

Seismic Damage Avoidance Concrete Shear Walls Using New Self-Centring Friction Dampers

Farhad Mohammadi Darani

A thesis submitted to
Auckland University of Technology in fulfilment of the
requirements for the degree of
Doctor of Philosophy (PhD)

Supervisors:
Prof. John Tookey
Dr. Amirhosein Ghaffarianhoseini

October 2020

School of Future Environments, Department of Built Environment Engineering

Auckland University of Technology (AUT), New Zealand

ABSTRACT

Past severe earthquakes imposed considerable life and financial loss to earthquake-prone countries. Therefore, in recent years, earthquake resiliency has become an important subject in political, social, economic and technical contexts. In the 2011 Christchurch earthquake, most of the buildings designed for the code requirements performed as expected and saved lives. However, a big financial loss was imposed on the economy to repair and rebuild the damaged buildings. Therefore, the importance of earthquake resiliency and a need to shift from life safety design philosophy to a more resilient design objective became clear. Researchers suggested that cost-efficient low-damage structural systems should be used in seismic resisting structures in order to achieve more resilient designs. Hence, developing new low-damage systems is an important part of this movement. In addition to a robust and predictable seismic response, new low-damage systems should be cost-efficient and easy to design and manufacture. Accordingly, the scope of this research is to develop a cost-efficient low-damage structural system that can be used in a variety of applications from buildings to bridges. New self-centring friction dampers have been selected as the low-damage connections providing repeatable energy dissipation and eliminating residual drifts. Rocking wall structural systems are known as seismic resisting systems in which less structural damage is expected compared to ductile systems. Also, reinforced concrete is a cheap and available material with suitable structural properties. In this study, these three different elements will be combined to achieve a new low-damage structural system. In this system, self-centring friction dampers together with rocking concrete shear walls form a seismic resisting structural system. In the next chapters, the friction dampers are studied first and then used in developing and large-scale testing of the proposed rocking concrete shear wall system. The seismic performance and design of the structures equipped with the developed system are also studied and verified through analytical and numerical investigations.

Attestation of Authorship

I hereby declare that this submission is my own work and that, to the best of my knowledge and belief, it contains no material previously published or written by another person (except where explicitly defined in the acknowledgements), nor material which to a substantial extent has been submitted for the award of any other degree or diploma of a university or other institutions of higher learning.

Signed:Farhad Mohammadi Darani.....

Date: 30 October 2020

Acknowledgement

I would like to express my thanks to my supervisor, Prof. John Tookey and Dr Amirhosein Ghaffarianhoseini.

I would like to thank the Ministry of Business, Innovation and Employment (MBIE) for their financial supports for this study. In addition, many thanks to Concrete NZ, Precast Sector for supporting us.

I would like to express my gratitude to all the mentors and professional technicians in the Engineering department of Auckland University of Technology, Dr Sherif Beskhyroun, Dave Crofts, Andrew Virtue and Allan Dixon, who have been big supports during the difficult times of this study. In addition, special thanks to Sajad Veismoradi and Mohamad Yousef-beik for all their times and helps during this research.

I would like to express my deepest love and gratitude to my father, my mother, my sister, and my brother for the infinite love that I received from them throughout my life. Last but not least, my love, Dr Niusha Navabian, my wife, my best friend and my soulmate who supported me countlessly and unconditionally throughout this journey. I would not have been able to finish this work without her support.

Dedication

This thesis is honourably dedicated to:

My lovely family

My wife, my parents and my siblings for all their support and the inspiration I received from them

Table of Contents

ABSTRACT.....	i
Attestation of Authorship.....	ii
Acknowledgement	iii
Dedication	iv
Table of Contents.....	v
List of Figures	viii
List of Tables	xii
Chapter 1: Introduction and Background.....	1
1.1 Introduction	1
1.2 Ductile concrete shear walls	3
1.3 Seismic Energy Dissipation Devices	18
1.4 This study	23
Chapter 2: Resilient Slip Friction Joint Performance: Component Analysis, Spring Model and Anti-Locking Mechanism	26
2.1 Introduction	26
2.2 Background	26
2.3 Resilient Slip Friction Joint (RSFJ).....	29
2.4 Energy damping mechanism in the RSFJ.....	32
2.5 Experimental validation	33
2.6 Load distribution between RSFJ grooves	33
2.7 Anti-Locking Mechanism.....	45
2.8 Summary and conclusion	54
Chapter 3: Development of a New Self-Centring Structural Connector for Seismic Protection of Structures	56
1.1 Abstract.....	56
3.2 Introduction	57
3.3 SSC PARTS	61
3.4 SSC PERFORMANCE.....	64
3.5 Experimental verification	69
3.6 The effect of various parameters on the damper behaviour	76
3.7 SSC Arrangements.....	79
3.8 Damper Applications.....	82
3.8.1 Braced frames	83
3.8.2 Moment resisting frames.....	84

3.8.3 Rocking structures.....	85
3.10 Conclusions	89
Chapter 4: Seismic Performance and Design of Rocking-wall Structures Equipped with Self-Centring Friction Connections.....	91
4.1 Abstract.....	91
4.2 Introduction	91
4.3 Displacement-based design of self-centring structures	94
4.4 Self-Centring Friction Dampers.....	99
4.4.1 Resilient Slip-Friction Joint (RSFJ)	99
4.4.2 Self-Centring Structural Connector (SSC).....	101
4.5 Seismic Design of the Prototype Structure	105
4.6 Load-displacement performance of rocking walls.....	109
4.7 Design of the prototype building	112
4.8 Nonlinear time-history analysis	120
4.9 Conclusions	124
Chapter 5: Concept Development and Experimental Verification of a New Rocking Concrete Shear Wall with Self-Centring Friction Connections	126
5.1 Abstract.....	126
5.2 Introduction	127
5.3 Concept development and analytical investigation.....	130
5.3.1 Self-Centring Friction Dampers.....	130
5.3.2 Load-displacement performance of Rocking Walls	134
5.3.3 Controlling Tension Cracks and Internal Bending Demand	137
5.4 Proposed Concept.....	141
5.5 Detailed design of the system.....	143
5.6 Experimental Investigation	146
5.6.1 Wall Panel Design.....	146
5.6.2 Test setup.....	149
5.7 RSFJ Shear Wall	151
5.8 SSC Shear Wall	155
5.9 Numerical Modelling.....	159
5.10 Non-linear time history analysis	163
5.11 Discussion and Conclusion	166
Chapter 6: Conclusions	169
6.1 Conclusions	169
6.2 Future studies	177

REFERENCES	182
Appendix A, Self-Centring Structural Connector SSC Patent.....	192

List of Figures

Figure 1. 1. Severe damage of code compliant concrete shear walls. a) Web crushing b) toe crushing	2
Figure 1. 2. Unexpected damage to a ductile designed concrete shear wall during the 2011 Christchurch Earthquake [2]. (a) Concrete removal; (b) fractured bar	3
Figure 1. 3. out of plane buckling of the boundary element of a ductile designed concrete shear wall [2]. (a) damaged wall; (b) close-up of the buckled region.	4
Figure 1. 4. 2011 Christchurch Earthquake (a) axial failure and (b) shear-axial failure [5].	5
Figure 1. 5. 2010 Chile Earthquake (a) axial compression failure and (b) diagonal shear failure [7].	5
Figure 1. 6. 2011 Christchurch earthquake (a) a moderately damaged concrete shear wall [2]. (b) Crack epoxy grout injection repair for the same wall [4].	6
Figure 1. 7 CTV Building (a) before, and (b) after Christchurch Earthquake.	7
Figure 1. 8 Rocking frame-wall structure with draped tendons and supplemental damping and fuse.	9
Figure 1. 9. Idealized hysteresis behaviour of traditional and self-centring systems [23].	10
Figure 1. 10. Typical details of rocking walls with and without supplementary energy dissipaters: (a) Single Rocking Wall (SRW) [27], (b) Precast concrete jointed wall system [24], (c) Hybrid wall with mild steel reinforcement [13, 28, 29], (d) Precast Wall with End Columns (PreWEC) using steel O-connectors [30].	12
Figure 1. 11. Unbonded post-tensioned precast wall (a) elevation and the section of wall base. (b) Hysteretic behaviour under lateral loading.	13
Figure 1. 12. Large-scale shake table testing of PRESSS system [24]: (a) UFP, (b) concrete crushing at wall base toe.	14
Figure 1. 13. Using mild still as internal yielding elements for energy dissipation [13, 28] (a) detail of energy dissipater (b) energy dissipater placed in foundation beam before pouring concrete (c) RHS members used as energy dissipaters.	15
Figure 1. 14. using external yielding and viscous dampers for energy dissipation [35, 36]: (a) Post-tensioned wall with viscous and TCY mild steel damper, (b) Buckled external TCY dissipaters.	16
Figure 1. 15. PreWEC system with O connectors [30, 37]: (a) The concept of PreWEC, and (b) Different failure modes of O connectors.	16
Figure 1. 16. Southern Cross Hospital after 2011 Christchurch Earthquake, unbonded PT walls with U shape flexural connectors [4].	17
Figure 1. 17. Different parts of a viscous damper	19
Figure 1. 18. High Force to Volume (HF2V) dampers [16, 47].....	20
Figure 1. 19 Elastomeric Spring Damper (ESD) [52]	21
Figure 1. 20. Friction ring spring, parts and performance [41, 55].....	22
Figure 1. 21. Resilient Slip-Friction Joint (RSFJ).....	23
Figure 2. 1. Resilient Slip Friction Joint: a) Parts, b) Assembly, c) Free body diagram.	29
Figure 2. 2. Flag shaped load-displacement hysteresis of RSFJ.	31
Figure 2. 3. Contribution of elastic springs and friction damping in RSFJ overall response.	32
Figure 2. 4. Experimental testing of a sample RSFJ: a) Test setup, b) Load-displacement responses.....	33
Figure 2. 5. Free body diagram of the RSFJ and deformed shapes of the grooves.....	36
Figure 2. 6. Shear and moment diagrams of the grooves.	36
Figure 2. 7. Equivalent grooves and their parameters: (a) Equivalent shear/flexure deformation segments (hatched), (b) Symmetric groove parameters, (c) Asymmetric groove parameters.	37
Figure 2. 8. Equivalent axial deformation segments and their parameters.	39
Figure 2. 9. RSFJ and its equivalent spring model: (a)The modelled RSFJ, (b) RSFJ structural spring model.....	39
Figure 2. 10. Test setup and instrumentation.....	41
Figure 2. 11. ABAQUS numerical model.....	42
Figure 2. 12. Comparison of experimental results with the numerical and analytical predictions on 2.the force-displacement response of the tested RSFJ.	42
Figure 2. 13. Distribution of internal forces in the spring model calculated based on the proposed analytical model.	44

Figure 2. 14. Comparison of test results with the analytical method (Note: FG and SG refer to the first and second gauges).	44
Figure 2. 15. Theoretical load-displacement response of RSFJs with ALM mechanism.....	46
Figure 2. 16. RSFJ components cyclic behaviour.	46
Figure 2. 17. Cyclic response of RSFJ when the ALM is activated.	49
Figure 2. 18. Comparison of component test results with their equivalent bi-linear model.....	50
Figure 2. 19. Anti-locking mechanism test specimen.	51
Figure 2. 20. Test loading protocol.....	52
Figure 2. 21. Comparison of experimental results with analytical backbone and last cycle.	52
Figure 2. 22. Yielding of the nuts as the result of concentrated bearing pressure induced by disc internal edge.	53
Figure 2. 23. Comparison of analytical and experimental results for the last three cycles.	53
Figure 3. 1. Self-Centring Structural Connector.	62
Figure 3. 2. Free body diagram and force-displacement response.	65
Figure 3. 3. Free body diagram of a cylinder with internal pressure.	67
Figure 3. 4. Belleville Spring (Left), and tube dimensions (Right).	70
Figure 3. 5. Manufactured tube.....	71
Figure 3. 6. Friction disc.....	71
Figure 3. 7. Applying the clamping force (a) Total length of friction discs and spacing between clamping bolts, and (b) torque meter used for clamping bolts.	72
Figure 3. 8. (a) End flanges dimensions, and (b) the assembly of friction discs and springs being inserted into the tube.....	73
Figure 3. 9. Test setup.	75
Figure 3. 10. Force-displacement response of SSC prototype.....	76
Figure 3. 11. The effect of pre-stressing force on the performance of SCC.....	77
Figure 3. 12. The effect of friction force on the performance of SCC.	78
Figure 3. 13. The effect of pre-stressing force on the performance of SCC.....	79
Figure 3. 14. (a) Multiple friction discs configuration, and (b) corresponding behaviour.	80
Figure 3. 15. SSC compression-only configurations.	81
Figure 3. 16. Double-acting configuration.	82
Figure 3. 17. Braced frame with tension-compression members using double-acting SSC.	83
Figure 3. 18. Braced frame with tension-only members using tension-only SSC.....	84
Figure 3. 19. The application of SSC in moment-resisting frames.	84
Figure 3. 20. The application of SSC in rocking wall systems.	86
Figure 3. 21. (a) Multi-Linear Elastic (MLE) link representing pre-stressed spring behaviour, and (b) Multi-Linear Plastic (MLP) link representing friction behaviour.	87
Figure 3. 22. Combination of MLE and MLP links.	88
Figure 3. 23. The comparison of experimental result with the numerical model prediction of SSC.	89
Figure 4. 1. Load-deformation response: a) Self-centring system with additional damping b) Elastic system with viscous damping.	95
Figure 4. 2. Hysteresis dissipated energy and equivalent viscous damping concept.	96
Figure 4. 3. Design parameters of an SDOF self-centring system.	97
Figure 4. 4. Equivalent SDOF system of a multi-story building.....	98
Figure 4. 5. Resilient Slip Friction Joint.	101
Figure 4. 6. Self-centring structural connector.	102
Figure 4. 7. Free body diagram and force-displacement response.	103
Figure 4. 8. Free body diagram of a cylinder with internal pressure.	104
Figure 4. 9. Structural plan and elevation of the modelled building.	106
Figure 4. 10. Acceleration design spectrum (Left) and Displacement design spectrum (Right).	107
Figure 4. 11. The free-body diagram of rocking walls equipped with double-acting self-centring connections.	109
Figure 4. 12. The free-body diagram of rocking walls equipped with tension-only self-centring connections.	111
Figure 4. 13. Experimental Verification: (a) RSFJ shear wall, and (b) SSC shear wall.	112

Figure 4. 14. RSFJ hysteresis behaviour designed for representing the double-acting joint (Left), and SSC hysteresis behaviour designed for representing the tension-only joint (Right).....	115
Figure 4. 15. Three-dimensional model of the designed structure.	115
Figure 4. 16. Elements used for the structural modelling of rocking walls with RSFJs.	116
Figure 4. 17. Load-displacement response of the RSFJ and SSC shear walls obtained from the analysis.....	117
Figure 4. 18. Combination of MLE and MLP links for modeling SSC.	118
Figure 4. 19. Elements used for the structural modelling of rocking walls with SSC.....	119
Figure 4. 20. Comparison of the response parameters of the re-designed SSC with the primary design:.....	120
Figure 4. 21. Comparison of the acceleration response spectra of the selected ground motions with the design spectra (red line).	122
Figure 4. 22. Comparison of maximum roof displacements obtained from NLTH analysis.....	123
Figure 4. 23. Hysteresis response of the connections under Tabas earthquake:	124
Figure 4. 24. Vertical distribution of inter-story drift for the modelled structure with SSC shear wall under the selected ground motions.....	124
Figure 5. 1. Observed failure modes of structural walls during past earthquakes: (a) Bar yielding followed by bar rupture, (b) Toe crushing, (c) Diagonal shear, (d) Compression failure and buckling [4].....	127
Figure 5. 2. Resilient Slip Friction Joint: a) Components, b) Assembly, c) Free body diagram, d) Flag-shaped response of RSFJ.....	131
Figure 5. 3. Self-centring Structural Connector (SSC).....	132
Figure 5. 4. Free body diagram and force-displacement response.	132
Figure 5. 5. Free body diagram of a cylinder with internal pressure.	134
Figure 5. 6. a) Free-body diagram of rocking walls equipped with double-acting self-centring connections and b) load-displacement response of the wall.....	135
Figure 5. 7. The free-body diagram of rocking walls equipped with tension-only self-centring connections.	137
Figure 5. 8. Structural plan and elevation of the modelled building.	139
Figure 5. 9. Concrete stress-strain relationship.	139
Figure 5. 10. Comparison of overall load-displacement performance of the system with the elastic and plastic concrete models.....	140
Figure 5. 11. Comparison of the joint load-displacement performance of the system with the elastic and plastic concrete models.....	141
Figure 5. 12. Different components and construction phases of the proposed rocking pre-cast concrete wall system.	144
Figure 5. 13. Free body diagram of the post-tensioned wall at the ultimate lateral loading stage.	146
Figure 5. 14. Concrete panel reinforcement: a) shop drawings, b) reinforced wall before the concrete pour, c) post-tensioning rod.	148
Figure 5. 15. Rocking wall base plate: a) base plate connected to the strong floor and b) arrangement of the holes.	149
Figure 5. 16. Lateral support: a) Test setup, b) schematic elevation view, c) schematic plan view.	150
Figure 5. 17. Out-of-plane shear keys.	151
Figure 5. 18. Instrumentation of the specimen: a) draw wire, b) LVDTs, and c) instrumentation diagram.	152
Figure 5. 19. RSFJ component testing: a) middle plate dimensions, b) cap plate dimensions, c) assembled joint tested in UTM, d) observed load-displacement performance.	153
Figure 5. 20. Details of the RSFJ: a) connection to the shear wall and base plate b) bracket section view, c) elevation view of the bracket.	154
Figure 5. 21. RSFJ shear wall: a) Test setup, b) comparison of analytical and experimental results, c) minor concrete spalling at toes.	155
Figure 5. 22. SSC component test: a) comparison of analytical and experimental performance, b) test setup.	156
Figure 5. 23. SSC connection to shear wall and foundation: a) connection at the top of the joint, b) connection at the bottom of the joint, c) rotation compatibility with rocking motion, d) shear keys.....	158
Figure 5. 24. SSC shear wall: a) test setup, b) comparison of analytical and experimental results, and c) results under high-frequency loading.	159

Figure 5. 25. Numerical modelling of the proposed concept: a) general components, b) connection details for double-acting connections, and c) connection details for tension-only connections.....	161
Figure 5. 26. Combination of MLE and MLP links for modelling the SSC.....	161
Figure 5. 27. Axial stress distribution in the models: a) RSFJ shear wall, and b) SSC shear wall.	162
Figure 5. 28. Comparison of numerical and experimental results: a) RSFJ shear wall, b) SSC shear wall.	163
Figure 5. 29. Flag-shaped behaviour of the modelled RSFJs (Left), and Response of the proposed rocking wall system under cyclic loading for the lateral force acting at the top (H=4000mm) (Right)	164
Figure 5. 30. Roof displacement demand for selected ground motions.....	165
Figure 5. 31. Maximum top floor drift ratio for the selected earthquake events.	165

List of Tables

Table 2. 1. the properties of the tested RSFJ.....	34
Table 2. 2 Stiffness parameters of the tested RSFJ.....	43
Table 2. 3. Strain predictions and measurements at the joint load of 550 kN.....	45
Table 2. 4. Rod M18 grade 8.8 tension test results.....	50
Table 2. 5. Properties of RSFJ tested for ALM mechanism.....	51
Table 3. 1 The properties of the tested SSC.....	70
Table 3. 2. SSC design parameters.....	73
Table 3. 3. Cyclic testing load protocol.	74
Table 3. 4. Numerical modeling parameters of the tested SSC.....	89
Table 4. 1. Multi-Degree of Freedom System (MDOF) parameters of the prototype building.....	108
Table 4. 2. Vertical distribution of seismic load and story shears of the modelled structure.....	108
Table 4. 3. Geometrical and mechanical properties of Wall A.	112
Table 4. 4. Force and displacement parameters calculated for Wall A with double-acting joints.	113
Table 4. 5. Force and displacement parameters calculated for Wall A with tension-only joints.....	114
Table 4. 6. Selected Ground-Motions and corresponding scale factors.	121
Table 5. 1. Design parameters of the tested wall.....	147
Table 5. 2. Design parameters of the tested RSFJ.....	153
Table 5. 3. Design parameters of tested SSCs.	156
Table 5. 4. Selected ground motions and scaling.....	164

Declaration of Contribution

Manuscript 1: Resilient Slip Friction Joint Performance: Component Analysis, Spring Model and Anti-Locking Mechanism

Manuscript 2: Development of a New Self-Centring Structural Connector for Seismic Protection of Structures

Manuscript 3: Seismic Performance and Design of Rocking-wall Structures Equipped with Self-Centring Friction Connections

Manuscript 4: Concept Development and Experimental Verification of a New Rocking Concrete Shear Wall with Self-Centring Friction Connections

	Manuscript 1		Manuscript 2		Manuscript 3		Manuscript 4	
	Contribution (%)	Description	Contribution (%)	Description	Contribution (%)	Description	Contribution (%)	Description
Farhad M.Darani	80	Main research and paper writing	82	Main research and paper writing	82	Main research and paper writing	84	Main research and paper writing
Pouyan Zarnani	5	Supervision and review	10	Supervision and review	10	Supervision and review	5	Supervision and review
Pierre Quenneville	5	Supervision and review	8	Supervision and review	8	Supervision and review	5	Supervision and review
Ashkan Hashemi	4	Advice, review and technical feedback on the experiments	0	N/A	0	N/A	0	N/A
Sajad Veismoradi	3	Review and feedback	0	N/A	0	N/A	3	Technical feedback on the experiments
Mohamad Mahdi Yousef-beik	3	Technical feedback on the experiments and modeling	0	N/A	0	N/A	3	Technical feedback on the experiments

I hereby declare that my contribution in this research is as mentioned in the table above			
Farhad M.Darani	Date	26/10/2020	Signature
Pouyan Zarnani	Date	5/11/20	Signature
Pierre Quenneville	Date	5 Nov 2020	Signature

Ashkan Hashemi	Date	5/11/2020	Signature
Sajad Veismoradi	Date	5/11/2020	Signature
Mohamad Mahdi Yousef-beik	Date	5/11/2020	Signature Mohamad

Manuscript 1: Paper under review submitted to Journal of Structures

Manuscript 2: Paper under review submitted to Journal of Construction Steel Research

Manuscript 3: Paper in preparation for submission

Manuscript 4: Paper in preparation for submission

Chapter 1: Introduction and Background

1.1 Introduction

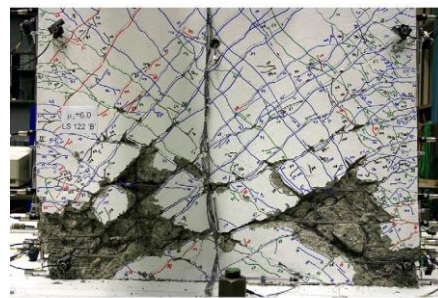
Concrete shear walls have been used widely in earthquake resisting systems. High stiffness and high strength, as well as acceptable ductility levels, can be named as positive aspects of these lateral load-resisting systems. The yielding of the longitudinal bars is the main source for dissipating seismic energy in these walls to provide the required ductility. To achieve this level of ductility, many details should be considered which makes the design procedure of conventional concrete shear walls complicated, in addition to the permanent damage. For example, the concrete confinement, reinforcing of the potential plastic hinge regions and avoiding brittle failure modes, could be named as the design and practical challenges. shear failure, wall toe crushing, and local buckling of the wall segments are some of the brittle failure modes which are observed during past earthquakes and should be avoided. Furthermore, the traditional design, which is based on ductile design concepts, is costly to be repaired or reconstructed after moderate to severe earthquakes. It should be noted that the cost of business interruption should be also be added to the above-mentioned costs.

Following the 2010 and 2011 Christchurch earthquakes and the consequent economic and social impacts, researchers and engineers got more inclined to move from ductile design concepts to low-damage ones given the advantages involved. This was a significant step to achieve a resilient society against natural disasters. The low-damage design concept is based on the fact that the earthquake energy should be dissipated in certain structural elements as sacrificial fuses which can be easily repaired or replaced after moderate to severe earthquakes. To minimise the earthquake damage in addition to satisfying the life-safety of the occupants, researchers and engineers' focus have been on the development of low-damage concepts for concrete shear walls where they could still have the benefits of reinforced concrete such as desired structural performance, low cost and availability. The initial solution introduced was the rocking wall systems in which the rocking

motion is controlled using post-tensioned cables. In earthquake-resistant rocking systems, the seismic input energy will be dissipated by the energy required to induce base uplift in the wall. Even though such systems have shown acceptable seismic performance in comparison to the traditional ductile design, the lack of damping leads to high acceleration and displacement demands. This lack of damping makes the design more challenging in terms of the deformation compatibility, occupants' comfort, and protection of non-structural components. Adding supplemental damping devices is proposed by researchers to improve the seismic response of the rocking wall systems. Yielding, friction and viscous damping systems are proposed, tested and used in rocking shear walls. While these rocking walls with additional damping have become more reliable given the improved performance, there are still some challenges involved with these systems. For example, yielding elements providing energy dissipation should be inspected after each intense event and repaired or replaced if required. In addition, as the residual capacity of these sacrificial elements might be affected during the main shocks, the structure is more vulnerable to the aftershocks until getting fully repaired by replacing the damaged fuses. Therefore, there is still a remaining step to achieve an ideal maintenance-free rocking wall system that provides the desired level of performance during earthquakes and aftershocks.



(a)



(b)

Figure 1. 1. Severe damage of code compliant concrete shear walls. a) Web crushing b) toe crushing

No table of figures entries found.

1.2 Ductile concrete shear walls

Ductile concrete shear walls are designed and detailed to dissipate earthquake energy by the yielding of the longitudinal reinforcements at boundary elements. After moderate to severe earthquakes, the level of damage in these walls imposes considerable repair and even reconstruction costs to the owners and/or the government. Fig. 1.1 shows two ductile concrete shear walls tested up to the design earthquake level [1]. As it is clear from the pictures, even though the walls performed as expected, reconstruction would be necessary if they were used in a real building.

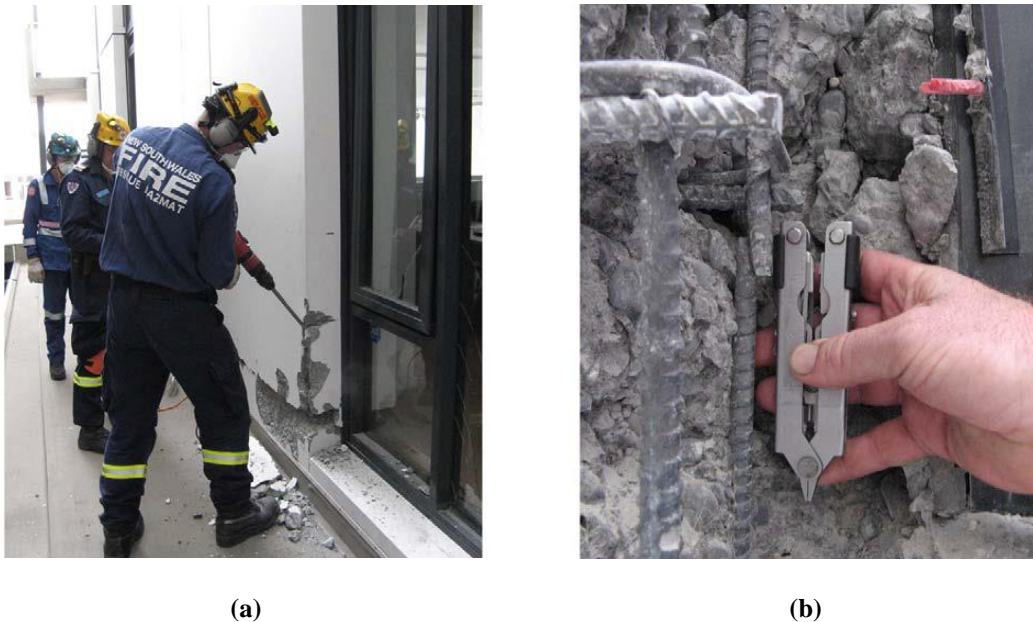


Figure 1.2. Unexpected damage to a ductile designed concrete shear wall during the 2011 Christchurch Earthquake [2]. (a) Concrete removal; (b) fractured bar.

Furthermore, some ductile designed concrete shear walls have shown unexpected failure modes during recent earthquakes [3, 4]. For example, as it is shown in Fig. 1.2, the longitudinal rebar rupture at lower level tensile strains has occurred in some ductile designed concrete shear walls during the 2011 Christchurch earthquake. Out of plane buckling of boundary elements can also be mentioned as another common unexpected failure mode observed in the 2011 Christchurch Earthquake. Large tensile strain demands at boundary elements of plastic hinge regions cause severe crack opening and undesired gaps in these regions. When the previously tensioned boundary

element is subjected to the earthquake compression cycle, the effective thickness of the wall in these severely cracked regions is already decreased dramatically leading to the occurrence of buckling.



Figure 1. 3. out of plane buckling of the boundary element of a ductile designed concrete shear wall [2]. (a) damaged wall; (b) close-up of the buckled region.

This phenomenon is shown in Fig. 1.3 [2]. These unexpected failure modes are considered by researchers as poor seismic behaviour of concrete shear walls requiring more investigation to improve the design guidelines presented in the codes [2, 3]. In addition to the unexpected damage to ductile designed walls, many other brittle failure modes were observed in concrete shear walls designed in compliance with the recent concrete codes. Axial and different types of shear failure in the 2011 Christchurch earthquake are just a few examples of such failures. Poor design, detailing and construction quality are the main reasons for such observed brittle failure modes. Fig. 1.4(a) shows the axial failure in a wall at the rebar splice region which is as a result of poor detailing. A combined axial-shear failure is also shown in Fig. 1.4(b) [5].



(a)



(b)

Figure 1. 4. 2011 Christchurch Earthquake (a) axial failure and (b) shear-axial failure [5].

Also, in the 2010 Chile Earthquake, severe damages were observed in ductile designed concrete shear walls. Axial compression was one of the commonly observed failure modes [6]. Concrete crushing and rebar buckling at the boundary element of a wall after the 2010 Chile earthquake is shown in Fig. 1.5(a). The damage started at the boundary element and then continued to the wall web [7]. The different shear failure modes of concrete shear walls can be initiated by the diagonal tension, diagonal compression and sliding shear. As it can be seen in Fig. 1.5(b), shear failure is very critical in perforated and coupled walls [7].



(a)



(b)

Figure 1. 5. 2010 Chile Earthquake (a) axial compression failure and (b) diagonal shear failure [7].

Shear failure should be avoided in ductile concrete shear walls. One of the most difficult aspects of designing ductile shear walls is taking into account all of the possible failure modes and

designing the wall in the way that the desired ductile flexural failure occurs before other brittle failure modes, within a safe margin [8]. After more than a hundred years of research and application of concrete structures, the complexity of reinforced concrete behaviour surprises the engineers by unexpected failures in real earthquake loading condition.



Figure 1. 6. 2011 Christchurch earthquake (a) a moderately damaged concrete shear wall [2]. (b) Crack epoxy grout injection repair for the same wall [4].

Other problems with traditional concrete structures appear when the repair methods of damaged shear walls are considered. There are some methods to repair concrete walls with minor to moderate earthquake damage. For example, Fig. 1.6(a) shows a damaged wall after the 2011 Christchurch earthquake [2] and Fig. 1.6 (b) shows the same wall after repairing [4]. The most important challenge for repairing reinforced concrete is to detect the damage and to realize how serious the damage is. It is difficult to assess the level of damage, especially the yielding of the reinforcements inside the concrete. This can be more challenging for the elements and connections which are not visible nor accessible.



(a)



(b)

Figure 1. 7 CTV Building (a) before, and (b) after Christchurch Earthquake.

For example, in February 2011 the Christchurch earthquake with a magnitude of 6.3 causing 185 casualties, 115 people died in the CTV building (Fig. 1.7). According to the investigations carried out by Professor John B. Mander based on the inquiry of Canterbury Earthquake Royal Commission into the collapse of the CTV building, it was reported that the building had already been weakened and considerably damaged by the Darfield Earthquake occurred that in September 2010 with a higher magnitude of 7.1. However, the local authority permitted the building to be re-occupied because of the lack of proper understanding about the condition of the buildings after the first earthquake. The CTV Building was inspected by engineers after the first strong earthquake and was declared safe. However, based on Professor Mander's report, the building must have also hidden (unobserved and/or unobservable) damage in specific structural components because the level of ground motion sustained by the building was close to the level that the design code NZS4203 called for. In addition, on several occasions' eyewitnesses reported that the CTV building was uncomfortably lively. These issues could be considered as a signal for Red Sticker for the building.

This example emphasizes that damages to the concrete structures are really hard to detect and evaluate. Therefore, this can be considered as a weakness for the current design philosophy which is based on controlled damages in certain locations in the structure. It has been quite a while since the 1990s that researchers have been emphasizing the need to move beyond ductility [9, 10]. Repair

and reconstruction, business interruption and residual deformations are challenges that impose financial and social loss to the community after earthquakes. All of these concerns were proven correct after the 2010 and 2011 Christchurch earthquakes. Therefore, a low-damage based design philosophy could be a more reliable option for concrete structures [11].

In conclusion, regardless of the code modifications required for the ductile design of concrete shear walls, a shift from a high-damage to a low-damage concept seems to be necessary as there is still a huge repair and business interruption cost for traditional concrete structural walls. Given the complex behavioural aspects and failure modes of concrete structures, the risk of relying on yielding and plastic deformation in reinforced concrete for dissipating earthquake energy is high. In addition, damage detection and repairing of concrete structures are challenging and quite costly. In recognition of this fact, researchers have strongly intended to adopt low-damage design concepts for concrete structure. Low-damage concrete structures can be identified as structures with minor cracks without crushing of the concrete and/or yielding or rupture of the reinforcements. In these systems, the earthquake energy is dissipated through an external repairable or resilient mechanism. Therefore, the repair is cost-efficient and the need for reconstruction is un-likely after severe earthquakes. The benefits of such systems are further discussed in the following sections.

Low-damage and damage-avoidance concrete shear walls

the term damage avoidance has been used for the structures that incorporate systems to provide energy dissipation and bring the structure back into its upright position after an earthquake [9, 10, 12]. Damage Avoidance Design (DAD) philosophy is the basis of the seismic design of the structures aimed not to suffer from damage due to Design Base Earthquake (DBE) [9]. The desired characteristics of damage avoidance systems are repeatable and predictable hysteresis damping and reliable self-centring. Different damage-avoidance systems have been introduced and tested successfully [13-18]. These systems have been incorporated experimentally in different configurations such as moment resisting concrete [16] and steel [19] frames and rocking concrete

shear walls and rocking bridge piers [10, 14, 20]. In the following section, more details are given about two rocking wall damage-avoidance systems developed and tested previously.

As shown in Fig 1.8, a rocking wall framed structure was proposed using tendons [14, 21]. Draped tendons were used to connect the rocking wall to the foundation. A parallel combination of a fuse and a damper connects the tendon to the foundation. A yielding element represents the fuse behaviour. Different type of dampers such as Elastomeric Spring Dampers (EDS) can be used to represent the behaviour of the damper in the fuse-damper configuration [21, 22]. The tendon is draped to form the same shape as the bending moment diagram along with the height of the structure due to the design earthquake. This configuration contributes to effectively reducing the displacement and acceleration demands. The results of this study proved that rocking concrete walls are a suitable alternative to traditional ductile walls as the level of expected damage is significantly less. Damage Avoidance Design (DAD) philosophy was proved to be the alternative for traditional ductile design as the damage was controlled in the proposed system designed with DAD. Sensitivity analysis on tendon prestressing force mentioned that the response is not sensitive to this parameter. However, a minimum amount of pre-stressing is required to prevent the tendons from the slack.

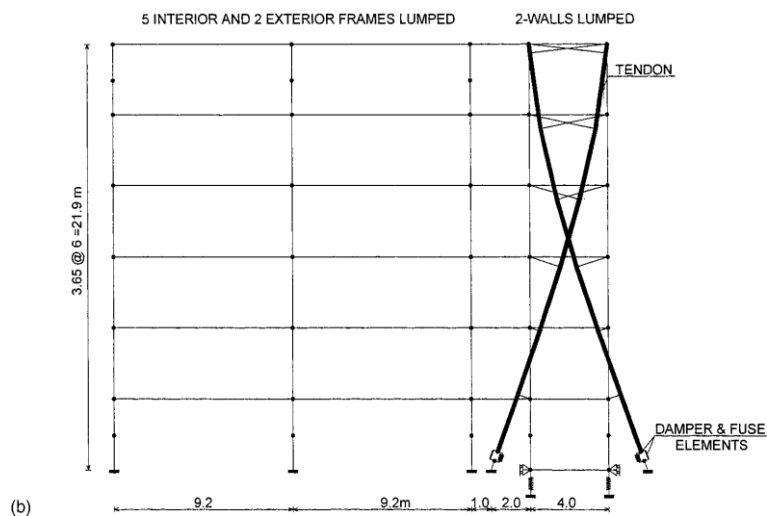


Figure 1. 8 Rocking frame-wall structure with draped tendons and supplemental damping and fuse.

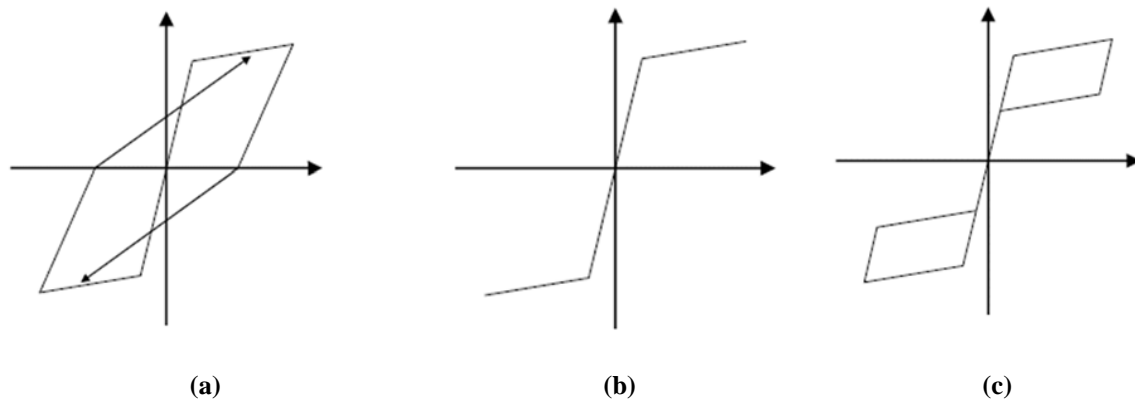


Figure 1. 9. Idealized hysteresis behaviour of traditional and self-centring systems [23].

To minimise the earthquake damage in addition to satisfying the life-safety of the occupants, researchers and engineers' focus have been on the development of low-damage concepts for concrete shear walls where they could still have the benefits of reinforced concrete such as construction cost, availability and formability. As discussed in the previous section, yielding of the reinforcements is the main source for energy dissipation in traditional reinforced concrete (RC) walls. However, the strength and stiffness degradation are expected due to the degradation of concrete mechanical properties during cyclic loading (Fig. 1.9(a)). The initial solution introduced for low-damage concrete shear walls was the rocking wall systems in which the rocking motion is controlled using post-tensioned tendons [24]. In earthquake resistant rocking systems, the seismic input energy will be dissipated by the energy required to induce base uplift in the wall [25]. Research has been performed on rocking concrete shear walls with post-tensioned (PT) tendons. As it is shown in Fig. 1.9(b), the ideal load-deformation response of rocking walls consists of a bilinear elastic graph in which the softening in the response represents starting of the gap opening between the wall base and the foundation. The tendons are post-tensioned to a certain magnitude of force holding the wall in its position. When lateral loading starts, the post-tensioning force should be overcome first before the lateral load could separate the wall base from the foundation

(when rocking motion starts). At this stage, the response of the wall is very stiff there is only internal deformation rather than rigid body rotation. As soon as the clamping force is equal to the earthquake force, the softer response due to rod elongation and therefore the rocking motion starts. This completely bilinear elastic behaviour may result in greater force and displacement demands which makes using additional energy dissipation mechanisms necessary. Fig. 1.9(c) shows the flag shape hysteresis of a rocking system with additional damping.

The schematic views of the unbonded post-tensioned precast concrete rocking walls without (Fig. 1.10(a)) and with different types of additional energy dissipaters (Fig. 1.10(b) to 1.10(d)) are shown in Fig. 1.10 [26]. A brief explanation about the concepts shown in Fig. 1.10 is given here. As shown in Fig. 1.10(a), unbonded post-tensioning of the wall to the foundation results in a controlled rocking motion of the wall when subjected to lateral loading. The performance of the wall can be controlled by the amount of post-tensioning force applied to the tendon. The softening of the wall response at the onset of rocking movement results in reduced seismic demand on the structure. However, one can still argue that the displacement demand is high due to small resistive force during the rocking motion. Accordingly, researchers have suggested providing additional energy dissipation to reduce the displacement demand and to better control the rocking motion. Such concepts with additional energy dissipations are mentioned in Fig.1.10(b), (c) and (d). Further explanation on how these additional damping will contribute in the response improvement will be discussed later in this chapter. In this section, the literature related to the performance and application of rocking walls as low-damage structural systems is reviewed.

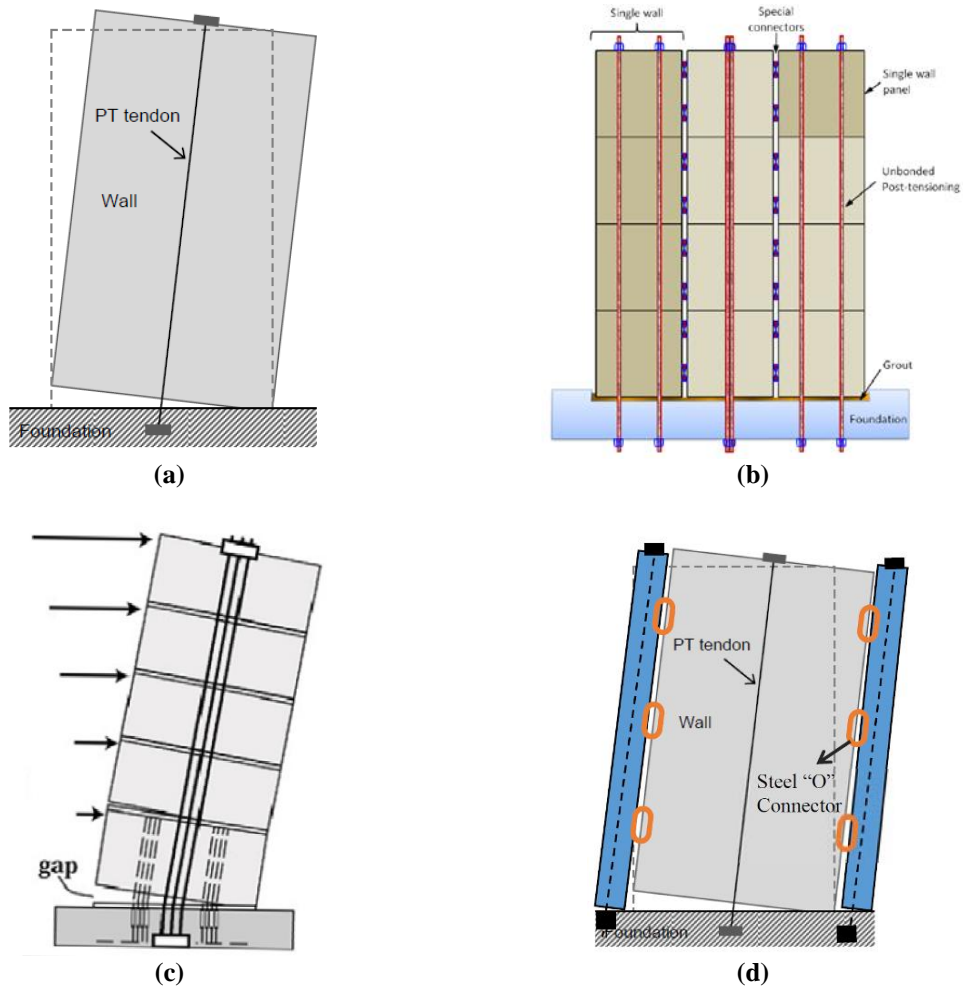


Figure 1. 10. Typical details of rocking walls with and without supplementary energy dissipaters: (a) Single Rocking Wall (SRW) [27], (b) Precast concrete jointed wall system [24], (c) Hybrid wall with mild steel reinforcement [13, 28, 29], (d) Precast Wall with End Columns (PreWEC) using steel O-connectors [30].

A joint US-Japan research program entitled PREcast Seismic Structural Systems (PRESSS) was initiated in the early 1990s to develop seismic-resilient precast structures. As part of this program, it was suggested to use unbonded post-tensioned cables to improve the seismic performance of beam-column connections in precast concrete frames [31]. The idea of using unbonded post-tensioning was then adopted in rocking concrete walls to assess their cyclic performance [27].

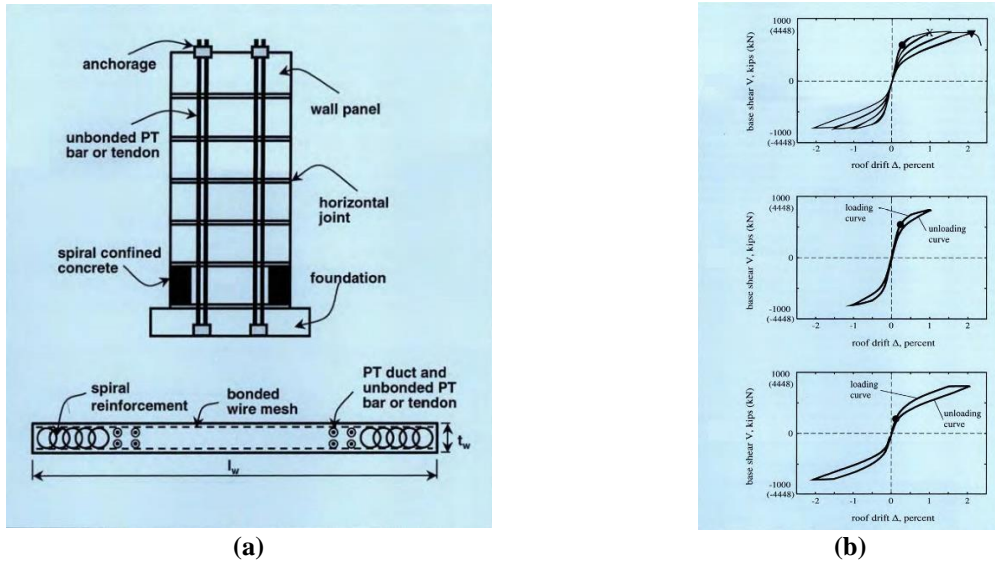


Figure 1. 11. Unbonded post-tensioned precast wall (a) elevation and the section of wall base. (b) Hysteretic behaviour under lateral loading.

A detailed analytical study on the behaviour of single rocking walls was done by Kurama et al [27]. As shown in Fig. 1.11(a), special reinforcements are needed at the wall base corners to limit the concrete crushing at the wall toe. Nonlinear behaviour of concrete in compression in these areas causes some nonlinearity in the response of the rocking structure as shown in Fig. 1.11a. The nonlinear behaviour of steel strands could also be considered as another source of softening in the response of the system. The displacement demand of the system is higher than the equivalent ductile shear walls because of the lack of damping in the system. Accordingly, Kurama [32, 33] performed a series of analytical studies to assess the performance of single rocking walls with additional supplemental friction and viscous dampers. The results showed that additional dampers effectively reduce the seismic demands if they are properly designed.

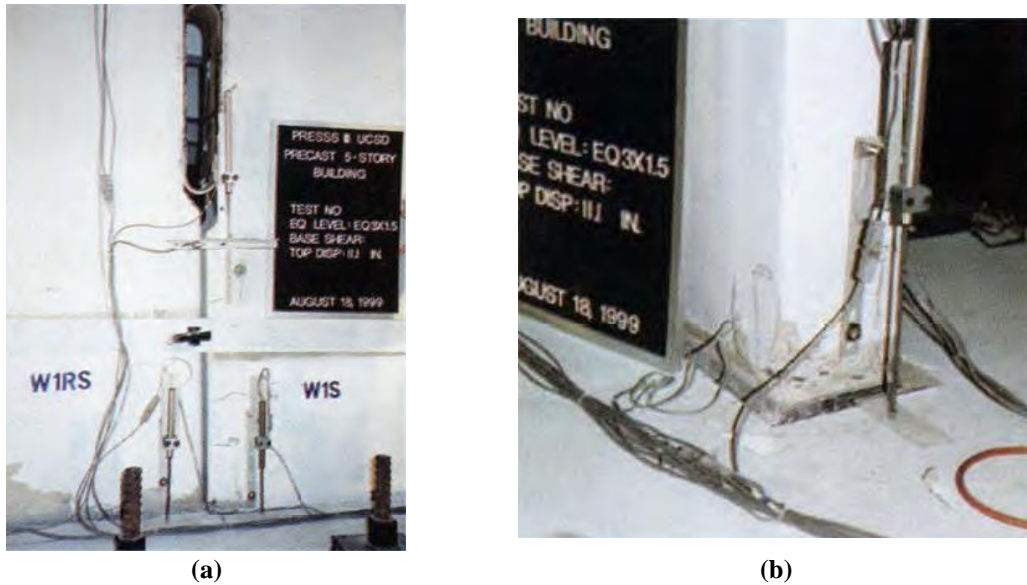


Figure 1. 12. Large-scale shake table testing of PRESSS system [24]: (a) UFP, (b) concrete crushing at wall base toe.

The precast concrete jointed wall system with U-shaped Flexural Plates (UFPs) was tested by Priestly et al. [24]. U-shaped dissipaters were used as additional yielding dampers (Fig. 1.12(a)). A large-scale shake table testing was carried out for the final stage of PRESSS program. The response of the structure to an earthquake 50% stronger than the design level was determined as suitable with minor damage. However, because of the smaller lever arm, these walls provide less moment capacity than that of comparable traditional ductile walls. The response of UFPs is also unpredictable [34] and they should be replaced after moderate to severe earthquakes. Spalling of the concrete was observed at the wall base at the compression toes which can be considered as repairable damage. Fig. 1.12(b) exhibits the spalling of concrete at the wall toes.

Other efforts were made for using internal grouted mild steel reinforcement for additional damping in unbonded post-tensioned walls [13, 28, 29]. In this concept, the yielding of the unbonded and/or tapered part of the rebars is the main source for energy dissipation (Fig. 1.13). These bars are hard to replace if rupture occurs after severe earthquakes. Therefore, regardless of their acceptable seismic performance, their application in areas with high seismicity might be problematic.

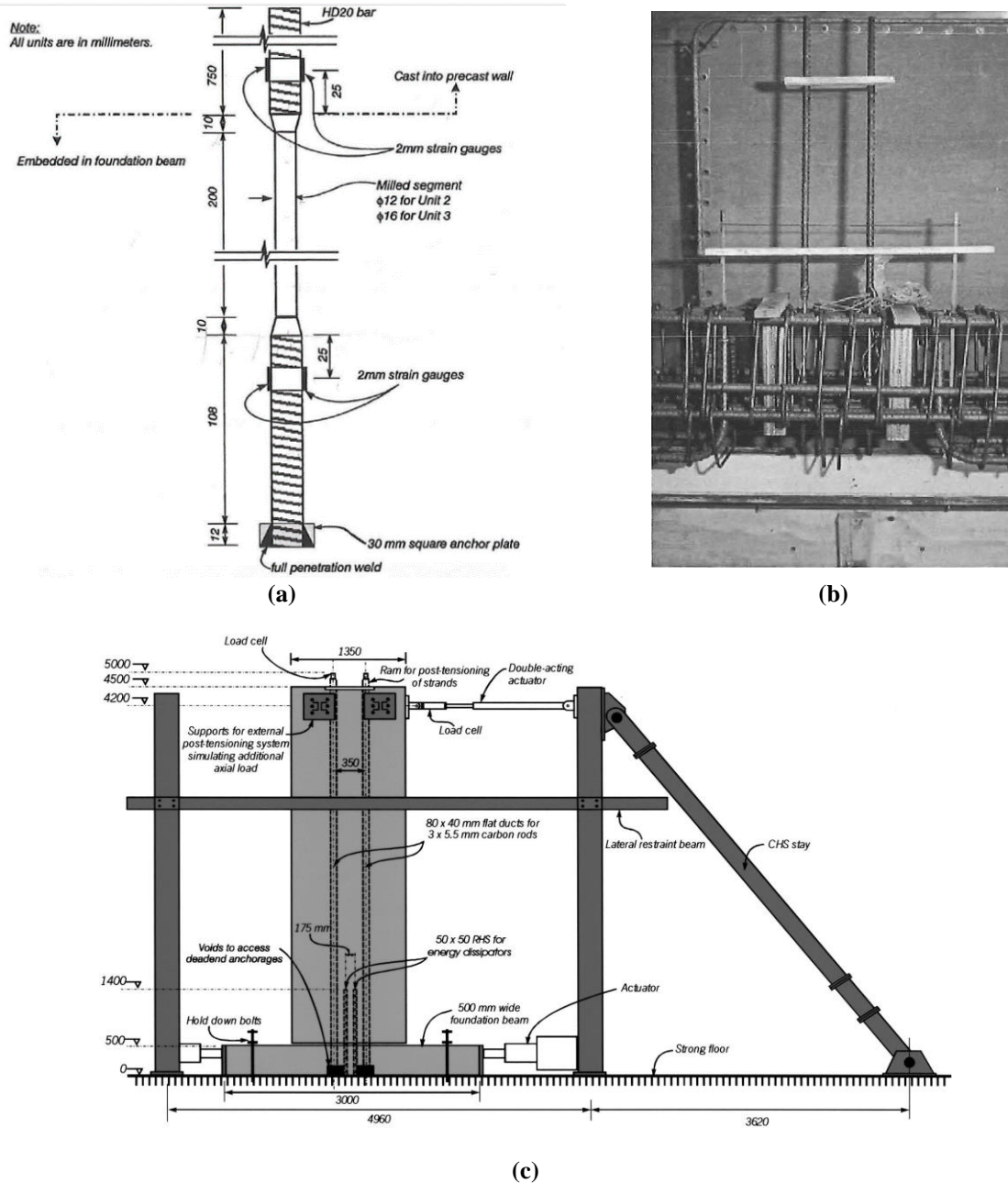


Figure 1.13. Using mild steel as internal yielding elements for energy dissipation [13, 28] (a) detail of energy dissipater (b) energy dissipater placed in foundation beam before pouring concrete (c) RHS members used as energy dissipators.

Externally mounted mild steel, Tension and Compression Yielding (TCY) dampers, as well as viscous dampers, were designed and tested by Marriot et al [35, 36]. In their proposed system (Fig. 1.14(a)), different combinations of TCY and viscous dampers were assessed using analytical and experimental data. An epoxy injected steel confining tube was used to cover the tapered part of

TCY dampers. However, these dampers are prone to buckling and should be properly designed (Fig. 1.14(b)).

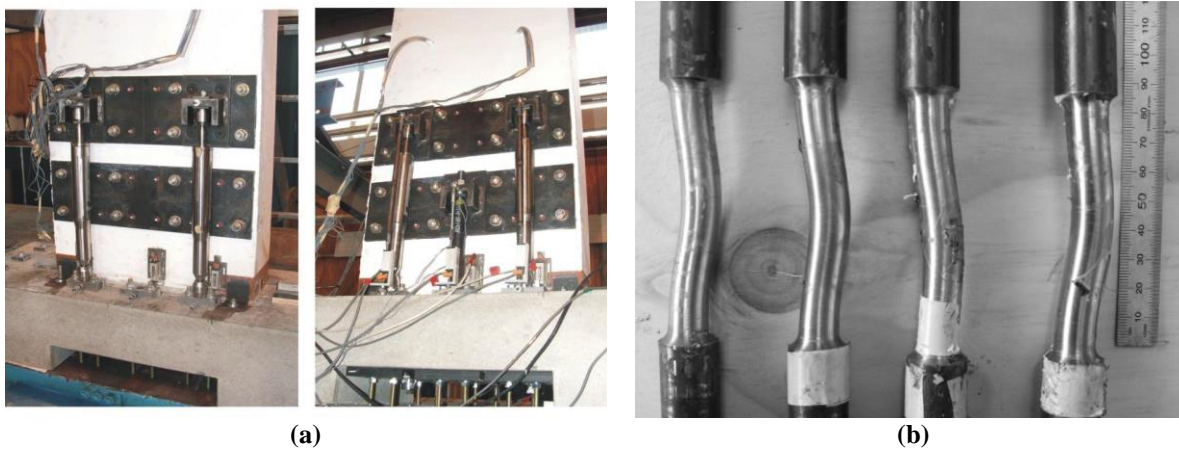


Figure 1.14. using external yielding and viscous dampers for energy dissipation [35, 36]: (a) Post-tensioned wall with viscous and TCY mild steel damper, (b) Buckled external TCY dissipaters.

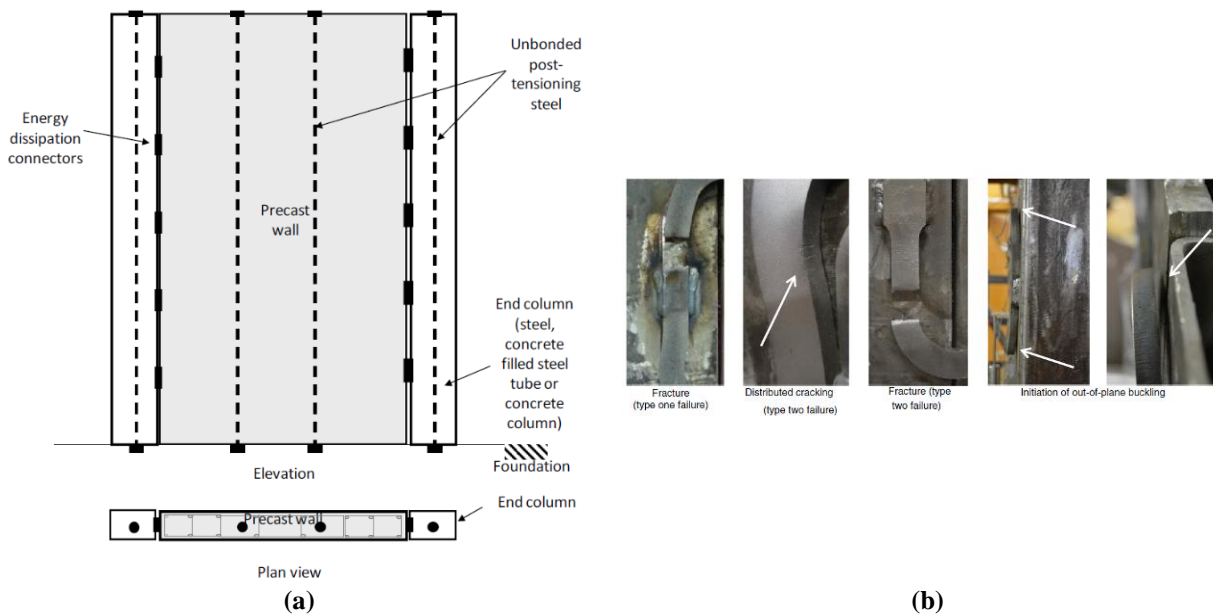


Figure 1.15. PreWEC system with O connectors [30, 37]: (a) The concept of PreWEC, and (b) Different failure modes of O connectors.

Following the work done on unbonded PT walls during the PRESSSS program [24], Sritharan et al [30] suggested a more effective system as Precast Wall with End Columns (PreWEC). In the proposed system, instead of using coupled walls with expensive U shape connectors, the wall will be coupled with end columns using welded mild steel oval shape connections named O connectors (Fig. 1.15(a)). Even though the system works efficiently in design earthquake levels, different

unexpected failure modes of O connectors were observed during experimental investigations [37]. These observations are shown in Fig. 1.15(b). The observed failure modes as shown in Fig. 1.15(b) consist of the fracture of the O connector in the Heat Affected Zone (HAZ) close to welds to where the connector is welded to the wall plates. Also, fracture failure is observed due to low-cycle fatigue where the bending stresses in the connector are maximum. Out-of-plane local buckling as the result of load-eccentricity and micro cracks due to high-rate loading are some other observed failures.

Several buildings with rocking walls and additional hysteretic dampers have been constructed since the development of these systems. As reported by Kam et al [4], Southern Cross Hospital in Christchurch resisted the 2011 earthquake using post-tensioned hybrid walls with minor damage (Fig. 1.16). However, U shape flexural dissipaters experienced inelastic deformations and more assessment was needed to be undertaken to see if a replacement was required.



Figure 1. 16. Southern Cross Hospital after 2011 Christchurch Earthquake, unbonded PT walls with U shape flexural connectors [4].

To sum up, the acceptable seismic performance of unbonded post-tensioned rocking walls is verified through past analytical and experimental studies as well as real earthquakes. However, higher construction cost compared to traditional cast in place walls, the need for unbonded post-tensioning tendons with complex behaviour and practical problems, and challenges related to yielding dissipaters can be named as disadvantages of such systems. After severe earthquakes, these systems should be inspected to observe possible damage in PT tendons or energy dissipaters.

The structure could become vulnerable to aftershocks if any damage has occurred during the mainshocks.

1.3 Seismic Energy Dissipation Devices

Ground shaking during an earthquake leads to kinematic energy being transferred to the structures located in the earthquake-affected areas. From the seismic engineering point of view, the structure should be able to dissipate this input energy reliably to ensure that the design objective is achieved. Different solutions from ductile fuses to base isolations have been introduced and developed to deal with the earthquake input energy. Energy dissipation devices are one of the solutions that have been around for quite a while. These devices have been used as either structural members, such as Buckling Restrained Braces (BRBs) [38], or connections, such as friction dampers [39, 40]. Energy dissipation devices can be classified into three different categories. 1- deformation sensitive dampers 2- velocity-sensitive (rate dependent) dampers and 3- a combination of both deformation and velocity-sensitive dampers or hybrid dampers.

For damping devices with reliable performance for seismic applications, the self-centring ability is a bonus. Self-centring capability can be looked at in two different ways. First, damping devices can re-centre the structure by pushing it back to the original position such as ring springs [41]. Second, damping devices that allow the structure to re-centre itself by inherent elastic action after the earthquake loading is finished [42]. It should be noted that preserving elastic base fixity up to the maximum design displacement is a requirement of this self-centring concept. A brief description of these self-centring dampers is given as follows.

Viscous Dampers

In viscous dampers, the input energy is dissipated through the forced movement of the viscous liquid through an orifice [43, 44]. The forced movement of the viscous liquid converts the kinematic energy to heat. The amount of the energy being dissipated, and the magnitude of the

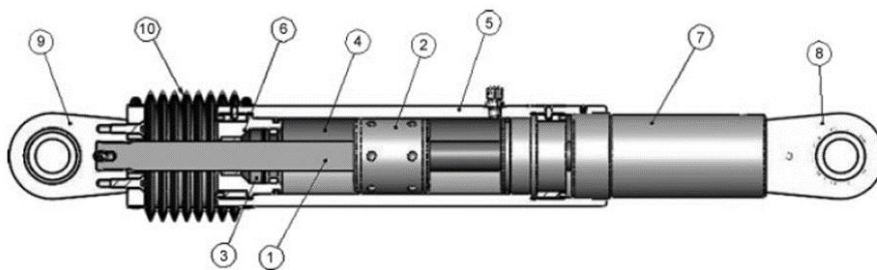
resisted force is a function of relative velocity as the behaviour is dominated by laws of fluid mechanics.

Different parts of a viscous damper are shown in Fig. 1.17 [45]. When the piston moves, the liquid flows through the orifices in the piston resulting in a damping force being generated.

In viscous dampers, energy dissipation is repetitive and predictable. Damage to the damper and its parts is also unlikely considering the fact that there is not a yielding element within the damper. Also, when combined with the elastic action of the structure, the system is fully self-centred after the earthquake loading and the structure can be reoccupied quickly. It should be noted that viscous dampers are not inherently self-centring. Since there is no residual force within the damper when the earthquake load is gone the elastic action of the structure will bring it back to the initial upright position.

However, viscous dampers are rather expensive, and they get quite large in dimensions when high capacity dampers are required. This is a limiting aspect of viscous dampers from an architectural point of view. In addition, as viscous dampers are velocity dependent, analysis and design of viscous dampers are rather complex making it difficult for the wider engineering community to deal with the design of structures equipped with these dampers.

Different variations of this damper have been developed by researchers to achieve different dampening performances[42, 46].



1. Piston rod, 2. Piston, 3. Seals/seal bearings, 4. Fluid, 5. Cylinder, 6. End cap,
7. Extender, 8. End clevis, 9. Spherical bearing, 10. Bellows

Figure 1. 17. Different parts of a viscous damper

HF2V Dampers

High Force to Volume HF2V Dampers [16, 47] were developed based on Lead Extrusion energy dissipaters [48]. HF2V dampers provide stable load-displacement cycles. The HF2V device consists of a steel cylindrical container filled with lead and a moving bulged shaft Fig 1.18. HF2V dampers are smaller than their ancestors, lead extrusion dampers, making them a suitable choice for structural applications. These dampers are also cost-efficient and easy to manufacture [47]. HF2V dampers have been experimentally proved to be a suitable replacement for yielding dissipaters [16, 49-51]. A big portion of the residual force in HF2V dampers will be released due to relaxation within a couple of hours after loading. Force relaxation results in almost no residual deformation after earthquakes.

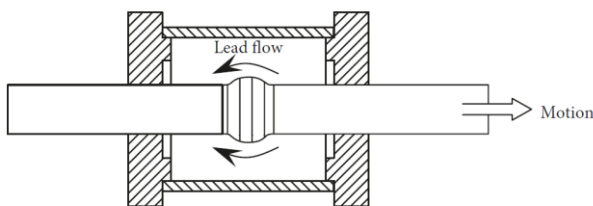


FIGURE 1: HF2V device schematic.



Figure 1. 18. High Force to Volume (HF2V) dampers [16, 47]

Elastomeric Spring Damper

Elastomeric Spring Dampers (ESD) contain a silicon-based elastomer. This material can be compressed to the desired force and also gives a viscous attribute. Therefore, elastic response and hysteretic energy dissipation are both provided by this material. Fig. 1.19 mentions a double-acting ESD [52]. When the piston moves into the cylinder, the elastomer is pushed further resisting the force by its spring action. Also, the elastomer tends to escape from the space around the piston

head. This generates rate-dependent damping resistance. ESDs have been tested successfully in several structural configurations and used in some real-world applications [12, 21, 52].

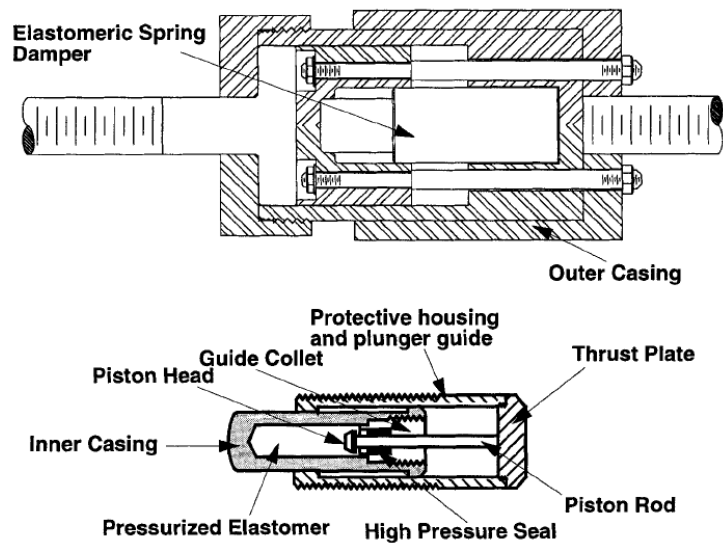


Figure 1. 19 Elastomeric Spring Damper (ESD) [52]

Ring-Spring Damper

Ring-spring dampers are self-centring friction dampers developed and used for industrial applications [53, 54]. Reliable yet low-maintenance hysteretic energy dissipation and self-centring are the main characteristics of ring-springs making them a good choice for shock absorber in industrial applications. Parts and components of a ring-spring are mentioned in Fig. 1.20 [41, 55]. An axial pre-stressing force will result in a normal force acting on the grooves of inner and outer rings. This normal force results in friction between the inner and outer rings while contracting and expanding respectively due to the axial deformation of the damper assembly.

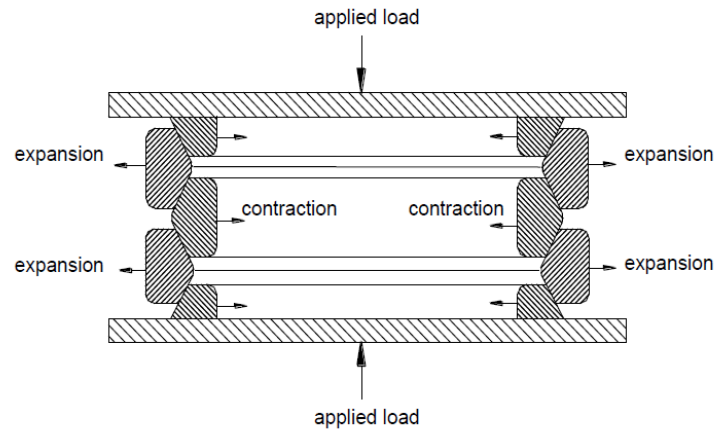


Figure 1. 20. Friction ring spring, parts and performance [41, 55]

During unloading, the elastic action of the rings restores the dampers deformation to its primary position providing robust self-centring ability.

Ring springs are suitable candidates for seismic Damage Avoidance Design (DAD) because of integrating both self-centring and energy dissipation. They have been tested experimentally and investigated analytically to be used in different structural applications [56, 57].

Ring spring dampers can be designed to achieve different force and displacement capacities. Therefore, researchers have been interested in developing more structural applications for Ring-springs [58].

Resilient Slip-Friction Joint (RSFJ)

Resilient Slip-Friction Joint (RSFJ) [59] is a self-centring friction damper for seismic protection of structural systems (Fig. 1.21). The conceptual framework of the RSFJ is similar to ring springs. However, some improvements have been made. In the RSFJ, the concept of friction between inclined grooves and using spring action for re-centring is the same as ring springs. However, grooved cap and middle plates are used instead of rings. This provides flexibility in design and manufacturing. Also, as contraction and expansion are not expected in the grooved plates, adoption of the plates' material will be less concerning. In addition, pre-stressing force is applied axially absorbing a portion of the displacement capacity of the damper. However, the pre-stressing is

applied perpendicular to the main axis of the RSFJ using Belleville springs giving the designer more flexibility in designing force and displacement capacities independent from each other. A detailed discussion about the RSFJ is presented in Chapter 2 of this thesis.

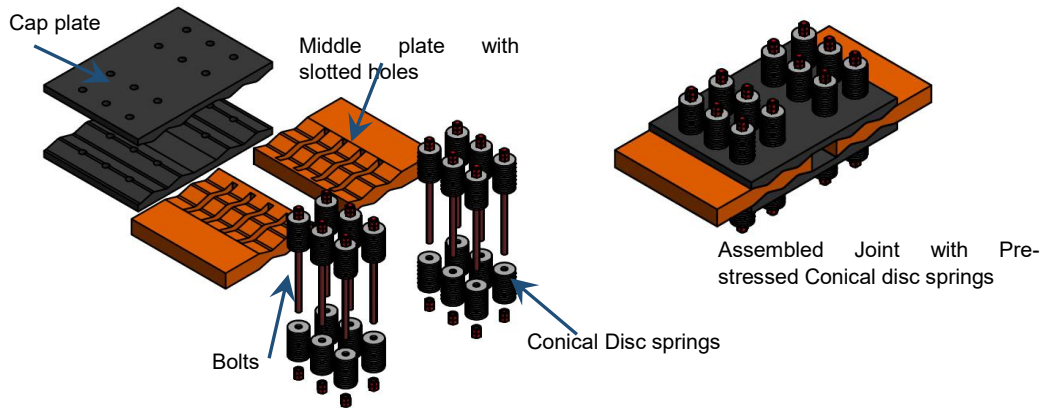


Figure 1. 21. Resilient Slip-Friction Joint (RSFJ)

1.4 This study

The use of self-centring dampers in rocking concrete shear walls has not been previously studied. In the dampers presented within this thesis, energy dissipation and self-centring are provided in one device. Such devices are capable of controlling the rocking motion in rocking walls. In this study, the application of self-centring dampers, friction dampers in particular, in rocking concrete shear walls is investigated. The main purpose of this research is to introduce a structural system in which the challenges related to unbonded post-tensioning is resolved while a robust yet cost-efficient energy dissipation system is used rather than yielding elements.

For example, there are always complexities involved in using Post-Tensioning (PT) cables on the construction site especially when the structural members are mounted vertically. The main purpose of this research is to develop a rocking concrete shear wall system in which on-site post-tensioning work is not required and post-tensioning is not used for connecting the wall to the foundation. Furthermore, as for the energy dissipation mechanism, the use of friction will be investigated as

an alternative for yielding mechanisms. Accordingly, the scope of this research is to develop a rocking concrete shear wall with self-centring friction dampers.

The Resilient Slip-Friction Joint (RSFJ) is selected for this study as the required characteristics of the desired damper can be found in the RSFJ. In the first section of this study, the performance of the RSFJ is investigated analytically and experimentally. The governing load-displacement equations are updated to correctly account for the effect of the friction coefficient. Also, a simplified analysis procedure is developed to minimise the required design and optimisation work for the RSFJ. Finally, the possibility of implementing a secondary fuse within the damper as an anti-locking mechanism is studied analytically and experimentally. This part of the research is presented in Chapter 2 of the thesis.

A new self-centring friction damper is also patented and developed (as one of the unique contributions of this research) which is named as Self-Centring Structural Connector (SSC). The SSC is a cost-efficient simple concept that provides the desired energy dissipation characteristics of a self-centring friction damper suitable to be implemented in Damage Avoidance Design (DAD). In Chapter 3, the development of this damper from concept to detailed design and experimental verification are presented. First, the concept is established and analytical equations are derived. Then, an experimental study is carried out to verify the performance of a prototype SSC. Finally, the effect of different design parameters on the performance of the damper is investigated and different applications of the damper are introduced.

In Chapter 4, the seismic performance and design of multi-story rocking wall structures equipped with RSFJs and SSCs as hold-downs are studied. A displacement-based design approach is discussed, and a prototype building is designed based on the proposed procedure. A set of Non-Linear Time History (NLTH) analysis is performed on the prototype building to assess the seismic response of the building and to verify the design procedure used.

In Chapter 5, a comprehensive study is designed and conducted to develop a robust concrete rocking wall system using self-centring friction dampers. The concept, design and performance of the system are analytically discussed and then verified through a large-scale experimental test. Numerical analysis procedures are introduced as a tool for the fast assessment and design of the developed system. The numerical procedure is also verified against the experimental results. The outcome of the research and suggestions for future research are summarised in Chapter 6.

Chapter 2: Resilient Slip Friction Joint Performance: Component Analysis, Spring Model and Anti-Locking Mechanism

2.1 Introduction

In recent years, there has been more interest in the utilisation of slip friction connectors among researchers, due to their energy dissipation without any yielding of the components. Resilient Slip Friction Joint (RSFJ) is a damage avoidance friction damper in which energy dissipation and self-centring features are provided in one device. This is achieved by controlled friction sliding of especially grooved steel plates which are designed to take the induced tension, bending and shear stresses. In order to perform in accordance with damage avoidance philosophy, the RSFJ plates should remain elastic. Hence, in this paper, the performance of RSFJ components is initially investigated through numerical, analytical and experimental studies. New simplified equivalent spring models are developed in this research for analysis and design of the plates. Also, to prevent the sudden stiffness increase of the joint after locking at its maximum deflection, a new mechanism is introduced and named Anti-Locking Mechanism (ALM). The new ALM is presented and studied experimentally in this research. The ALM is in fact a secondary fuse for the RSFJ in which the clamping bolts elongate providing more ductility for the joint and solving the locking issue of the damper while the re-centring feature is still preserved without any compromise. Therefore, the RSFJ equipped with ALM could prevent the formation of seismic shocks to the structure during unpredictable seismic events beyond the design level.

2.2 Background

New or existing buildings are expected to respond satisfactorily to small and medium earthquakes and even survive severe seismic events without any collapse hazard. On this basis, buildings tolerate severe earthquakes by dissipating the seismic energy through the introduction of inelastic ductile behaviour of the structural elements in carefully detailed locations (such as braces in CBFs,

or beam plastic hinges in steel or RC-MRFs [60]). Although the safety of residents is ensured, some level of residual deformation might accumulate in buildings which may eventually lead to their demolition. Previous studies imply that for an earthquake-hit building with residual drift greater than 0.5%, the repairing costs are usually greater than reconstruction; while FEMA-P58 [61] recommends complete demolition of buildings with residual drift bigger than 1.0%. While high amounts of residual drifts could negatively influence the residents' feelings about the safety of the buildings, it can also affect the frames vulnerability against upcoming aftershocks and increase the collapse risk of the buildings [62]. Damage Avoidance Design (DAD) concept [9] is a solution to above-mentioned problems. In this design philosophy, damage protected energy dissipation is combined with self-centring capability[10]. Systems designed based on damage-avoidance concept are capable of being immediately occupied after Design Based Earthquakes (DBE)[21]. Different systems have been developed and tested based on DAD philosophy [14]. Elastomeric Spring Dampers [22], yielding dampers [63-65] and lead extrusion HF2V dampers have been used in the experiments conducted to verify DAD philosophy. the experiments proved that the DAD concept minimises the expected damage so that one can be 90% sure that the structure sustains no damage after DBE earthquakes[51]. Therefore, earthquake resilient structures with damage avoidance self-centring components have become one of the focal topics among scholars and structural engineering communities.

A self-centring (SC) system has two main features: 1) energy dissipation and 2) restoring. The first feature is similar to the conventional dampers which can be provided by either metal yielding[66-68], friction sliding [69-71] or viscous resistance [12, 42, 72]; while the self-centring feature or restoring force is mainly provided by Shape Memory Alloy (SMA) materials [67, 73, 74], pre-stressed cable strands [75] or disc springs and ring springs [41, 76-78]. Elastomeric Spring Dampers can also be named as self-centring energy dissipaters[12, 21, 52]. Based on the energy dissipation and self-centring mechanism being utilised in SC-systems, different types of self-

centring dampers have been proposed and investigated in the literature. Resilient Slip Friction Joint (RSFJ) [59, 70] is one of the systems that could provide self-centring feature as well as energy dissipation in one device. The joint consists of specially grooved outer cap plates and slotted middle plates, which have been clamped together using pre-stressed conical disc springs. The seismic energy is dissipated through relative sliding of the plates, while the damper self-centring is provided by pre-stressed disc springs. The joint can be implemented in different structural systems (rocking shear wall systems, moment-resisting frames, bracing systems, etc. [70, 79, 80]) as the main seismic resisting system or supplemental damping device. The overall performance of the RSFJ is similar to friction ring springs [41] as in both concepts pre-stressing and friction are combined together to provide self-centring and energy dissipation capability. The main difference is in how pre-stressing force is applied in each concept making the RSFJ a good choice for higher structural capacities.

While the experimental and numerical performances of the RSFJ seem to be quite promising, there are some points to consider when it comes to designing the damper components themselves. First and foremost, to fulfil the damage avoidance philosophy, it is expected for the RSFJ to maintain its functionality after strong earthquakes. This requires all the joint components including the cap and middle plates to be carefully designed to remain elastic during the sliding movement of the damper. Considering the unique shapes of the middle and cap plates for different design objectives, it is rather time-consuming and computationally demanding to perform finite element analyses for each plate design. Therefore, it is preferred to utilise simplified analytical spring models to investigate the elastic performance of the plates during friction sliding.

Another point related to the RSFJ design is associated with the "locking mechanism" of the RSFJ which is somehow similar to conventional friction dampers. On this basis, when the friction dampers reach their sliding displacement capacity, the pre-stressed bolts suddenly increase the force demand in the joint as they are acting as restraints [81]. This sudden stiffness rise could

increase the base shear in the structure and impose some inelastic deformation on the system as well. It should be noted that similar locking mechanisms in traditional friction devices have been witnessed and investigated by other researchers (see for example [82, 83]). To decrease the probability of locking, the joint can be designed for higher displacement capacity than the design requirement (for example 130% of the design displacement calculation, as recommended by FEMA-356 [84]). However, such an over-design approach is not financially favourable and yet the problem would remain albeit with a lower probability of occurrence. To overcome the locking issue of the RSFJ, an internal yielding mechanism is allocated to the damper called anti-locking mechanism (ALM), which can tackle the sudden demand increase issues of the damper in extreme events while preserving the self-centring features of the joint as well. ALM mechanism is the unique contribution of this research.

2.3 Resilient Slip Friction Joint (RSFJ)

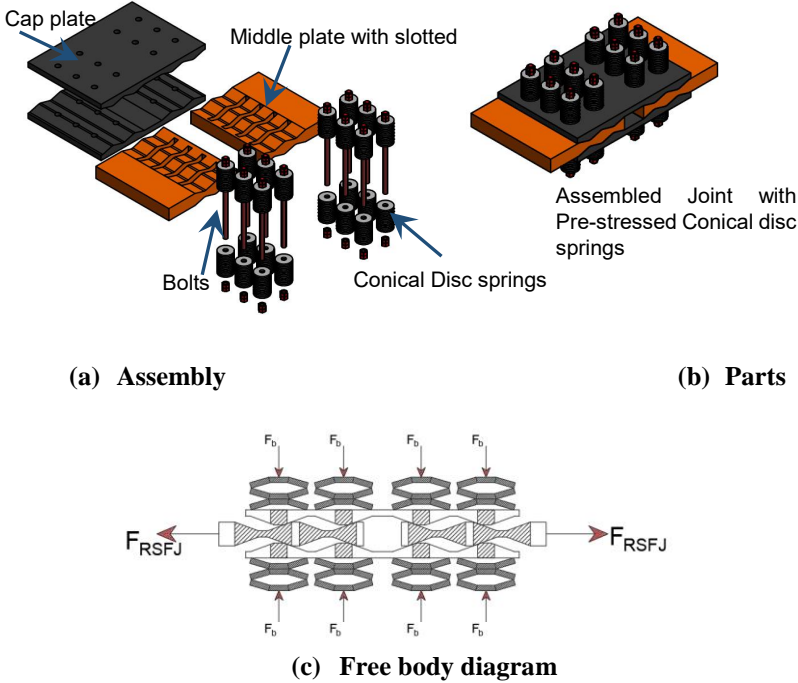


Figure 2. 1. Resilient Slip Friction Joint: a) Parts, b) Assembly, c) Free body diagram.

The typical Resilient Slip Friction Joint (RSFJ) is depicted in Fig. 2.1. The friction between the grease-lubricated grooved plates provides damage-avoidance energy dissipation and the elastic action of the pre-stressed disc springs provides the self-centring.

The force-displacement response of the joint in the loading and unloading phase can be obtained as follows [85]:

$$F_{RSFJ,loading} = 2n_b F_b \alpha \quad (2.1)$$

$$F_{RSFJ,unloading} = 2n_b F_b \beta \quad (2.2)$$

where,

$$F_b = F_{b,pr} + k_{spring} \delta_{spring} \quad (2.3)$$

$$\alpha = \frac{\sin \theta + \mu \cos \theta}{\cos \theta - \mu \sin \theta} \quad (2.4)$$

$$\beta = \frac{\sin \theta - \mu \cos \theta}{\cos \theta + \mu \sin \theta} \quad (2.5)$$

The term n_b is the number of the bolts, F_b represents the clamping force produced in each bolt and the related disc springs and $F_{b,pr}$ denotes the pre-stressing force in each bolt. The parameters k_{spring} and δ_{spring} are the stiffness and displacement of the stack of disc springs, while θ denotes the angle of grooves and μ is the coefficient of friction. Considering that RSFJ plates present some flexibility and the fact that pre-stressing pressure is not uniformly distributed on the grooves' surfaces, some slips and stops occur in microscopic scale between the plates at the initial movement phase and the end of each loading/unloading phase. On this basis, a certain distinction between static and kinetic friction forces could not be observed. This phenomenon is known as Paradox in Sudden Friction Drop [86]. Therefore, instead of utilising different static and kinetic coefficient of frictions, only one coefficient of friction (μ) is employed to represent the overall response of the RSFJ. Accordingly, the flag-shaped hysteresis of the RSFJ is shown in Fig. 2.2.

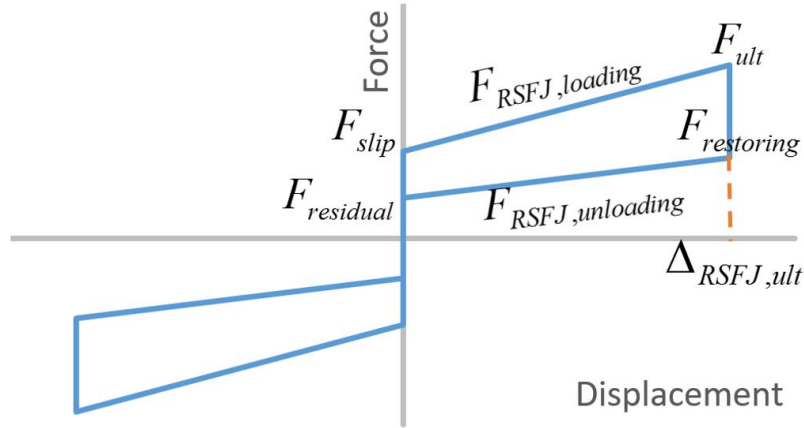


Figure 2. 2. Flag shaped load-displacement hysteresis of RSFJ.

As can be seen, four different phases in the RSFJ flag-shaped response can be defined. When the external load (F_{RSFJ}) overcomes the pre-stressing and friction forces between the grooves, the joint initiates slipping. After the slipping phase, as the load increases, the disc springs are being compacted until their ultimate displacement capacity, in which they are fully flattened. At this point, the ultimate load (F_{ult}) and its associated displacement ($\Delta_{RSFJ,ult}$) are reached. When the unloading phase initiates, the forces from the elastically deformed disc springs overcome the external load which is denoted as $F_{restoring}$ and then restoring phase starts. Finally, the re-centring movement will be stopped where the residual load in the system is decreased to $F_{residual}$. The displacement of the joint can be correlated to the displacement of the disc springs using the following equation.

$$\delta_{spring} = \frac{\Delta_{RSFJ}}{n_j} \tan \theta \quad (2.6)$$

In which, Δ_{RSFJ} is the joint displacement and n_j is the number of joints in a series arrangement.

For instance, a case of $n_j=2$ is shown in Fig. 2.1(b).

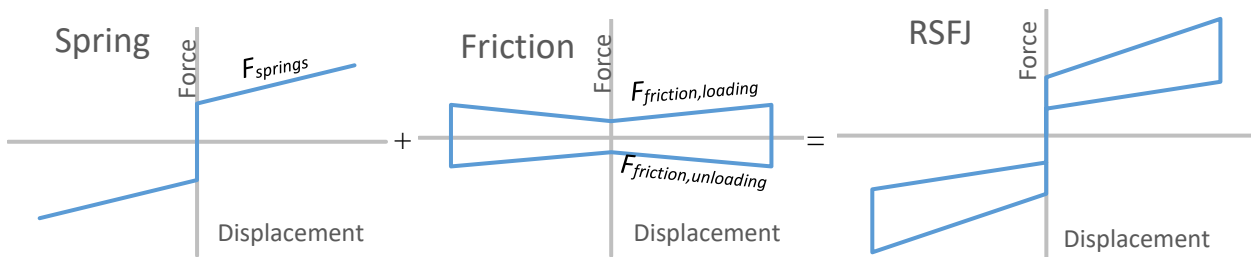


Figure 2. 3. Contribution of elastic springs and friction damping in RSFJ overall response.

2.4 Energy damping mechanism in the RSFJ

In RSFJ, energy damping is provided by friction while self-centring is provided by pre-stressed disc springs and the overall response is the combination of these two actions (Fig. 2.3). However, there is an interaction between the friction and springs forces due to the simultaneous relative vertical and horizontal movement produced by inclined grooves. The contribution of springs and friction action can be calculated based on RSFJ load-displacement equations (Eqs. (2.1) and (2.2)). This can be accomplished by considering $\mu=0$ and calculating the contribution of the springs (F_{spring}) without friction:

$$F_{RSFJ} = F_{spring} = 2n_b F_b \tan \theta \quad (2.7)$$

When the springs portion is known as per Eq. (2.7), the friction portion can be derived by substituting the spring portion into the following equations.

$$F_{RSFJ,loading} = F_{spring} + F_{friction,loading} = 2n_b F_b (f_{spring} + f_{friction,loading}) \quad (2.8)$$

$$F_{RSFJ,unloading} = F_{spring} - F_{friction,unloading} = 2n_b F_b (f_{spring} - f_{friction,unloading}) \quad (2.9)$$

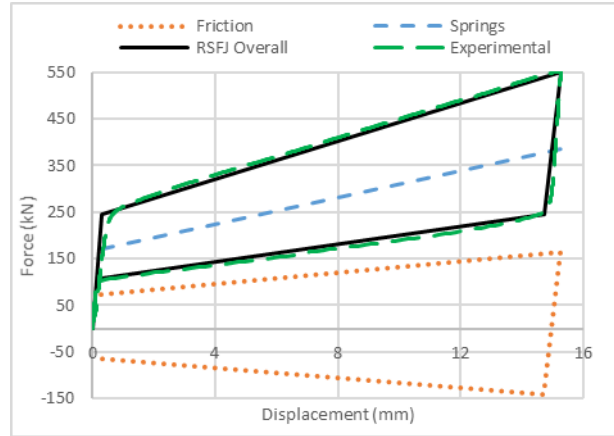
In which, f_{spring} is the equivalent coefficient for spring portion, $f_{friction}$ is the force carried by friction and $f_{friction}$ is its equivalent coefficient. As $f_{spring} = \tan \theta$, the friction portion for loading and unloading stages can be calculated using the following equations.

$$f_{friction,loading} = \alpha - f_{spring} = \frac{\mu}{\cos^2 \theta - \mu \sin \theta \cos \theta} \quad (2.10)$$

$$f_{friction,unloading} = f_{spring} - \beta = \frac{\mu}{\cos^2 \theta + \mu \sin \theta \cos \theta} \quad (2.11)$$



(a) Test setup



(b) Load-displacement responses

Figure 2. 4. Experimental testing of a sample RSFJ: a) Test setup, b) Load-displacement responses
Note: the set-up and joint was previously designed by others[87], the test and instrumentation was done by the authors of this research

2.5 Experimental validation

The load-displacement response of an RSFJ which was observed through testing is compared to the analytical model. In addition, the contributions of friction and springs are calculated using the proposed equations. The properties and parameters of the tested RSFJ are summarised in Table 2.1. The test setup that was previously designed is shown in Fig. 2.4(a). The experimental load-displacement response is compared to the analytical predictions in Fig. 2.4(b). As it can be seen from the graphs, the response is well predicted using the analytical model. The contribution of friction and springs is also mentioned on the graph. At the ultimate load of 550 kN, 30% of the load was carried by friction (165 kN out of 550 kN) and the remaining 70% was carried by springs.

2.6 Load distribution between RSFJ grooves

To design the plates of the RSFJ, the performance of the plate should be precisely investigated. While the finite element models show an accurate representation of the RSFJ plates, they require a large amount of computational effort and obviously, the FE analysis should be conducted for each design. Accordingly, a simplified analytical spring model with enough accuracy can save both time and computational effort as a more efficient design method. RSFJ in most of its

applications is being used as an axially loaded element. It is also composed of triangular grooves and flat plates. This type of simplicity in loading and geometry has made an opportunity to develop a simplified analytical model for load distribution between RSFJ parts. As such, a stiffness-based model is developed for predicting the load distribution between RSFJ parts. The RSFJ is divided into several parts and each part is modelled by an appropriate shear, flexure or axial spring. The results are then verified via experimental and numerical modelling.

Table 2. 1. the properties of the tested RSFJ.

Parameter	Value
θ	25°
μ	0.15
n_j	2
Number of Bolts per joint (n_b)	6
Number of discs in one stack	7
Discs internal height	1.55 mm
Discs ultimate capacity	110 kN
Bolts Pre-stressing force ($F_{b,pr}$)	30 kN

As shown in Fig. 2.5(a), axial loading of the joint, F , and disc spring forces, F_b , which are considered as external loads, produce internal normal and friction stresses on the grooves' surfaces. These stresses can be converted to resultant horizontal, F_h , and vertical, F_v , forces (Fig. 2.5(b)). The distribution of the external forces inside the joint depends on the relative stiffness of the segments. To define such stiffness, shear and flexural deformation (Fig. 2.5(c)) are considered for grooves only while axial deformation for flat plates including the grooves (Fig. 2.5(d)). The appropriate stiffness of these segments can be calculated using mechanics of materials theories. It should be noted that the acting points for the resultant forces on the grooves' surfaces (e.g. F_v and F_h) should be calculated based on the relative sliding of the middle and cap plate grooves at desired

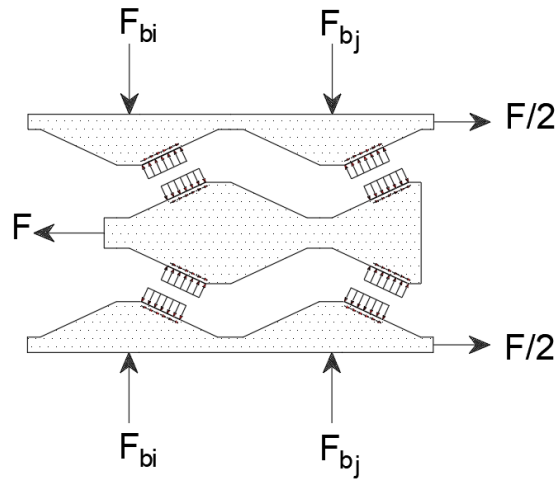
design displacement. For design purposes, joint ultimate displacement can be selected for defining the free body diagram. In the first attempt for calculating the forces and acting points, parts can be assumed to be rigid and the joint axial force is distributed uniformly between the grooves. This assumption will be then modified for the next iteration until achieving the desired convergence. It is worth noting that such a process can be implemented in spreadsheet software as well.

The unit load method is used for calculating the shear and flexural stiffness of the triangular grooves. As can be noted in Fig. 2.6, each groove is assumed to be a cantilever column. Only the effect of the horizontal load, F_h , is considered for calculating the deformations while the effect of vertical load, F_v , is neglected as the vertical axial deformations can be ignored for horizontal load distribution. Bending deformation due to F_v is also negligible as the effect of this force is counterbalanced by the vertical force coming from the other touching groove. Considering the shear and bending diagrams of the grooves (Fig. 2.6), the derived deformation integrations are given by Eqs. (2.12) and (2.13).

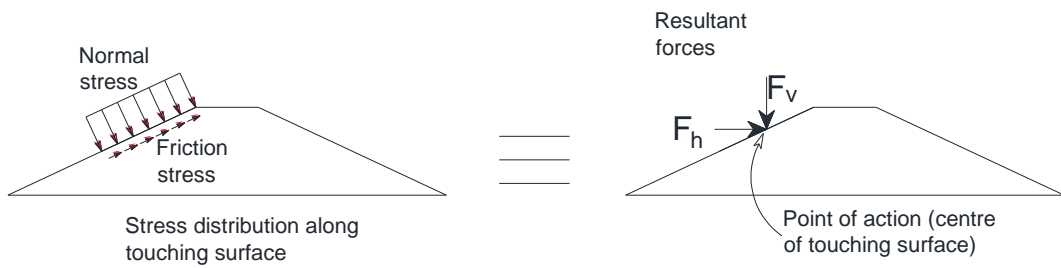
$$\Delta_b = \int_0^h \frac{\bar{m}M}{EI(y)} dy \quad (2.12)$$

$$\Delta_v = \frac{6}{5} \int_0^h \frac{\bar{v}V}{A(y)G} dy \quad (2.13)$$

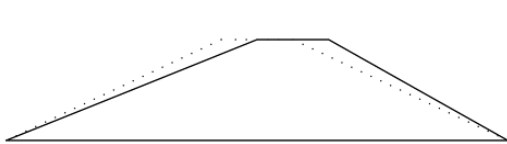
where Δ_b is the bending deformation of the grooves while Δ_v denotes the shear deformation of the groove. The parameters \bar{m} and \bar{v} are internal moment and shear due to virtual unit load acting on the same point and direction as F_h , while M and V are internal moment and shear due to F_h , E and G are moduli of elasticity and rigidity, respectively. $I(y)$ and $A(y)$ are section moment of inertia and section area, respectively which are variable along with the height of the grooves.



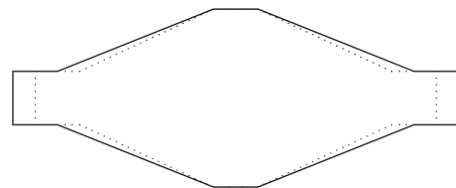
a) RSFJ free body diagram



b) Stresses acting on each groove and their equivalent horizontal and vertical forces



c) Shear and flexural deformation of the grooves



(d) Axial deformation of plates and grooves

Figure 2. 5. Free body diagram of the RSFJ and deformed shapes of the grooves.

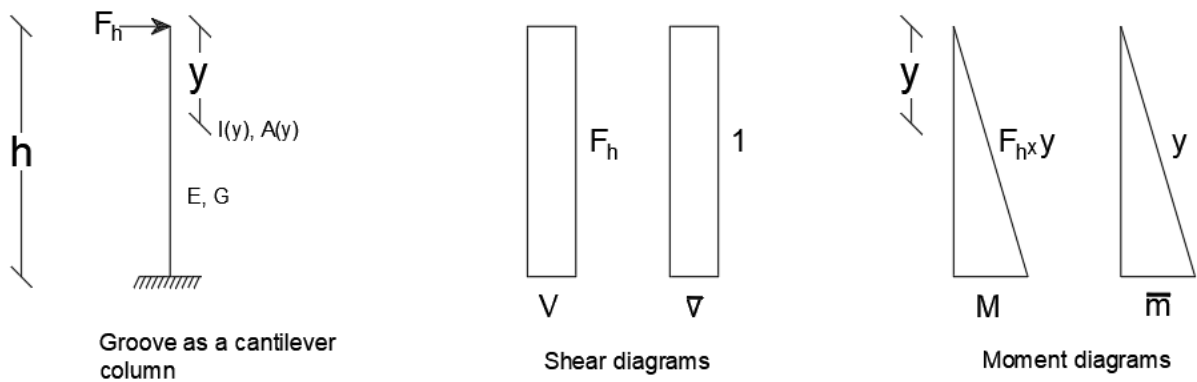


Figure 2. 6. Shear and moment diagrams of the grooves.

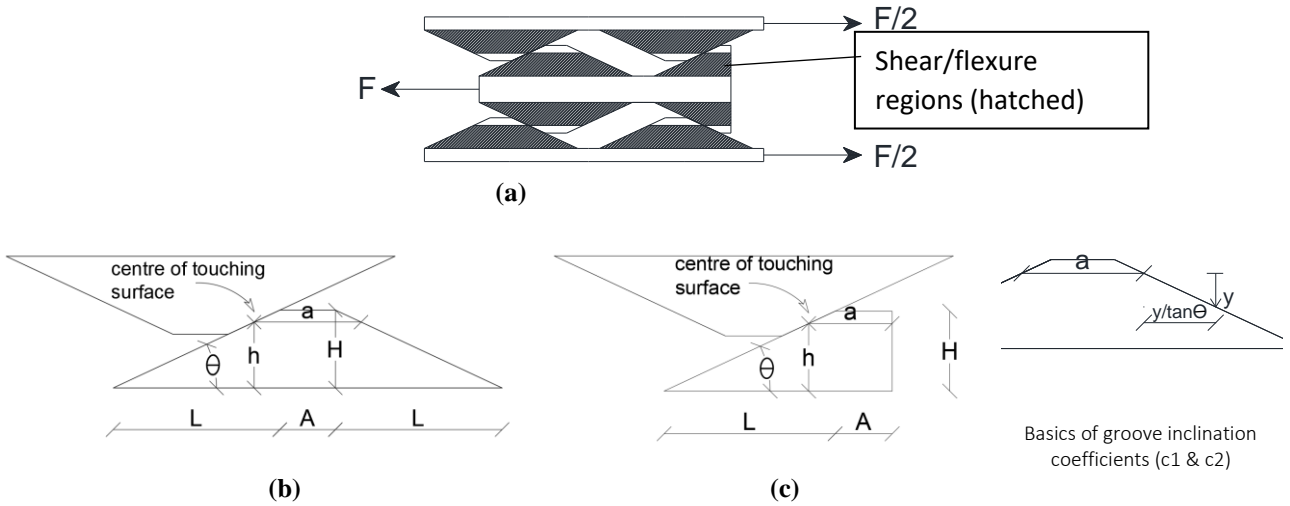


Figure 2. 7. Equivalent grooves and their parameters: (a) Equivalent shear/flexure deformation segments (hatched), (b) Symmetric groove parameters, (c) Asymmetric groove parameters.

The hatched areas (shown in Fig. 2.7(a)) are considered effective segments under shear and flexure deformation. The parameters for symmetric and asymmetric groove cases are shown in Figs. 2.7(b) and 2.7(c), respectively. By substituting the parametric values of the internal actions and groove dimensions into Eq. (2.12) and Eq. (2.13), the parametric deformation integrations can be derived and solved as follows.

$$\Delta_b = \frac{12F_h}{b_e E} \int_0^h \frac{y^2}{(a + c_1 y)^3} dy$$

$$\Delta_b = \frac{12F_h}{b_e E c_1^3} \left(\ln(c_1 h + a) + \frac{2a}{c_1 h + a} - \frac{a^2}{2(c_1 h + a)^2} - \ln a - \frac{3}{2} \right) \quad (2.14)$$

$$\Delta_v = \frac{6}{5} \frac{F_h}{b_e G} \int_0^h \frac{dy}{a + c_1 y}$$

$$\Delta_v = \frac{6}{5} \frac{F_h}{b_e G c_1} (\ln(c_1 h + a) - \ln a) \quad (2.15)$$

where b_e is the effective width of the plates which is equal to the gross width of the section for the cap plates and net width of the middle plates (gross width reduced by the total thickness of the slotted holes). The parameter c_1 denotes the groove inclination coefficient which is equal to $2/\tan \theta$ for symmetric groove case and $1/\tan \theta$ asymmetric groove case. h and a are the effective

height and width of the groove measured from the centre of the touching surface which can be calculated using the following equations.

$$h = \frac{1}{2} (\Delta_{RSFJ} \frac{\tan \theta}{n_j} + H) \quad (2.16)$$

For symmetric groove:
$$a = A + \frac{H - (\Delta_{RSFJ}/n_j) \tan \theta}{\tan \theta} \quad (2.17)$$

For asymmetric groove:
$$a = A + \frac{H - (\Delta_{RSFJ}/n_j) \tan \theta}{2 \tan \theta} \quad (2.18)$$

The term Δ_{RSFJ} is the joint displacement in which the load distribution is desired.

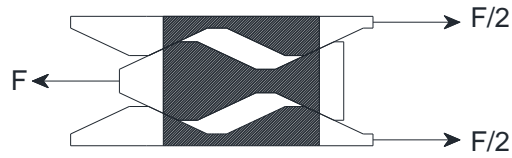
To calculate the deflection of the RSFJ, the axial deformation of the plates should also be considered in the load distribution model of the joint. The length between the centres of touching surfaces of two consecutive grooves (Fig. 2.8(a)) is considered as the effective length for calculating axial deformations. To simplify, this axial deformation segment is divided into three different segments as shown in Fig. 2.8(b). It is obvious from Figs 2.8(b) and 2.8(c) that the axial deformation of the left segment is equal to the right one. This arrangement has been made to make the analysis easier. Therefore, the right segment is selected for calculating the equivalent stiffness. The required geometric parameters are defined in Fig. 2.8(c). The deformation for each segment can be calculated using the following equations.

$$\Delta_1 = \frac{2F}{Eb_e} \int_0^L \frac{dx}{t_{thin} + c_2 x} \quad (2.19)$$

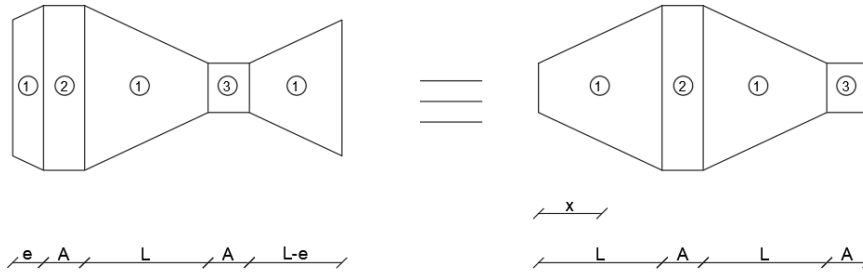
$$\Delta_1 = \frac{2F}{Eb_e c_2} (\ln(t_{thin} + c_2 L) - \ln t_{thin}) \quad (2.20)$$

$$\Delta_2 = \frac{FA}{Eb_e t_{thick}} \quad (2.21)$$

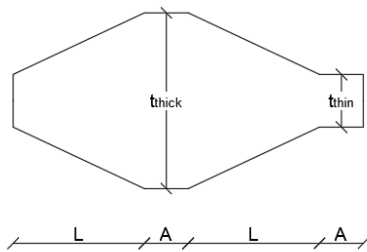
$$\Delta_3 = \frac{FA}{Eb_e t_{thin}} \quad (2.22)$$



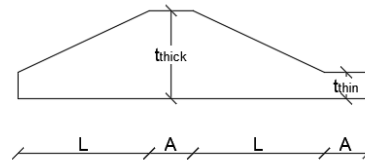
(a) Axial deformation segments



(b) Different parts for calculating axial deformations

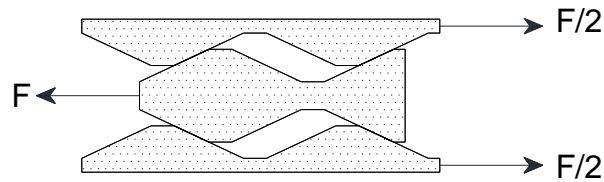


(c) Middle plate axial-segment parameters

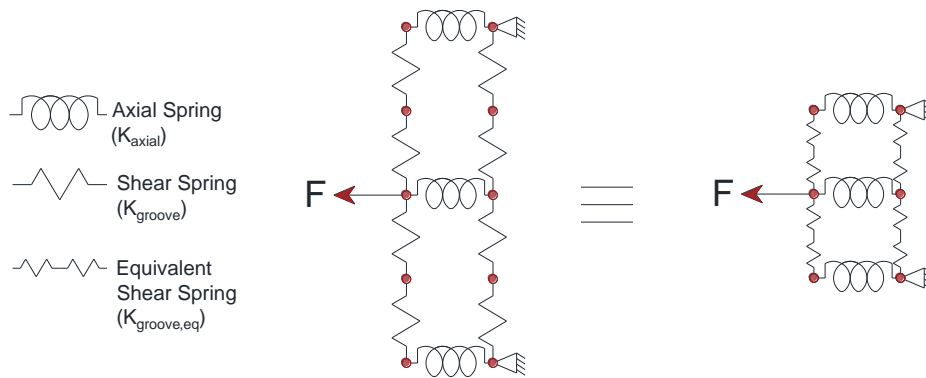


(d) Cap plate axial-segment parameters

Figure 2. 8. Equivalent axial deformation segments and their parameters.



(a)



(b)

Figure 2. 9. RSFJ and its equivalent spring model: (a)The modelled RSFJ, (b) RSFJ structural spring model.

In which, F is the internal axial load in the segment and c_2 is the groove inclination coefficient for axial deformations which is equal to $2 \tan \theta$ for middle plate and $\tan \theta$ cap plate. For the next step, the structural model of the RSFJ was created using the equivalent springs (Figs 2.9(a) and 2.9(b)). This model consists of axial and shear springs. The properties of these springs are calculated based on the deformation equations derived using the following equations.

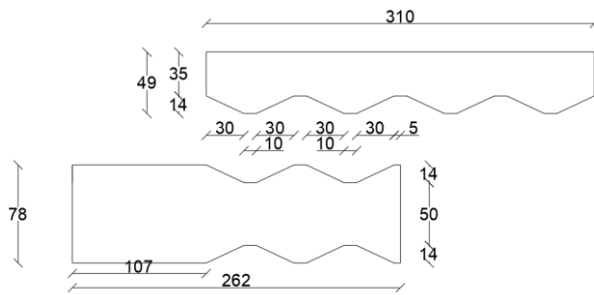
$$k_{groove} = \frac{F_h}{\Delta_b + \Delta_v} \quad (2.23)$$

$$k_{groove,eq} = \frac{k_{groove,cap} k_{groove,middle}}{k_{groove,cap} + k_{groove,middle}} \quad (2.24)$$

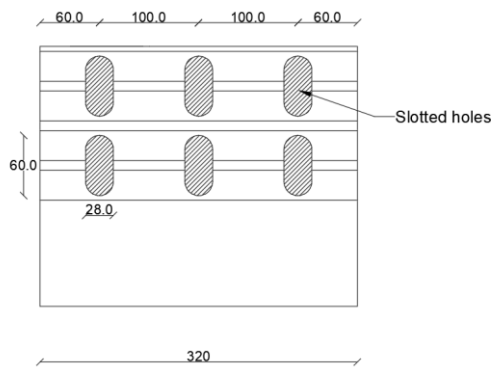
$$k_{axial} = \frac{F}{\Delta_1 + \Delta_2 + \Delta_3} \quad (2.25)$$

where k_{groove} is the stiffness of the grooves, $k_{groove,eq}$ is the equivalent stiffness of each two touching grooves as they are working in series and k_{axial} is the equivalent stiffness of the axial segments. While the stiffness model can be advantageous in terms of providing an efficient analysing method for joint optimization, it could also predict the elastic deformation of the joint under each loading demand. The elastic deformation of the joint should be considered given it is important to limit the joint displacement before the slip which could be critical in some applications in order to satisfy the design serviceability limit states.

To verify the developed analytical spring model, an experimental study was carried out. The dimensions of the tested joint are depicted in Fig. 2.10(a). The test setup and instrumentation are shown in Figs 2.10(b) and 2.10(c). As it can be noted, the strain gauges are attached between the middle plate grooves to measure the relative axial strain of the flat part between the grooves. Since the geometry is symmetric, the middle plate centre line is in pure tension and the relative strains are in direct relation with the relative stresses (Fig. 2.10(d)). The ratio of the second gauge measurement to the first gauge measurement represents the portion of the load which is being carried by the second groove. This ratio can then be compared to the calculated ratio using the spring model.



(a) The dimensions of the test specimen



Middle Plate Top View

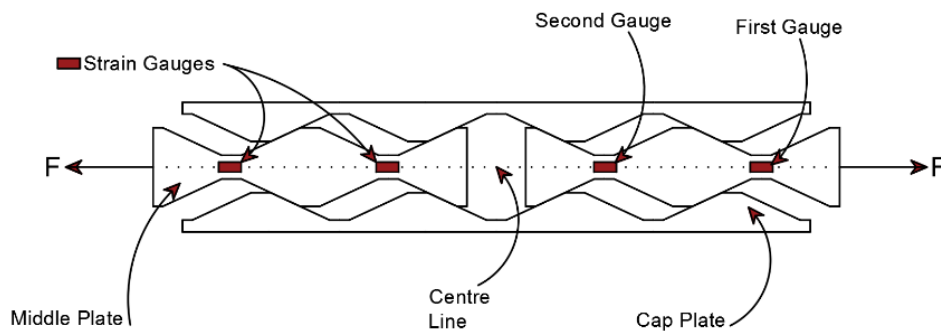
(b)



(c) Test setup



(d) Attached strain gauges



(e) Instrumentation sketch

Figure 2. 10. Test setup and instrumentation.

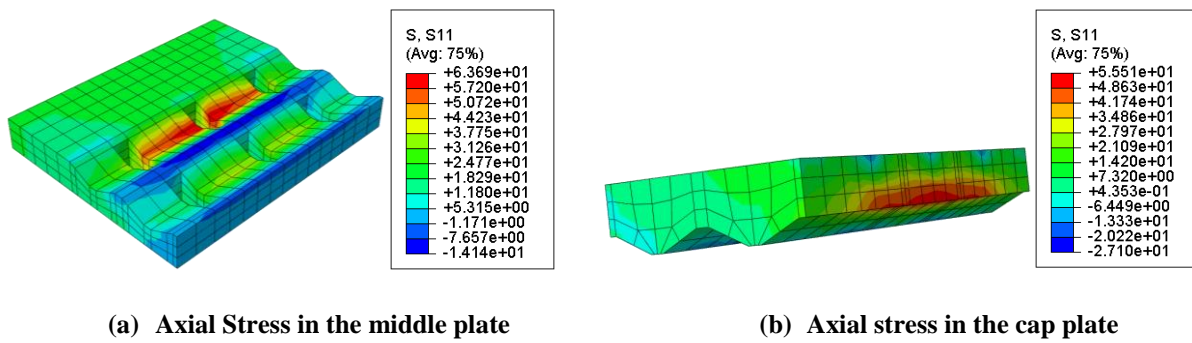


Figure 2. 11. ABAQUS numerical model.

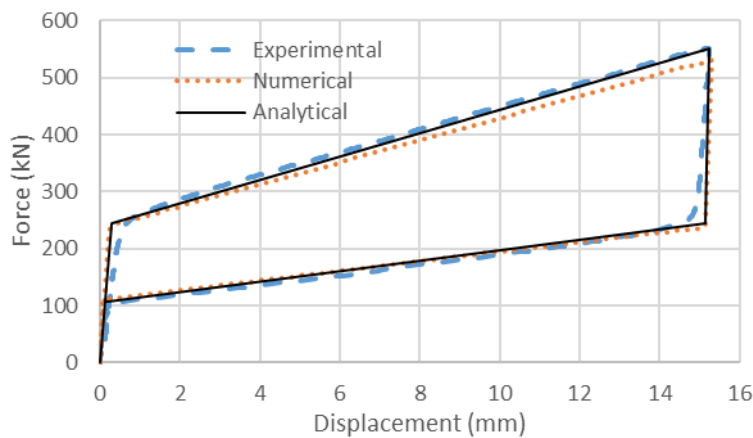


Figure 2. 12. Comparison of experimental results with the numerical and analytical predictions on the force-displacement response of the tested RSFJ.

A finite element model is also made and analysed by the ABAQUS software package version 6.14, in order to capture the strain distribution in the model and compare the results with the spring model and experimental data. The same dimensions as shown in Fig. 2.10 have been used for modelling the connection. Only half of one cap plate and half of one middle plate have been modelled. This means that only one fourth of the joint have been modelled considering the symmetry of the joint in across and along directions. Symmetric boundary conditions have been assigned to the bottom surface of the middle plate and external edge of the cap plate. Simple friction models with a coefficient of friction, μ , of 0.15 has been used for modelling the friction. A mesh sensitivity study was carried out until convergence occurred in the slip force F_{slip} .

The elastic properties of the high-strength steel material (Bisalloy 80) were used for modelling. Plastic properties such as yielding, and rupture have not been modelled as the scope is to verify the developed elastic mechanical model. Therefore, the nonlinearity of the material is not modelled. Also, considering the magnitude of forces and design of the tested RSFJ, nonlinear deformations it was unlikely that the model experience nonlinear deformations.

The axial stress (S11) for both the middle and cap plates are shown in Fig. 2.11. It can be deduced that the first groove resists the higher portion of the load due to non-uniform load distribution among the grooves. The comparison between experimental results, the FE model and the analytical spring model is shown in Fig. 2.12. As can be seen, the experimentally observed overall load-displacement response of joint is well predicted by the numerical model as well as agreeing with the analytical model predictions.

The stiffness parameters calculated using Eq. 2.23 to Eq. 2.25 for the tested joint are presented in table 2.2. Also, the distribution of the relative stiffness and relative forces in the physical model of the damper, as introduced in Fig. 2.9, are depicted in Fig. 2.13.

Table 2. 2 Stiffness parameters of the tested RSFJ.

Parameter	Middle plate	Cap plate
$A_{symmetric}$ (mm)		10
$A_{asymmetric}$ (mm)	5	---
H (mm)		14
D_{RSFJ}		15
n_j		2
b_e (mm)	257	320
t_{thin} (mm)	50	35
t_{thick} (mm)	78	49
L (mm)		30
K_{axial} (kN/mm)	40120	33130
$K_{groove,eq}$ (kN/mm)		*49930
$K_{groove,eq}$ (kN/mm)		#30580

Note: *two symmetric grooves are touching.

#one symmetric and one asymmetric groove are touching.

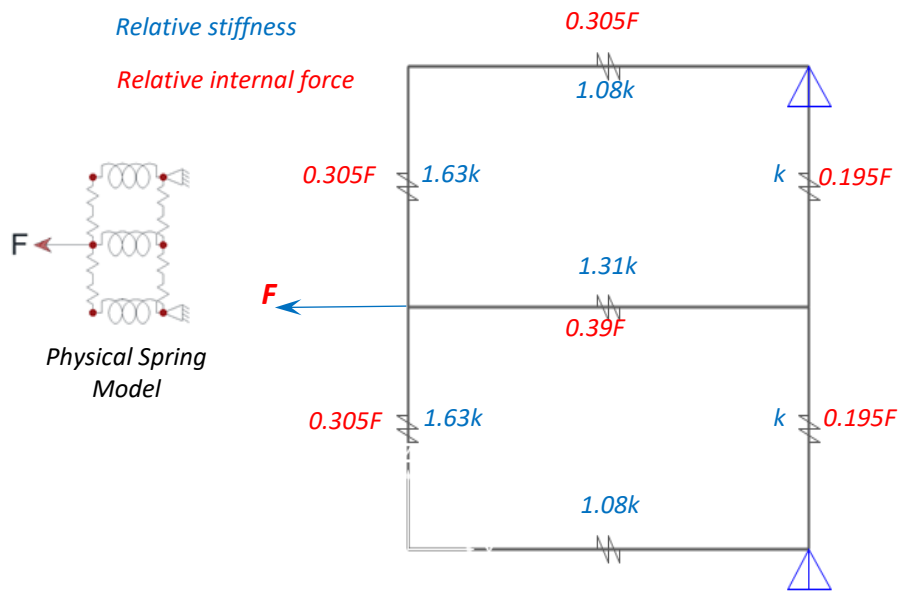


Figure 2.13. Distribution of internal forces in the spring model calculated based on the proposed analytical model.

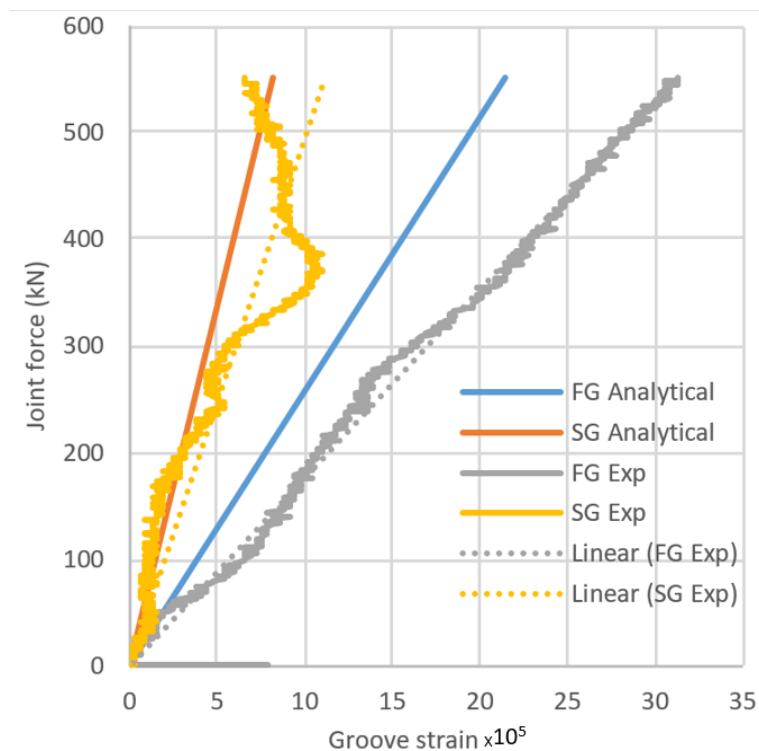


Figure 2.14. Comparison of test results with the analytical method (Note: FG and SG refer to the first and second gauges).

As shown in Fig. 2.14, the experimental results are compared with the analytical predictions. Considering that the dimensions of the joint in different directions are relatively close, the distribution of the stresses is complex. Accordingly, strain gauge readings are sensitive to the

position and direction. In addition, there is bending in the joint as the result of imperfections. The trendlines of the experimental results are used to be compared with the analytical results. In general, it seems that the model has predicted an average of 40% higher stiffness than the experiment which might be because of the difference between the actual material modulus of elasticity and the value used in analytical calculations. However, As mentioned in Table 2.3, the stiffness ratios (SG/FG) are 39% and 36% for the analytical and experimental results respectively. Therefore, the accuracy of the proposed model is verified by the experiments. The analytical, numerical and experimental strains for the joint ultimate load of 550 KN are summarised in Table 2.3. As can be observed from the table, the results validate the proposed spring model.

Table 2. 3. Strain predictions and measurements at the joint load of 550 kN.

Average strain at ultimate load	First gauge	Second gauge	Ratio (second/first)
Analytical	21.4×10^{-5}	8.35×10^{-5}	0.39
Numerical	21.4×10^{-5}	9.59×10^{-5}	0.45
Experimental	31.1×10^{-5}	11.12×10^{-5}	0.36

2.7 Anti-Locking Mechanism

When the joint reaches its maximum displacement capacity (i.e., when the conical discs are flat), with further displacement demand in the joint, the force rapidly increases which is denoted as the locking phase in the damper. Due to the uncertain nature of earthquakes, there is always a possibility that the seismic input loading would be higher than the joint design capacity. One obvious solution is to design for higher displacement capacities than design requirements. However, over-designing of the joint is not an economical solution and the problem of locking would remain, albeit with lesser probability. To tackle the issue, the authors propose an internal yielding mechanism inside the joint. In this concept, one of the joint components starts to yield at a certain load level to keep the produced actions in the joint supporting elements less than the design capacities. Here, the clamping bolts/rods, as mentioned in Fig. 2.1, are selected as the

elements to be yielded in tension (as a secondary fuse) when discs are flattened. The main advantage of considering rods or bolts as the yielding elements is that they can be easily replaced after the earthquake events that are stronger than the design expectations.

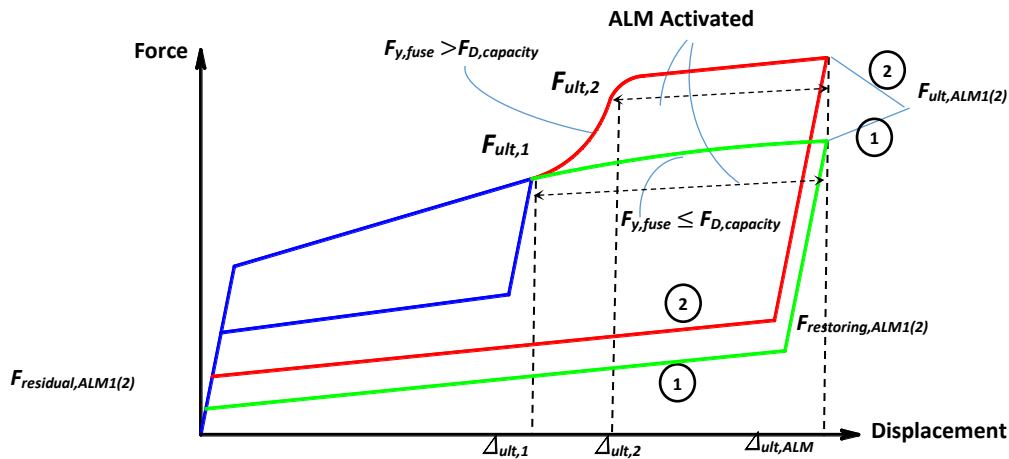


Figure 2. 15. Theoretical load-displacement response of RSFJs with ALM mechanism.

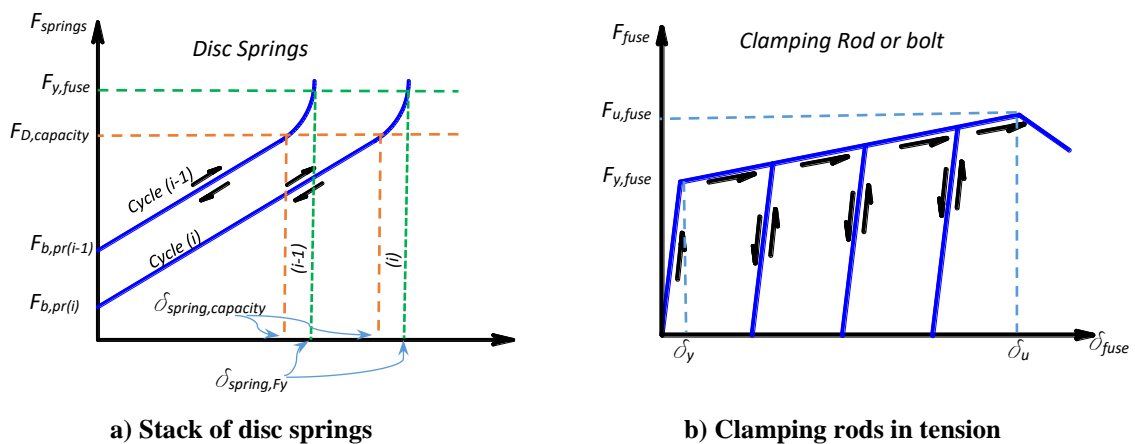


Figure 2. 16. RSFJ components cyclic behaviour.

As shown in Fig. 2.15, two different load-displacement responses for the joints with the yielding mechanism are expected based on the relative yielding strength of the rods to the disc springs capacity. In the case that rod yielding strength is less than or equal to disc capacity (the green line in Fig. 2.15), the rods start to yield before the discs start to flatten (F_{ult1}, Δ_{ult1}). It should be noted while the disc springs loading response is fully elastic, it has two different linear and nonlinear steps (Fig. 2.16(a)). The nonlinear step starts with a gradually increasing slope behaviour when the

discs are close to being completely flat. The capacity of the disc springs ($F_{D,Capacity}$) is defined as the force in which the increasing nonlinear part starts (Fig. 2.16(a)). In case the yielding strength of the rods is higher than the disc capacity, the joint is expected to follow an increasing response after $F_{ult,1}$ up to the force where rods start to yield in tension (F_{ult2}, Δ_{ult2}), as shown with the red line in Fig. 2.15. The ultimate load of the joint with the Anti-locking mechanism and its corresponding displacement ($F_{ult,ALM}, \Delta_{ult,ALM}$) for each case are shown in Fig. 2.15. On this basis, different parameters of the load-displacement graph can be calculated using the following equations. It should be noted that index 1 in the equations refers to the parameters related to the green-line and index 2 refers to the red-line parameters.

$$F_{ult1} = 2n_b\alpha \times \min\{F_{D,capacity}, F_{y,fuse}\} \quad \alpha = \frac{\sin \theta + \mu \cos \theta}{\cos \theta - \mu \sin \theta} \quad (2.26)$$

$$\Delta_{ult1} = \frac{n_j}{\tan(\theta)} \delta_{spring,capacity} \quad (2.27)$$

$$F_{ult2} = 2n_b\alpha F_{y,fuse} \quad (2.28)$$

$$\Delta_{ult2} = \frac{n_j}{\tan(\theta)} \delta_{spring,fy}^* \quad (2.29)$$

$$F_{ult,ALM1(2)} = \frac{k_{p,fuse} \delta_{p,fuse1(2)} + F_{y,fuse}}{F_{y,fuse}} \times F_{ult1(2)} \quad (2.30)$$

$$F_{restoring,ALM} = 2n_b\beta(k_{p,fuse} \delta_{p,fuse1(2)} + F_{y,fuse}) \quad \beta = \frac{\sin \theta - \mu \cos \theta}{\cos \theta + \mu \sin \theta} \quad (2.31)$$

$$F_{residual,ALM} = 2n_b\beta(F_{b,pr} - \frac{k_{spring} \delta_{p,fuse1(2)}}{2}) \quad (2.32)$$

In which, $F_{y,fuse}$ is the yielding strength of the rods as shown in Fig. 2.16(b), $\delta_{spring,capacity}$ is the displacement at the start point of the increasing nonlinear response of disc springs (Fig. 2.16(a) 2.16(b)) and $\delta_{spring,fy}^*$ is the modified displacement of the disc springs corresponding to the yielding force of the rods calculated using Eq. (2.33). k_{spring} is the initial stiffness of the discs stack. $k_{p,fuse}$ and $\delta_{p,fuse}$ are plastic stiffness and plastic deformation of the rods and can be calculated using Eq. (2.34) and Eq. (2.35).

$$\delta_{spring, fy}^* = \frac{2AE_{fuse}(\delta_{spring, fy} - \delta_{spring, capacity}) + (F_{y, fuse} - F_{D, capacity})L_{0, fuse}}{2AE_{fuse}} \quad (2.33)$$

$$+ \delta_{spring, capacity}$$

$$k_{p, fuse} = \frac{F_{u, fuse} - F_{y, fuse}}{\delta_u - \delta_y} \quad (2.34)$$

$$\delta_{p, fuse1(2)} = \frac{2(\Delta_{ult, secondary} - \Delta_{ult1(2)})}{n_j} \tan \theta \quad (2.35)$$

In which, AE_{fuse} is the axial stiffness of the unit length of the rods, $\delta_{spring, fy}$ is the disc springs deflection at rod yielding force and $L_{0, fuse}$ is the clear length of the rod between the nuts. It should be noted that the parameter $\delta_{spring, fy}^*$ used in Eq. (2.29) and Eq. (2.30) represents the effect of reduction in the equivalent stiffness due to the fact that the rod and the discs stack work together in series. However, this effect is just considerable for the region between Δ_{ult1} and Δ_{ult2} where the stiffness of the rods and discs are relatively close. $F_{u, fuse}$ is the ultimate strength of the rods while δ_u and δ_y are ultimate and yielding deformation of the rods, respectively. The maximum displacement of the joint ($\Delta_{ult, ALM}$) should be kept limited in order to prevent the rods from fracture. In addition, the stack of discs will become loose if the rod plastic deformation is more than the pre-stressing displacement of the disc springs stack. Therefore, the maximum allowable $\Delta_{ult, ALM}$ should be considered as the minimum value related to the above-mentioned requirements:

$$\Delta_{ult, ALM1(2)} < \min \left\{ \frac{n_j(\delta_u - \delta_y)}{2 \tan(\theta)} + \Delta_{ult1(2)}, \frac{n_j F_{b, pr}}{k_{spring} \tan(\theta)} + \Delta_{ult1(2)} \right\} \quad (2.36)$$

where k_{spring} is the initial stiffness of each discs stack. After each cycle where the anti-locking is initiated, the load-displacement response of the joint will be changed for the next cycles. This is due to the decrease in disc springs pre-stressing force resulted from residual plastic deformation in the rods and an increase in cyclic yield strength of the rods. The cyclic behaviour of disc springs with pre-stressing loss and the cyclic behaviour of the rods are shown in Fig. 2.16. The following equations are derived to measure each cycle's corresponding parameters. These hysteresis

parameters are then used for calculating the load-displacement response of the RSFJ in cycle (i) after the cycle (i-1) in which the anti-locking was activated.

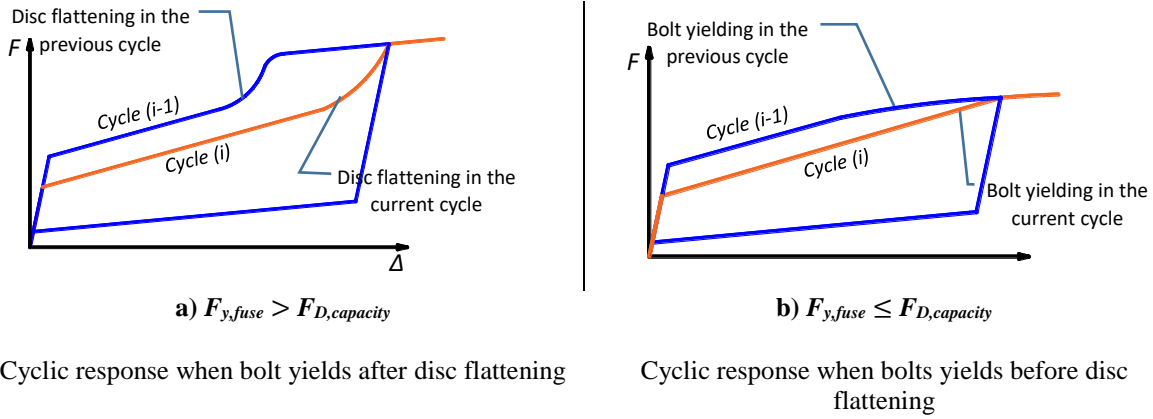


Figure 2. 17. Cyclic response of RSFJ when the ALM is activated.

As shown in Fig. 2.17, two different responses are expected based upon the relative rod yielding strength and disc spring capacity. When $F_{y,fuse} < F_{D,capacity}$, the current cycle response would be linear up to the maximum point of the previous cycle where the rods start to yield. When $F_{y,fuse} > F_{D,capacity}$, the current cycle response would be elastically nonlinear with an increasing slope up to the yielding force of the rods.

$$F_{b,pr(i)} = F_{b,pr(i-1)} - \frac{1}{2}k_{spring}\delta_{p,fuse(i-1)} \quad (2.37)$$

$$F_{slip(i)} = 2n_b F_{b,pr(i)} \alpha \quad (2.38)$$

$$F_{y,fuse(i)} = F_{y,fuse(i-1)} + k_{p,fuse}\delta_{p,fuse(i-1)} \quad (2.39)$$

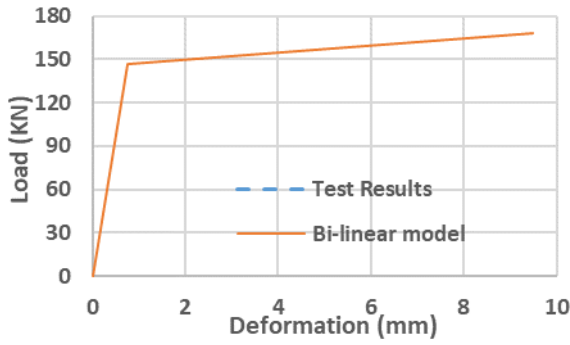
$$\delta_{spring,capacity(i)} = \delta_{spring,capacity(i-1)} + \frac{\delta_{p,fuse(i-1)}}{2} \quad (2.40)$$

$$\delta_{spring,fy(i)}^* = \delta_{spring,fy(i-1)}^* + \frac{\delta_{p,fuse(i-1)}}{2} \quad (2.41)$$

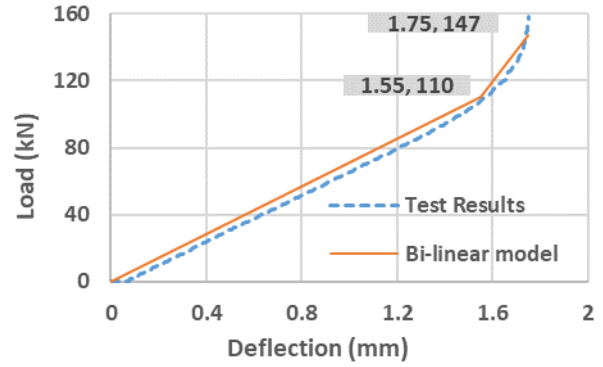
To verify the proposed equations, an experimental study was carried out. First, in order to capture the properties of the rods as the yielding elements, a set of rod component testing (five tests) was performed on rod M18 grade 8.8. The average values of the results, as mentioned in Table 4, can be used for analysis purposes. However, it is suggested to limit the ε_{max} (strain at ultimate load) to the minimum value of 0.043 to measure the δ_u used in Eq. (2.36).

Table 2. 4. Rod M18 grade 8.8 tension test results.

Test	L_0 (mm)	$A \times E$ (kN)	F_y (kN)	F_u (kN)	Δ_{max} (mm)	ϵ_{max}
1	165	31907.7	145.64	166.07	7.79	0.047
2	190	33202.5	146.42	167.64	10.58	0.056
3	52.1	37628.7	149.45	168.21	2.22	0.043
4	50.5	41617.56	148.18	168.40	2.43	0.048
5	52.5	39525.15	145.53	169.64	2.99	0.057
Average		36776.32	147.04	167.99		0.050



a) Rod M18, grade 8.8



b) Single disc spring

Figure 2. 18. Comparison of component test results with their equivalent bi-linear model.

The load-displacement graph corresponding to test (2) in Table 2.4, is shown in Fig. 2.18(a). The performance of a single disc spring was also tested. As shown in Fig. 2.18(b), an equivalent bi-linear response has been matched to the test results to be used in the developed analytical equations. As it can be seen from the graph, the deflection in the disc at the end of its linear response ($\delta_{D,capacity}$) and the force corresponding to the rod yield force ($\delta_{D,fy}$) are measured as 1.55 mm and 1.75 mm respectively. It should be noted that this graph represents the behaviour of a single disc spring. The equivalent spring properties for the disc stack should be calculated using the following equations:

$$\delta_{spring,capacity} = \left(1 - \frac{F_{b,pr}}{F_{D,capacity}}\right) n_D \delta_{D,capacity} \quad (2.42)$$

$$\delta_{spring, fy} = \delta_{spring, capacity} + (\delta_{D, fy} - \delta_{D, capacity})n_D \quad (2.43)$$

$$k_{spring} = \frac{F_{D, capacity}}{n_D \delta_{D, capacity}} \quad (2.44)$$

where n_D is the number of the discs in each stack.



Figure 2. 19. Anti-locking mechanism test specimen.

The same joint was utilised for a new testing with different number of bolts, discs and pre-stressing force (Fig. 2.19). These parameters are summarised in Table 2.5. The tested RSFJ is shown in Fig. 2.19. As can be seen from the picture, two nuts were used at each side of the rods to make sure that the root diameter will yield before thread stripping occurs.

Table 2. 5. Properties of RSFJ tested for ALM mechanism.

Parameter	Value
n_b	3
n_d	3
$F_{b, pr}$	60 kN

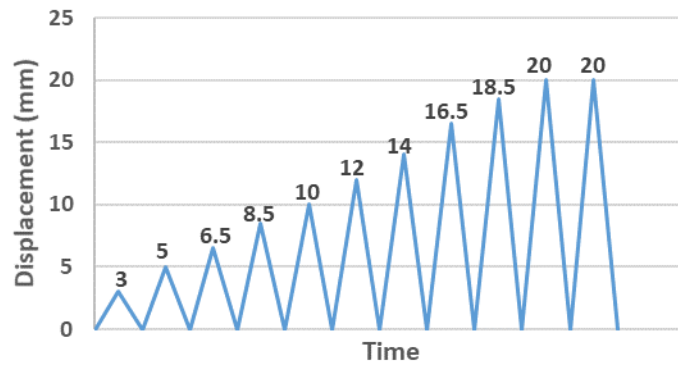


Figure 2. 20. Test loading protocol.

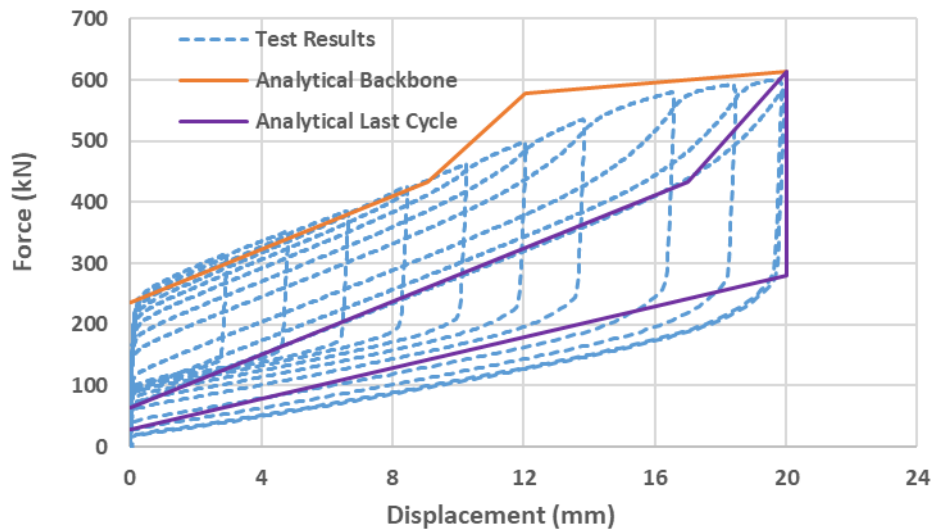


Figure 2. 21. Comparison of experimental results with analytical backbone and last cycle.

Note: the initial stiffness of both experiment and analysis have not been included in these graphs for brevity

A displacement-controlled loading protocol (shown in Fig. 2.20) was used for the cyclic loading. Fig. 2.21 compares the experimental load-displacement response of the specimen with the analytical backbone graph. The analytical prediction for the last cycle is also shown in the graph. As it can be seen, the analytical response does not match with the experimental results where the increment in the slope before yielding of the rods predicted by the equations is not observed during the test. However, the predictions for the last cycle perfectly matches the experimental results. As shown in Fig. 2.22, the reason for the disagreement between experimental and analytical results for the backbone curve refers to the unexpected yielding due to bearing which occurred in the nuts. As the inside diameter of the discs is larger than the standard bearing diameter of the nuts, high

stress-concentration at the nut edge resulted in yielding of the nuts in bearing from the early stages of the loading. The plastic bearing deformations accumulated gradually during each cycle of the test resulting in increasing the bearing surface automatically during the test. accordingly, when the bearing area was finally adjusted to bear the stress between the nuts and discs without any plastic deformation (Fig. 2.22), the difference between analytical predictions and observed behaviour became negligible for the last few cycles in the same test (Fig. 2.21). The comparison between the analytical and experimental results for the last three cycles is shown in Fig. 2.23. As it is demonstrated in the graph, the analytical and experimental results are in agreement with each other when the response is not affected by the yielding of the nuts. Therefore, the accuracy of the analytical model can be verified based on the experimental results.

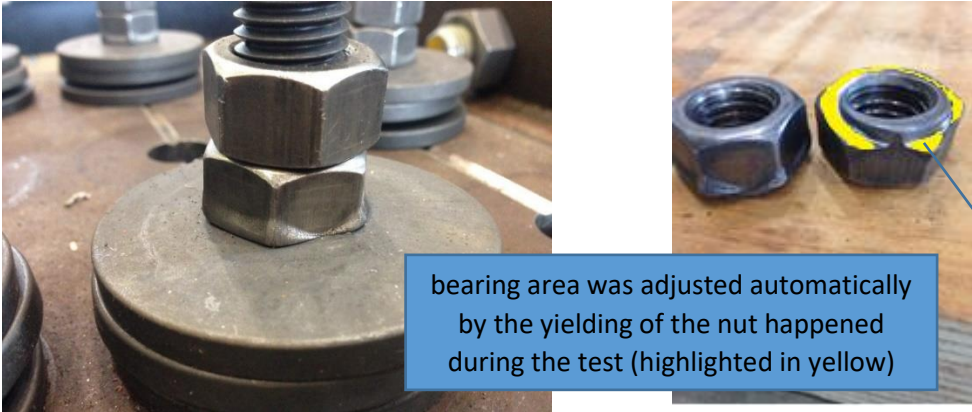


Figure 2. 22. Yielding of the nuts as the result of concentrated bearing pressure induced by disc internal edge.

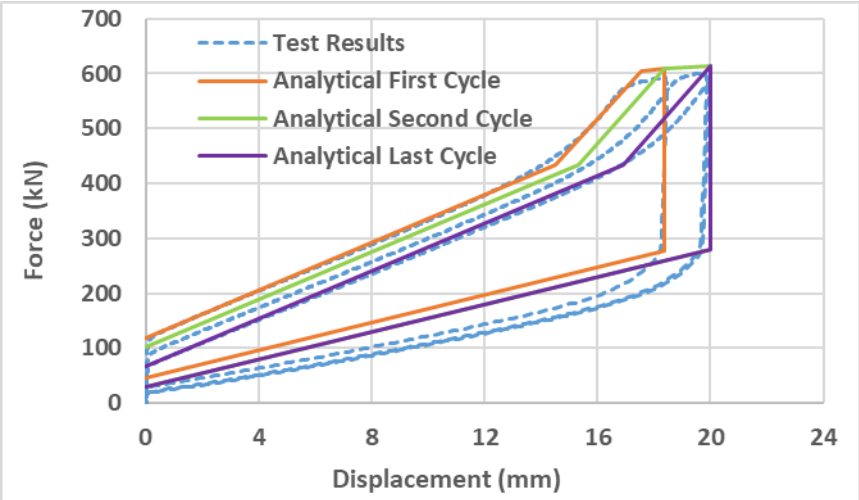


Figure 2. 23. Comparison of analytical and experimental results for the last three cycles. Note: the initial stiffness of both experiment and analysis have not been included in these graphs for brevity

In order to improve the performance of the anti-locking mechanism, it is suggested to select the size and the material type of the rods or bolts in a way that bolts start to yield immediately before discs start flattening. This results in a smooth load-displacement curve without increasing the slope due to discs flattening. In addition, customised rods with a slightly reduced cross-section in the middle of the rod (dog-bone shaped) can be used to achieve the desired yielding force. Another suggestion could be calibrating the capacities of the discs to the rod mechanical properties. Washer plates between the discs and the nuts should be used to increase the bearing interface and avoid the yielding of the nuts. It is necessary to make sure that the rods are installed straight without inclination to avoid additional bending in them. Therefore, further experimental studies are suggested. Finally, a series of nonlinear time history analysis at the structural level needs to be done to assess the effect of yielding, slope changing in load-displacement response and degradation of slip force in each cycle after yielding of the rods.

2.8 Summary and conclusion

This paper investigated the component performance of the Resilient Slip Friction Joint as a self-centring friction damper. First, the performance of the plates was analysed, and a simple equivalent spring model was developed to investigate the distribution of the load among the grooves as well as calculating the joint elastic deflection. This spring model was then verified by experimental and finite element modelling. With regards to the locking issue of the damper, a new anti-locking mechanism (ALM) was introduced and experimentally validated where the clamping bolts or rods yielding force is calibrated to prevent the increasing force associated with locking of the damper at the discs flattening point. While this technique can prevent the locking issue of the damper, it can still preserve the self-centring feature of the joint. Therefore, the RSFJ equipped with ALM could prevent the formation of seismic shocks to the structure during unpredictable seismic events beyond the design level. However, suggestions have been made to improve the performance of the

RSFJ equipped with ALM which requires further experimental studies at the joint component level as well as non-linear time history analysis at the structural level.

Chapter 3: Development of a New Self-Centring Structural Connector for Seismic Protection of Structures

1.1 Abstract

The concept of seismically low-damage structures was introduced by researchers to decrease the likelihood of irreparable damage as well improving the response of the structure. The need to shift from conventional ductile design to a less ductility (damage) oriented design was emphasised by different researchers in New Zealand and across the world back in the 1990s and 2000s. Damage Avoidance Design (DAD) philosophy introduced in the early 2000s took the idea of low-damage design to another level. Self-centring is the main aspect of a DAD designed. However, the need to change the seismic design philosophy was mostly felt by the community and decisions makers after the considerable financial and social loss that resulted from the 2011 Christchurch earthquake. Several damage-avoidance concepts and solutions have been introduced and developed in the past. However, most of these solutions have not been widely implemented in practice because of the complexity and extra construction costs. This research aims to overcome this gap by introducing a new solution that can be easily adopted by the construction industry without imposing extra complexity and construction costs. This paper presents the development of a new innovative seismic device named as Self-Centring Structural Connector (SSC) as a new self-centring friction damping device. The main purpose of this device is to provide a cost-efficient yet flexible solution to achieve a range of efficient DAD structures in practice. In this paper, the principles of the force-deflection relationship for the SSC is analytically developed and validated through experimental investigation. In addition, the influence of various parameters affecting the joint performance are studied through an analytical model. Finally, some possible applications of this device are introduced. As per the findings based on the analytical modelling and experimental investigation,

it can be observed that the joint performs well to achieve the design and construction objectives making it a suitable solution for DAD.

3.2 Introduction

Most of the current building codes have been developed based on the design concept of ductility to mitigate the earthquake force demands on the structure [8]. In this concept, the earthquake input energy is dissipated through cyclic yielding of a ductile element. Collapse prevention and suitable energy dissipation are two main advantages of such structures [2]. On the other hand, plastic yielding is generally a complex phenomenon and can be sacrificed by undesired failure modes [5, 88, 89]. Ductile structures should be designed, detailed and constructed precisely in order to achieve the desired performance. However, during the past earthquakes, undesired seismic behaviour and failure modes have been observed even in precisely designed and constructed structures [90]. Residual deformation and significant repair or reconstruction costs are expected for ductile structures after moderate to severe earthquakes [6, 91].

Therefore, researchers have introduced the low-damage design concept, a design philosophy in which the earthquake-induced motion is dissipated in reparable or replaceable fuses [12, 21, 25, 39, 82, 92, 93]. A variety of systems such as yielding [38, 94], friction [39, 40, 95, 96], and viscous [93, 97, 98] dampers and different types of base-isolators [92, 99-101] have been introduced, tested and used in different types of structures. Experimental tests and previous earthquakes have proved the advantages of low-damage systems compared to ductile structures [89, 102-107]. Repetitive energy dissipation, larger displacement capacities and smaller demands in addition to less repair cost can be named as some of these advantages.

For a seismically low-damage structure, self-centring is a bonus. A self-centring structure, when appropriately designed, can bring the structure to almost a damage-avoidance level [9, 108-111]. Most of the low-damage structures experience residual deformations after moderate to severe earthquakes. This residual deformation can be a source of some problems. For example, the

likelihood of collapse due to aftershocks will be increased when there is a residual displacement within the structure after the main shocks [9, 62].

Furthermore, it can be a costly and complicated process to bring the structure back into its initial position and it can be even more problematic for the repair and replacement of low-damage elements. When designing a low-damage structure, designers should not consider using replaceable seismic elements as a member of the gravity resisting system. Besides, when there are already residual displacements after an earthquake, the structure is resisting the additional imposed actions due to p-delta effects. Therefore, it is not safe to remove the lateral-load resisting elements for repair purposes as it could endanger the stability of the structure. Consequently, it is required to bring the structure back into its initial vertical position before replacing or repairing low-damage elements.

Damage Avoidance Design (DAD) philosophy was introduced in the early 2000s and took the idea of low-damage design to another level [9]. Self-centring is the main aspect of a DAD designed structure [10, 14, 21, 63]. Residual deformation is considered a type of damage that should be controlled based on DAD [13, 16, 22, 64]. Several damage-avoidance concepts and solutions have been introduced and developed in the past confirming the advantages of such systems [19, 49, 50, 58, 112, 113].

DAD solutions have been implemented in various applications such as concrete moment frames [49-51, 65], steel moment frames [19] and rocking walls and piers [10, 13, 14, 17, 18, 20, 21, 114]. As mentioned before, residual deformations are not desired and therefore, the main advantage of DAD structures is to overcome the residual displacement issue. In a DAD structure, not only the repair costs will be decreased, but also the structure is more likely to remain fully operational after severe earthquakes [63]. The ability to keep the building fully functional is one of the essential benefits of DAD structures. For example, lifelines such as hospitals can remain fully operational after severe earthquakes if a properly designed self-centring system is adopted and used.

Different types of self-centring systems and devices have been introduced and tested by researchers. Energy dissipation in such systems is usually provided in forms of friction, yielding and viscous damping [24, 27, 31, 115]. In order to add a re-centring capability to such systems, a reserved force is required, which is generally produced using pre-stressing [116, 117]. When the earthquake action being unloaded, the reserved force can push the structural elements and the seismic weight of the structure back into their initial positions. It is required to store the pre-stressing force in elements, which are capable of deforming within a compatible range to earthquake-induced deformation demands.

A common method to incorporate self-centring capacity within a structural system is to use steel-strand cables known as post-tensioning cables. Post-tensioning cables have been used in various types of self-centring structures [118-122] such as concrete and timber rocking walls [115, 123], steel and concrete Moment Resisting Frames (MRFs) [124, 125], and steel braces [126]. For example, a hospital building designed and constructed in Christchurch, New Zealand using self-centring rocking concrete walls performed reasonably well in the 2011 Christchurch earthquake with limited non-structural damages [89]. An additional energy dissipation mechanism is usually adopted for cable-based self-centring systems. U-shaped flexural dampers in PRESSS rocking-wall technology [127, 128], or BRBs equipped with post-tensioning cables [129], are some of the examples where a yielding element is implemented to provide energy dissipation. Another example is cable-based self-centring braces with frictional plates [130]. Similar concepts have been used in steel moment frames where post-tensioning cables and frictional end connections or yielding endplates have been used together [131].

Another way of looking at self-centring is to implement devices that are capable of dissipating earthquake-induced motion and then directing the structure to return to its initial position. Such devices can be used as structural connectors. Structural springs such as Belleville springs and Ringfeder springs [41, 58, 132] are used in these devices to provide self-centring. In addition to

suitable structural capacity, one of the key features for such springs is to have the potential of tolerating large displacement generated by earthquake actions. Resilient Slip-Friction Joint (RSFJ) [59, 133] and Ringfeder springs [41, 134] are two examples of self-centring devices in which friction is also incorporated to provide energy dissipation. Several applications in different structural systems have been developed by researchers to use self-centring devices for earthquake protection of building structures [111, 135-138]. There have been other self-centring connections developed and implemented in the past. High Force to Volume (HF2V) dampers are lead extrusion viscous dampers that work based on yielding of lead inside a cylinder [16, 47, 49, 50]. Various types of fluid self-centring viscous dampers [42, 46, 58, 113, 132] and ratcheting devices have been also developed by different researchers [139]. Elastomeric Spring Dampers can also be named as self-centring energy dissipaters [12, 21, 52].

As discussed above, several damage-avoidance concepts and solutions have been introduced and developed in the past. However, most of these solutions have not been widely implemented in practice because of the complexity and extra construction costs. This research aims to overcome this gap by introducing a new solution that can be easily adopted by the construction industry without imposing extra complexity and construction costs. This paper presents the development of a new innovative seismic device named Self-Centring Structural Connector (SSC) [78] as a new self-centring friction damping device. The main purpose of this device is to provide a cost-efficient yet flexible solution to achieve a range of efficient DAD structures in practice.

SSCs can be used in different applications for seismic protection of buildings, bridges and industrial structures. In this paper, the parts and performance of SSC are explained and equations for predicting the load-displacement performance of the device are determined. An experimental study at the component level is carried out to verify the performance and performance equations developed. A parametric study is then carried out in order to assess the effect of various parameters on the response of the damper. As per the findings of this study, it can be observed that the SSC

performs well to achieve the design and construction objectives making it a suitable solution for DAD.

3.3 SSC PARTS

As shown in Fig. 3.1, one of the parts of the SSC are the friction discs. The main responsibility of these discs is to create friction in contact with the internal surface of the tube. In fact, these discs along with the tube take the important task of energy dissipation in the damper. The normal force, which is perpendicular to the surface of the tube, is applied to these discs through the clamping bolts pushing the longitudinal tabs of the tube towards each other. Pre-stressed Belleville springs are used to provide self-centring.

The relative movement between the friction discs and the tube creates friction. End rods are used to connect the SSC to the structural elements being protected against seismic actions. Another function of the longer rod is to assemble the stack of Belleville springs and friction discs together and then to apply a pre-stressing force to the stack of the Belleville springs. This pre-stressing force can be applied by tightening the nuts at each end of the rod. The length of these friction discs is designed to have the required tributary length to make sure the designated normal force from the bolts is applied to the discs. The edges of the friction disc have been chamfered in order to prevent stress concentration and possible scratching. In addition, some grooves have been made around the friction disc to keep the contact surface lubricated during the movement (Fig. 3.1).

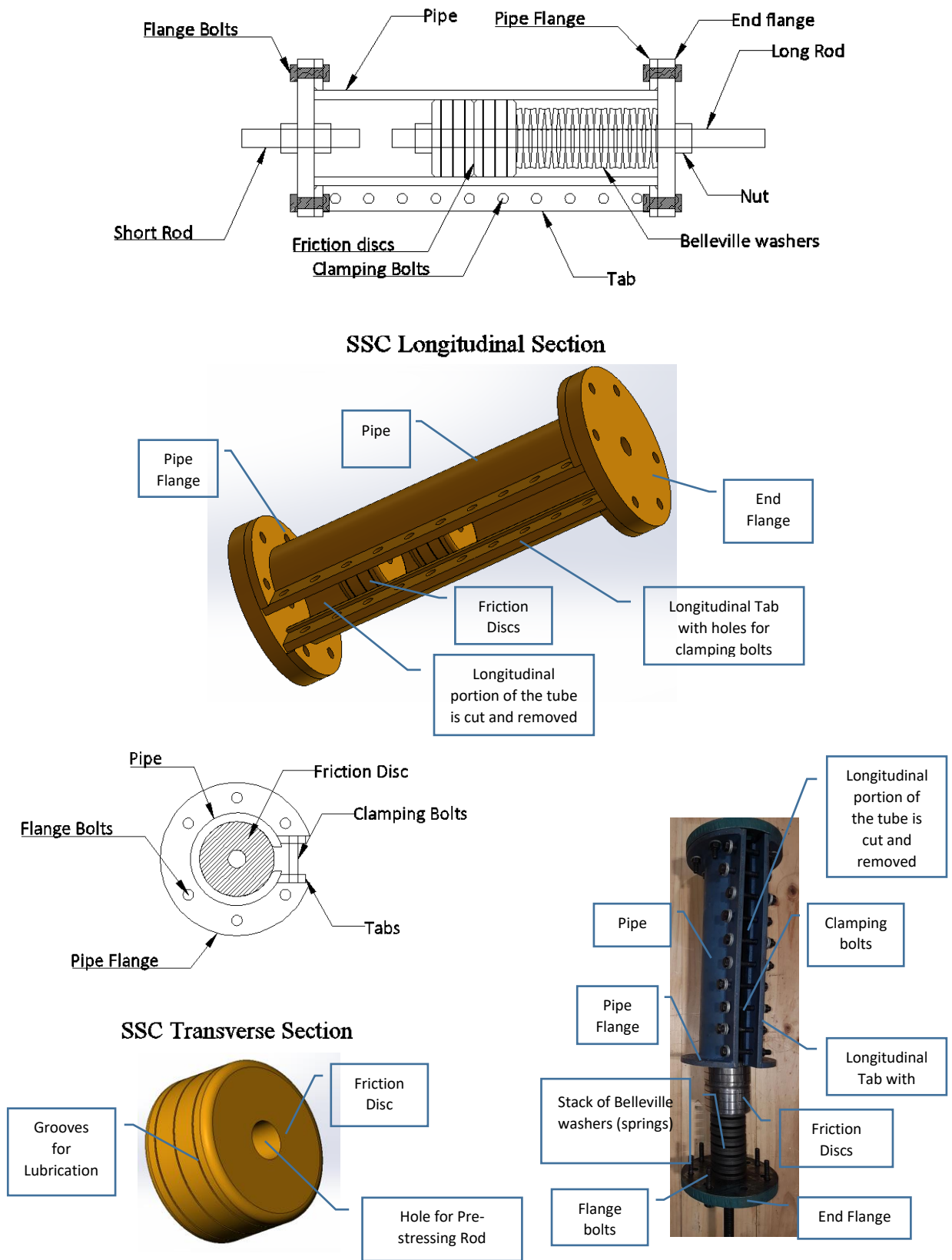


Figure 3. 1. Self-Centring Structural Connector.

Belleville washers are responsible for the self-centring capability. Belleville washers are conical springs that only work in compression. It should be mentioned that this type of springs is usually

stacked using various layouts of series and/or parallel arrangements in order to achieve the desired force-displacement performance. Every single spring has a specific displacement capacity, Δs , and a corresponding load capacity, F_s , at the maximum flatness displacement, which is called flatness load. It is noteworthy that the displacement capacity will be increased by placing more springs in a series layout and the load capacity will be increased by placing more springs in the parallel layouts. In the design of the SSC, the springs have been placed in the series layout. The number of these springs are selected based on the required displacement capacity of the SSC. In addition, it should be mentioned that the stack of springs should be pre-stressed to the desired pre-stressing force before being inserted inside the tube.

One short and one long size rod have been used as the load transferring elements. The long rod is implemented in order to pre-stress the springs and friction discs as well as transferring the seismic forces from the structure to the SSC. The stack of the springs should be pre-stressed up to the desired force. Then, these parts are connected to the main tube using some nuts.

The tube is another critical element of the SSC given the sliding friction between the internal surface of the tube and the friction rings is the source of energy dissipation. The mechanism of this energy dissipation is explained in this section. The external diameter of the friction discs is equal to the internal diameter of the tube. After the friction discs have been put inside the tube, the flange bolts will be finger-tightened. It is noteworthy that the diameter of the bolt holes on the flanges are considered large than the diameter of the bolts so that the bolts do not create resistance for the tube deformation at the time of clamping the tube. At this stage, the tube clamping bolts are pre-stressed to the required clamping force creating the normal force perpendicular to the sliding surface. This normal force results in the frictional resistance between the disc and the tube. It should be mentioned that torque meters can be used to control the accuracy of the applied force to the bolts. At the end of this step, the flange bolts will be properly tightened, and the damper is ready for loading.

It should be noted that the internal surface of the tube and the external surface of the rings are lubricated using grease in order to control the surface damage as the result of friction sliding. A special type of grease has been used with a long working lifetime, more than 50 years. In addition to the reduction of damage due to friction, such as scratching, galling, and wearing, the use of this grease can reliably make repeatable force-displacement response for the SSC and prevent surface rusting over time.

It should be noted that different configurations of the SSC such as tension-only, compression-only and double-acting can be designed. In the following section, the performance of the tension-only variation is discussed in more details. Later on in this paper, the concept for other variations are introduced.

3.4 SSC PERFORMANCE

In this section of the paper, the force-displacement performance of the SSC is analysed. As can be seen from Fig. 3.2, the developed damper in this study has a flag-shaped force-displacement response. This force-displacement curve is the main characteristics of self-centring dampers which shows the presence of damping and self-centring at the same time. This curve usually comes from the combination of an elastic-perfectly-plastic response, which represents the friction behaviour, and a bilinear elastic response, which represents the behaviour of the pre-stressed springs. Applying the pre-stressed force to the springs is essential given this force should overcome the existing friction in the system and return the damper to its initial position at the unloading stage.

At the beginning of the loading stage, the force inside the damper is increased with an increase in the external force F . At this stage, the friction force ($F_{friction}$) and the pre-stressing force ($F_{prestressing}$) inside the springs resist the movement. The damper displacement starts when the external force becomes equal to the summation of the above-mentioned forces. The equivalent force corresponding to the damper displacement is called F_{slip} . This force can be obtained using the following equation:

$$F_{slip} = F_{friction} + F_{prestressing} \quad (3.1)$$

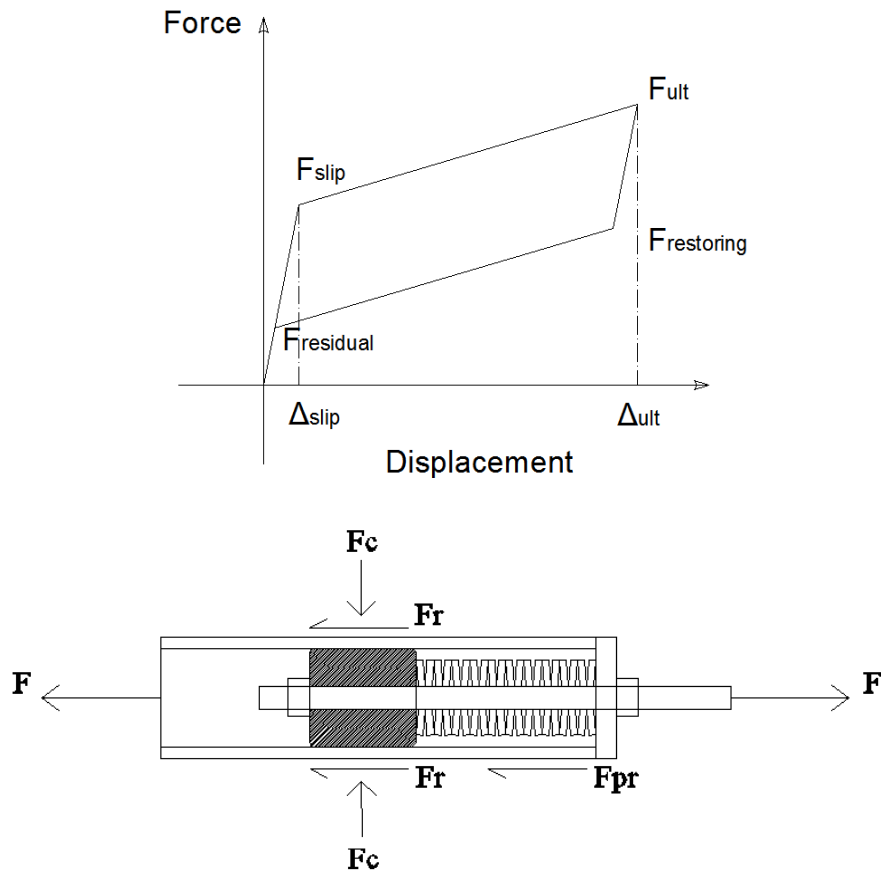


Figure 3. 2. Free body diagram and force-displacement response.

In seismic design, the amount of F_{slip} is determined based on the design requirements and performance objectives. As a general rule, F_{slip} should be considered large enough, so that the lateral movement of the structure is restricted at the Serviceability Limit State (SLS) loading level in the event of small-scale earthquakes and high wind loading. The displacement of the external force at the slip (Δ_{slip}) is equal to the elastic deformation of the internal components of the damper. The calculation of Δ_{slip} can be done simply using the mechanics of materials principles. The accurate assumption of Δ_{slip} is essential in order to calculate the initial stiffness of the system to estimate the seismic demand of the structural system based on the natural frequency and design spectrums provided in the seismic codes.

The initiation of the movement after slip results in the compaction of the springs and consequently the increase of the applied load. Therefore, while the spring force increases, the friction force remains constant. At this stage, the displacement of the damper increases until the maximum displacement capacity of the springs is reached or in another word, the springs get flattened. At this flat load, the damper has been theoretically reached its maximum force capacity (F_{ult}). F_{ult} can be estimated using the following equation.

$$F_{ult} = F_{friction} + F_{prestressing} + K\Delta = F_{friction} + F_s \quad (3.2)$$

Where K is the equivalent stiffness of the set of springs and Δ is the displacement capacity of the springs after pre-stressing. F_s represents the force capacity of the springs.

It should be mentioned that from the seismic design point of view, the maximum force of the damper is equal to the maximum earthquake force that the structure is designed for. To create a safety margin in real design, it is better to consider the maximum design force less than the theoretical F_{ult} to prevent the damper to reach its maximum displacement during the design level earthquake.

At the unloading stage, the spring tries to return the structure to its initial position when the external force is decreasing. At this stage, the spring force should be able to overcome the internal friction and the external force. When both the friction force and the external force are equal to the maximum force created in the spring, the structure starts to move toward its initial position. From now on, the displacement of the damper decreases as the external force decreases. The restoring force, $F_{restoring}$, can be calculated using the following equation.

$$F_s = F_{friction} + F_{restoring} \rightarrow F_{restoring} = F_s - F_{friction} \quad (3.3)$$

Eventually, the displacement reaches zero with the decrease in the force completing a full cycle of loading and unloading. The external residual force in the system at this stage, $F_{residual}$, can be obtained using the following equation:

$$F_{prestressing} = F_{friction} + F_{residual} \rightarrow F_{residual} = F_{prestressing} - F_{friction} \quad (3.4)$$

In order to obtain the self-centring condition, the pre-stressing force of the spring must be greater than the friction force. If this condition is not met, an additional external force should be applied to push the structure back to zero displacement position. In the design of this damper, the value of $F_{residual}$ can ideally be considered to be zero. In such a situation, the area of the force-displacement curve is maximized and therefore, the damping reaches its maximum possible value.

$$F \geq 0 \rightarrow F = F_{prestressing} - F_{friction} \geq 0 \rightarrow F_{prestressing} \geq F_{friction} \quad (3.5)$$

From the seismic design point of view, a designer can select the residual force greater than zero due to the fact that in a real structure, there is always friction between the structural members that needs to be overcome. This is more important when designing moment resisting or braced frames, in which the weight of the structure does not take part in re-centring such as in rocking structures. The design philosophy of the friction force in this damper is based on the movement of a piston inside a cylinder. However, it should be mentioned that in the design of SSC, the normal force acting on the surface between the piston and the cylinder can be adjusted by the external clamping force. This force (F_c) is applied using the tube clamping bolts and nuts. Through the clamping force of F_c , the internal surface of the cylinder pressurise the piston (i.e., friction disc), and the normal stress on the surface is evenly distributed between the tube and the friction disc. This pressure distribution is similar to the pressure distribution in pressure vessels.

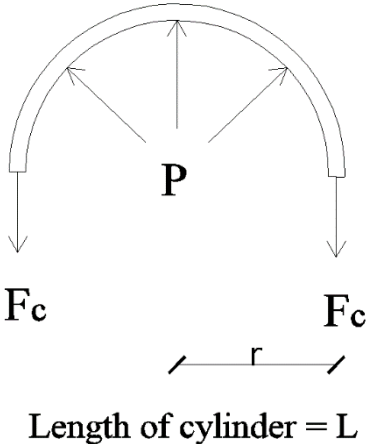


Figure 3. 3. Free body diagram of a cylinder with internal pressure.

As shown in Fig. 3.3, considering the equilibrium equations for the longitudinal section of the cylinder, the relationship between the clamping force (F_c) and the pressure (P) on the tube can be obtained using the following equation for a cylinder with a radius of r and the length of L .

$$2F_c = 2PrL \rightarrow F_c = PrL \quad (3.6)$$

At this stage, the friction force (F_{fr}) can be calculated using the pressure on the tube (P) and the friction coefficient, μ , between two greased steel surfaces, which is considered to be 0.15, as per test results.

$$F_{fr} = 2\pi r \mu PL$$

By substituting P from equation (3.6):

$$F_{fr} = 2\pi \mu F_c \quad (3.7)$$

This equation calculates the friction force in the SSC. It can be understood from this equation that the circular pattern of the pressure has an advantage in terms of the level of the normal force on the sliding surface of the tube. By placing π and μ in Eq. 7, the F_{fr} almost equates the F_c ($F_{fr} = 0.95 \times F_c$). It means that the friction force is approximately equal to the pre-stressing force, which is considered a worthy advantage in using the concept of cylinder and piston when compared to flat plates. It should be mentioned that in flat friction plates, a high clamping force in bolts is required for achieving the desired friction resistance. Despite using grease, a considerable friction force can still be achieved given the coefficient of 0.95.

In this section, the relationships governing the performance of the disc springs are discussed. Each Belleville spring has an ultimate force (F_s) and an ultimate displacement (Δ_s), in which the spring is completely flat. F_s and Δ_s will be used as the main characteristics of Belleville springs in order to develop other design calculations related to springs stack performance. By considering n springs with a series layout, their maximum displacement (Δ_{max}) is calculated using the following equation:

$$\Delta_{max} = n\Delta_s \quad (3.8)$$

In a series layout of springs, the required force for flattening the springs is equal to the required force for flattening one spring. Therefore, the stiffness of the series springs (K) can be obtained using the following equation:

$$K = \frac{F_s}{\Delta_{max}} = \frac{F_s}{n \times \Delta_s} \quad (3.9)$$

If the pre-stressing force in the springs is equal to F_{pr} , the displacement of the stack of springs (Δ_{pr}) can be calculated using the following equation.

$$F_{pr} = K \Delta_{pr} \rightarrow \Delta_{pr} = n F_{pr} \frac{\Delta_s}{F_s} \quad (3.10)$$

The maximum displacement of the springs stack after pre-stressing is equal to the maximum displacement capacity of the damper, Δ_{ult} , which can be calculated using the following equation.

$$\Delta_{ult} = \Delta_{max} - \Delta_{pr} = n \Delta_s - n \Delta_s \frac{F_{pr}}{F_s} = n \Delta_s \left(1 - \frac{F_{pr}}{F_s}\right) \quad (3.11)$$

The above equation presents the relationship between the pre-stressing force in springs and the maximum displacement expected from the SSC. Therefore, by using the derived equations, it is possible to design the SSC for the desired force (F_{ult}) and displacement (Δ_{ult}). F_{pr} can be obtained using Eq. 11 when the characteristics and the number of Belleville washers are known. By applying the self-centering condition according to Eq. 3.5, the friction force (F_{fr}) and then, the required force for clamping the cylinder (F_c) can be obtained using equation (7). This design procedure is repeated until an optimized design is achieved. In the next section, the equations already discussed are verified using a series of experimental tests.

3.5 Experimental verification

In this section, a sample of the new damper has been designed and manufactured. The obtained results from the experiments have been compared with the predictions. The initial design has been based on a maximum force (F_{ult}) of 135 kN and a maximum displacement (Δ_{ult}) of 20 mm. To achieve this performance, springs with a displacement capacity (Δ_s) of 1.8 mm and force capacity (F_s) of 110 kN were selected. The dimensions of these springs are shown in Table 3.1.

Table 3. 1 The properties of the tested SSC.

Parameter	Value
Discs internal height	1.80 mm
Discs ultimate capacity	110 kN

By considering the outer diameter of springs equal to 70 mm (Fig. 3.4(a)), approximate diameter of 100 mm was selected for the friction discs. Then, a tube with an internal diameter of 92.1 mm was chosen from the available steel tube sizes in the market. The cross-section of the selected tube for this damper is also shown in Fig. 3.4(b).

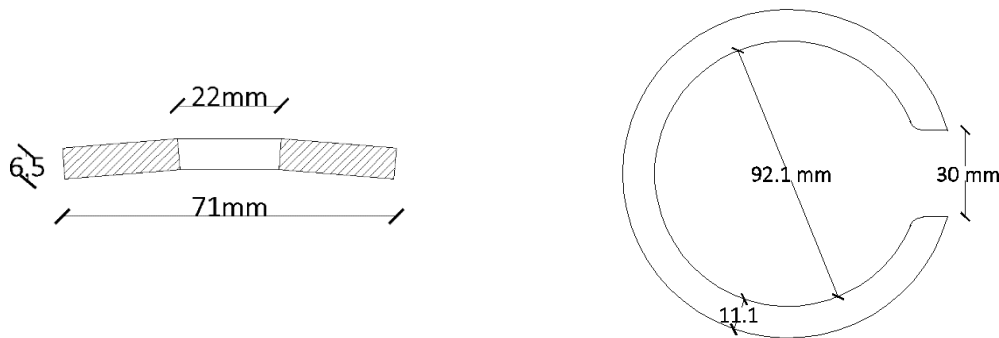


Figure 3. 4. Belleville Spring (Left), and tube dimensions (Right).

As can be seen in Fig. 3.5, a portion of the tube along its length with an approximate width of 30 mm has been cut and removed. The dimension of this slot can be less or more depending on the design and the application. In this prototype, the slot width has been selected to be wide enough to observe the performance of the internal components during loading and unloading. The other components of the tube, such as tabs and flanges, have been welded to the tube.



Figure 3. 5. Manufactured tube.

As mentioned in Fig. 3.5, the friction discs have been manufactured with the same outer diameter as the internal diameter of the tube. Therefore, the manufacturing precision for these friction discs is crucially important, as their outer diameter should be properly equal to the inner diameter of the tube, otherwise there would be a need for extra clamping force in the bolts to overcome the gap. The length of the friction discs has been selected long enough so that the normal stress acting on the tube is equal to the designated normal force to provide the friction. Therefore, a length of 50mm has been selected for the friction discs. Details of the friction discs are shown in Fig. 3.6.

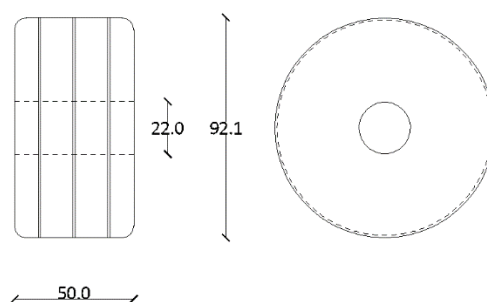
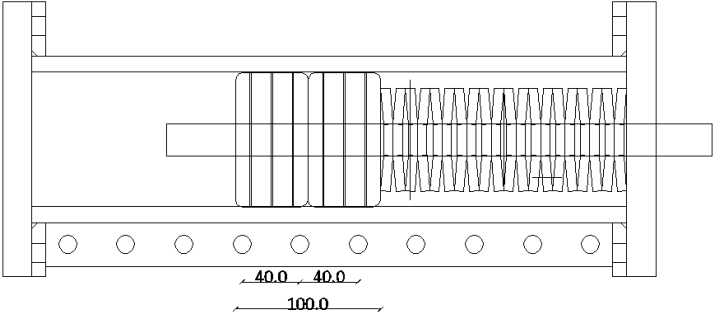


Figure 3. 6. Friction disc.

The normal force acting on the friction discs is a function of the length of friction discs and the distance between the clamping bolts. In the sample manufactured for this experiment, two friction discs have been put beside each other to shape a longer friction disc of 100 mm and the distance between the clamping bolts is 40 mm. Therefore, the number of effective bolts in applying the

perpendicular force on the friction discs is equal to $100/40= 2.5$ (Fig. 3.7(a)). This means the pre-stressing force of each bolt times the effective number of bolts is equal to the clamping force (F_c) acting on the friction discs. The clamping force is applied to the bolts using a calibrated torque meter as shown in Fig. 3.7(b).



(a)



(b)

Figure 3. 7. Applying the clamping force (a) Total length of friction discs and spacing between clamping bolts, and (b) torque meter used for clamping bolts.

The dimensions of the end flanges are shown in Fig. 3.8(a). In order to assemble the damper, first the end flange, springs, and friction discs are stacked using the rod passing through them and then tightened using the nuts. The selected rod for the damper is a high strength steel (grade 10.9) threaded rod as shown in Fig. 3.8(b).

In this stage, the assembly of friction discs and springs can be pre-stressed until the desired pre-stressing force is reached using a hydraulic jack. As mentioned in the previous section, the pre-stressed force of the rod can be estimated using the equations developed for the damper. In this section, to achieve the desired performance, the required pre-stressing force is calculated, as per Table 3.2.

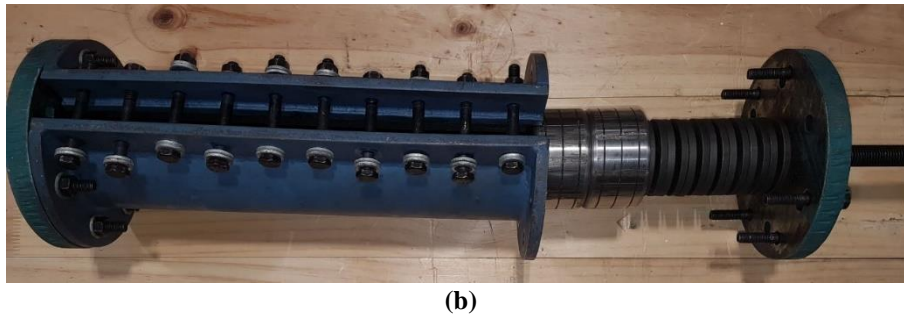
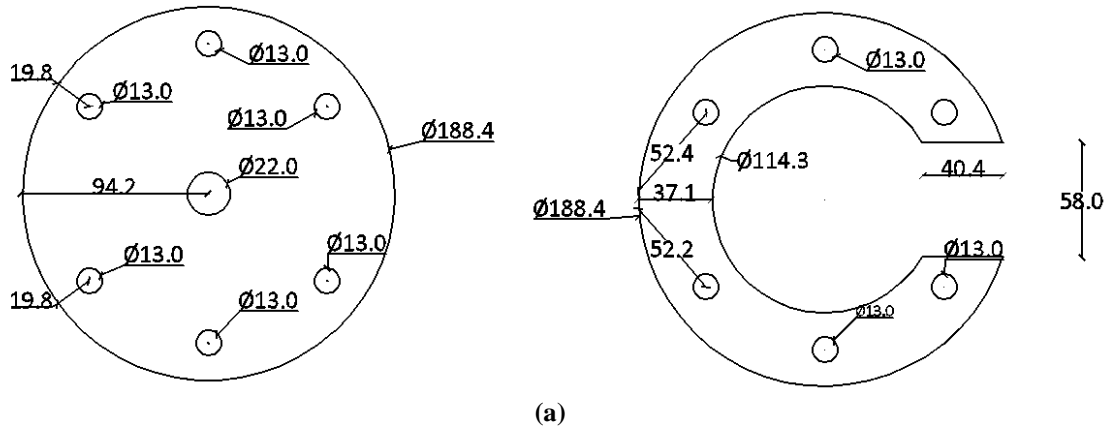


Figure 3. 8. (a) End flanges dimensions, and (b) the assembly of friction discs and springs being inserted into the tube.

Table 3. 2. SSC design parameters.

Parameter	Value	Equation
F_{ult} (kN)	135	
F_s (kN)	110	Eq. 3.2
$F_{friction}$ (kN)	25	
Δ_{ult} (mm)	20	
Δ_s (mm)	1.8	
F_{pr} (kN)	49	Eq. 3.11
F_c (kN)	26.5	Eq. 3.7
F_b (kN)	10.6	$F_c/2.5$
F_{slip} (kN)	74	
$F_{restoring}$ (kN)	85	
$F_{residual}$ (kN)	24	

These design target values for the damper performance are verified in the following section by experimental testing.

A Universal Testing Machine (UTM) has been used for the experimental verification. The input force and displacement by the UTM were recorded via the data acquisition system at each pre-defined interval time. Different load protocols can be defined for testing the damper. Some of the standards, such as AISC [140] and ASCE [141] provide various loading protocols for testing seismic devices. Most of the testing procedures suggested by the codes have been developed based on the criteria for testing yielding dampers. However, in this test, yielding is not expected, and low cycle fatigue and cumulative damage are not likely to happen due to the self-centring capability of SSC. Therefore, a loading protocol has been developed for this test to make sure that the desired performance of the device can be achieved during earthquakes. In the suggested protocol, the device will be tested under quasi-static cyclic loading at four different displacement levels. If the ultimate design displacement is Δ_{ult} , the amplitudes are 25%, 50%, 75% and 100% of Δ_{ult} . At each displacement level, the device will be tested for three full cycles in order to verify the repeatability of the performance.

In order to evaluate the performance of the SSC according to the suggested load protocol, the displacement levels for testing the device are calculated based on the ultimate design displacement of 20mm, summarized in Table 3.3.

Table 3. 3. Cyclic testing load protocol.

Percentage (%)	Displacement (mm)
25	5
50	10
75	15
100	20

The test setup is shown in Fig. 3.9. The prototype was loaded in the UTM through the end connections. It should be noted that this test is a tension only test, therefore, the performance of the connection has been only evaluated under tensile loading.



Figure 3. 9. Test setup.

The results obtained from the experimental test is shown in Fig. 3.10. As can be seen from the graph, the test result matches very well with the analytical predictions. This agreement between the analytical and experimental results proves the accuracy of the developed equations for predicting the performance of the SSC. In addition, it can be concluded that the SSC can present a uniform repetitive behaviour under cyclic loading, which shows a reliable performance to resist seismic loads.

It should be noted that the device should be designed for a maximum force of 25% more than the design level earthquake force as per the AISC loading protocol. Therefore, in the conducted experimental test, it is assumed that the maximum force of the SSC is equal to 1.25 times the design earthquake force.

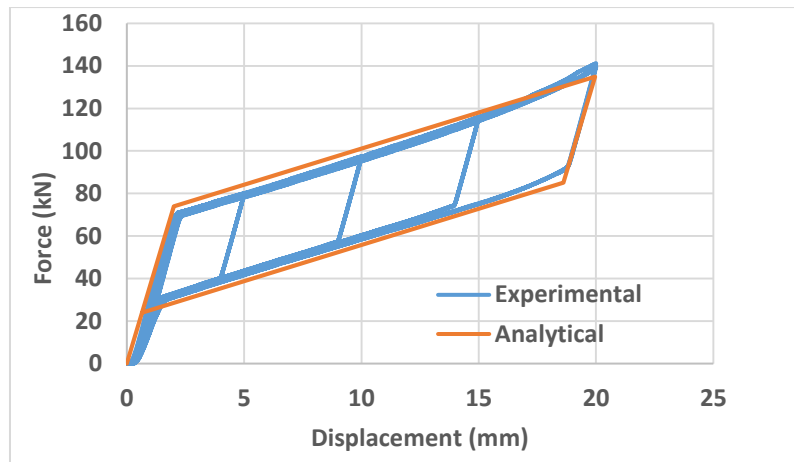


Figure 3. 10. Force-displacement response of SSC prototype.

3.6 The effect of various parameters on the damper behaviour

Before discussing the SSC parametric study, a brief discussion of the equivalent damping ratio is presented in this section. As a general rule, the more the damping ratio is, the better the seismic response of the structure will be in terms of displacement and acceleration demands. Therefore, it seems necessary to have a proper definition of the damping ratio and then assess the effect of various SCC parameters on this ratio. Different references have presented different definitions for equivalent damping ratio based on nonlinear force-displacement hysteresis curves. It should be mentioned that in the dynamic equilibrium equation of motion for a linear system, the damping ratio affects the structural response based on the velocity. Therefore, when considering an equivalent damping ratio for a nonlinear force-displacement response, some estimations are involved. However, as a general principal, the following damping ratio calculation method has been utilised in the literature [142] according to Fig. 3.11.

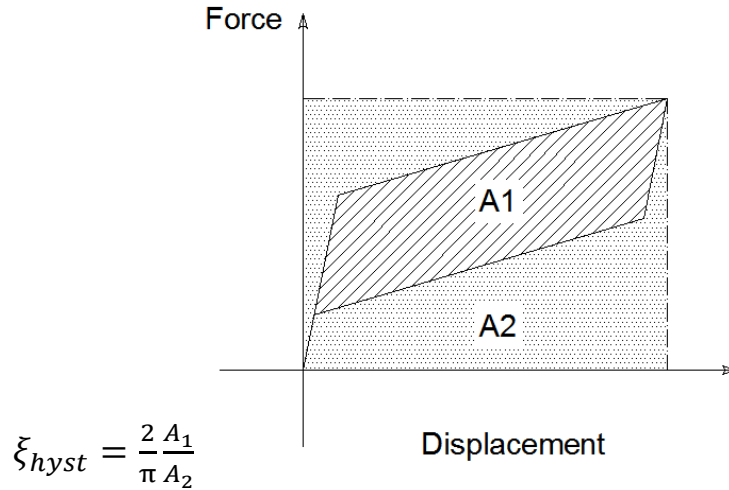


Figure 3. 11. The effect of pre-stressing force on the performance of SSC.

In this part of the paper, the effect of various parameters on the behaviour of the SSC has been evaluated. Two parameters that are involved in the design of the damper are the friction force and the pre-stressing force of the springs. According to the equations developed in the previous sections, the friction force is a function of the pre-stressing force of the bolts and friction coefficient between the tube and the friction disc. By considering a constant friction coefficient, the only effective parameter in friction force is the clamping force of the bolts (F_c). Here, the effect of changing the friction force (F_f) on the behaviour of the SSC has been investigated. As mentioned in the previous section, to achieve a self-centring condition, the pre-stressing force of the springs (F_{pr}) must be more than the friction force (F_f). As such, the dimensionless parameter of $\left(\frac{F_{fr}}{F_{pr}}\right)$ is considered to investigate the effect of changes in the friction force. The maximum amount considered for this parameter is equal to 1. This means that the self-centring condition is still satisfied. In the graph shown below, the force-displacement of the damper has been depicted for three different ratios of $\frac{F_{fr}}{F_{pr}}$. As can be seen from Fig. 3.12, the area enclosed within the graph increases as the friction force increases. This result means that the equivalent damping ratio of the joint (and accordingly the structure) is increased with the increase of the friction force. Another noteworthy point is that the changes in the slip force and the ultimate force is achievable without changing the ultimate displacement. This fact is one of the advantages of the SSC which means

the friction and pre-stressing can be independently adjusted. During the design, with a constant value of pre-stressing force and ultimate displacement, the desirable slip force and ultimate force can be tuned by changing the friction force. This demonstrates the flexibility of the SSC to be used in different applications.

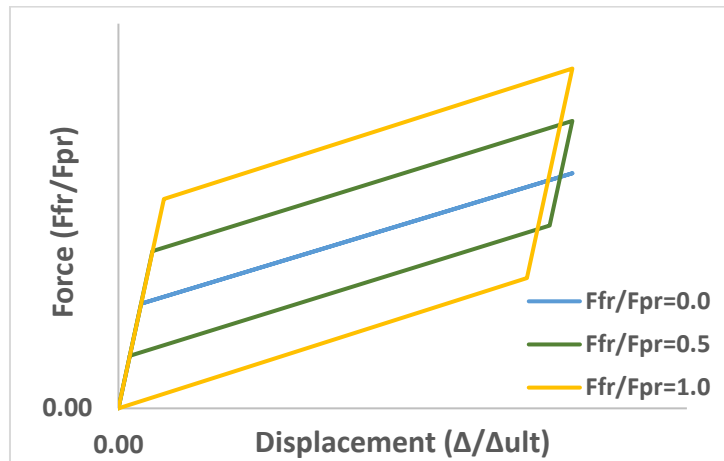


Figure 3. 12. The effect of friction force on the performance of SCC.

The other parameter investigated is the pre-stressing force of the rod. This parameter has been investigated by changing the dimensionless ratio of $\frac{F_{pr}}{F_s}$. As it is evident from Fig. 3.13, once the pre-stressing force is equal to zero, the full self-centring will not happen and there may be some residual displacement in the system. However, it should be mentioned that the Δ_{ult} in this arrangement is the maximum possible displacement expected from the stack of springs. With increasing the pre-stressing force, the amount of slip force will be increased, however, the ultimate force and the difference between the slip force and the restoring force remain constant. In addition, as a result of more pre-stressing, the ultimate displacement, Δ_{ult} , is decreased depending on the springs compaction. Another parameter that does not change with increasing the pre-stressing is the equivalent damping ratio. This ratio is a function of damping energy in each cycle of loading, which is a function of dissipated energy by friction and is independent of the pre-stressing force of the springs.

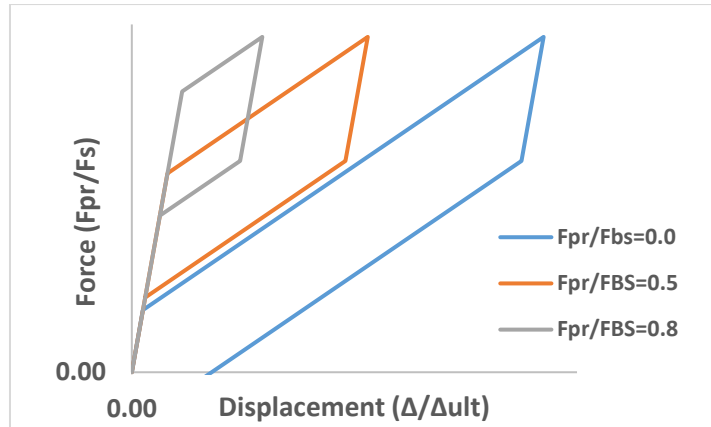


Figure 3. 13. The effect of pre-stressing force on the performance of SCC.

3.7 SSC Arrangements

In the previous sections, a tension-only SSC was investigated analytically and experimentally. As mentioned earlier, different arrangements of the SSC parts and different configurations can be developed and tested to achieve different performances. Some of the possible configurations for the SSC are introduced and discussed in this section including multiple-sliding SSC (Fig. 3.14), Compression SSC (Fig. 3.15) and double-acting SSC (Fig. 3.16).

Multiple-sliding SSC is a combination of two stacks of discs and springs as mentioned in Fig. 3.14. The main purpose of this arrangement is to provide a secondary fuse within the damper to prevent a sudden increase in stiffness when the damper reaches its maximum displacement and springs are flat. As can be seen from Fig 3.14, when F increases, the first stack, with a smaller clamping force F_c , starts to slide first at F_{slip1} . This is the main designated slip force of the damper. In a code-compliant structure, this force can be considered as SLS earthquake force. Beyond this point, by increasing F , the damper reaches its ultimate force and displacement designed for the ULS earthquake. At this stage, the force pushing the second stack has reached to sliding threshold of the second stack (F_{slip2}). It should be noted that a larger clamping force is applied to the second friction disc compared to the first one in order to make sure that the sliding occurs late enough immediately after the ultimate stage. Beyond this point, all of the moving parts (first and second

stack) are moving together resulting in a smaller loading stiffness as more springs are now working together in a series arrangement.

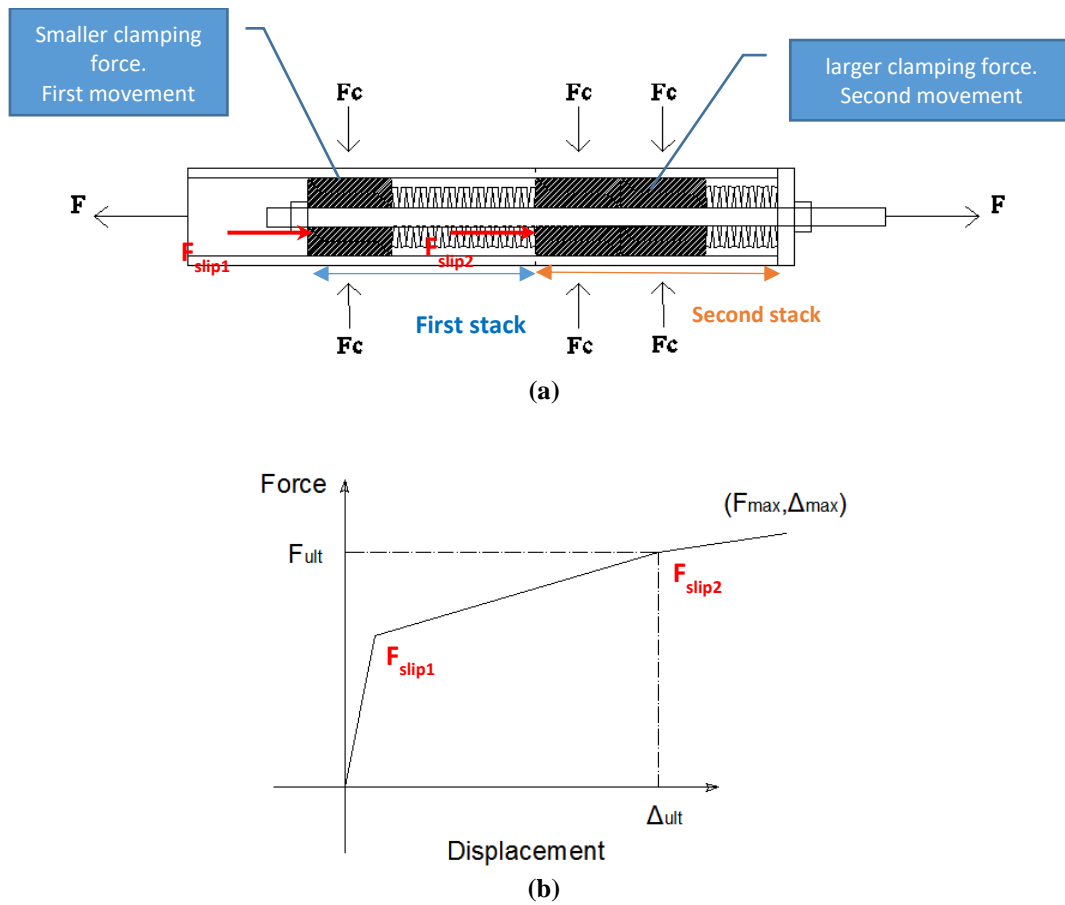


Figure 3. 14. (a) Multiple friction discs configuration, and (b) corresponding behaviour.

As mentioned before, one of the applications of such configuration can be considered for a situation when the actual earthquake is stronger than the design earthquake. In this case, this concept can be used as a secondary fuse. As can be seen from the graph, the slope of the loading curve is decreased after the ultimate force. Therefore, when this secondary fuse is implemented, it is possible to design the structure for a smaller force when for capacity design purposes at the Maximum Considered Earthquake (MCE) level. This could enhance the reliability and safety of the structure during stronger earthquakes than the design earthquake.

In the previous sections, the tension-only configuration of the damper was introduced. It should be mentioned that the SSC can be also designed for compression-only and double-acting configurations. Two configurations of the SSC related to the compression-only arrangement can

be seen in Fig. 3.15. In the first state, the damper is adjusted for compression-only configuration by adding a tab to one end of the tube and applying force to its other end. The second configuration for the compression-only SSC is shown in Fig. 3.14(b). According to this configuration, the set of springs and friction discs is pre-compressed and placed inside the tube. Then, this set is loaded using the external pistons.

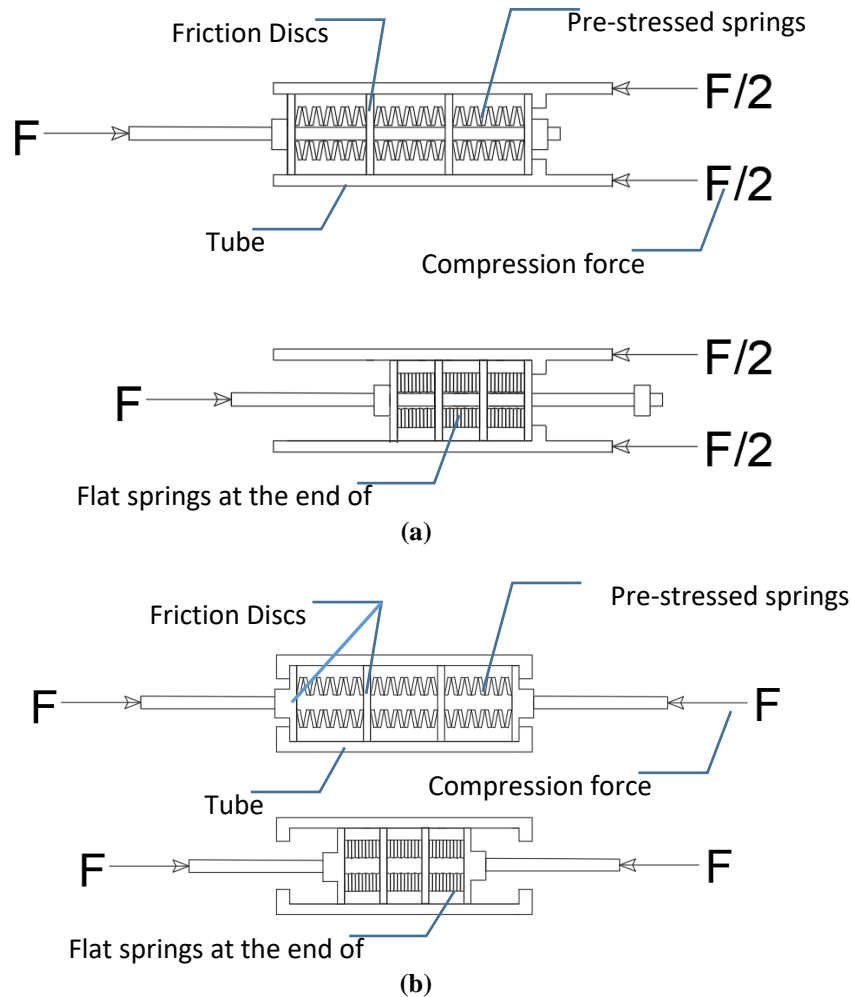


Figure 3. 15. SSC compression-only configurations.

In this section, a brief description is provided for the double-acting configuration (Fig. 3.16). In this configuration, the damper works in both tension and compression. Therefore, some engaging tabs should be placed at both ends of the tube, so that the friction discs are pressing and bearing against the tabs. Therefore, the damper has the capability for applying the force in tension and compression directions. As mentioned, different configurations of this damper can be utilised for

various applications. In the following section, some of the applications of SSC have been introduced.

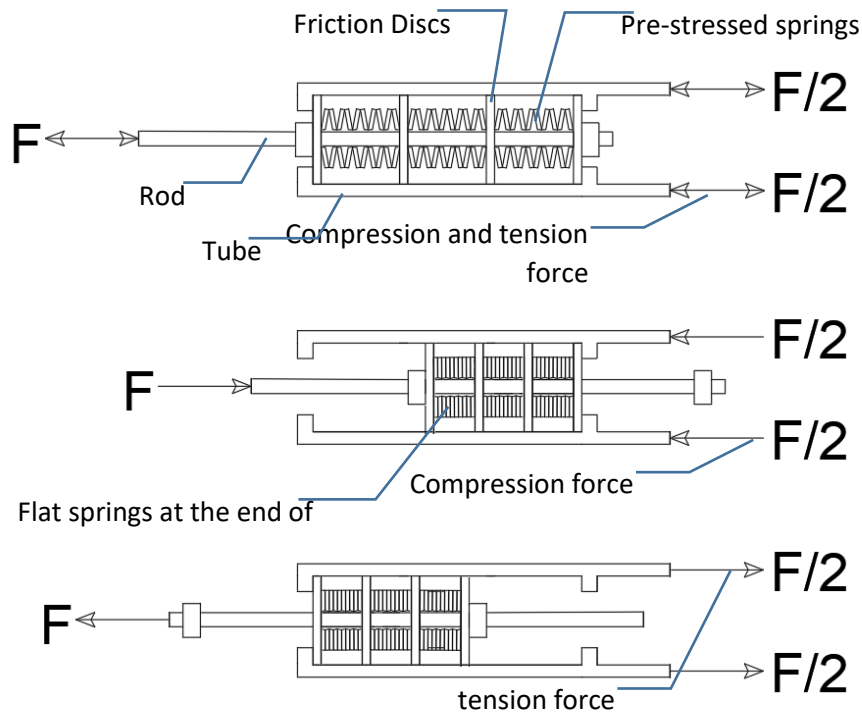


Figure 3. 16. Double-acting configuration.

3.8 Damper Applications

In this section, different applications of the SSC are discussed. In general, SSC can be used for dissipating dynamic energy due to seismic movements. However, it should be mentioned that self-centring is considered as one of the main features of the structures in which the SSC will be used. In structural applications, usually, the damper starts to dissipate the energy after the external force is above a certain threshold. Such feature brings efficiency to the system given the seismic resisting structures should have limited lateral displacement against the low to moderate magnitude earthquake and wind events, in order to preserve the comfort of the occupants. However, once the lateral loads exceed a certain threshold, such systems are able to resist large displacements and dissipate the energy for maintaining the safety of the users. It is noteworthy that in these systems, in addition to the safety of the occupants during the design earthquake, the structure can be

reoccupied after the design earthquake and is ready to resist the probable aftershocks. In the following, a brief description of the various applications of this damper will be presented.

3.8.1 Braced frames

Braced frames are one of the common seismic resisting systems. Their suitable flexibility in design and application has made them one of the popular systems for designers. SSC can be utilised with two different configurations in braced frames, which will be discussed in the following section.

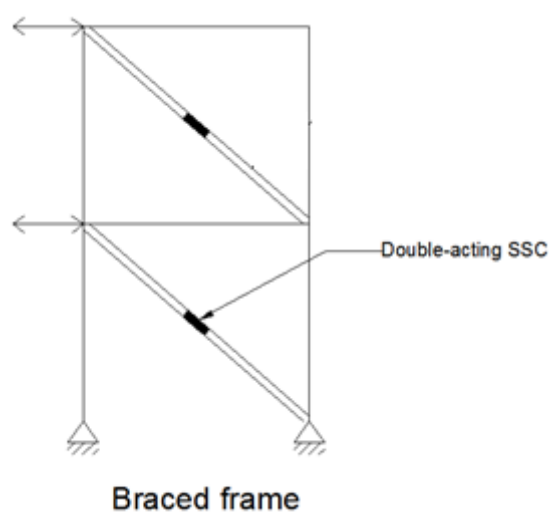


Figure 3. 17. Braced frame with tension-compression members using double-acting SSC.

According to the first configuration shown in Fig. 3.17, the structure can be designed using the Double acting configuration of this damper. It should be mentioned that in case of using such configuration, the brace member should be designed for both tension and compression forces. In addition, this system can be used for both steel and timber structures. If the tension-only configuration of this damper is adopted, cables or bars can be used as tension-only members. This application can be applied for the strengthening of existing structures. Fig. 3.18 presents a schematic view of such an application.

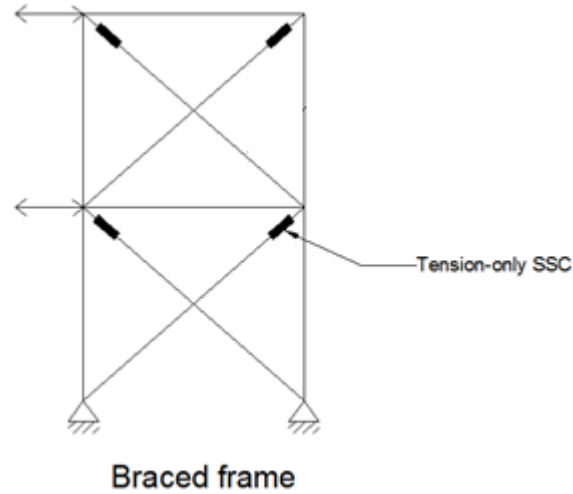


Figure 3. 18. Braced frame with tension-only members using tension-only SSC.

3.8.2 Moment resisting frames

Moment resisting connections with self-centring dampers have been studied in the past[56]. These connections are capable of dissipating the input energy through rotation at the end of the moment-resisting beams. In Fig. 3.19, the SSC applications in moment resisting frames is introduced where the connections are fixed. In the beam-to-column connection, two SSC's have been placed on top and bottom of the section to resist the bending moments (in both positive and negative directions) through coupled actions. These SSCs are in tension-only configuration and the force is transferred through the connection between the end of the beam and the column flange. For shear transformation, a shear connection is considered on the beam web with the slotted holes.

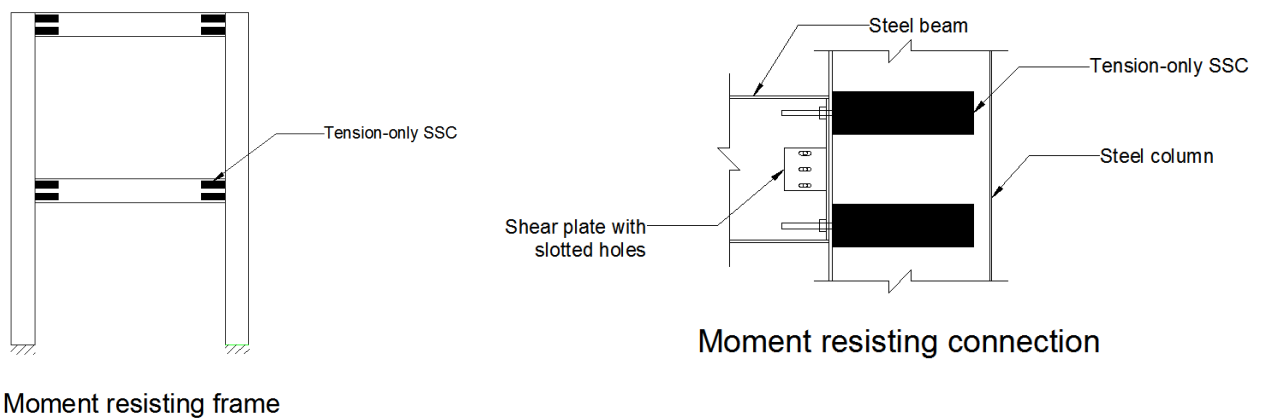


Figure 3. 19. The application of SSC in moment-resisting frames.

3.8.3 Rocking structures

As another potential application, the SSC could be used as a damper in rocking structures. In general, shear walls are one of the common lateral-load resisting systems in rocking structures. These walls can be made of timber, steel, or concrete materials. The main principle of rocking systems is based on the fact that the structure rocks around its toes during loading and the earthquake force will be balanced by the force required for swinging the structure. After unloading, the structure returns to its initial balanced position due to its self-weight. The important point that needs to be considered for rocking systems is the energy dissipation and the control of rocking movement. The energy dissipation happens by adding the energy dampers to the system. In addition, it should be mentioned that the presence of dampers in the structure can control the rocking movement and decrease the negative impact of pounding during unloading. The rocking shear wall systems can be designed using different methods. Some of the methods are detailed in Fig. 3.20. It should be mentioned that all of the rocking systems presented here can be designed using both tension-only and double-acting dampers. It should be noted that the self-centring aspect of the SSC negates the use of post-tensioning PT tendons as the rocking motion can be controlled by the SSC.

3.9 Numerical Modelling

In this section of the paper, the behaviour of the SSC is numerically investigated. In order to model the SSC in SAP2000 software, a parallel combination of two predefined links with similar self-centring and damping characteristics to the SSC being modelled is utilised.

To model the self-centring aspect, the behaviour of the pre-stressed springs can be simulated using a multi-linear elastic link. Pre-stressed springs have a bilinear response as mentioned in Fig. 3.21(a) where the pre-stressing force corresponds to the onset of softening. The softening stiffness (movement of the springs) of the bilinear curve is the same as of the springs with the maximum

point of (Δ_{ult}, F_s) as previously defined in this paper. Further explanation about the initial stiffness of the springs bilinear curve will be given later on in this section.

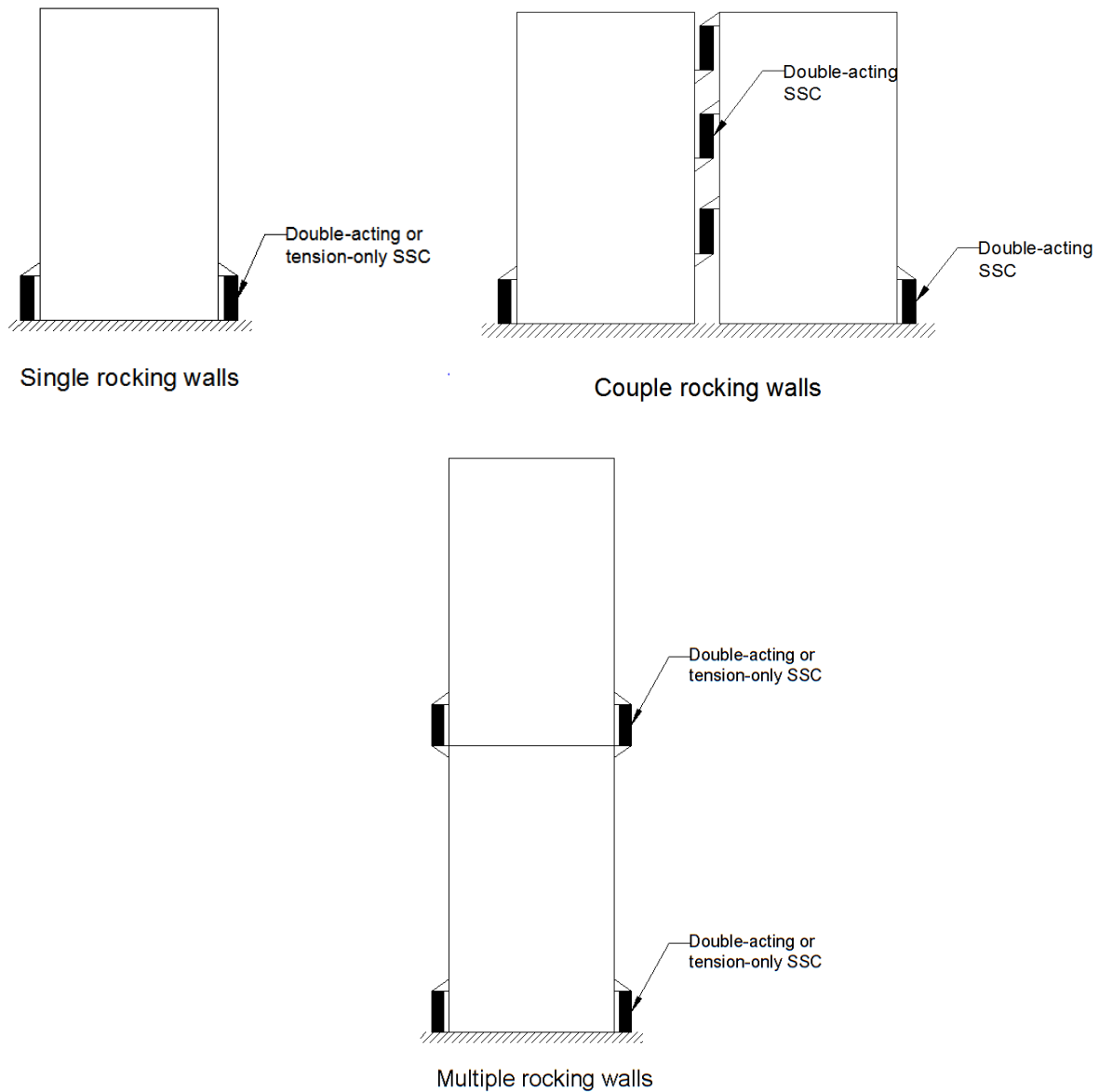


Figure 3. 20. The application of SSC in rocking wall systems.

For modelling the energy dissipation aspect of the SSC, a multi-linear plastic link is selected. It is a well-known approach for modelling friction behaviour using an Elastic Perfectly Plastic (EPP) curve. As shown in Fig. 3.21b, the friction force, F_{fr} , introduced in previous sections, represents the yielding force of the EPP curve and continues up to the maximum displacement (Δ_{ult}). The hysteresis damping of the EPP link is the equivalent of the energy being damped by friction in the SSC.

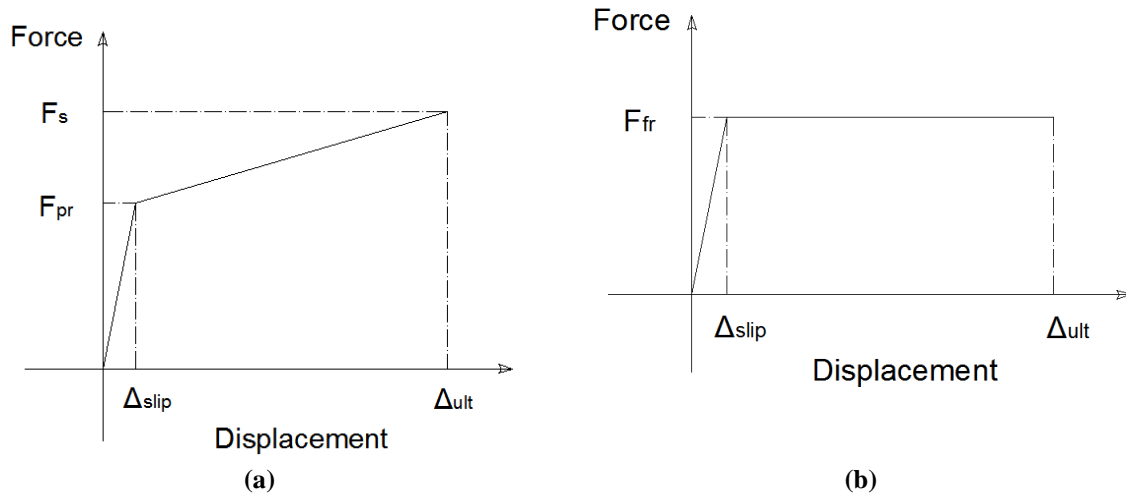


Figure 3. 21. (a) Multi-Linear Elastic (MLE) link representing pre-stressed spring behaviour, and (b) Multi-Linear Plastic (MLP) link representing friction behaviour.

The final link to be used for modelling consists of a parallel combination of the abovementioned links as mentioned in Fig 3.22a. The analytical combination of the two links results in the flag-shaped curve mentioned in Fig. 3.22b. The reader is referred to Eq. 3.1 to Eq. 3.5 for further detail on how friction and spring actions are combined.

For modelling the initial stiffness of the combined link it is crucial to know the elastic deformation of the SSC (Δ_{slip}) being modelled. as mentioned in the diagram in Fig 3.22c, at the slip stage the MLE link takes the spring force of F_{pr} and the MLP link takes the friction force of F_{fr} . The deformation of each link at this stage should be the same and equal to Δ_{slip} . As the links work in parallel the displacement of the assembly is equal to the displacement of each individual compartment. Therefore, as mentioned in Fig. 3.21a and 3.21b, the expected elastic deformation of the damper at the slip stage is considered to be the threshold of the initial stiffness of each MLE and MLP link.

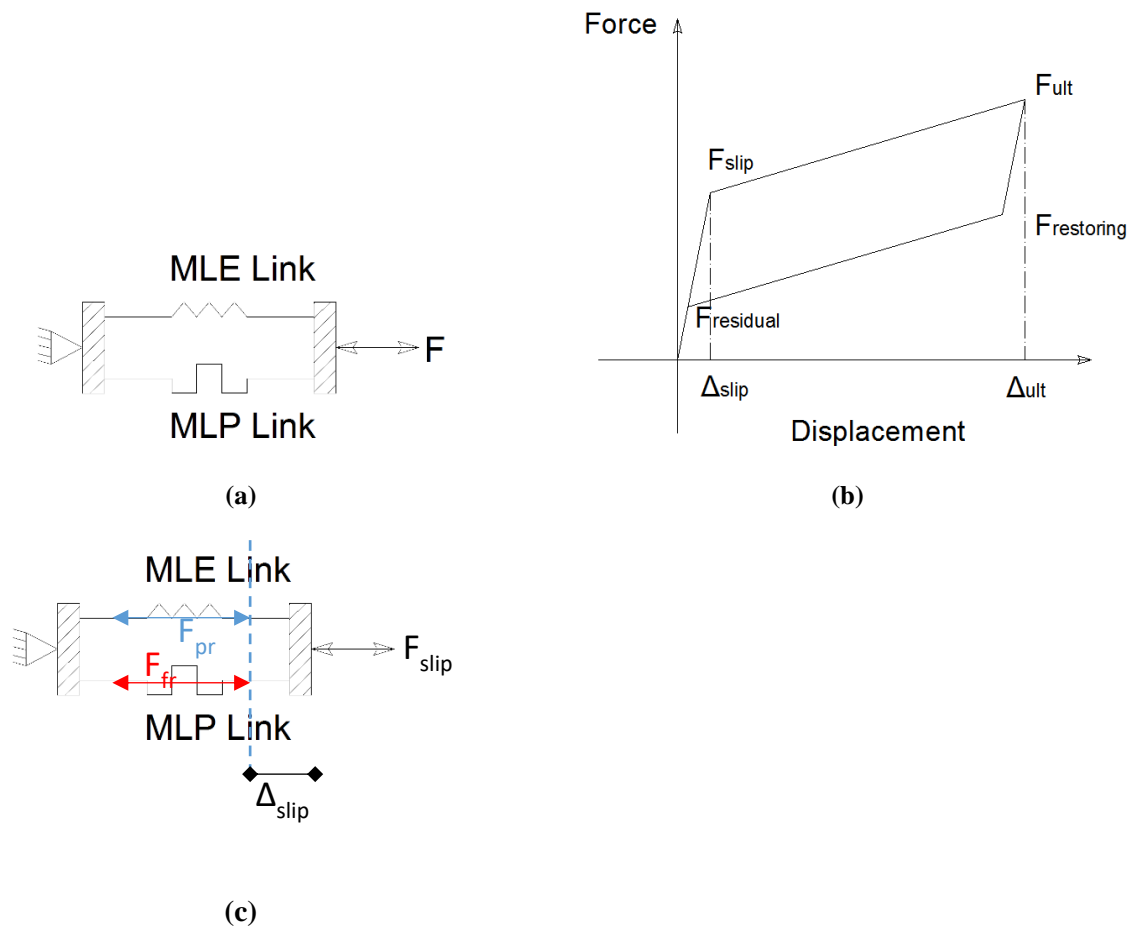


Figure 3. 22. Combination of MLE and MLP links.

In order to verify the accuracy of the modelling approach, a structural model of the SSC in SAP2000 [143] has been made as shown in Fig. 3.23 and compared to the experimental results. As it can be observed from the graph, good agreement is achieved for slip and ultimate forces. There is a negligible difference between the unloading lines which is mainly due to the convergence accuracy of unloading. However, As can be seen from the graphs, the area enclosed by the experimental and numerical curves are almost the same which results in the same energy dissipation characteristics. Accordingly, the results verify the use of the model for dynamic analysis purposes. The modelling parameters are summarised in table 3.4.

Table 3. 4. Numerical modeling parameters of the tested SSC

Parameter	Value
F_s (kN)	110
F_{pr} (kN)	49
F_{fr} (kN)	25
Δ_{slip} (mm)	2
Δ_{ult} (mm)	20

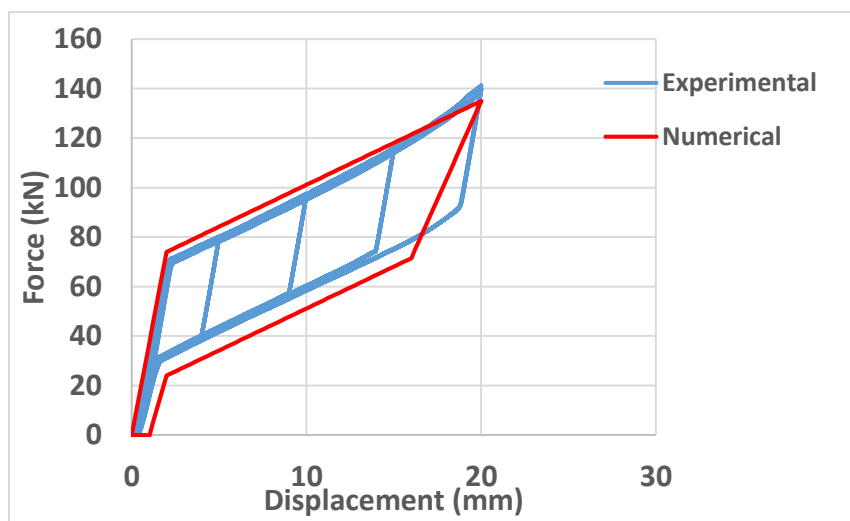


Figure 3. 23. The comparison of experimental result with the numerical model prediction of SSC.

3.10 Conclusions

In this manuscript, a new damper named SSC is introduced and presented. The SSC is a self-centring energy damper that dissipates the input energy through friction. The mechanism and different components of the damper have been explained and the equations governing the damper behaviour have been developed in this paper. Further, these equations have been verified using experimental test results. Also, the effect of different parameters such as pre-stressing force and friction have been investigated. It was observed that the increase in pre-stressing force can increase the ultimate capacity of the damper, but it does not make any change in the damping ratio. On the other hand, the displacement capacity of the damper is decreased. The capacity of the SSC and the damping ratio get enhanced with the increase in friction. However, it should be considered that the

self-centring capability of the damper should not be sacrificed by increasing the friction. In this paper, various configurations and variations of the damper have been proposed and the potential applications of the SSC in different LLRSs have been discussed. Finally, a general approach for modelling the damper using the structural analysis software, SAP, has been introduced. Given the accuracy of the numerical model, the design engineers could use common analyses and design software packages for modelling the structures equipped with SSC.

Chapter 4: Seismic Performance and Design of Rocking-wall Structures Equipped with Self-Centring Friction Connections

4.1 Abstract

Traditional ductile concrete shear walls have performed adequately in terms of saving lives in past earthquakes, as per the codes main performance objective. However, extensive repair or reconstruction costs are expected after moderate to severe earthquakes. As a solution, rocking concrete walls were introduced as a seismically low-damage system. Seismic assessment and design of rocking structures could be challenging considering the complexity of the performance. In this paper, a seismic design procedure is proposed for rocking concrete walls equipped with the new self-centring friction connections. The proposed design procedure is based on the Direct Displacement-Based Design (DDBD) method with an emphasis on the equivalent damping ratio rather than the ductility factor. First, the seismic design procedure is discussed, followed by its implementation in designing a prototype multi-story building. The structure is designed for two different configurations of lateral load resisting system; 1) rocking shear walls with double-acting hold-down connections using Resilient Slip Friction Join (RSFJ) and 2) rocking shear walls with tension-only hold-down connections using Self-Centring Structural Connectors (SSC). Finally, the seismic-performance measures of the designed structures are assessed using the Nonlinear Time History Analysis (NLTHA). The NLTHA results have shown that the performance requirements are met for the structures designed using the proposed approach.

4.2 Introduction

Ductile concrete shear walls dissipate the earthquake input energy mostly through the yielding of longitudinal reinforcements in flexure [8]. Other minor sources of energy dissipation are also observed such as yielding of transverse reinforcement, concrete crushing, aggregate inter-lock friction and sliding shear [144]. However, these behavioural modes are not desirable due to

associated brittle failure modes. In general, ductile concrete shear walls have performed well to meet the life-safety requirement of the code in the past earthquakes [145]. Strength, stiffness, ductility and energy dissipation, are the good seismic resisting characteristics of RC walls [146]. The plastic hinge region of the RC walls should be detailed adequately in order to represent the repetitive cyclic damping and to achieve the desired ductility [147].

In some cases, unexpected failure modes such as local instability, bar rupture and web crushing have been observed in the research and past earthquakes [1, 89]. Residual deformation is expected in RC shear walls after moderate to severe earthquakes. This residual displacement along with the damage in concrete and reinforcements imposes extensive repair or reconstruction costs [91]. Therefore, researchers suggested a move from ductile shear walls towards rocking shear walls as damage avoidance systems [9, 24].

Damage Avoidance Design (DAD) philosophy is the basis of the seismic design of the structures aimed not to suffer from damage due to Design Base Earthquake (DBE) [9]. The desired characteristics of damage avoidance systems are repeatable and predictable hysteresis damping and reliable self-centring. Different damage-avoidance systems have been introduced and tested successfully [13-18].

In order to achieve a structural system with advantages similar to RC walls, rocking concrete shear walls have been developed, tested and even used in real constructions [14, 34-36, 148]. The damage is controlled in rocking concrete shear walls as the yielding of reinforcement and concrete crushing is not expected in these systems [14, 20, 51, 111]. Also, controlled self-centring could be provided by either unbonded post-tensioning [10, 18, 24, 128, 148] or self-centring connections [111]. Therefore, problems related to damage and residual deformation are almost overcome in rocking walls designed based on DAD philosophy.

Unbonded post-tensioning was used in pre-cast concrete walls in PREcast Seismic Structural Systems (PRESSSS) in the early 1990s [31]. Detailed analytical studies on the behaviour of Single

Rocking Wall (SRW) systems was done by Kurama et al. [149]. They suggested using additional Spiral reinforcement at the wall toes to mitigate the damage of concrete due to crushing. Kurama and colleagues [33] also performed a series of studies on the unbonded PT walls with additional supplemental damping such as yielding, friction or viscous damping. The results showed that the additional dampers effectively reduce the seismic demand if they are properly designed. Priestley [24] used U-shaped Flexural Plates (UFPs) in coupled rocking wall systems. Other efforts were made for using internal grouted mild steel reinforcement for additional hysteresis damping [28, 29]. Externally mounted mild steel, Tension and Compression Yielding (TCY) dampers, as well as viscous dampers, were also designed and tested by Marriot et al. [35]. Sritharan and colleagues [34] suggested a PT rocking wall system as Pre-cast Wall with End Columns (PreWEC). In this paper, a rocking wall concept has been introduced in which post-tensioning tendons have been replaced with self-centring friction dampers as hold-down connections.

The Performance-Based Earthquake Engineering (PBEE) [150] such as Direct Displacement Based Design (DDBD) method [151] have been developed for seismic design of structures when other performance objectives are of more interest than the base shear determined by the force-based design method. In these concepts, performance objectives are selected at the beginning of the design stage. As such, the final design should meet the selected design objectives. For low-damage systems, damage control is the main design objective. Therefore, PBEE methods are the preferred design approaches when it comes to low-damage structures [152]. Usually, the maximum drift ratio is selected as the design objective. The DDBD has been used for the seismic design of rocking wall structures and the results were evaluated using experimental investigations [115]. In this paper, a DDBD approach will be outlined and used for the seismic design of self-centring structures and will be verified by designing a prototype structure.

In this study, the seismic performance and design of self-centring systems are discussed. DDBD is implemented while the concept of damping ratio and effective stiffness are used rather than the

ductility factor. It is emphasised that the response of self-centring systems with hysteresis damping can be the counterpart of an elastic system with viscous damping. Then, the proposed procedure is used for designing a multi-story structure equipped with rocking concrete shear walls. Two new different types of self-centring connections are used for designing the structure. The Resilient Slip-Friction Joint (RSFJ) [59] is used to represent a double-acting (tension and compression) hold-down connection. Also, The Self-Centring Structural Connector (SSC) [153] is used to represent a tension-only hold-down connection. Accordingly, the performance of the connections is discussed and verified with experimental results. Later, the performance of each structural configuration is discussed and verified as well. The prototype structure is designed based on the proposed design method. Finally, the performance of the structure is verified using the Nonlinear Time History (NLTH) analysis through the comparison of performance measures with the primary design objectives.

4.3 Displacement-based design of self-centring structures

Generally, self-centring structures can be considered as elastic structures having a bilinear performance. Accordingly, the seismic design of such structures is less complex than in-elastic or ductile structures. Such a conclusion could be made based on the following two points. First, in self-centring structures, residual displacement is not expected, and the structure will be at its initial position at the end of loading. Therefore, the use of the ductility concept, which is associated with plastic deformations, is hardly justifiable for self-centring structures. The second point refers to the fact that self-centring systems show a repetitive cyclic behaviour without strength or stiffness degradation. This means that the hysteretic energy being damped is equal in each cycle and there is less uncertainty in the assumption of damping ratios.

Considering the above-mentioned points, for self-centring structures, the use of elastic-design concepts based on stiffness and damping ratio is more applicable rather than in-elastic design concepts, which are based on ductility and yielding force. Self-centring structures usually have a

flag-shaped load-displacement response (Fig. 4.1). As can be seen from Fig. 4.1, a single degree of freedom system with flag-shaped behaviour and non-viscous damping, which is usually produced by yielding or friction, can be considered equal to an SDOF system with viscous damping.

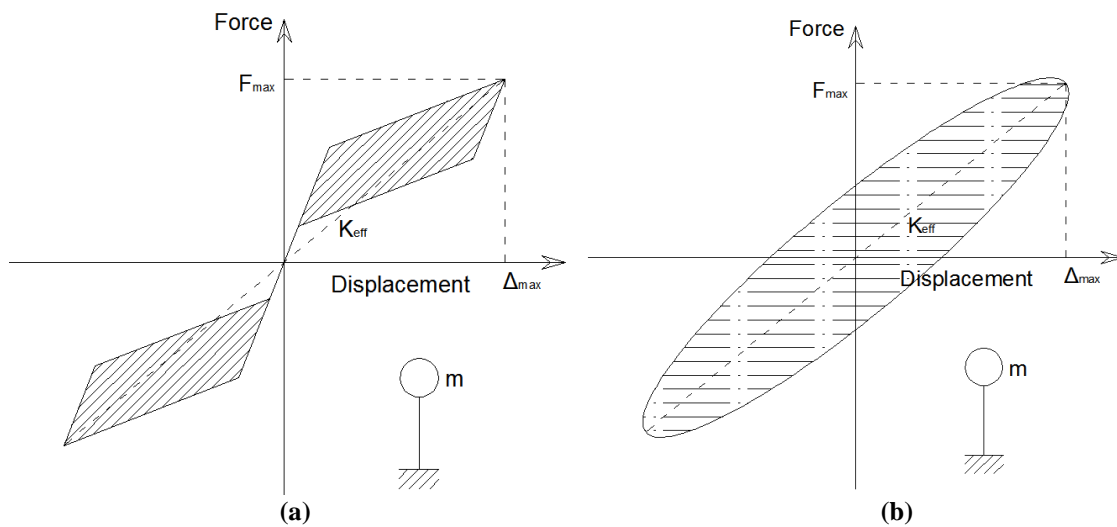


Figure 4. 1. Load-deformation response: a) Self-centring system with additional damping b) Elastic system with viscous damping.

Based on the graphs shown in Fig. 4.1, a self-centring structure is an equivalent of an elastic structure with similar effective stiffness when the damped energy in both systems are equal at the desired displacement demand of Δ_{max} .

The main difference between the two above-mentioned systems is the source of energy dissipation. In the elastic system, the viscous damping dissipates the energy while in the self-centring system, the energy is dissipated by yielding or friction. Unlike viscous damping, hysteretic damping is not a function of the system velocity. Therefore, different approaches should be used to model and solve the dynamic equilibrium equation. However, it has been shown [142, 154] that the hysteretic damping can be modelled as an equivalent viscous damping (ξ_{eq}) with an acceptable level of accuracy. Accordingly, a brief description of equivalent viscous damping is provided as follows. Equivalent viscous damping ratio (ξ_{eq}) is the combination of hysteretic damping ratio (ξ_{hys}) and the inherent viscous damping of the system at the period of vibration (ξ_v). The concept of hysteretic

damping ratio (ξ_{hys}) is illustrated in Fig. 4.2. It can be expressed by Eq. 4.1 which is a function of the hysteretic damped energy to elastic restored energy. Therefore, (ξ_{eq}) can be calculated using Eq. 4.2. It should be noted that, for the first design attempt, ξ_{hys} should be adopted based on an engineering judgment as the characteristics of the flag-shaped response are unknown at this stage.

$$\xi_{hys} = \frac{1}{4\pi} \frac{E_D}{E_S} \quad (4.1)$$

$$\xi_{eq} = \xi_{hys} + \xi_v \quad (4.2)$$

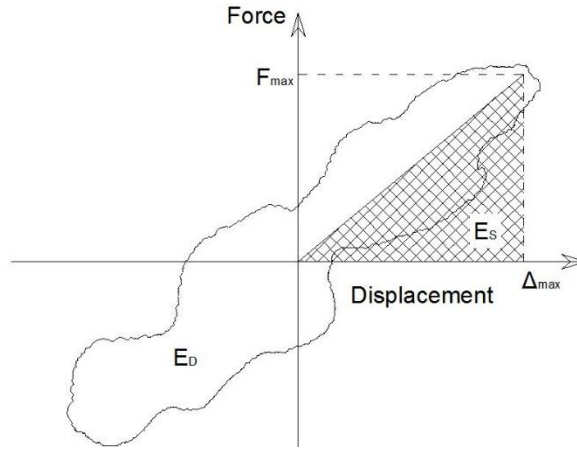


Figure 4. 2. Hysteresis dissipated energy and equivalent viscous damping concept.

In order to solve the equilibrium equation, in addition to the damping ratio, ξ_{eq} , we need to have the natural vibration period of the system (T_n). From Fig. 4.1, the maximum expected displacement, Δ_{max} , should be defined by the designer as a design objective. Δ_{max} or the displacement demand can be linked to the spectral acceleration based on Eq. 4.3 and Eq. 4.4.

$$\Delta_{max} = S_d = \frac{T_n^2}{4\pi^2} S_a R_\xi \quad (4.3)$$

$$R_\xi = \left(\frac{0.07}{0.02 + \xi_{eq}} \right)^{0.5} \quad (4.4)$$

where S_d is spectral displacement, S_a is spectral acceleration and R_ξ is the spectrum modification factor for the damping ratio being considered. Δ_{max} is known and the design spectrum, S_a , is available in the seismic code, T_n can be calculated using Eq. 4.3. When T_n is calculated, the ultimate force at the considered seismic hazard level can be obtained using Eq. 4.5 and Eq. 4.6.

$$k_{eff} = \frac{4\pi^2}{T^2} m \quad (4.5)$$

$$F_{max} = k_{eff} \Delta_{max} \quad (4.6)$$

where k_{eff} is the effective stiffness of the system at the ultimate displacement as mentioned in Fig. 4.1, m is the seismic mass of the system and F_{max} is the design seismic force. When F_{max} and Δ_{max} are known, the self-centring system can be designed based on the flag-shaped response parameters mentioned in Fig. 4.3. The details of this step are discussed as follows.

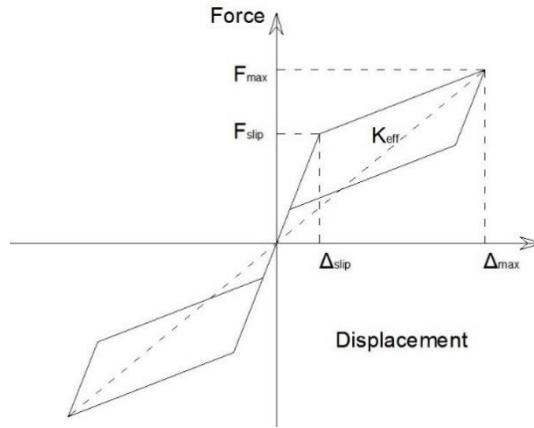


Figure 4. 3. Design parameters of an SDOF self-centring system.

Considering the response parameters mentioned in Fig. 4.3, F_{slip} and Δ_{slip} should be assumed by the designer. These parameters can be assumed based on different criteria selected by the designer considering the design requirements and performance objectives. Some of these criteria can be named as occupants' comfort, protection of non-structural components for serviceability limit state (SLS) earthquake and lateral wind deformation control. The following limits should be satisfied for the consideration of F_{slip} and Δ_{slip} .

$$\Delta_{slip} \leq \Delta_{SLS} \quad (4.7)$$

$$F_{slip} \geq F_{SLS} \quad (4.8)$$

where Δ_{SLS} and F_{SLS} are displacement and force at the SLS earthquake. When the required parameters are assumed based on Fig. 4.3, the system ultimate and slip forces and displacements should be redistributed in the structure in order to quantify the force and displacement demands of the self-centring connection components. Then, each component will be designed based on the

criteria required. At this stage, the preliminary design of the system is completed, and the design outcome should be verified.

In order to verify the primary design, a cyclic pushover analysis should be carried out. The structure should be laterally loaded up to the design displacement and then unloaded to its initial position under a reversed cycling loading for at least one full cycle. ξ_{hys} is calculated using Eq. 4. 1 based on the obtained force-displacement response. If the obtained ξ_{hys} from the graph is equal to the adopted ξ_{hys} in the first step, the design and analysis process has been converged and the design is completed. Otherwise, the previous steps should be repeated until convergence is achieved.

The procedure defined in the previous section is developed for single-degree of freedom (SDOF) systems. In order to extend the procedure to be used for multi-degree of freedom (MDOF) systems, the following equations can be used [151]. The indicative MDOF system and its equivalent SDOF system are mentioned in Fig. 4.4.

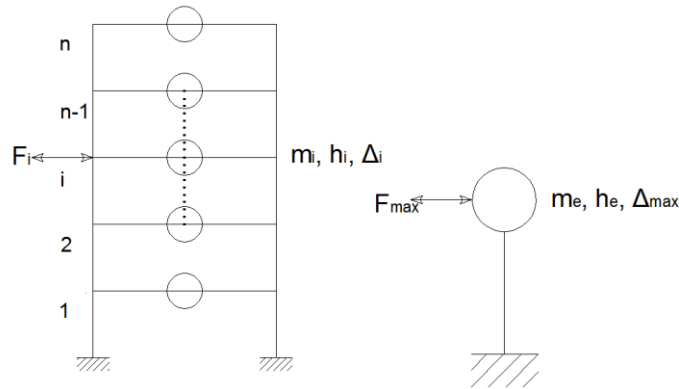


Figure 4. 4. Equivalent SDOF system of a multi-story building.

$$\Delta_{max} = \frac{\sum_1^n m_i \Delta_i^2}{\sum_1^n m_i \Delta_i} \quad (4.9)$$

$$F_i = F_{max} \frac{m_i \Delta_i}{\sum_1^n m_i \Delta_i} \quad (4.10)$$

$$m_e = \frac{\sum_1^n m_i \Delta_i}{\Delta_{ult}} \quad (4.11)$$

$$h_e = \frac{\sum_1^n m_i \Delta_i h_i}{\sum_1^n m_i \Delta_i} \quad (4.12)$$

where F_i , m_i , h_i and Δ_i are the seismic force, seismic mass, height and displacement of i^{th} degree of freedom, respectively. m_e and h_e are the seismic mass and height of the equivalent SDOF system. n is the number of freedom degrees in the direction being considered.

4.4 Self-Centring Friction Dampers

In the previous section, the seismic design of self-centring structures was discussed. There are several ways to provide the self-centring ability in a structure. It is important to note that a suitable self-centring system should provide enough damping in addition to its restoring capacity. Different concepts have been developed and tested to achieve self-centring and damping in the connection level. These self-centring concepts are generally based on viscous damping [42, 46], Friction [41, 130], a combination of friction and viscous [58, 132], shape memory alloys [66, 155] and lead extrusion High Force to Volume (HF2V) dampers [47, 50, 51].

Friction dampers have been widely studied and applied in earthquake resisting structures [39, 156, 157]. Adequate and repetitive energy dissipation along with flexibility in design and application are some of the advantages of friction dampers [158]. Accordingly, when the energy dissipation through friction is combined with self-centring capacity, a robust device could be achieved in terms of both re-centring and repetitive cyclic energy dissipation. There have been several devices developed by incorporating these characteristics [41, 57, 108, 130].

In this paper, the application of two new self-centring friction dampers in rocking concrete shear walls is studied in the seismic design of a prototype structure. The Resilient Slip-Friction Joint (RSFJ) is used to represent a double-acting hold-down connection [59]. Also, the Self-Centring Structural Connector (SSC) is used to represent a tension-only hold-down connection [153]. The performance of each damper is introduced in the following sections.

4.4.1 Resilient Slip-Friction Joint (RSFJ)

In RSFJs, the restoring force comes from the disc springs combined with the specific groove shape of the steel plates which are tied through high strength bolts [159]. By slipping of grooved plates,

the input energy is dissipated through frictional resistance. Based on the free-body diagrams presented in Fig. 4.5, the design procedure is developed for the prediction of the performance of the RSF joint [59]. The slip force (F_{slip}) and residual force (F_{res}) can be determined by Eq. 4. 13 and Eq. 4. 14:

$$F_{RSFJ,slip} = 2n_b F_{b,pr} \left(\frac{\sin \theta + \mu \cos \theta}{\cos \theta - \mu \sin \theta} \right) \quad (4.13)$$

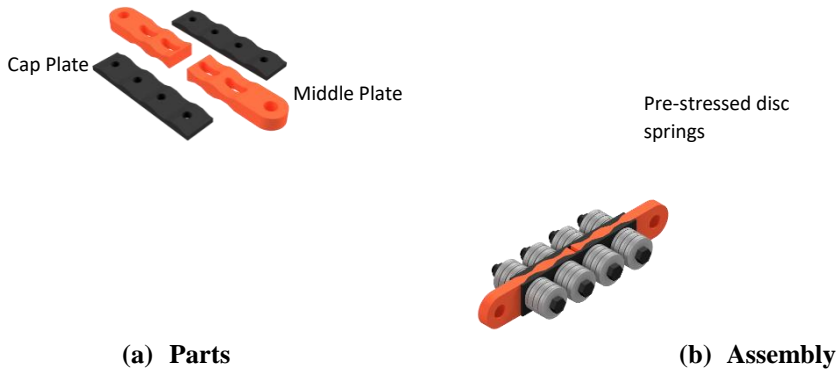
$$F_{RSFJ,res} = 2n_b F_{b,pr} \left(\frac{\sin \theta - \mu \cos \theta}{\cos \theta + \mu \sin \theta} \right) \quad (4.14)$$

where n_b is the number of bolts on each splice, θ is the groove angle, $F_{b,pr}$ is the clamping force of pre-stressing and μ is the coefficients of friction [160]. The general hysteresis behaviour of RSFJ is illustrated in Fig. 4.5(d). $F_{ult, loading}$ and $F_{ult, unloading}$ are the joint forces at the maximum disc springs displacement and bolts force during loading and unloading.

$$F_{b,u} = F_{b,pr} + K_s \Delta_s \quad (4.15)$$

K_s is the stiffness of each stack of springs and Δ_s is the displacement of the stacks. $F_{b,u}$ is the maximum force generated in the bolts. F_{ult} and $F_{restoring}$ are derived by replacing the bolt forces in Eq. 4.13 and Eq. 4.14 by Eq. 4.15.

The ultimate displacement of the joint (Δ_{ult}) is equal to $2\Delta_s / \tan \theta$



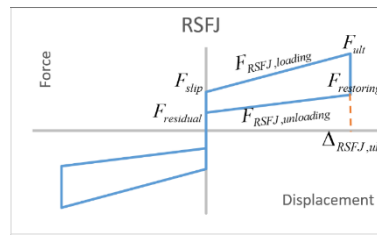
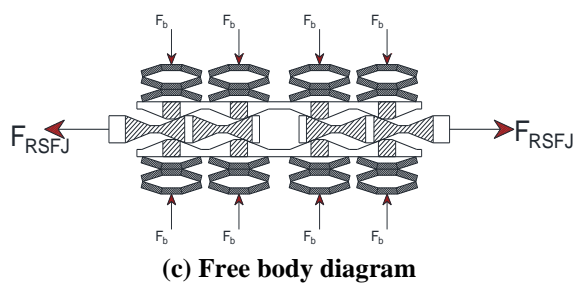


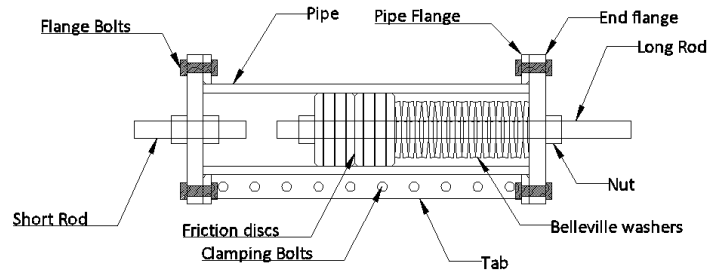
Figure 4. 5. Resilient Slip Friction Joint.

Several different applications of RSFJ have been developed and tested. For example, timber rocking walls [160], timber braces [161], tension-only braces [162]. Also, there are other applications under investigation [135, 138].

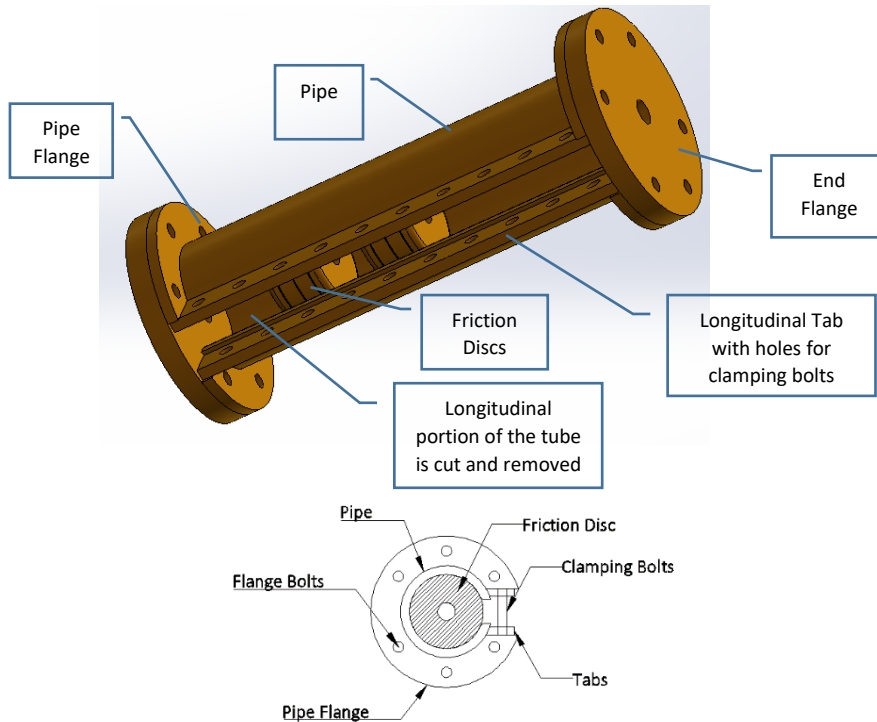
4.4.2 Self-Centring Structural Connector (SSC)

In this section, the arrangement of the components of SSC and its performance are discussed [163]. As shown in Fig. 6, one of the parts of the SSC is the friction discs. These discs along with the tube take the major role of energy dissipation in the damper. The normal force, which is perpendicular to the surface of the tube, is applied to these discs through the clamping bolts in the longitudinal tabs and split in the tube. The friction will be developed as the result of relative movement between the tube and the discs. The earthquake force is applied to the friction discs through rods.

Springs are responsible for the self-centring capability. In the SSC, Belleville washers are used for the spring members. Every single spring has a specific displacement capacity, Δ_s , and a corresponding load capacity, F_s , at the maximum displacement, which is called flatness load. In the design of SSC, the springs have been placed in the series layout. The number of these springs are selected based on the required displacement capacity of the SSC. It should be mentioned that the stack of the springs should be pre-stressed to the desired pre-stressing force before being inserted inside the tube.



SSC Longitudinal Section



SSC Transverse Section

Figure 4. 6. Self-centring structural connector.

The tube is another main component of the SSC. The sliding friction between the internal surface of the tube and the friction rings is the source of energy dissipation. At this stage, the tube clamping bolts are pre-stressed creating the normal force (perpendicular to the surface) between the disc and the tube to achieve the required slip friction force

In this section of the paper, the force-displacement performance of the SSC is analysed. As can be seen from Fig. 4.7, the developed damper in this study has a flag-shaped force-displacement response.

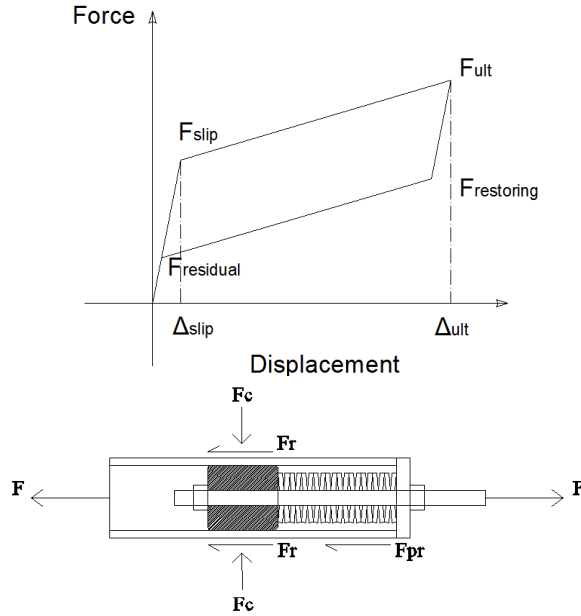


Figure 4. 7. Free body diagram and force-displacement response.

At the beginning of the loading stage, the force inside the damper is increased with an increase in the external force F . At this stage, friction force ($F_{friction}$) and the pre-stressing force ($F_{prestressing}$) inside the spring resist against the movement. The F_{slip} can be obtained using the following equation:

$$F_{slip} = F_{friction} + F_{prestressing} \quad (4.16)$$

The Δ_{slip} can be calculated using the principles of mechanics of materials. When the discs are flat, the damper has theoretically reached its maximum force capacity (F_{ult}). F_{ult} can be estimated using the following equation.

$$F_{ult} = F_{friction} + F_{prestressing} + K\Delta = F_{friction} + F_s \quad (4.17)$$

where K is the equivalent stiffness of the set of springs and Δ is the displacement capacity of the springs after pre-stressing. F_s represents the force capacity of the springs. The restoring force, $F_{restoring}$, can be calculated using the following equation.

$$F_{restoring} = F_s - F_{friction} \quad (4.18)$$

Eventually, after unloading, the damper returns to zero displacement. The external residual force in the system at this stage, $F_{residual}$, can be obtained using the following equation:

$$F_{residual} = F_{prestressing} - F_{friction} \quad (4.19)$$

In order to meet the self-centring condition, the pre-stressing force of the spring set should be greater than the friction force.

$$F \geq 0 \rightarrow F = F_{prestressing} - F_{friction} \geq 0 \rightarrow F_{prestressing} \geq F_{friction} \quad (4.20)$$

In the design of SSC, the normal force acting on the surface between the piston and the cylinder can be adjusted by the external clamping force. This force (F_c) is applied using the tube clamping bolts and nuts.

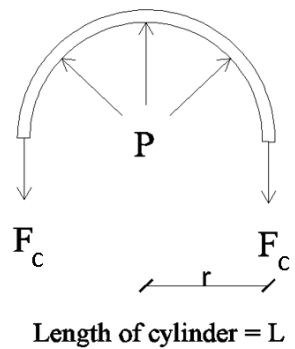


Figure 4. 8. Free body diagram of a cylinder with internal pressure.

As shown in Fig. 4.8, considering the equilibrium equations for the longitudinal section of the cylinder, the relationship between the clamping force (F_c) and the pressure (P) on the tube can be obtained using the following equation for a cylinder with a radius of r and the length of L .

$$F_c = PrL \quad (4.21)$$

At this stage, the friction force (F_{fr}) can be calculated using the pressure on the tube (P) and the friction coefficient, μ , between the two sliding steel surfaces. As per the test results, the μ , is considered to be 0.15 given the lubrication.

$$F_{fr} = 2\pi\mu F_c \quad (4.22)$$

In this section, the relationships governing the performance of the disc springs are discussed. Each disc spring has an ultimate force (F_s) and an ultimate displacement (Δ_s), in which the spring is completely flat. By considering n number of springs stacked in series, their maximum displacement (Δ_{max}) is calculated using the following equation:

$$\Delta_{max} = n\Delta_s \quad (4.23)$$

The stiffness of the series of springs (K) can be obtained using the following equation:

$$K = \frac{F_s}{\Delta_{max}} = \frac{F_s}{n \times \Delta_s} \quad (4.24)$$

The displacement of the stack of springs (Δ_{pr}) under the pre-stressing force of F_{pr} , can be calculated using the following equation.

$$F_{pr} = K\Delta_{pr} \rightarrow \Delta_{pr} = nF_{pr} \frac{\Delta_s}{F_s} \quad (4.25)$$

The maximum displacement of the springs stack after pre-stressing is equal to the maximum displacement capacity of the damper, Δ_{ult} , which can be calculated using the following equation.

$$\Delta_{ult} = \Delta_{max} - \Delta_{pr} = n\Delta_s - n\Delta_s \frac{F_{pr}}{F_s} = n\Delta_s \left(1 - \frac{F_{pr}}{F_s}\right) \quad (4.26)$$

The above equation presents the relationship between the pre-stressing force in springs and the maximum displacement expected from the SSC.

4.5 Seismic Design of the Prototype Structure

In this section, a five-story structure is analysed and designed based on the procedure described in the previous section. The gravity load-resisting system in this structure is a steel frame. The steel beams are connected to the steel columns using pin connections. Therefore, the steel structure only can resist the vertical loads. As for the lateral load resisting system, the rocking concrete shear walls are used. The plan and elevation dimensions of this structure are shown in Fig. 4.9. The dead load considered for each floor is 3.5 kPa including the weight of the structure, floors, ceilings and walls. The imposed live loads of 2.0 kPa and 0.5 kPa are considered for the floors and the roof, respectively. The required parameters for the response spectrum analysis are detailed as follows.

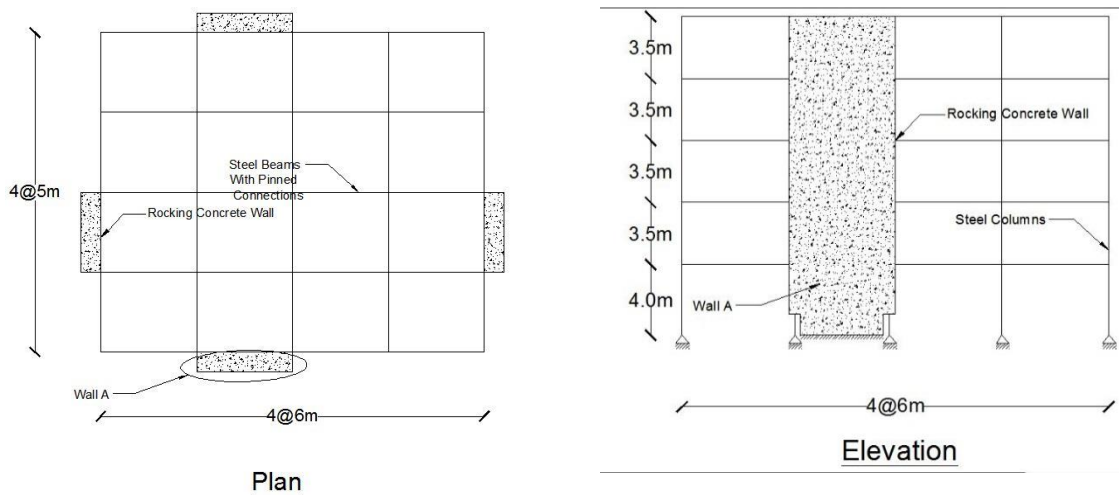


Figure 4. 9. Structural plan and elevation of the modelled building.

The structure is located in Christchurch, New Zealand on soil type class C or shallow soil site as per NZS 1170.5 [164]. The hazard factor, Z , for the Christchurch region is 0.3. A design working life of 50 years is adopted for this structure and the importance level of this building is considered to be 3. As per 1170.5 recommendations, the maximum inter-story drift of 2.5% is suggested for the ultimate limit state (ULS) earthquake. However, the experience from past earthquakes such as the Christchurch earthquake has shown that a smaller drift of 1.5% is a more realistic assumption [165]. Therefore, 1.5% maximum inter-story drift for the ULS earthquake is selected for the building modelled in this paper.

It should be noted that the selection of the design displacement limit should be based on a rational judgment considering the design performance objectives. Some of the criteria for adopting the design displacement demand can be named as follows. The occupancy type and importance level of the structure are significant factors. For example, the level of expected displacements in a hospital would be less than in a residential building. Also, the structural material, the deformation compatibility of the lateral load resisting system with the gravity system and the ability of the non-structural components to undergo the earthquake-induced deformation could be considered as criteria for adopting the design displacement limit. For example, the columns in the gravity resisting system should be analysed and checked at Δ_{max} for the effect of possible additional internal forces and the P-delta secondary effects.

The acceleration design spectrum can be derived from the code based on the parameters defined earlier. Accordingly, the annual probabilities of exceedance of 1/1000 for the ULS and 1/25 for the SLS earthquakes are considered based on the New Zealand standard 1170.0 [166]. Therefore, the return period factors are 1.3 and 0.25 for the ULS and SLS earthquakes, respectively. The S_a spectrum is mentioned in Fig. 4.10a. The displacement spectrum, S_d , is derived using Eq. 4. 3 and Eq. 4. 4 and is defined in Fig. 4.610b. h_e , m_e and Δ_{max} can be calculated using Eq. 4.9 to Eq. 12. These calculations are summarised in Table 4.1. It should be noted that as the first attempt, 15% equivalent damping ratio, ξ_{eq} , is assumed for this building. For, damage avoidance structures cracking of structural members is not as likely as ductile structures. Furthermore, less engagement between structural and non-structural components is provided due to the required displacement compatibility at larger drifts. Accordingly, less inherent viscous damping, ξ_v , is expected in damage avoidance structures compared to ductile ones and therefore the response is less sensitive to inherent viscous damping [167]. It is recommended that $\xi_v = 2\%$ can be a good assumption for analysis and design purposes [167] for rocking structures with additional supplemental damping. Therefore, the expected hysteresis damping for this structure, ξ_{hys} , can be calculated as 15%-2%=13%. The accuracy of this assumption will be examined later on in the final step of the design and should be adjusted if the archived damping is different from the first assumption.

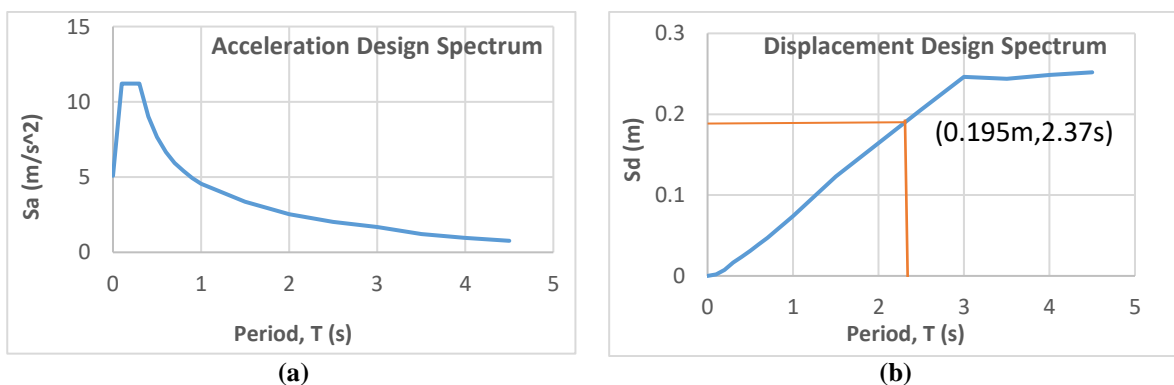


Figure 4. 10. Acceleration design spectrum (Left) and Displacement design spectrum (Right).

Table 4. 1. Multi-Degree of Freedom System (MDOF) parameters of the prototype building.

Story	h_i (m)	w_i (kN)	Δ_i (m)	$w_i\Delta_i$	$w_i\Delta_i^2$	$w_i\Delta_i h_i$
5	18	1680	0.27	453.6	122.472	8164.8
4	14.5	1968	0.2175	428.04	93.0987	6206.58
3	11	1968	0.165	324.72	53.5788	3571.92
2	7.5	1968	0.1125	221.4	24.9075	1660.5
1	4	1968	0.06	118.08	7.0848	472.32
sum		9552		1545.84	301.1418	20076.12

$$h_e = 13m$$

$$\Delta_{max} = 0.195m$$

$$m_e = 809 \text{ tons}$$

Based on the calculated Δ_{max} , the natural period $T_n = 2.37s$ is obtained from the design displacement spectrum as mentioned in Fig. 4.6b. The effective stiffness and ultimate base shear can be calculated using Eq. 4. 5 and Eq. 4. 6.

$$k_{eff} = 5685 \text{ kN/m}$$

$$F_{max} = 1107 \text{ kN}$$

The base shear is distributed along with the height of the structure using Eq. 4. 10 and the structure can be analysed accordingly. The vertical distribution of seismic load and the storey shears are summarised in Table 4.2.

Table 4. 2. Vertical distribution of seismic load and story shears of the modelled structure.

Story	F_i (kN)	V_i (kN)
5	324.99	324.99
4	306.68	631.66
3	232.65	864.31
2	158.63	1022.94
1	84.60	1107.54

When the analysis is completed, the forces and displacements in the self-centring connections are determined and the connections can be designed for the demand actions. As mentioned in Fig. 4.5, in this paper, Wall A is selected for a detailed design. In order to analyse the selected wall, the performance equations of a rocking wall equipped with self-centring Hold-downs are developed in the following section and the force generated in each self-centring connection is calculated.

4.6 Load-displacement performance of rocking walls

First, the performance of rocking walls with double-acting hold-downs are assessed and the equations are developed. Second, the same assessment is conducted for the rocking walls with tension-only connections. The system-level behaviour of a structure fitted with either tension-only or double-acting devices can be broadly similar, depending upon design decisions. The free-body diagram of the system with double-acting connections is illustrated in Fig. 4.11. The reader is referred to [168] for more details.

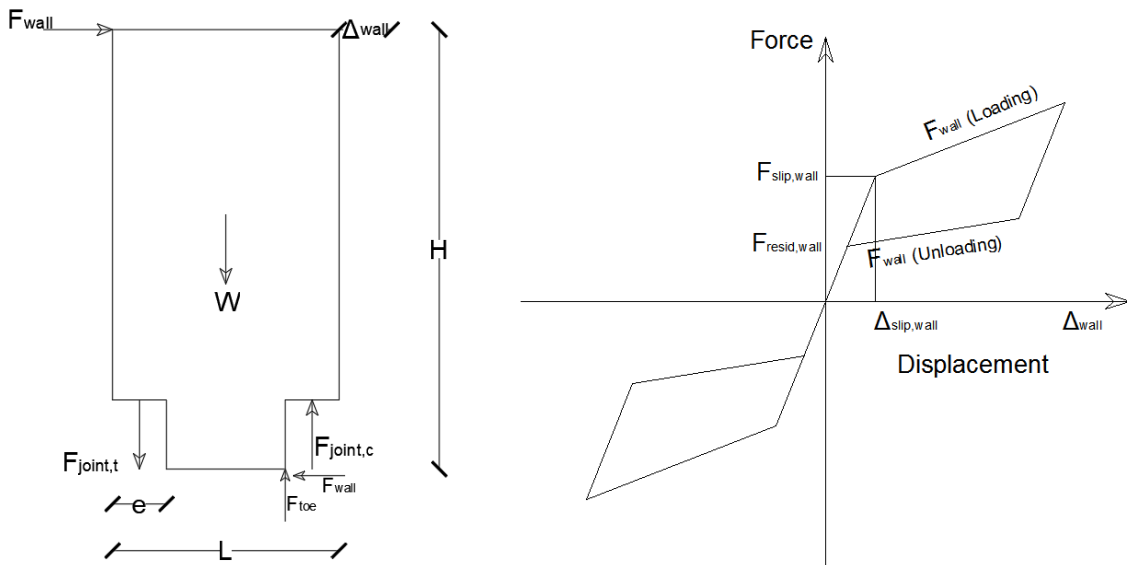


Figure 4. 11. The free-body diagram of rocking walls equipped with double-acting self-centring connections.

$$F_{slip,wall} = \frac{1}{H} \left[F_{slip,joint} (L - e) + w \frac{L - 2e}{2} \right] \quad (4.27)$$

$$F_{wall} = \frac{1}{H} \left[F_{joint,t} \left(L - \frac{3e}{2} \right) + w \frac{L - 2e}{2} + F_{joint,c} \frac{e}{2} \right] \quad (4.28)$$

$$\Delta_{wall} = \Delta_{elastic} + \Delta_{rot} \quad (4.29)$$

$$\frac{\Delta_{rot}}{H} = \frac{\Delta_{joint,t}}{L - \frac{3e}{2}} = \frac{\Delta_{joint,c}}{\frac{e}{2}} \quad (4.30)$$

$$\Delta_{elastic} = \frac{F_{wall}H^3}{3EI} \quad (4.31)$$

During the loading stage:

$$F_{joint,c} = \frac{e}{2L - 3e} (F_{joint,t} - F_{slip,joint}) + F_{slip,joint} \quad (4.32)$$

During the unloading stage:

$$F_{joint,c} = \left(\frac{e}{2L - 3e} - 1 \right) (F_{joint,t} - F_{resid,joint}) + F_{joint,t} \quad (4.33)$$

Where, $F_{slip,wall}$ is the lateral load acting on the wall at the onset of rocking motion, $F_{slip,joint}$ is the connections slip force and W is the weight of the wall. Other geometric parameters are mentioned on the wall. F_{wall} , is the lateral force acting on the wall during the loading stage of rocking motion, $F_{joint,t}$ is the force in the connection under tension and $F_{joint,c}$ is the force in the connection under compression. F_{fr} is the friction force generated at the bottom plates, the reader is referred to [168] for more details on how to calculate F_{fr} . $\Delta_{elastic}$, is the elastic deformation of the wall due to F_{wall} . $\Delta_{joint,t}$ and $\Delta_{joint,c}$ are the joints displacement under tension and compression due to F_{wall} , respectively. E and I are the modulus of elasticity and moment of inertia of the wall section. The residual force in the wall ($F_{resid,wall}$) can be obtained by replacing $F_{slip,joint}$ by $F_{resid,joint}$ in Eq. 4. 27. $F_{resid,joint}$ is the residual force in the joint at the end of the unloading stage.

The same analogy can be used for developing the equations governing a rocking wall with tension-only connections. The free body diagram of such a system is mentioned in Fig. 4.12. There is a main difference between tension-only and double-acting system. In tension-only systems, the governing equations are the same for before and after the onset of rocking motion (Eq. 4. 34). As for the displacements, the same equations as those developed for the double-acting systems can be used.

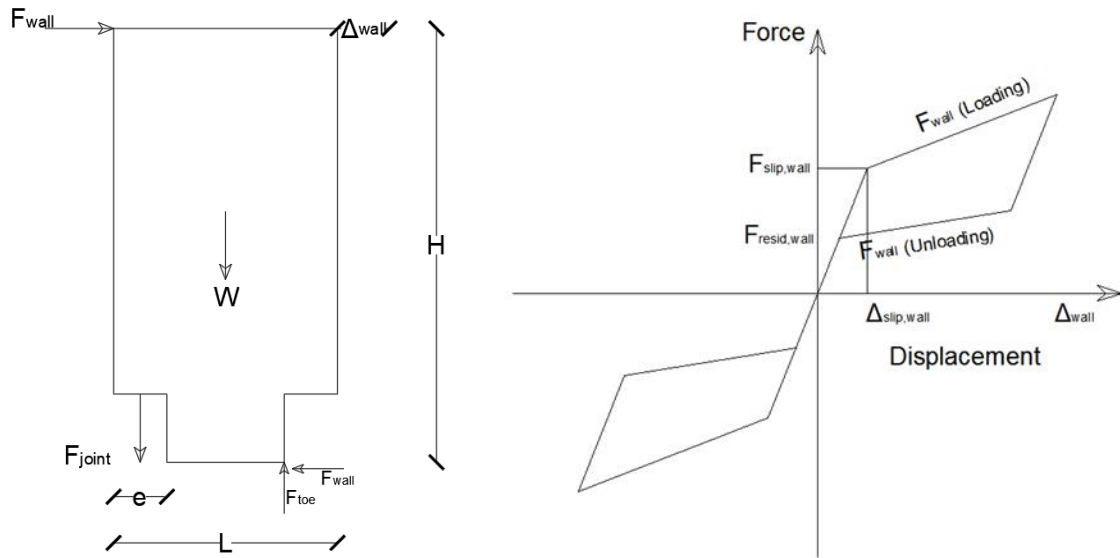
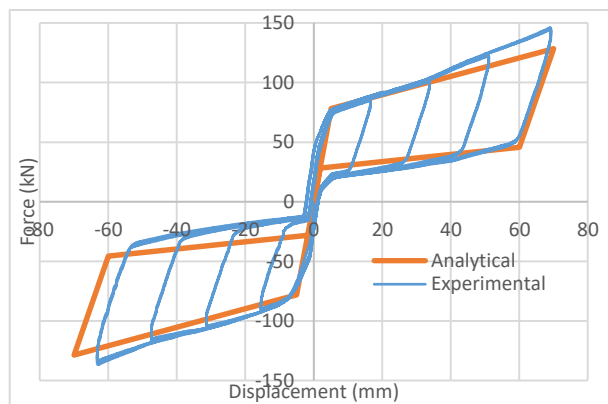


Figure 4.12. The free-body diagram of rocking walls equipped with tension-only self-centring connections.

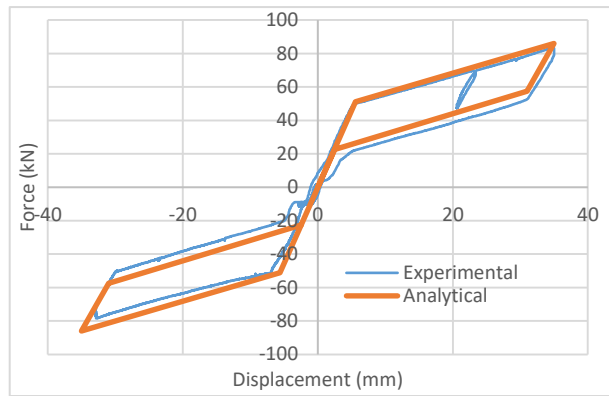
$$F_{wall} = \frac{1}{H} \left[F_{joint} \left(L - \frac{3e}{2} \right) + w \frac{L - 2e}{2} \right] \quad (4.34)$$

$$\frac{\Delta_{rot}}{H} = \frac{\Delta_{joint,t}}{L - \frac{3e}{2}} \quad (4.35)$$

The developed equations are verified through experimental investigation. The test demonstrations are illustrated in Fig. 4.13. the reader is referred to [168] for more details about the experimental testing and verification of the models developed. As can be seen from the graph, the load-displacement performance of the walls equipped with RSFJs and SSCs are accurately predicted by the developed equations.



(a)



(b)

Figure 4. 13. Experimental Verification: (a) RSFJ shear wall, and (b) SSC shear wall.

4.7 Design of the prototype building

For the prototype structure illustrated in Fig. 4.9, the force and displacement demands on the connections of Wall A can be calculated based on the developed equations. These calculations are made for both the RSFJ double-acting joint and the SCC tension-only joint. The required parameters for wall performance calculations are summarised in Table 4.3. First, the double-acting joint is considered. The prototype structure is considered to be symmetric. Therefore, half of the earthquake force in the longitudinal direction is taken by Wall A. The calculations for this wall are summarised in Table 4.4.

Table 4. 3. Geometrical and mechanical properties of Wall A.

H (mm)	18000
h_e (mm)	13000
L (mm)	6000
e (mm)	300
W (N)	810000
E (Mpa)	27500
I (mm ⁴)	5.40E+12

Table 4. 4. Force and displacement parameters calculated for Wall A with double-acting joints.

F_{wall}	560
$\Delta_{elastic}$	2.76
Δ_{wall}	195
Δ_{rot}	192
$\Delta_{joint,t}$	82.1
$\Delta_{joint,c}$	2.2
$F_{slip,wall}$	373
$F_{slip,joint}$	467
$F_{joint,t}$	905
$F_{joint,c}$	479

Force: kN
Displacement: mm

Therefore, the wall should be designed for $F_{wall} = 560\text{kN}$. A design displacement, Δ_{wall} , of 195mm is also obtained for the wall. All of the other parameters required for the design of the wall are summarised in Table 4.4. As mentioned before, $F_{slip,wall}$ should also be determined before analysing the structure for hold-down demands. The slip force should be assumed based on the performance requirements and the designer's judgment; however, it could be larger than the expected SLS earthquake force. In such a case, the displacement is limited to the elastic deformations at the SLS earthquake as the connection slip and wall rocking would not occur beforehand. It should be noted that the $F_{slip,wall}$ is also a function of the adopted self-centring connections. As obvious, the characteristics of the self-centring connection will govern the final flag-shaped response of the structure.

The double-acting connection can be designed based on the demands calculated in this section. A Resilient Slip-Friction Joint (RSFJ) is designed for the double-acting hold-down. The force-displacement response of the joint is shown in Fig. 4.14(a). To achieve the required displacement and damping, the RSFJ groove angles should be adopted precisely. The smaller the angle is, the

more displacement and damping is expected from the joint. For this particular design (Fig 4.14 a) the small groove angle (15°) resulted in a small restoring force (87 kN) and the unloading line visually get closed to the horizontal origin line.

Similar to the procedure explained above for a double-acting joint, Wall A is analysed for a tension-only joint. The design and analysis parameters for tension-only configuration is summarised in Table 4.5. Accordingly, a Self-centring Structural Connector (SSC) [153] is designed to represent the behaviour of the tension-only connection for Wall A. The load-deformation characteristics of this tension-only joint is shown in Fig. 4.14(b).

It should be noted that in the RSFJ, the friction and pre-stressing are coupled together as by increasing the displacement during loading, the friction increases due to more clamping force coming from the grooves. During un-loading, however, the friction decreases as the clamping force decreases at this stage. Different friction forces during loading and unloading results in different loading and unloading slopes as can be seen from Fig. 4.14a.

However, the same loading and unloading stiffness can be observed for SSC, as mentioned in Fig. 4.14b, as friction and pre-stressing are uncoupled and act independently in this concept.

Table 4. 5. Force and displacement parameters calculated for Wall A with tension-only joints.

F_{wall}	560
$\Delta_{elastic}$	2.76
Δ_{wall}	195
Δ_{rot}	192
$\Delta_{joint,t}$	82
$F_{slip,wall}$	373
$F_{slip,joint}$	480
$F_{joint,t}$	918

Force: kN

Displacement: mm

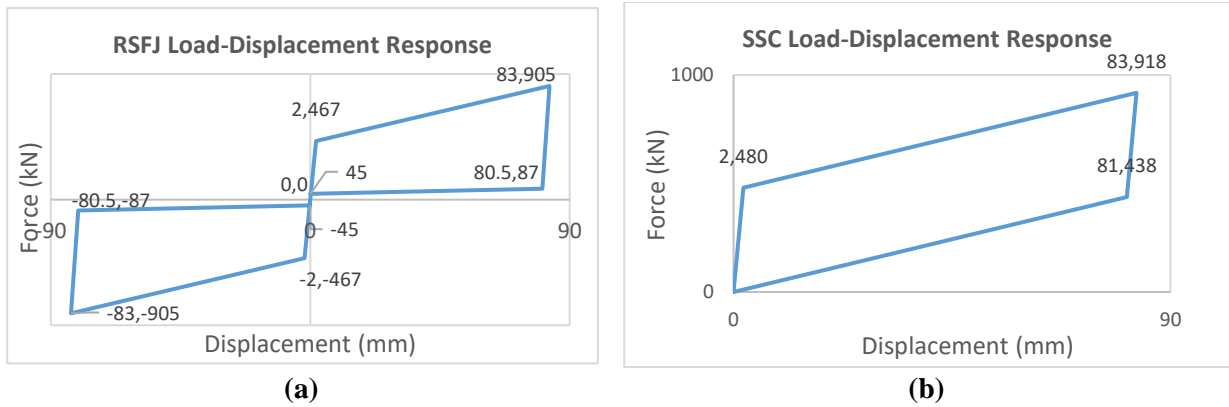


Figure 4. 14. RSFJ hysteresis behaviour designed for representing the double-acting joint (Left), and SSC hysteresis behaviour designed for representing the tension-only joint (Right).

At this stage, a numerical model of the structure is made and analysed under cyclic pushover analysis. Firstly, the structure is designed under the gravity load. The New Zealand Standard for Designing Steel Structures, NZS 3404 [169], has been used for this purpose. The designed section for the beams is 310UB47 and for the columns is 310UC118, the design yield strength of 350 MPa is considered for the steel material. The three-dimensional model of the structure is shown in Fig. 4.15. The beams end connections and column base connections are considered as pins. The shear walls are located at the external frames and connected to the structure. The seismic mass is assigned to the centre of mass on each floor. A brief description of the modelling of the rocking walls and their connections to the floors is provided, as follows.

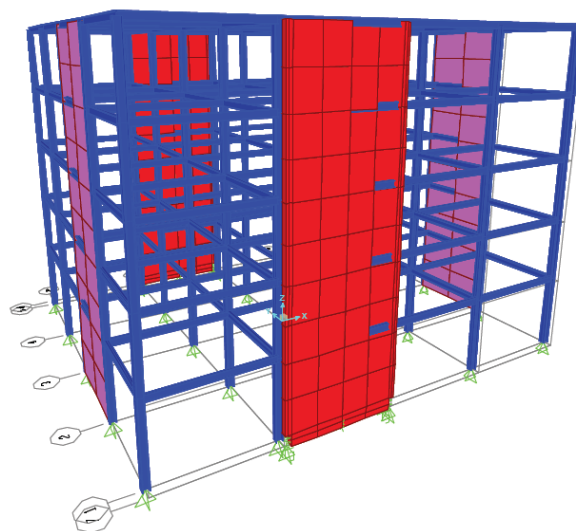


Figure 4. 15. Three-dimensional model of the designed structure.

In order to model the rocking walls in SAP2000, different elements have been used as shown in Fig. 4.16. The RSFJs are modelled using the Friction-Spring links. The Gap elements represent the compression-only connection of the wall to the top of the foundation. The Gap elements, with zero opening dimension, allow the wall to rock about its toes. To restrain the wall in the horizontal direction, shear keys should be used. In the model, the middle point at the bottom of the wall is restrained against horizontal movement to represent the shear key behaviour. Finally, the connection of the wall to the foundation should be modelled.

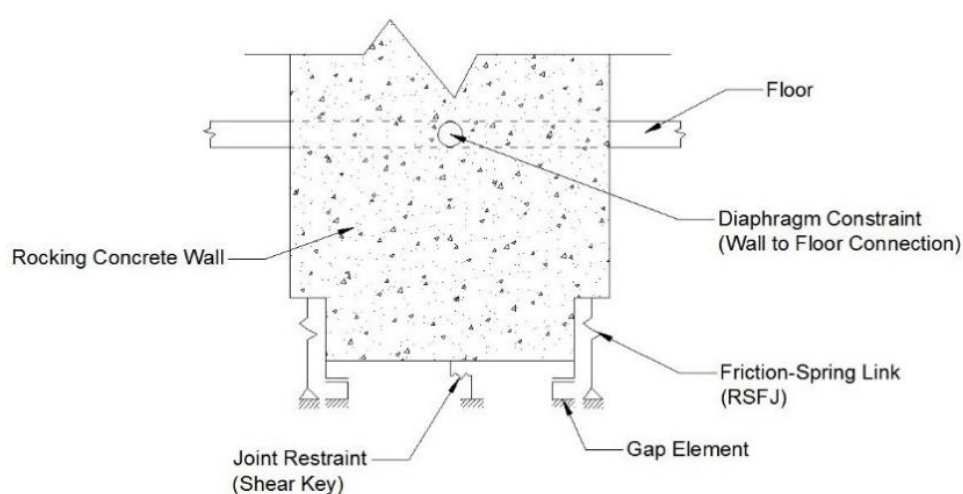


Figure 4. 16. Elements used for the structural modelling of rocking walls with RSFJs.

The performance of the wall to floor connection is important both in practice and numerical modelling. This connection should be capable of transferring the seismic loads from floors to rocking walls. Therefore, a rigid horizontal connection is required between the wall and floor. At the same time, the connection should allow the relative vertical movement between the wall and floor as the result of wall uplift during rocking. Accordingly, the wall will be able to rock freely without being restrained by the floor, otherwise, there would be additional bending demand on the floors and gravity would also contribute to self-centring. A variety of solutions have been proposed by researchers to provide such a flexible connection [170-172]. In this research, all of the nodes at the roof and the central node of the wall at the same level are horizontally constrained as a diaphragm. The diaphragm constrains the nodes to move together horizontally but allows them

to move separately in the vertical direction. As such, for modelling this connection, there is no need to use any kind of elements.

The modelled structure was loaded under gravity loads and then analysed under cyclic pushover analysis for seismic actions. The pushover hysteresis curves for both SSC equipped and RSFJ equipped structures are shown in Fig. 4.17. It should be noted that the vertical load distribution obtained in previous sections was used to perform the pushover analysis.

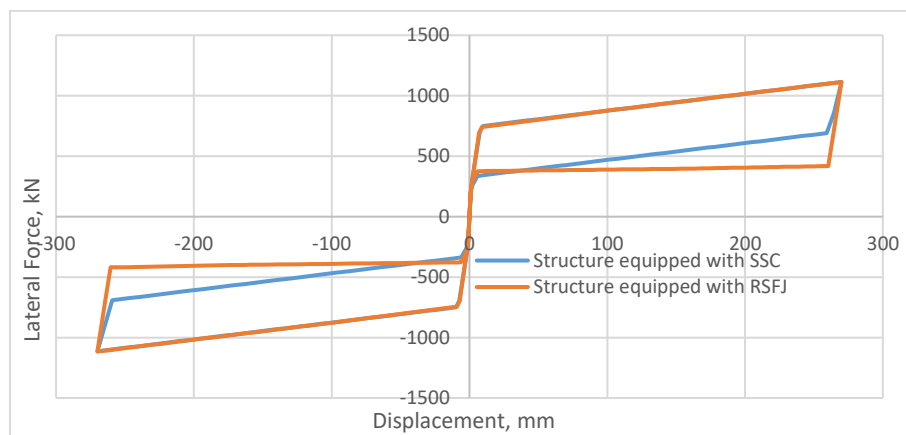


Figure 4. 17. Load-displacement response of the RSFJ and SSC shear walls obtained from the analysis

In this section, the assumed damping ratio for the first attempt should be compared to the damping ratio obtained from the graph. For the RSFJ shear wall, the hysteric damping ratio, ξ_{hys} of 14%, is obtained for the graph shown in Fig. 4.17 (orange graph) using Eq. 4. 1. The hysteresis damping ratio determined here is slightly higher than the assumed hysteresis damping ratio of 13% at the first step. However, in terms of design, it is conservative as this damping is more than what was expected primarily. Therefore, further design iteration is not required. The equivalent viscous damping ratio of 16% (= 2% + 14%) is achieved for this structure. In the next section, the reliability of the proposed design procedure will be verified against non-linear time history analysis.

As the final check, the displacement of the structure for the SLS earthquake is compared to the code requirements. The SLS base shear can be calculated as $R_s F_{wall} / R_u$ which is equal to 213kN (=0.25/1.3*1107). As per NZS1170.5, the lateral drift at the SLS level should be kept at less than 0.33%. This requires the roof lateral displacement to be less than 59mm at the SLS earthquake. As

per the graph shown in Fig. 4.12, the roof displacement is less than 59mm which is the maximum displacement allowed as per the code. Therefore, the SLS earthquake requirement is met.

In this part of the paper, the structural model of the wall equipped with tension-only connectors is presented. The Self-centring Structural Connectors (SSC) is selected for the tension-only hold-downs. The energy dissipation mechanism of SSC is slightly different from the RSFJ. Therefore, the modelling approach for the connections is also different. In order to model the SSC, Multi-Linear Plastic (MLP) and Multi-Linear Elastic (MLE) links should be connected in paralleled configuration to make a single link. The reader is referred to [163] for more information in this regard. The modelling approach is illustrated in the diagram shown in Fig. 4.18. Another different aspect of modelling is how to consider the tension-only behaviour for the connections. As shown in Fig. 4.19, the Hook element is used for connecting the SSCs to the foundation. The Hook elements work only in tension and prevent any compression force to be generated in the connections.

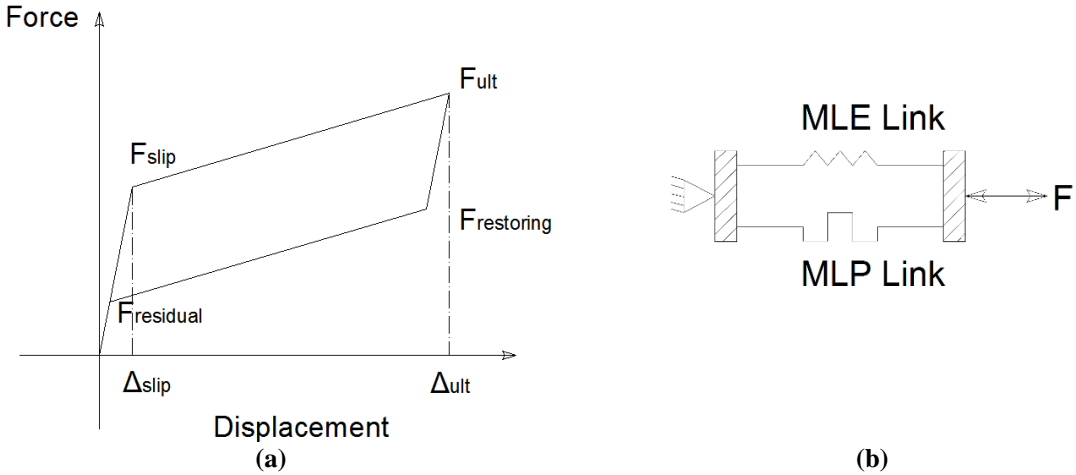


Figure 4. 18. Combination of MLE and MLP links for modeling SSC.

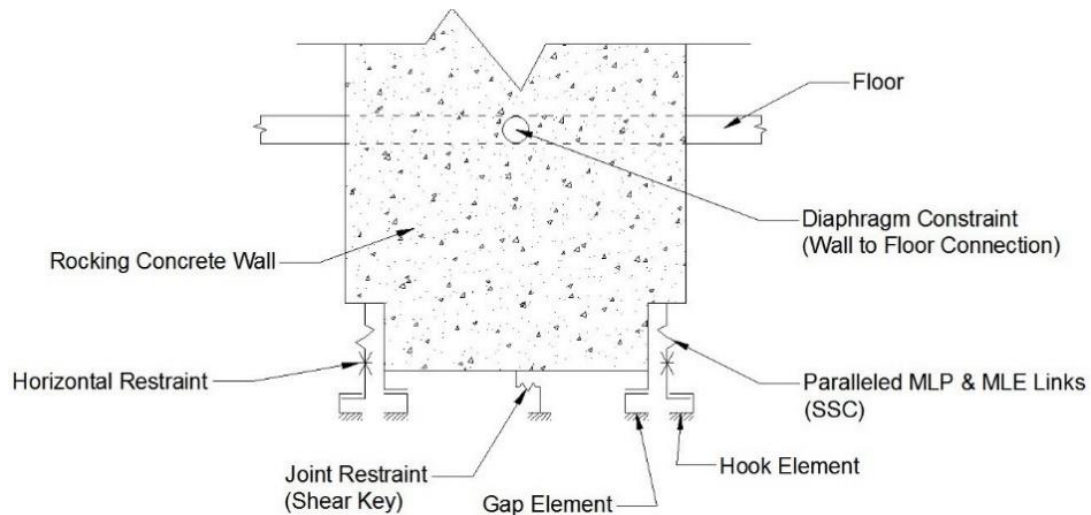


Figure 4.19. Elements used for the structural modelling of rocking walls with SSC.

The structure is loaded and analysed under cyclic pushover analysis. The load-displacement graph is shown in Fig. 4.17. The ξ_{eq} of 12% is calculated for this structure which is less than the primary assumption of 15%. There are two approaches for the next design attempt. First, the previous steps can be repeated with new ξ_{eq} of 12% and continue until reaching a convergence. Second, the design of the dampers can be reconsidered to achieve a higher damping ratio. Then, the cyclic pushover analysis and the measurement of ξ_{eq} should be repeated until convergence. Any approach has its challenges which depends on the structure being considered, the adjustability of the selected damper and design performance objectives. In this paper, the second approach is selected as finally a higher damping ratio is achieved. The design of SSCs are reconsidered and new joints are designed to achieve a higher damping ratio. To achieve a higher damping ratio in the SSC, the slip force of the damper is increased. The load-displacement performance of the re-designed damper is mentioned in Fig. 4.20(a). The structure is analysed under displacement controlled cyclic loading and the flag-shaped response of the structure is obtained as mentioned in Fig. 4.20(b). A ξ_{eq} of 0.15 is achieved for the structure with new SSCs which is equal to the primary assumption of the equivalent damping ratio. Therefore, the design of the structure equipped with tension-only SSC is finished.

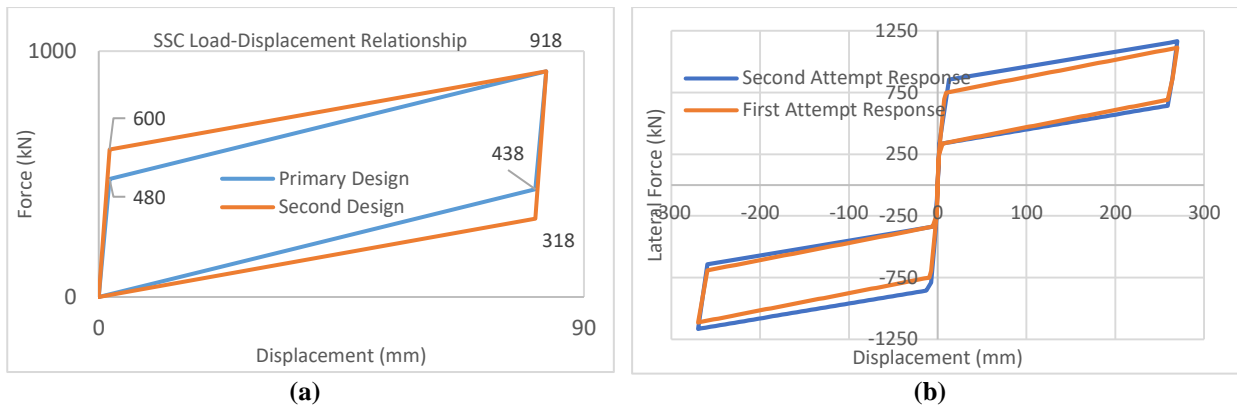


Figure 4.20. Comparison of the response parameters of the re-designed SSC with the primary design:
a) at the component level, and b) at the global level.

4.8 Nonlinear time-history analysis

In this section, the multi-story building designed based on the proposed design procedure in the previous section is analysed under nonlinear time-history analysis. The NLTHA will be carried out for both structures equipped with double-acting and tension-only seismic connections. Eight different earthquake scenarios are selected and scaled based on New Zealand Seismic code. The results are only discussed for the seismic excitation in the x-direction.

In order to scale the ground motions, the following assumptions are made. The structural performance factor, S_p , defined in NZS 1170.5 is selected as equal to one. The S_p factor in the code is considered for taking into account the effect of the over-strength of the yielding materials as well as the additional damping of the non-structural components contributing to the seismic response of the structure. In the structures designed using seismic dampers, especially those with self-centring capacity, the effect of such parameters is negligible. Therefore, a structural performance factor of one seems to be more applicable for such structures when scaling the ground motions.

Another important factor in the scaling of ground motions is to select an appropriate period range of interest. As per NZS1170.5 and its commentary recommendations [173], for rocking structures, it is better to select the upper limit of the period range of interest equal to the effective period of the structure at the maximum expected displacement in the limit state being considered.

Accordingly, the effective stiffness, K_{eff} , should be used to calculate the upper limit of the period range. Even though there is not a specific recommendation for the lower limit of the period range in the code, it is mentioned that additional considerations should be considered for selecting the lower limit based on the design objectives and design conditions. In this research, the lower band of the period range is selected as the period in which the spectral acceleration in the design spectra starts to decrease after the constant acceleration range. Therefore, the lower range is selected as 0.3s for this scaling. Consequently, a wider range of periods for scaling the ground motions is considered. The selected ground motions and the scale factor of each ground motion are summarised in Table 4.6. The acceleration spectra of the scaled ground motions are compared with the design spectra as shown in Fig. 4.21.

Table 4. 6. Selected Ground-Motions and corresponding scale factors.

Year	Ground Motion	Station	Scale Factor
1979	Imperial Valley	El Centro	0.89
1978	Tabas	Tabas	0.47
2010	Darfield	Hororata School	0.48
1994	Northridge	Saticoy St.	0.58
1989	Lomapieta	Saratoga	0.85
1995	Kobe	Amagasaki	0.69
1999	Duzce	Duzce	0.55
2011	Christchurch	Botanical Gardens	0.57

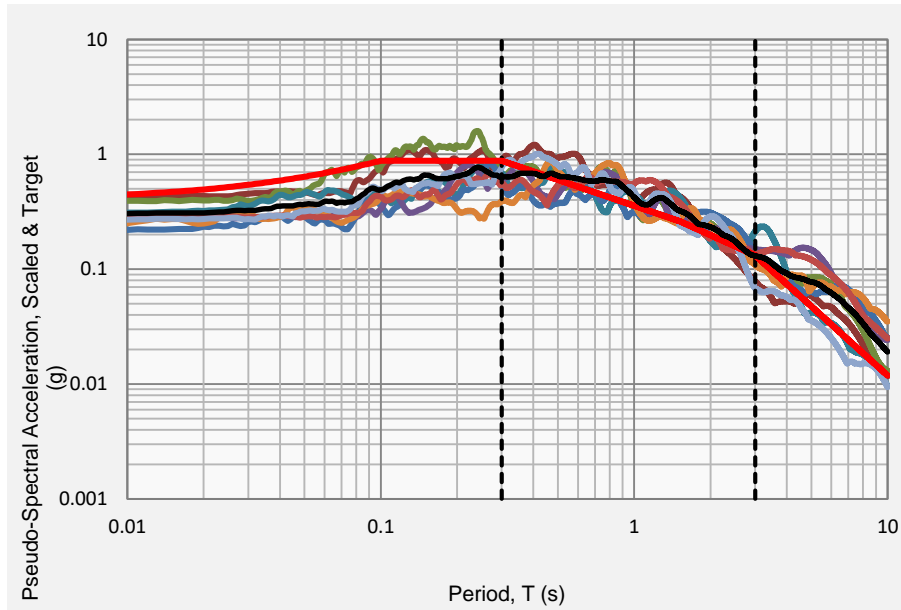


Figure 4. 21. Comparison of the acceleration response spectra of the selected ground motions with the design spectra (red line).

When the ground motions are scaled, the time history analysis can be performed. An important point for performing the nonlinear response-history analysis is to select a suitable viscous damping ratio, ξ_v . There have been some recommendations on how to select the viscous damping in nonlinear time history analysis when the intention is to verify a displacement-based design approach [151]. The ξ_v used for time-history analysis, should be consistent with the ξ_v used for the primary design (Eq. 4.2). In general, ξ_v is a function of system tangent stiffness. However, the viscous damping is modelled as a function of initial stiffness in most of the available software for nonlinear response history analysis. As per recommendations made by Priestley et al. [151], if constant damping, based on the initial stiffness method, is used in the analysis, the damping should be less than that of the damping used for the primary design. In this research, $\xi_v=2\%$ was selected for the design. As this damping is small, it is not expected that the overall response of the structure to be affected significantly by the viscous damping selected for the analysis. Therefore, the same damping ratio of $\xi_v=2\%$ is selected for the dynamic analysis. It should be noted that in the structures with higher viscous damping ratios, such as conventional concrete structures, additional considerations should be taken into account for the damping ratio to be selected for the analysis.

In this section, the analysis results are discussed, and the performance of the structure is assessed and compared to the primary design. First, the global response of the structure is considered. The design displacement at the roof level is 270mm based on the design procedure implemented in the previous section. In the graph shown in Fig. 4.22, the maximum observed demand for the structure equipped with a double-acting mechanism is 225mm and for the structure equipped with a tension-only mechanism is 210mm both observed for the case of the Tabas earthquake. The average of eight ground motions is also illustrated in the graph below which is 181mm and 139mm for the double-acting and tension only mechanisms, respectively.

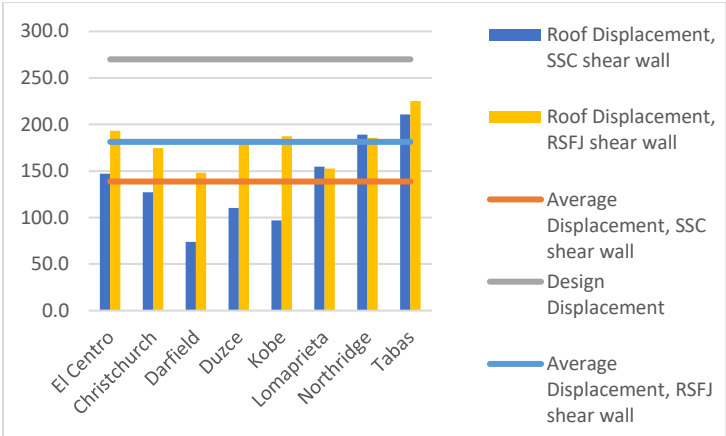


Figure 4. 22. Comparison of maximum roof displacements obtained from NLTH analysis.

As obvious, the drift demand for all the selected ground motions is less than the 1.5% demand targeted as the primary design objective. Therefore, the time-history analysis verified that the design is capable to achieve the desired performance. However, the designer might decide to repeat the design process by selecting a smaller design drift such as 1.25% or even 1.0%.

In this section of the paper, the local performance of the structural elements and more detailed response parameters are assessed and discussed. The hysteresis performance of the hold-downs for the selected ground motions are shown in Fig. 4.23. As can be seen from the graphs, the RSFJ hold-downs experienced both tension and compression while the SSC hold-downs performed only in tension. However, the response of the RSFJ in compression is almost linear and the energy dissipation mechanism was not activated in compression. The elastic deformation of the wall and

the joint are large enough to absorb the deformation demand on the compression side and the joints react almost elastic in compression.

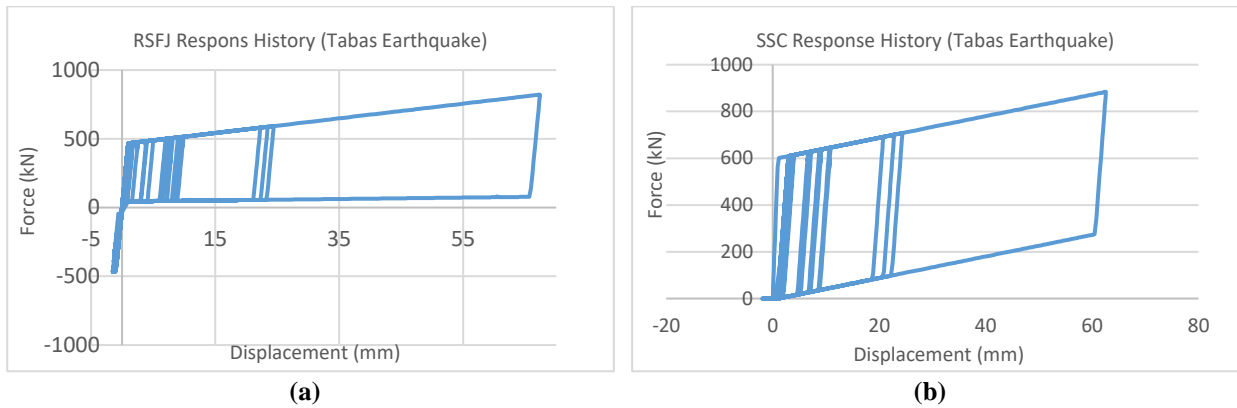


Figure 4. 23. Hysteresis response of the connections under Tabas earthquake:

a) RSFJ shear wall, and b) SSC shear wall.

The maximum drift profile of the structure equipped with SSCs is shown in Fig. 4.24. It can be observed from the graph that for all the ground motions at each story, the drift limit of less than 1.5% is met.

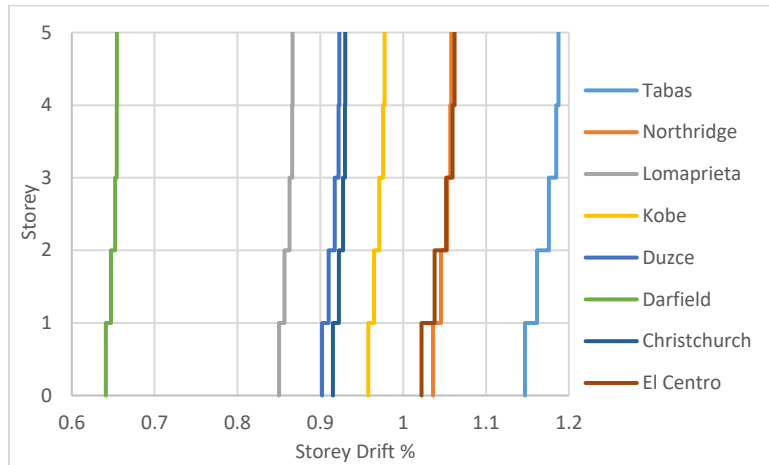


Figure 4. 24. Vertical distribution of inter-story drift for the modelled structure with SSC shear wall under the selected ground motions.

4.9 Conclusions

In this paper, the seismic performance and design of rocking concrete wall structures with self-centring friction connections were discussed. Firstly, a design procedure was proposed based on Direct Displacement Based Design method. It was emphasised that self-centring structures can be compared to elastic structures given the residual displacement and therefore ductility demand is

not expected in such structures. Accordingly, the proposed design procedure was developed based on the equivalent damping ratio and effective stiffness instead of ductility and yielding concepts. A five-story building equipped with concrete rocking shear walls and new self-centring friction dampers was designed based on the proposed design procedure. Two new different types of self-centring dampers were selected for this study. The Resilient Slip-Friction Joint (RSFJ) was selected to represent the performance of a double-acting connection and Self-centring Structural Connector (SSC) was selected to represent the performance of a tension-only connection. The structure was designed for two different systems based on the proposed procedure. The non-linear pushover analysis was used to capture the load-displacement performance of the systems. Also, the nonlinear Time-History analysis was carried out in order to verify the seismic performance of the designed buildings. A series of earthquake ground motions were selected and scaled as per the requirements of the New Zealand standard 1170.5. The seismic response of the structure was assessed against the desired response parameters such as the roof displacement and the maximum inter-story drift. The structures performed as expected and the response parameters complied with the maximum design limits and within less than 1.5% drift ratio. Therefore, the proposed design procedure can be used for the seismic design of rocking wall structures equipped with self-centring dampers.

Chapter 5: Concept Development and Experimental Verification of a New Rocking Concrete Shear Wall with Self-Centring Friction Connections

5.1 Abstract

In recent years, the intention towards developing and utilising low-damage systems in seismic resisting structures has been increasing amongst researchers and engineers. Replaceability and repairability after earthquakes even greater than the Ultimate Limit State (ULS) design level, more reliability against aftershocks, and being immediately occupiable after severe earthquakes are some of the advantages of these systems. Different types of rocking concrete shear walls have been developed and used as low-damage structural systems. In this paper, a new low-damage rocking concrete shear wall has been introduced, developed and tested. Self-centring friction dampers are used as wall to base connections to control the rocking motion in the proposed system. Two different configurations of connections are suggested including double-acting and tension-only self-centring dampers. Resilient Slip-Friction Joint (RSFJ) and Self-Centring Structural Connector (SSC) are used for each configuration, respectively. First, the conceptual framework and the analytical procedure to design each system in detail and predict the performance are presented. Afterwards, an experimental program is designed and conducted to verify the analytical procedure developed. Later, the numerical investigation and digital modelling of the rocking wall system is presented. The numerical outcome is also compared to the test results and the models are verified accordingly. Finally, in order to assess the seismic performance of the system within a structure, a Non-Linear Time History (NLTH) analysis is carried out on a single-degree-of-freedom prototype structure. The selected response parameters are compared to the code requirements and the outcome of NLTH analysis is discussed.

5.2 Introduction

Ductile concrete shear walls dissipate earthquake input energy mostly through the yielding of longitudinal reinforcements in flexure [8]. Other minor sources of energy dissipation are also observed such as yielding of transverse reinforcement, concrete crushing, aggregate inter-lock friction and sliding shear [144]. However, these behavioural modes are not desirable due to associated brittle failure modes. In general, ductile concrete shear walls have performed well in saving lives, the main purpose that they were designed to, in the past earthquakes [145]. Providing strength, stiffness, ductility and energy dissipation are the good seismic resisting characteristics of Reinforced Concrete (RC) walls [146]. The plastic hinge region of the RC walls should be detailed adequately in order to represent the repetitive cyclic damping and to achieve the desired ductility [147]. However, ductile detailing is complex and requires strong engineering and construction skills and experiments.

In some cases, unexpected failure modes such as local instability, bar rupture and web crushing have been observed in the experimental studies and past earthquakes (Fig. 5.1) [1, 89]. Residual deformation is expected in RC shear walls after moderate to severe earthquakes. This residual displacement along with the damages in concrete and reinforcements imposes extensive repair or reconstruction costs [91]. Therefore, researchers suggested a move from ductile shear walls towards rocking shear walls as damage avoidance systems [9, 24].

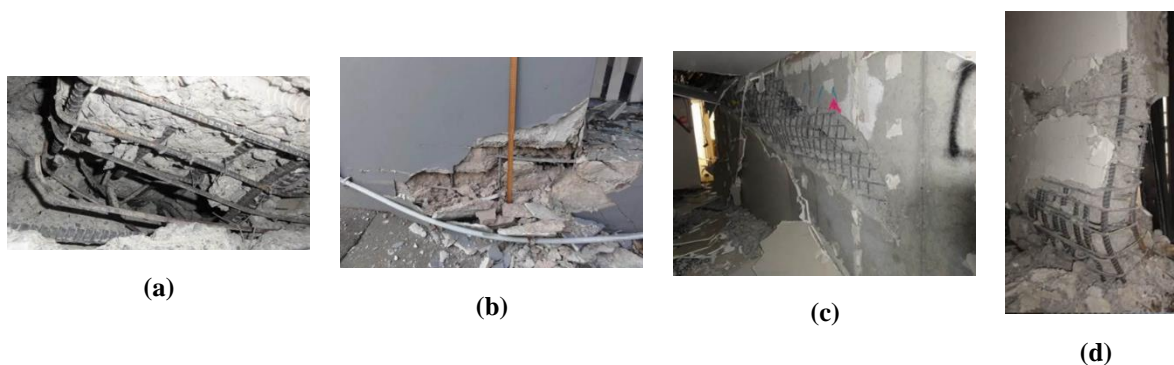


Figure 5. 1. Observed failure modes of structural walls during past earthquakes: (a) Bar yielding followed by bar rupture, (b) Toe crushing, (c) Diagonal shear, (d) Compression failure and buckling [4].

End users and authorities expect resilient structures. A resilient structure has negligible structural and minor non-structural damage after a severe earthquake. Researchers introduced Damage Avoidance Design (DAD) philosophy to achieve resilient structures [9]. DAD aims to achieve a repeatable and damage avoidance cyclic energy dissipation in addition to zero or negligible residual deformation. Therefore, the building could be occupied immediately after earthquakes and is ready to withstand aftershock without any deterioration in the structural characteristics [13-18]. Rocking concrete shear walls have been developed as a damage avoidance solution for DAD [14, 34-36, 148]. In rocking concrete shear walls, traditional reinforcement yielding and concrete crushing are not expected [14, 20, 51, 111]. Unbonded post-tensioning [10, 18, 24, 128, 148] and self-centring dampers [111] have been used to control the rocking motion and to provide controlled self-centring capability. Therefore, problems related to damage and residual deformation are almost overcome in rocking walls designed based on DAD philosophy.

The concept of rocking motion has always been a point of interest for seismic researchers and engineers [25, 174-179]. During the past earthquakes, it has been observed that the structures which unexpectedly rocked around their base suffered from less damage compared to those of fixed base [25]. Therefore, several different systems incorporating rocking motion have been introduced for earthquake resistant structures. The rocking motion has been incorporated in both the foundation level [180-182] and throughout the structure. At the structure level, different concepts and structural materials have been used. For example, steel rocking braced frames [183-185], steel rocking shear walls [186-188], timber [189, 190] and concrete [35, 148, 191] rocking walls. Different structural configurations have also been developed to implement the rocking motion in the structures. Single rocking walls [148], coupled rocking walls [189, 192] for increasing the capacity and multi rocking walls [193] to decrease the higher mode effects in high-rise buildings can be named as some examples. Along with these new rocking systems, several design procedures have been developed [194, 195].

The most common way of implementing a controlled rocking behaviour is to use post-tensioning (PT) cables along with supplemental yielding dampers [23]. However, other types of energy dissipaters such as friction or viscous dampers have also been used in the PT rocking wall structures [35]. It should be noted that using on-site post-tensioning causes construction complexity and additional labour. Also, yielding dampers should be inspected after moderate to severe earthquake and repaired or replaced if required. Unbonded post-tensioning was used in pre-cast concrete walls in PREcast Seismic Structural Systems (PRESSSS) in the early 1990s [31]. Detailed analytical studies on the behaviour of Single Rocking Wall (SRW) systems were conducted by Kurama et al. [149]. They suggested using additional spiral reinforcement at the wall toes to mitigate the damage of concrete due to crushing. Kurama and colleagues [33] also performed a series of studies on the unbonded PT walls with additional supplemental damping such as yielding, friction or viscous damping. The results showed that the additional dampers effectively reduce the seismic demand if they are properly designed. Priestley [24] used U-shaped Flexural Plates (UFP's) in coupled rocking wall systems. Other efforts were made for using internal grouted mild steel reinforcement for additional hysteresis damping [28, 29]. Externally mounted mild steel, Tension and Compression Yielding (TCY) dampers, as well as viscous dampers, were designed and tested by Marriot et al. [35]. Sritharan and colleagues [34] suggested a PT rocking wall system as Pre-cast Wall with End Columns (PreWEC).

Considering the previous research related to the rocking wall structures, it is observed that a limited effort [185, 196] has been made in developing rocking walls with self-centring dampers. These devices provide self-centring and energy dissipation in one compact connection [58, 155] and can be used for controlling the rocking motion. The use of two self-centring dampers, the Resilient Slip-Friction Joint (RSFJ) [59] and Self-centring Structural Connector (SSC) [153], in rocking concrete walls, is investigated in this study. Two different configurations are introduced and studied analytically and experimentally. RSFJs are used as double-acting wall-to-base connections

and SSCs are used as tension-only connections. In this paper, the performance of each damper is explained, and the concept of the rocking system is introduced and analytically investigated. Then, the performance of the system is examined via large-scale cyclic testing. Also, a numerical modelling approach is introduced and verified by the experimental results. Finally, the seismic performance of a prototype structure designed based on this new rocking system is examined using NLTH analysis and compared to the code requirements.

5.3 Concept development and analytical investigation

5.3.1 Self-Centring Friction Dampers

Resilient Slip-Friction Joint (RSFJ)

In RSFJs, the restoring force is provided by the specific steel grooved plates, which are tied through high strength bolts and disc springs [159]. By slipping of grooved plates, the input energy is dissipated through frictional resistance. Based on the free-body diagrams presented in Fig. 5.2, the design procedure is developed for the prediction of the performance of the RSFJ. The slip force (F_{slip}) and residual force (F_{resid}) can be determined by Eq. (5.1) and Eq. (5.2):

$$F_{RSFJ,slip} = 2n_b F_{b,pr} \left(\frac{\sin \theta + \mu \cos \theta}{\cos \theta - \mu \sin \theta} \right) \quad (5.1)$$

$$F_{RSFJ,res} = 2n_b F_{b,pr} \left(\frac{\sin \theta - \mu \cos \theta}{\cos \theta + \mu \sin \theta} \right) \quad (5.2)$$

Where n_b is the number of bolts on each splice, θ is the groove angle, $F_{b,pr}$ is the clamping force of pre-stressing and μ is the coefficient of friction. The general hysteresis behaviour of RSFJ is illustrated in Fig. 5.2(d). F_{ult} and $F_{restoring}$ are the system forces at the maximum disc springs displacement and bolts clamping force.

$$F_{b,u} = F_{b,pr} + K_s \Delta_s \quad (5.3)$$

K_s is the stiffness of each stack of springs and Δ_s is the displacement of the stacks. $F_{b,u}$ is the maximum force generated in the bolts. F_{ult} , and $F_{restoring}$ are derived by replacing the bolt forces in Eq. 5.1 and Eq. 5.2 by Eq. 5.3.

The ultimate displacement of the joint (Δ_{ult}) can be calculated using Eq. 5.4.

$$\Delta_{ult} = \frac{2\Delta_s}{\tan\theta} \quad (5.4)$$

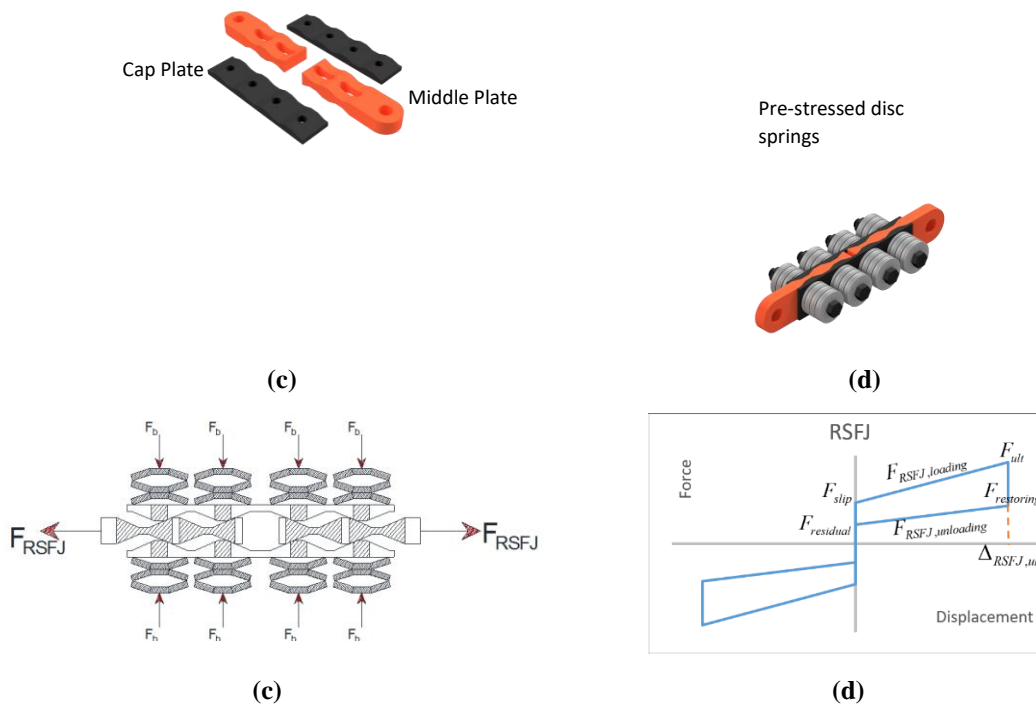


Figure 5. 2. Resilient Slip Friction Joint: a) Components, b) Assembly, c) Free body diagram, d) Flag-shaped response of RSFJ.

Several different applications of RSFJ have been developed and tested such as timber rocking walls [160], timber braces [161] and tension-only braces [162]. Also, there are other applications under investigation [135, 138].

Self-centring Structural Connector (SSC)

In this section, the performance and configuration of SSC are discussed [163]. Different components of SSC are shown in Fig. 5.3.

Disc springs are responsible for the self-centring capability. Every single spring has a specific displacement capacity, Δ_s , and a corresponding load capacity, F_s , at the maximum displacement, which is called flatness load. It should be mentioned that the stack of the springs should be pre-stressed to the desired pre-stressing force before being inserted inside the tube.

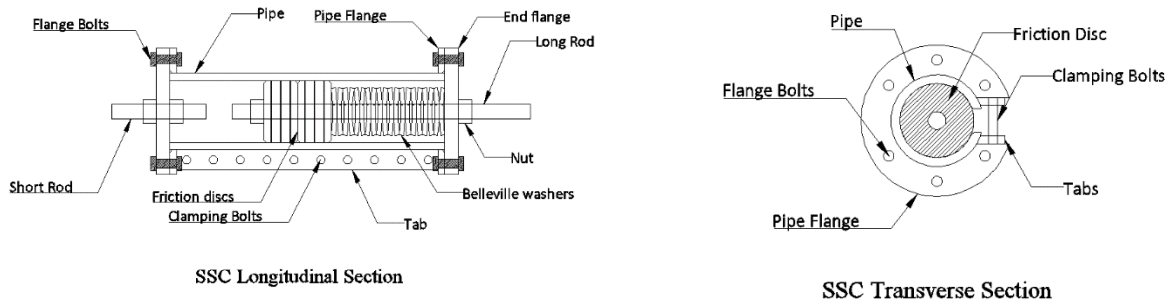


Figure 5. 3. Self-centring Structural Connector (SSC).

The friction of the internal surface of the tube with friction rings is the source of energy dissipation. At this stage, the tube clamping bolts are pre-stressed to the required clamping force. This force creates the normal force (perpendicular to the surface) between the disc and the tube for friction. In this section of the paper, the force-displacement performance of the SSC is analyzed. As can be seen from the Fig. 5.4, the SSC has a flag-shaped force-displacement curve.

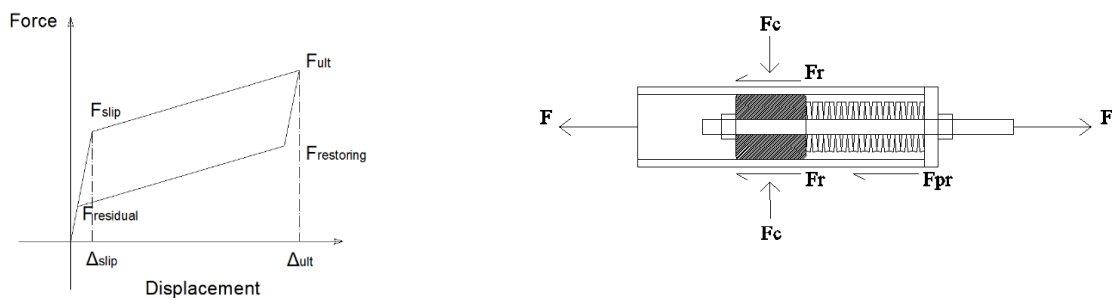


Figure 5. 4. Free body diagram and force-displacement response.

At the slip stage, friction force ($F_{friction}$) and the pre-stressing force ($F_{prestressing}$) inside the spring resist against the movement. F_{slip} can be obtained using Eq. 5.5:

$$F_{slip} = F_{friction} + F_{prestressing} \quad (5.5)$$

The calculation of Δ_{slip} using the mechanics of materials rule can be easily done. When the discs are flat, the damper has theoretically reached its maximum force capacity (F_{ult}). F_{ult} can be estimated using Eq. 5.6.

$$F_{ult} = F_{friction} + F_{prestressing} + K\Delta = F_{friction} + F_s \quad (5.6)$$

where K is the equivalent stiffness of the set of springs and Δ is the displacement capacity of the springs after pre-stressing. F_s represents the force capacity of the springs. The restoring force, $F_{restoring}$, can be calculated using Eq. 5.7.

$$F_{restoring} = F_s - F_{friction} \quad (5.7)$$

Eventually, the displacement reaches zero. The external residual force in the system at this stage, $F_{residual}$, can be obtained using Eq. 5.8:

$$F_{residual} = F_{prestressing} - F_{friction} \quad (5.8)$$

In order to obtain the self-centring condition, the pre-stressing force of the spring must be greater than the friction force.

$$F_{prestressing} \geq F_{friction} \quad (5.9)$$

In the design of SSC, the normal force acting on the surface between the piston and the cylinder can be adjusted by the external clamping force. This force (F_c) is applied using the tube clamping bolts and nuts and can be calculated using Eq. 5.10.

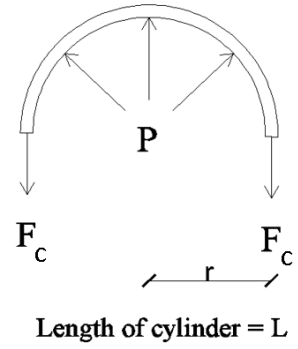


Figure 5. 5. Free body diagram of a cylinder with internal pressure.

As shown in Fig. 5.5, considering the equilibrium equations for the longitudinal section of the cylinder, the relationship between the clamping force (F_c) and the pressure (P) on the tube can be obtained using Eq. 5.10 for a cylinder with the radius of r and the length of L .

$$F_c = PrL \quad (5.10)$$

At this stage, the friction force (F_{fr}) can be calculated using the pressure on the tube (P) and the friction coefficient, μ .

$$F_{fr} = 2\pi\mu F_c \quad (5.11)$$

The maximum displacement of the springs stack after pre-stressing is equal to the maximum displacement capacity of the damper, Δ_{ult} , which can be calculated using Eq. 5.12.

$$\Delta_{ult} = n\Delta_s \left(1 - \frac{F_{pr}}{F_s}\right) \quad (5.12)$$

The reader is referred to (ref) for more details on the design and performance of the SSC.

5.3.2 Load-displacement performance of Rocking Walls

First, the performance of rocking walls with double-acting connections are assessed and the equations are developed. Second, the same assessment will be done for rocking walls with tension-only connections. The free-body diagram of the system with double-acting connections is mentioned in Fig. 5.6(a).

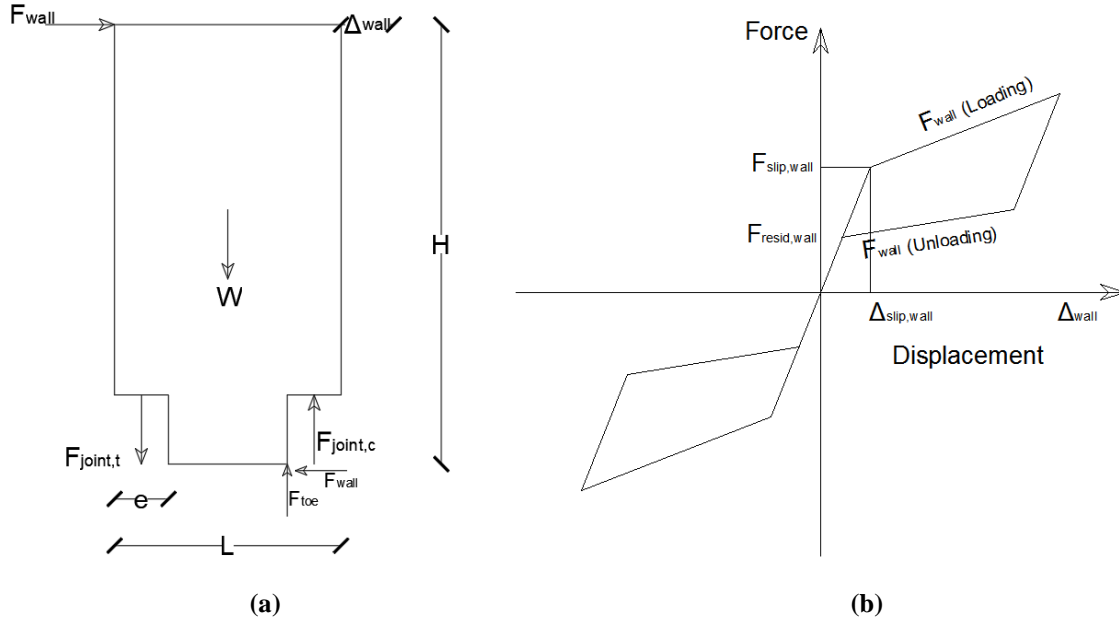


Figure 5. 6. a) Free-body diagram of rocking walls equipped with double-acting self-centring connections and b) load-displacement response of the wall.

Considering the free-body diagram of the wall at maximum lateral drift (Fig. 5.6(a)) and the load-displacement performance of the wall mentioned in Fig. 5.6(b), the performance parameters can be calculated as follows by taking moment around the wall toe. At the slip level, when joints have reached their slip force, the wall starts to rock.

$$F_{slip,wall} = \frac{1}{H} \left[F_{slip,joint}(L - e) + w \frac{L - 2e}{2} \right] \quad (5.13)$$

Where, $F_{slip,wall}$ is the lateral load acting on the wall at the onset of rocking motion, $F_{slip,joint}$ is the connections' slip force and W is the weight of the wall. Other geometric parameters are mentioned on the diagram (Fig. 5.6(a)).

After the onset of rocking movement, the tension and compression joints contribute to transfer the loads to the foundation based on their lever arm to the wall toe. The moment equilibrium at this loading stage results in Eq 14.

$$F_{wall} = \frac{1}{H} \left[F_{joint,t} \left(L - \frac{3e}{2} \right) + w \frac{L - 2e}{2} + F_{joint,c} \frac{e}{2} \right] \quad (5.14)$$

F_{wall} , is the lateral force acting on the wall during the loading and unloading stages of rocking motion, $F_{joint,t}$ is the force in the connection under tension and $F_{joint,c}$ is the force in the connection under compression. The residual force in the wall ($F_{resid,wall}$) can be obtained by replacing $F_{slip,joint}$ by $F_{resid,joint}$ in Eq. 5.13.

A relationship between $F_{joint,t}$ and $F_{joint,c}$ can be derived according to the displacement compatibility at the base by considering the "plane section remain plain" assumption. the wall as a rigid element. The displacement compatibility can be expressed by Eq. 5.15 which after being combined with the load-displacement performance of the joints, the relationship between the tension and compression forces for both loading and unloading stages can be presented (Eq. 5.16 and Eq. 5.17, respectively).

$$\frac{\Delta_{joint,t}}{L - \frac{3e}{2}} = \frac{\Delta_{joint,c}}{\frac{e}{2}} \quad (5.15)$$

$$F_{joint,c} = \frac{e}{2L - 3e} (F_{joint,t} - F_{slip,joint}) + F_{slip,joint} \quad (5.16)$$

$$F_{joint,c} = \left(\frac{e}{2L - 3e}\right) (F_{joint,t} - F_{resid,joint}) + F_{resid,joint} \quad (5.17)$$

$\Delta_{joint,t}$ and $\Delta_{joint,c}$ are the joint displacement due to F_{wall} under tension and compression, respectively. $F_{resid,joint}$ is the residual force in the joint at the end of the unloading stage.

The wall top displacement is a combination of the wall rigid body rotation due to rocking and its elastic deformation. The top displacement of the wall can be calculated using Eq. 5.18 to Eq. 5.20.

$$\Delta_{wall} = \Delta_{elastic} + \Delta_{rot} \quad (5.18)$$

$$\frac{\Delta_{rot}}{H} = \frac{\Delta_{joint,t}}{L - \frac{3e}{2}} = \frac{\Delta_{joint,c}}{\frac{e}{2}} \quad (5.19)$$

$$\Delta_{elastic} = \frac{F_{wall}H^3}{3EI} \quad (5.20)$$

$\Delta_{elastic}$ is the elastic deformation of the wall due to F_{wall} . E and I are the modulus of elasticity and moment of inertia of the wall section.

The same analogy can be used to develop the equations governing a rocking wall with tension-only connections. The free body diagram of such a system is illustrated in Fig. 5.7(a). There is a main difference between tension-only and double-acting systems. In tension-only systems, the governing equations are the same for before and after the onset of rocking motion (Eq. 5.21). As for the displacements, the same equations as those developed for the double-acting systems can be used.

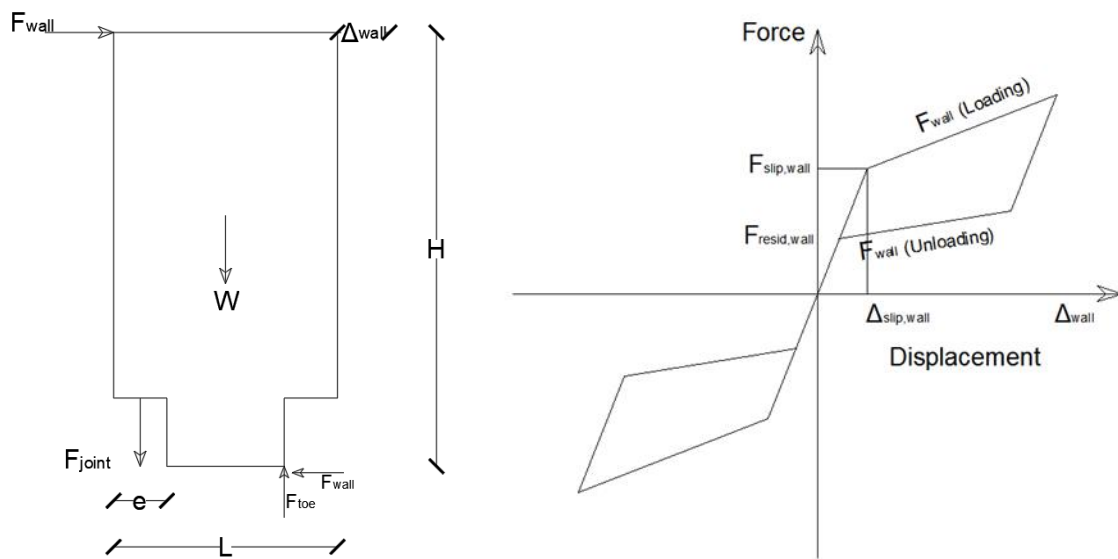


Figure 5. 7. The free-body diagram of rocking walls equipped with tension-only self-centring connections.

$$F_{wall} = \frac{1}{H} \left[F_{joint} \left(L - \frac{3e}{2} \right) + w \frac{L - 2e}{2} \right] \quad (5.21)$$

$$\frac{\Delta_{rot}}{H} = \frac{\Delta_{joint,t}}{L - \frac{3e}{2}} \quad (5.22)$$

The developed equations will be verified through experimental investigation presented in the upcoming sections.

5.3.3 Controlling Tension Cracks and Internal Bending Demand

When a reinforced concrete wall is subjected to bending, the tension cracks form and reduce the stiffness of the wall. Reduction in the stiffness results in reducing the displacement demands in the wall-to-base connections in a rocking concrete shear wall. For example, at the target lateral drift, a considerable portion of the deformation is due to tension cracks which is not desirable. Crack

opening and closing is a phenomenon without energy dissipation. Therefore, in a rocking wall with self-centring dampers as hold-downs, the total energy dissipation is decreased due to cracking and a less displacement demand in the connections providing the energy dissipation. In order to assess the effect of bending cracks in the overall response of the structure, a rocking concrete shear wall designed to resist the earthquake actions in a 5-story building has been selected (Fig. 5.8). The wall is analysed under nonlinear pushover analysis for the effect of cracking. The reader is referred to [197] for more details about the prototype structure.

A brief description about the pushover analysis is provided as follows. The rocking wall is analysed under two different scenarios; first, the concrete is modelled elastically, and the cracking is not allowed and second, the concrete is modelled plastically and the cracking is considered. The structure is analysed under cyclic loading and the roof load-displacement responses are compared for both cases. Furthermore, the load-displacement graphs of connections for the two cases are obtained and compared.

Software SAP2000 [198] is adopted for numerical analysis. In order to model the nonlinear behaviour of the concrete, the nonlinear concrete material and layered shell elements are used. In layered shell elements, the behaviour of the components of each element is modelled by different layers. The layers are connected and constrained at the element nodes. A stress-strain relationship should be assigned to each layer. As the effect of concrete cracking is being investigated in this research, only the nonlinearity of concrete is considered and the steel reinforcing bars are modelled elastically. The concrete stress-strain relationship proposed by [199] is selected to model the concrete material. For simplicity, the tension strength of the concrete is set to zero. The concrete stress-strain relationship is shown in Fig. 5.9. The steel reinforcing bars at the wall boundaries are designed based on the capacity design concept for the expected capacity of joints. Therefore, considering an over-strength factor of 1.15, the amount of longitudinal reinforcement can be calculated using Eq. 5.23.

$$A_s F_y = 1.15 F_{ult} \quad (5.23)$$

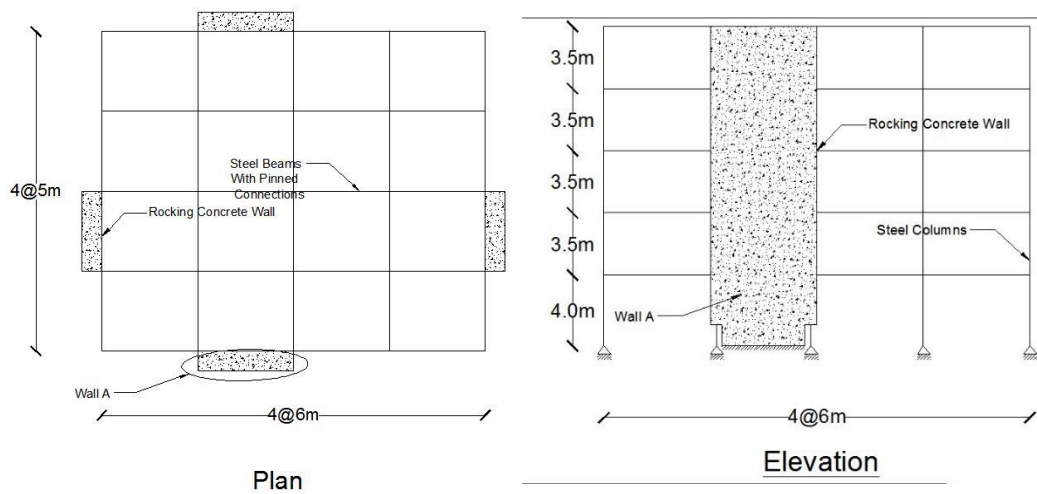


Figure 5. 8. Structural plan and elevation of the modelled building.

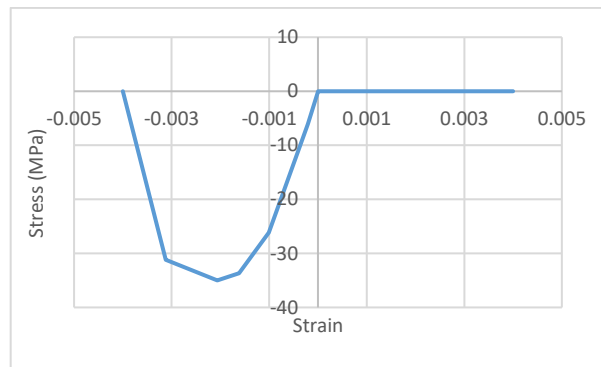


Figure 5. 9. Concrete stress-strain relationship.

where A_s is the area of longitudinal reinforcement and F_{ult} is the maximum force for which the joint is designed. Rebar grade 500E as per New Zealand Concrete Standard [200] is selected for the reinforcing steel with a minimum yield stress, f_y , of 500 MPa. For the joints, an ultimate capacity, F_{ult} , of 920kN is considered. Therefore, the A_s is calculated as 2116 mm² which is less than the maximum allowable reinforcement ratio of $16/f_y$, recommended by New Zealand standard. Longitudinal reinforcement in the wall web is designed as per the minimum reinforcement ratio of $\sqrt{f'_c}/4f_y=0.0029$, where the concrete compressive strength, f'_c , is 35 MPa.

The design lateral displacement at the top of the wall is 270 mm. The structure is analysed under cyclic-pushover analysis for the two cases of elastic and plastic concretes. First, the overall load-displacement responses of the different concrete behavioural models are compared. The

performance obtained is shown in Fig. 5.10. As it can be observed from the graph, the initial stiffness of the wall with the plastic concrete is 55% less than the wall with the elastic concrete. This observation verifies the necessity of considering the cracking behaviour of the concrete in the design, especially for controlling the Serviceability Limit State (SLS) drifts. It can be observed that after the slip stage, the loading and un-loading stiffness of the structure with the plastic concrete material is less than the one with elastic material. Also, the maximum base shear is slightly lower in the plastic concrete model. These observations confirm that less energy dissipation is expected when concrete cracks form. Accordingly, the concrete cracking results in less energy dissipation. For example, in the modelled structure, the equivalent viscous damping (ξ_{hys}) is about 9.0 % less than the case in the elastic concrete model.

The main reason for a decrease in energy dissipation is that the cracking decreases the demand in the joints which are responsible for energy dissipation. As shown in Fig. 5.11, the maximum displacement that occurred in the joints of the plastic concrete model was 5mm less than the elastic concrete model. Accordingly, the cracking reduces the efficiency of the system and should be seen as a disadvantage that needs extra consideration.

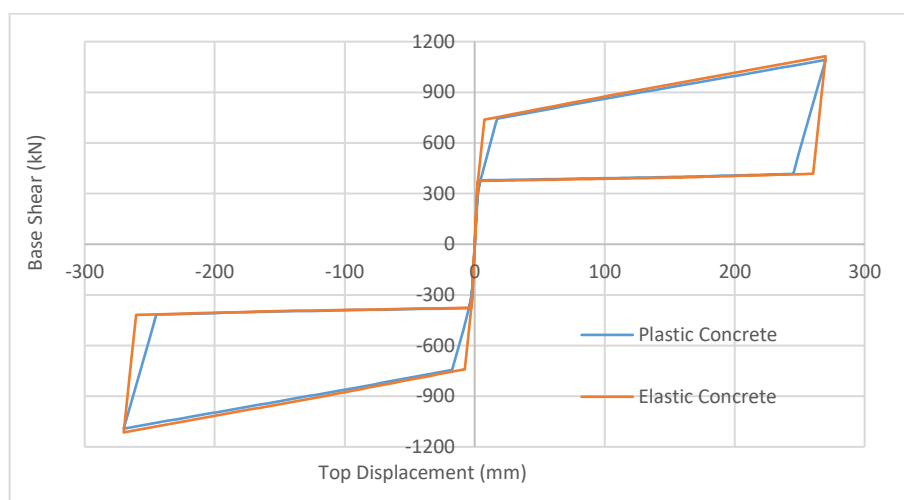


Figure 5. 10. Comparison of overall load-displacement performance of the system with the elastic and plastic concrete models.

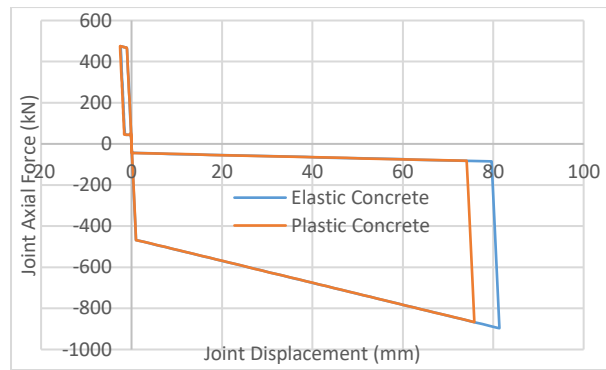


Figure 5. 11. Comparison of the joint load-displacement performance of the system with the elastic and plastic concrete models.

Another challenge in using self-centring dampers as hold-downs in rocking concrete walls is the connection of the hold-down to the wall. The connection should meet several requirements which limits the design options and could increase the complexity of the design. Some of the challenges can be named as follows. Capacity design requirements and complex failure modes such as concrete pull-out, bolt anchorage and splice requirements should be taken into account during the design. The amount of reinforcement is limited as per the code requirements and therefore undesirable larger boundary elements might be required to reduce the reinforcement ratio. This can be even more challenging at the location of the splices. In addition, from a practical point of view, dimension tolerances play an important role when dampers are to be connected to the anchor bolts sticking out from the concrete wall and the foundation. Considering the above-mentioned challenges in a traditional hold-down system along with the negative effect of the cracking in the performance of the wall, in this study, an alternative solution is proposed.

5.4 Proposed Concept

The proposed solution not only resolves the above-mentioned challenges but also has the advantage of optimising the amount of reinforcement required within the concrete panel. Also, this concept is suitable for prefabricated construction and promotes the use of pre-cast concrete in seismic resisting structures.

Pre-stressing has always been a well-accepted method to control the cracking and deflection in reinforced concrete. Pre-stressed and post-tensioned members have widely been used in the construction industry. The concept of off-site pre-stressing and/or post-tensioning of prefabricated reinforced concrete is not common for seismic resisting elements. Even though on-site unbonded post-tensioning is used for concrete rocking systems, the design complexity and the extra on-site work required for post-tensioning is one of the challenges from both design and construction points of view. In the proposed solution, the advantages of post-tensioning are used while on-site extra work is not required as the post-tensioning can be done in the factory.

In this concept, as shown in Fig. 5.12, a concrete panel that is already post-tensioned in the factory using unbonded rods is transferred to the construction site and then mounted and connected to the foundation using the self-centring hold-downs. It should be noted that the post-tensioning aims to prevent the wall from cracking and therefore an internal post-tensioning of the wall prior to mounting will suffice. This means that there is no need to use unbonded PT cables to connect the wall to its foundation. It is also not required to use complex connection detailing or a highly reinforced panel with special seismic detailing. In most cases, a minimum required reinforcement could be enough. The details of the developed concept are presented as follow.

As shown in Fig. 5.12, firstly, the concrete panel should be post-tensioned internally using unbonded rods up to a certain pre-stressing force level. The post-tensioning force can be applied using a rod or cable inserted through the ducts in the boundary regions of the wall and connected to the endplates (Fig. 5.12). In the next section, the concept is described in more details through designing the concrete panel used for the experimental investigations.

In order to eliminate the tension cracks, a pre-stressing concept is developed. In this concept, the pre-cast concrete panel is connected to the foundation using the self-centring dampers. This precast concrete panel is post-tensioned using unbonded cables or rods. After manufacturing and considering proper timing for the concrete curing, the pre-cast concrete panel will be compressed

using the unbonded tensioning elements. Post-tensioning can be done either at the factory or the construction site when the wall is laid down on the floor. This decreases the construction time and costs in comparison to the current on-site post-tensioning concepts. The wall can then be mounted vertically and get connected to the foundation using the brackets.

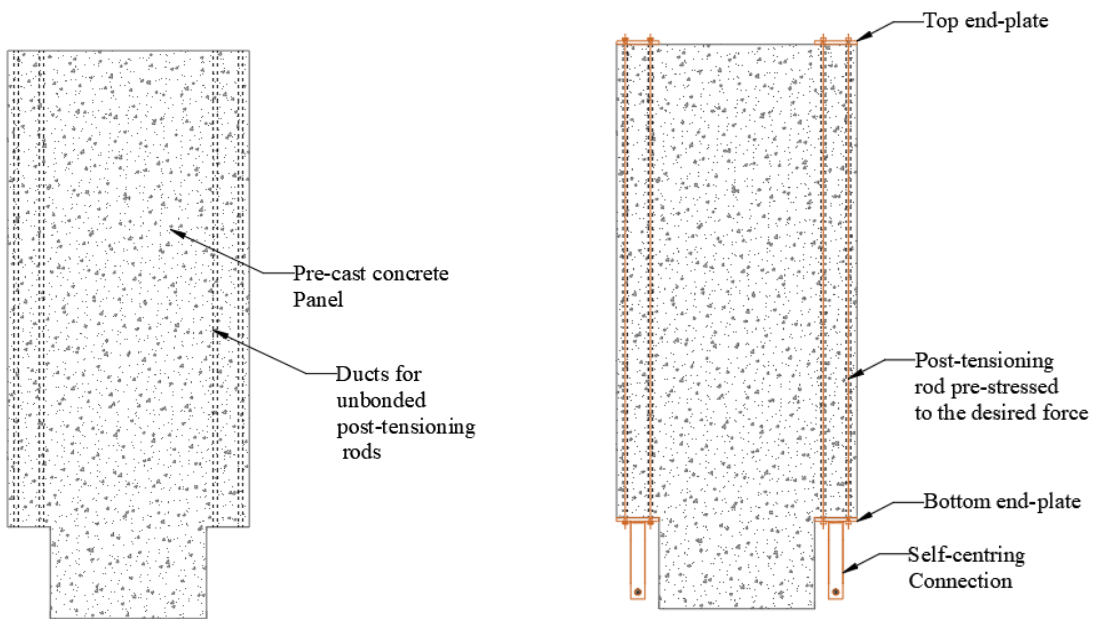
Another advantage of this system in comparison to the current post-tensioned rocking walls is that there is no need to design the post-tensioning elements for high displacement demands as the flexibility of the system comes from the dampers rather than the PT tendons.

5.5 Detailed design of the system

The required tensioning force in the Post Tensioning (PT) rods, F_{PT} , is calculated based on the maximum force in the joints (F_{ult}). The tensioning force at each side of the wall should be equal or greater than the joint ultimate force ($F_{PT} \geq F_{ult}$) in order not to allow the PT rods to deform elastically before the joint maximum design displacement. Accordingly, based on the capacity design concept, the required capacity of PT rods (N_u) is considered to be 25% higher than the joint design force.

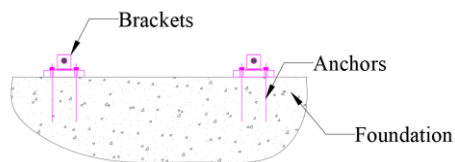
$$N_u = 1.25F_{ult} \quad (5.24)$$

By knowing the tensioning force, the free-body diagram of the wall can be drawn and analysed to obtain the internal forces and design the reinforcements. The wall will be analysed for two different cases. First, a rocking wall with double-acting joints and second, a rocking wall with tension-only joints. The free-body diagram of the double-acting joint at the final loading stage is shown in Fig. 5.13. As per the diagram in Fig. 5.13, when the wall is at its maximum lateral displacement, the tension force in the hold-down is F_{ult} . Accordingly, when $F_{joint,t} = F_{PT} = F_{ult}$, the internal forces can be calculated using Eq. 5.25 to Eq. 5.28.

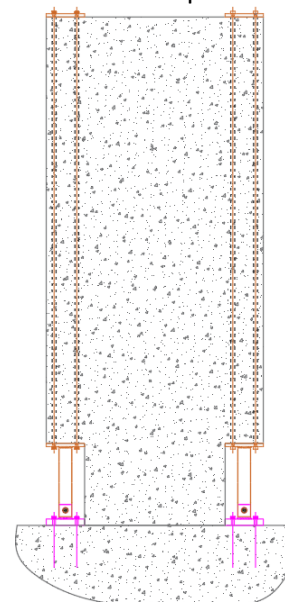


Phase 1: In the Factory
Pre-cast concrete panel

Phase 2: Either in the factory or on-site
Post-tensioning rods added and pre-stressed
with:
arrangement 1, self-centring connections already
welded to the bottom endplate
or,
arrangement 2, Self-centring connections to be
connected to the bottom endplate on-site using
bolts or pins



Phase 3: On-Site
Brackets anchored to the foundation



Phase 4: On-Site
Wall mounted and connected to the brackets

Figure 5. 12. Different components and construction phases of the proposed rocking pre-cast concrete wall system.

Axial compression:

$$N_{(x)} = 2F_{ult} + w_{(x)} \quad 0 \leq x \leq H - d \quad (5.25)$$

$$N_{(x)} = F_{ult} - F_{joint,c} + w_{(x)} \quad H - d \leq x \leq H \quad (5.26)$$

Bending moment:

$$M_{(x)} = F_{wall}x \quad 0 \leq x \leq H - d \quad (5.27)$$

$$M_{(x)} = F_{wall}x - (F_{ult} + F_{joint,c})\left(\frac{L - e}{2}\right) \quad H - d \leq x \leq H \quad (5.28)$$

Where $N(x)$ is the axial compression, and $M(x)$ is the bending moment. $W(x)$ is the weight of the wall at the top of the section considered at the distance x from the top. It should be noted that the wall only takes its self-weight and only takes seismic forces. When the internal forces are known, the reinforcement and concrete stresses can be calculated using Eq. 5.29. The wall is designed based on the desired level of stress distributed between the reinforcement and concrete.

$$\sigma = \frac{N_{(x)}}{A_{(x)}} + \frac{M_{(x)}C_{(x)}}{I_{(x)}} \quad (5.29)$$

where $A(x)$ is the sectional area, $C(x)$ is the distance from the section neutral axis and $I(x)$ is the moment of inertia of the section. The compression force at the toe, F_{toe} , can be calculated using Eq. 5.30.

$$F_{toe} = F_{ult} - F_{joint,c} + W \quad (5.30)$$

As for a rocking wall with tension-only self-centring hold-downs, the same equations as that of a double-acting joint (Eq. 5.25 to Eq. 5.30) can be used by considering $F_{joint,c}=0$.

In addition to general reinforcement, extra details should be considered for the local stress concentration. For example, the concrete crushing at toes may occur due to compression force concentrated at these regions during the rocking motion. Concrete crushing at toes has been observed in previous studies by different researchers [128, 148]. As a solution, steel angles with embedded anchors can be used at toes as external reinforcement. A more uniform stress distribution can be achieved by using the angle so that the force can be transferred to the concrete without localized damage. Furthermore, the compression strut at the toes should be confined using

stirrups. Concrete confinement increases the expected compression strength and crushing strains significantly. Therefore, the longitudinal reinforcement at the toes should be designed for the compression force, F_{toe} , and then appropriately confined as per the available guidelines for concrete confinement.

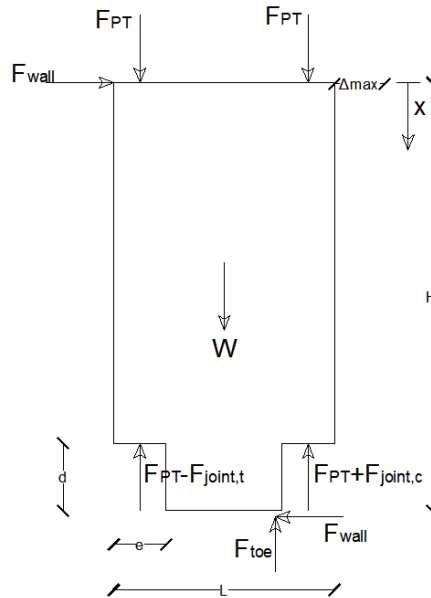


Figure 5. 13. Free body diagram of the post-tensioned wall at the ultimate lateral loading stage.

Extra consideration should be taken into account for the wall boundary elements surrounding the PT tendons or rods. The compression strut at the boundary elements should be designed for a compression force equal to F_{ult} . The developed design procedure will be used and verified in the experimental section of this paper.

5.6 Experimental Investigation

An experimental program is designed and conducted in order to verify the performance of the developed system. The details of the experimental program are presented in this section.

5.6.1 Wall Panel Design

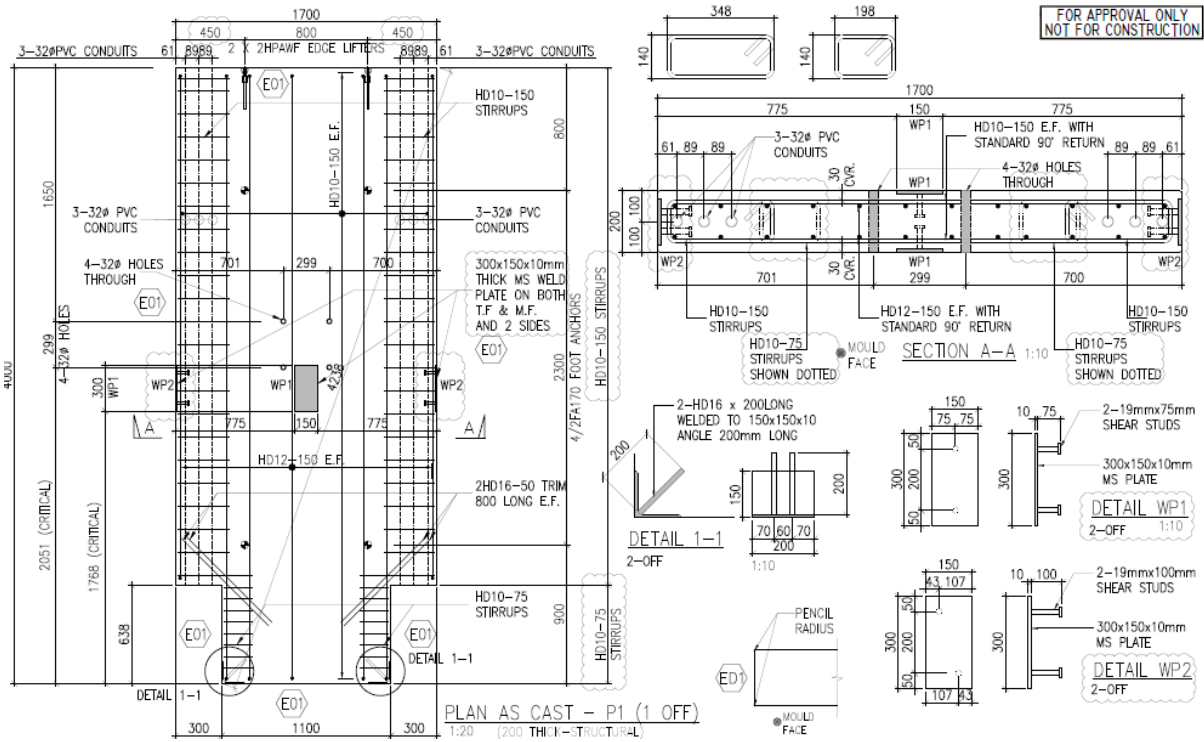
The required equations for designing the wall were developed in the previous section. The details of the designed concrete wall specimen are presented in Fig. 5.14(a). The wall dimensions are

summarised in Table 5.1. The wall was designed in a way that the maximum force induced in the self-centring joints were limited to 200 kN. The reason for selecting the 200 kN limit for designing the joints was the capacity of the available Universal Testing Machine (UTM) in the lab. The maximum drift of the wall at the ultimate force was considered to be 2.5% as per the recommendations of New Zealand Standard (NZSEE) [164] for the Ultimate Limit State (ULS) earthquakes. Accordingly, by knowing the external forces and dimensions of the wall, the internal forces can be calculated to design the wall. The wall has been designed using the procedure developed in the previous section. The reinforcement shop drawings and the wall reinforcement before pouring the concrete are shown in Fig. 5.14.

Table 5. 1. Design parameters of the tested wall.

L (mm)	1700
e (mm)	300
H (mm), Actuator level	2190
Total Height of Wall (mm)	4000
T (mm), Wall thickness	200
W (kN)	35350
F _c (MPa), concrete compressive strength	40
F _y (MPa), reinforcement yielding strength	500
E (MPa)	31600

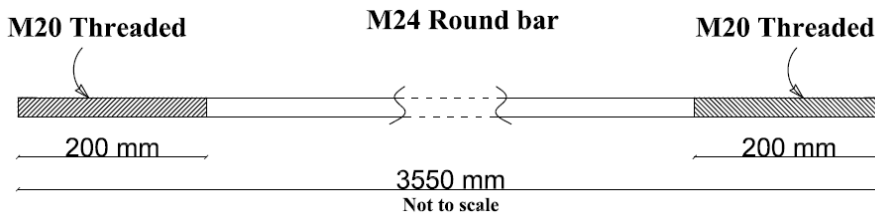
As can be seen from Fig. 5.14(b), three ducts are located at each boundary of the wall in order to pass the post-tensioning rods through them. The post-tensioning rods are size M24 Grade 8.8 threaded at the ends to M20 (Fig. 5.14(c)).



(a)



(b)



(c)

Figure 5. 14. Concrete panel reinforcement: a) shop drawings, b) reinforced wall before the concrete pour, c) post-tensioning rod.

5.6.2 Test setup

The details of the test setup and components are described in this section. As two different concepts have been tested, even though the wall and general setup were similar for both concepts, different details were considered for each test. As shown in Fig. 5.15(a), a mild steel base plate with a thickness of 50 mm has been used for connecting the wall and joints to the strong floor. The base plate is tightened to the strong floor using pre-tensioned high strength bolts. The amount of the pre-tensioning force should be enough to achieve a sliding friction resistance between the foundation and the strong floor. The sliding resistance should be more than the shear force acting on the contacting surface. The base plate drawings are illustrated in Fig. 5.15(b). The location of the required plain holes (for the base plate connection to the floor), as well as the threaded holes (for the hold-downs connection to the base plate), are mentioned on the drawing.

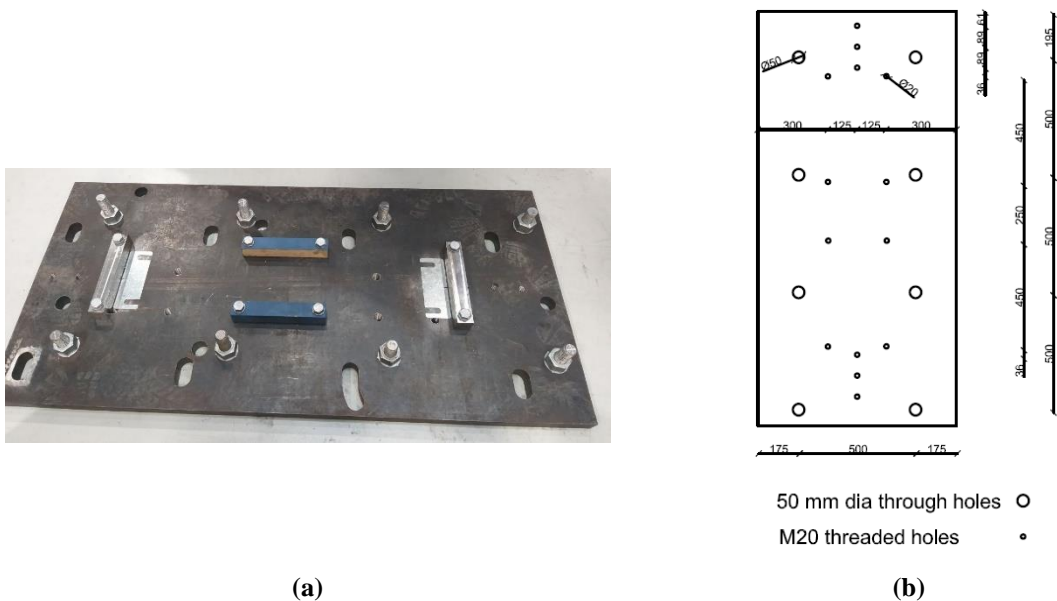


Figure 5. 15. Rocking wall base plate: a) base plate connected to the strong floor and b) arrangement of the holes.

Lateral support has been used in order to maintain safety and to restrain the wall in the out-of-plane direction. The lateral support consists of four columns located at the corners of the base plate and two tie-beams (Fig. 5.16). Timber spacers have been placed between the wall and the tie beams to prevent the wall from out-of-plane movement. The contacting surface between the wall and

timber spacers were lubricated with grease to eliminate the friction between the surfaces. As can be seen in Fig. 5.16, the beams were tied together using the straps in order to increase the overall stiffness of the set-up.

The lateral load was applied to the wall with an actuator equipped with a built-in load cell. The height of the actuator from the top of the steel base plate was 2190 mm. The push and pull forces were transferred from the actuator to the wall using the endplates with dimensions of 660*660*60mm (Fig. 5.16). The loading endplates were connected using four high strength M36 rods. The actuators were mounted close to the middle of the wall (rather than at the top) to facilitate the connection of the actuator to the specimen and the strong wall.

As shown in Fig. 5.17, two timber blocks have been used as out-of-plane shear keys. These shear keys prevent the wall from out-of-plane movement and twisting around its axis resulting from actuator imperfections.

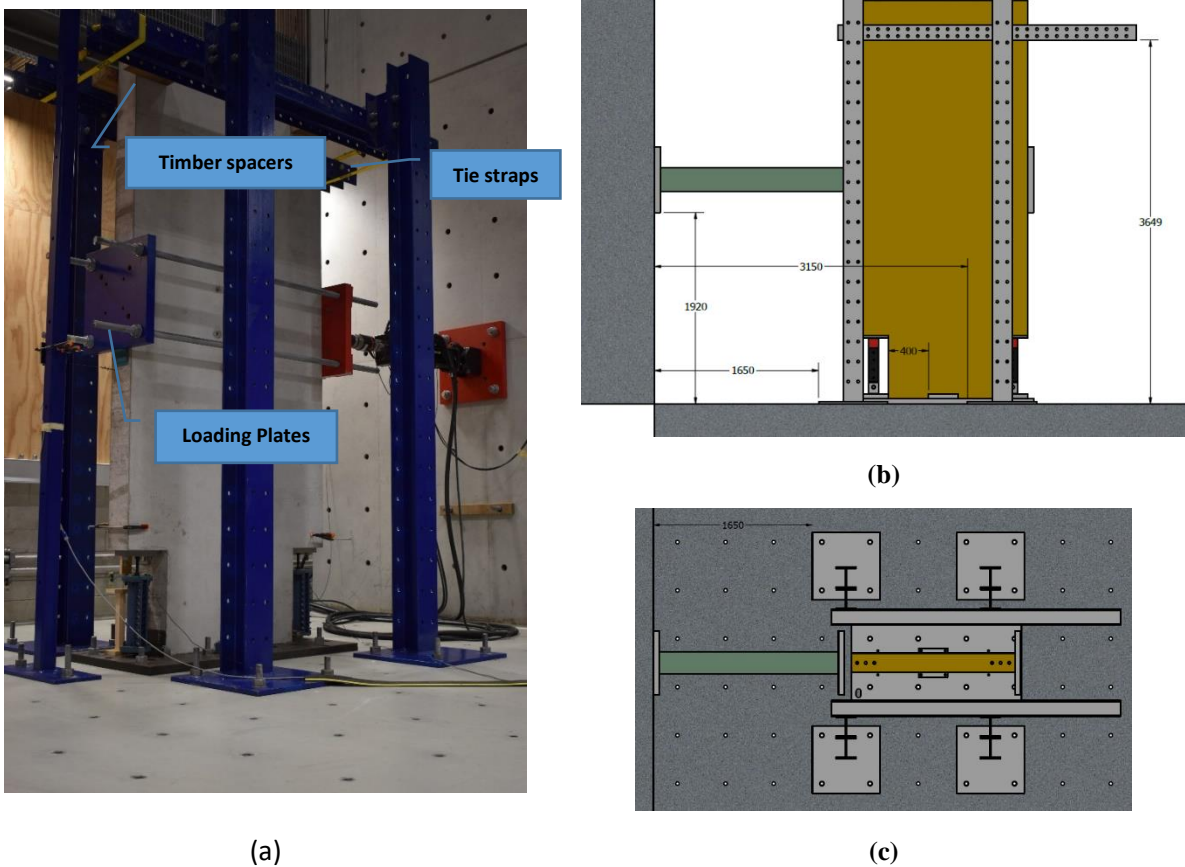


Figure 5.16. Lateral support: a) Test setup, b) schematic elevation view, c) schematic plan view.

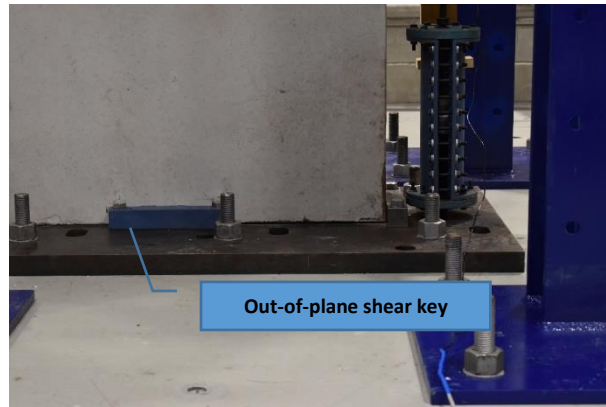
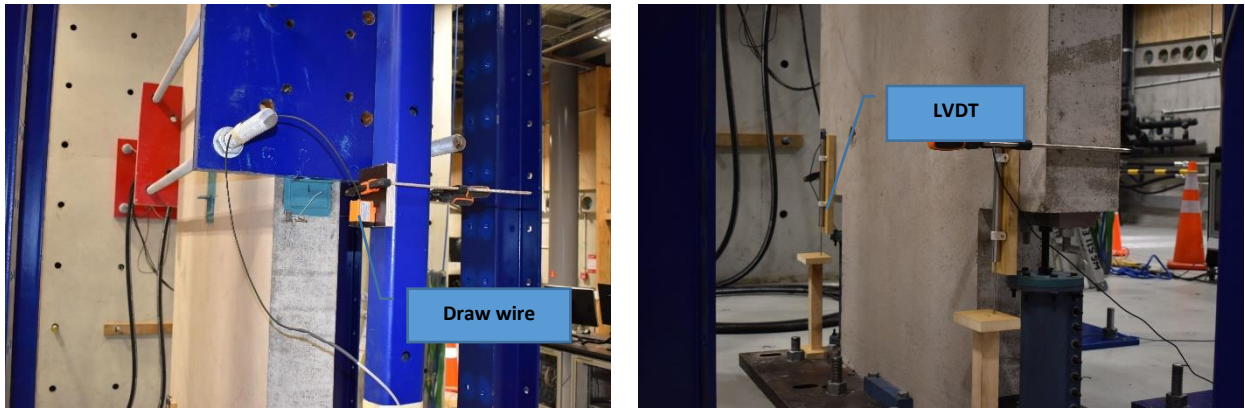


Figure 5. 17. Out-of-plane shear keys.

The specimen has been instrumented to measure different response parameters (Fig. 5.18). To measure the lateral displacement of the wall, a draw wire has been connected to the wall at the height of 1.85m (Fig. 5.18(c)). As illustrated in Fig. 5.18, two Linear Variable Differential Transformers (LVDT) have been used to measure the axial displacement of the joints. The actuator is equipped with a built-in load cell for measuring the applied force.

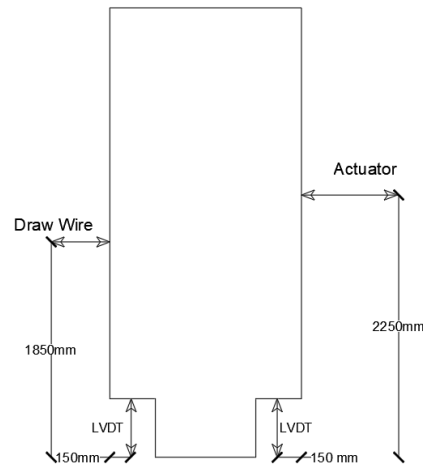
5.7 RSFJ Shear Wall

The RSFJs were designed for an ultimate force of 200 kN at the maximum displacement of 40mm. the joint dimensions and assembly are shown in Fig. 5.19. The width of the joints was 100 mm. the RSFJs were made of high strength steel Bisalloy 80 with a yield strength of 700 MPa. The clamping elements were M18 Grade 8.8 rods. In order to verify the performance of the joint, joint component testing has been done. The joints were tested in the Universal Testing Machine (UTM) as shown in Fig. 5.19c. The design parameters of the tested joints are summarised in Table 5.2. The test results and the analytical predictions are presented in Fig. 5.19(d). As can be seen from the graph, the experimental results are in good agreement with the analytical predictions.



(a)

(b)



(c)

Figure 5. 18. Instrumentation of the specimen: a) draw wire, b) LVDTs, and c) instrumentation diagram.

As illustrated in Fig. 5.20, the RSFJ had a fixed connection to the wall boundary and a pinned connection to the foundation. The RSFJ was connected to the wall from its fixed end using the PT rods prior to mounting the wall. In fact, the post-tensioning and the connection of the RSFJ to the wall were done at the same time. After the joints were connected, the rods needed to be pre-stressed up to the desired level. At the other end of the joint, a pin bracket with two tabs was used. The bracket was bolted to the base plate and then RSFJ was connected to the bracket using a pin. The designed detail allows the wall to rock around its toes while the joints can rotate freely without any additional moment to be imposed on the joints and the wall. The brackets endplates were thick enough to perform as the shear keys for the wall in-plane direction. The same material (high strength steel Bisalloy 80) as in RSFJs was used for manufacturing the brackets.

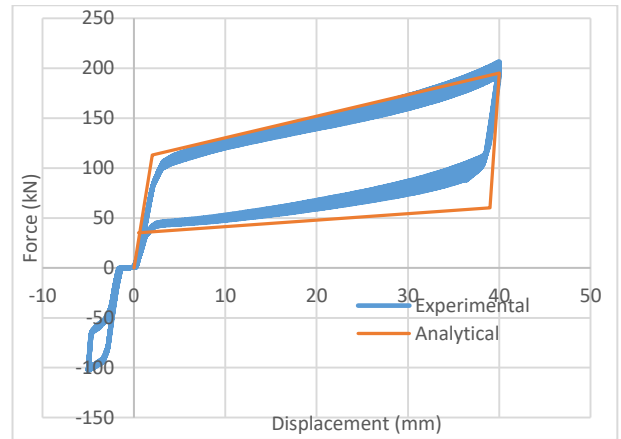
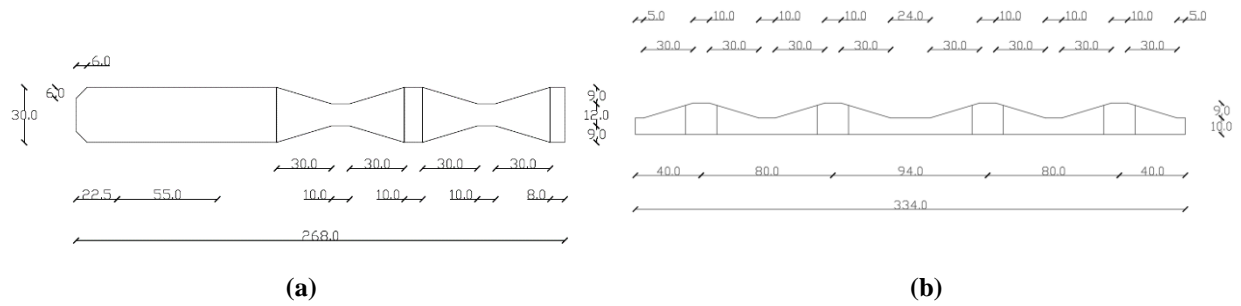
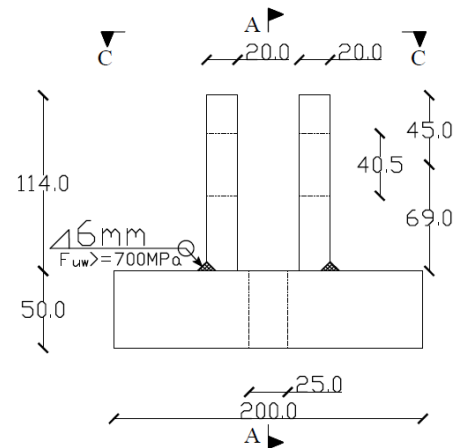
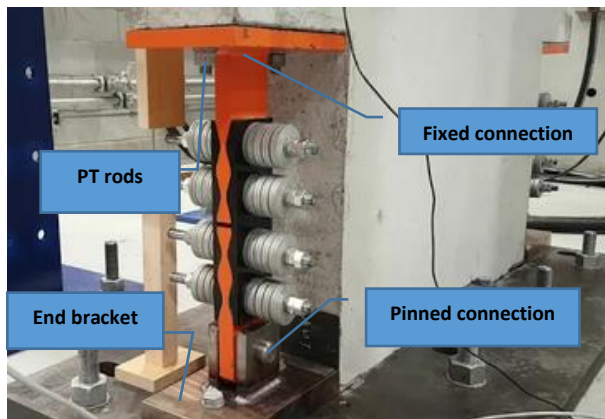


Figure 5. 19. RSFJ component testing: a) middle plate dimensions, b) cap plate dimensions, c) assembled joint tested in UTM, d) observed load-displacement performance.

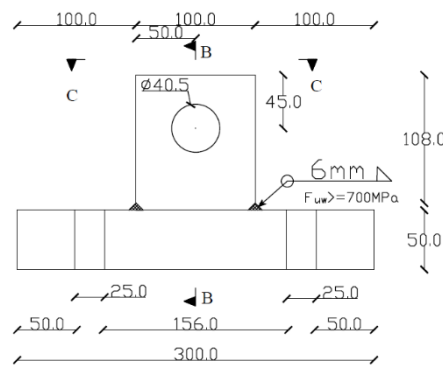
Table 5. 2. Design parameters of the tested RSFJ.

n_b	2
$F_{b,pr}$ (kN)	60
K_s (kN/mm)	7.9
Δ_s (mm)	6
μ	0.15
θ	16.7



(a)

(b)



(c)

Figure 5. 20. Details of the RSFJ: a) connection to the shear wall and base plate b) bracket section view, c) elevation view of the bracket.

The complete test set-up of the RSFJ shear wall is shown in Fig. 5.21(a). The wall was tested under reversed cyclic loading. The maximum lateral drift of 3.2% was applied by the actuator. The system has shown a stable response to lateral loading confirming the robustness of the system to be used as a new seismic resisting system. As can be seen in Fig 5.21(b), the load-displacement performance of the wall equipped with RSFJs is accurately predicted by the developed equations. The negligible difference between the experiment and the analytical results is due to some additional friction at the shear key level which was not accounted for in the analytical equations. The results verify the performance of the developed system where double-acting self-centring friction dampers are used as hold-downs. No major damage neither in the joints and connections nor in the wall was observed. Minor concrete spalling was observed at the toes which is the result

of stress concentration at the toes and minimal friction force generated in the shear keys during the rocking motion (Fig. 5.21(c)).

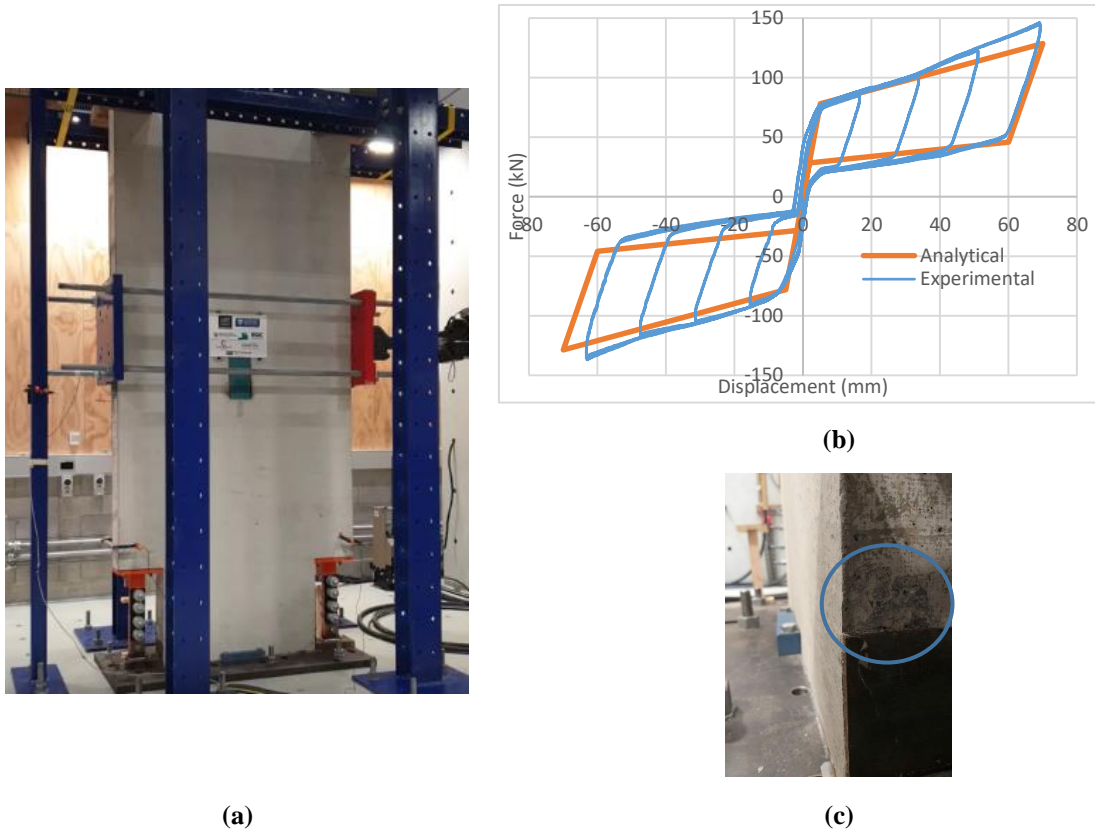


Figure 5. 21. RSFJ shear wall: a) Test setup, b) comparison of analytical and experimental results, c) minor concrete spalling at toes.

Note: displacements are inferred displacements at the actuator level based on draw-wire readings

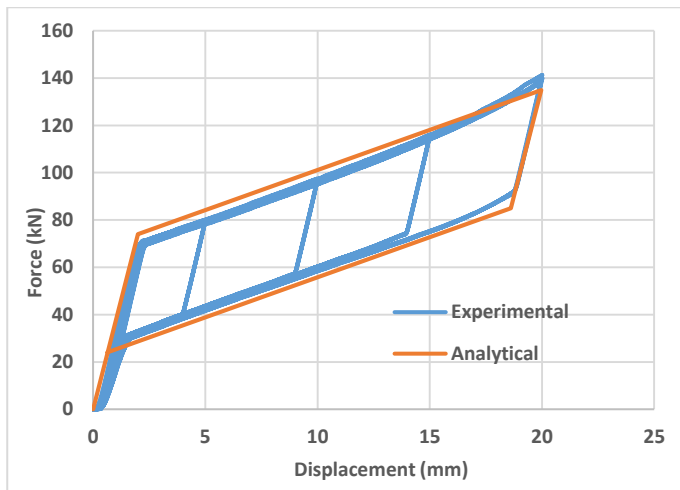
5.8 SSC Shear Wall

The SSC joints used for the rocking wall tests were originally designed for the proof of concept of the joints [163]. Later, the same joints were used for the rocking concrete shear wall test. The joints are designed for an ultimate force capacity of 135 kN and a maximum displacement of 20mm. The design parameters of the SSC are mentioned in Table 5.3. The SSCs were tested using the UTM machine to verify the load-displacement performance of the joints. The assembled joint in the UTM is shown in Fig. 5.22. The load-displacement response obtained from the test is compared to

the one predicted by the analytical equations verifying the accuracy of the developed model given the agreement between the results.

Table 5. 3. Design parameters of tested SSCs.

Δ_S (mm)	1.80
F_{pr} (kN)	49.00
F_S (kN)	110.00
n	20
Δ_{ult} (mm)	20.00
F_c (kN)	26.50
m	0.15
F_{fr} (kN)	25.00



(a)

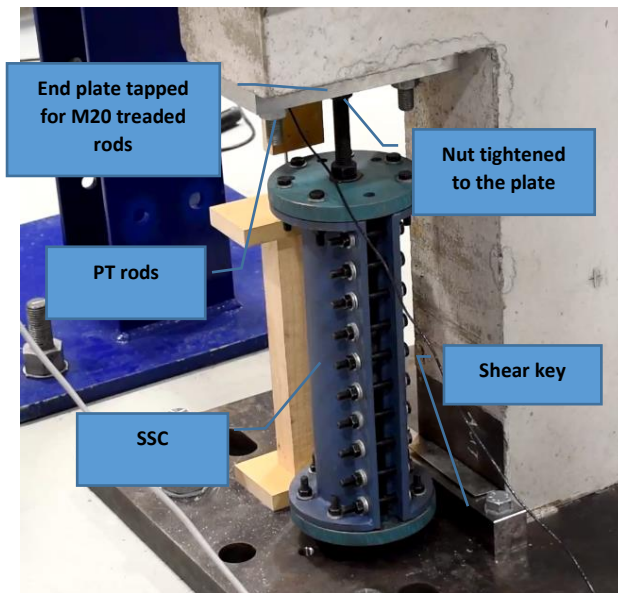


(b)

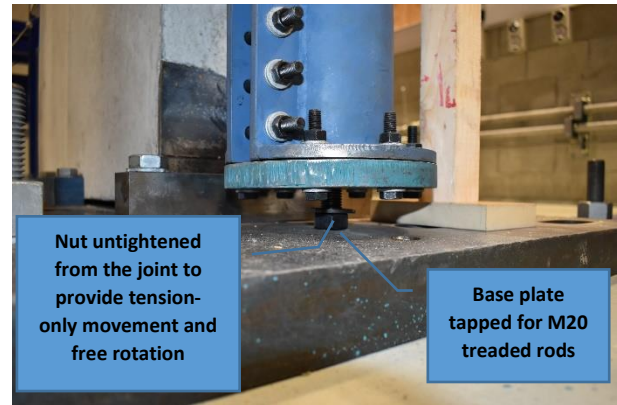
Figure 5. 22. SSC component test: a) comparison of analytical and experimental performance, b) test setup. In this section, the details related to the connection of the SSC to the wall and the foundation base plate is presented. Rod M20 Grade 10.9 has been used to connect the joint to the wall endplate and the foundation. As shown in Fig 5.23a and b, the wall endplate and the foundation base plate were tapped for the threaded holes required for the rod connection. The SSC needed to be connected to the wall first. This was done by turning the joint to screw it to the wall endplate while the wall was horizontally laid on the floor before mounting. When the wall was vertically mounted on the base plate, the SSC needed to be twisted around its axis to be screwed to the foundation base plate (Fig. 5.23(a)). There should be enough engagement length for the threads to maintain the desired

capacity. At this stage, the nut at the top of the SSC was tightened to the endplate restraining the joint from free rotation around its axis. Later, the nut at the bottom of the joint was tightened to the base plate to release the joint in compression and to prevent any compression force to be generated in the joint. In fact, the tension-only performance of the SSC was achieved by loosening the bottom nut as shown in Fig. 5.23(b). Also, it allows the joint to rotate from its bottom side to be compatible with the rotation induced by the rocking motion of the wall (Fig. 5.23(c)). For the SSC shear wall, two high strength steel blocks have been used at the wall toes to resist the shear force. These shear keys are shown in Fig. 5.23(d).

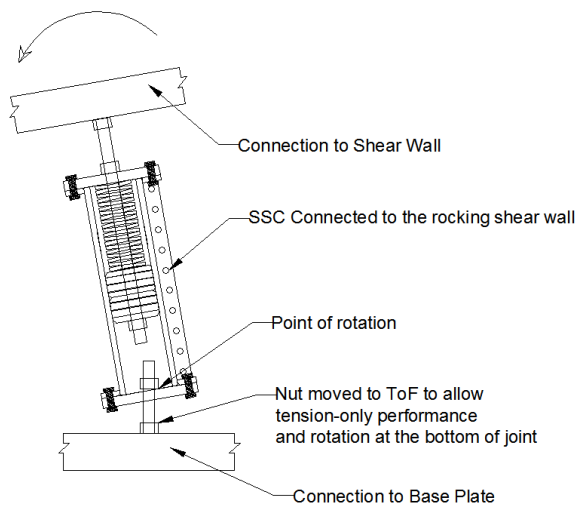
The completed test setup for the SSC shear wall is shown in Fig. 5.24(a). The wall was tested under 5 full cycles of lateral drift up to 1.6% where the maximum capacity of the joints was achieved. The load-displacement performance of the tested wall with the SSC dampers are shown in Fig. 5.24(b). The results have shown that the developed system is capable of resisting lateral loading with a repetitive and predictive response. As can be seen from the graph, the actual performance of the wall is well predicted by the analytical model. The performance of the wall was also tested under high frequency reversed cyclic testing as shown in Fig. 5.24(c). A repetitive load-displacement performance was achieved for five full cycles with a loading frequency of 0.75 Hz. The wall, joints and their connection were observed thoroughly after the test and no significant damage was detected confirming the robustness of the rocking-wall system developed with self-centring friction dampers as hold-downs.



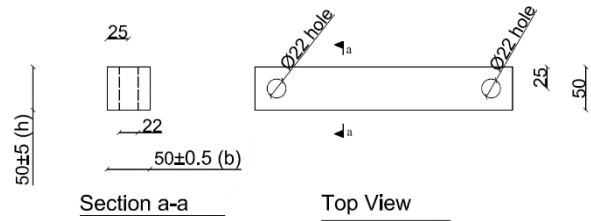
(a)



(b)



(c)

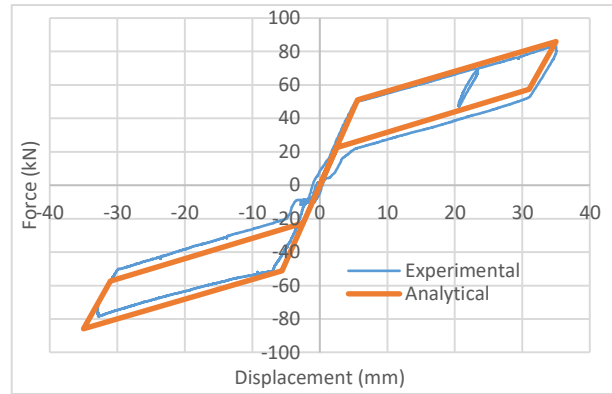


(d)

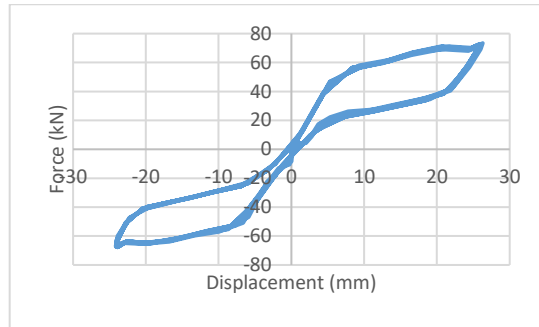
Figure 5. 23. SSC connection to shear wall and foundation: a) connection at the top of the joint, b) connection at the bottom of the joint, c) rotation compatibility with rocking motion, d) shear keys



(a)



(b)



(c)

Figure 5. 24. SSC shear wall: a) test setup, b) comparison of analytical and experimental results, and c) results under high-frequency loading.

Note: displacements are inferred displacements at the actuator level based on draw-wire readings

5.9 Numerical Modelling

A numerical model of the proposed rocking wall system is developed and analysed using the SAP2000 software [198]. The accuracy of the model is verified with the experimental results. Developing an accurate computer model using widely used commercial software is important as it facilitates the analysis of the structures by engineers. The details of the model are shown in Fig. 5.25. The non-linear shell elements were used for modelling the concrete and the reinforcements. The compressive strength of 40 MPa was considered for the concrete.

As shown in Fig. 5.25(a), the Damper-Friction Spring link element was used for modelling the RSFJs. For modelling the SSCs, the Multi-Linear Plastic and Multi-Linear elastic links can be

combined to form a unit element as illustrated in Fig. 5.26. The reader is referred to [163] for more details on how to model the SSC. The cable elements were used to model the post-tensioning elements and the pre-stressing force was applied to them as an initial deformation. The endplates were modelled as gap elements to accurately model the proposed pre-stressing method. Gap elements were also used for modelling the wall and foundation interface, allowing the wall to rock at its toes.

It should be noted that a staged construction loading case should be defined. The purpose of staged construction loading is to apply the prestressing force in the rods and the gravity force before connecting the self-centring joints to the structure. The joints are added to the structure when the wall was already pre-stressed in the previous stage. It should be noted that this modelling technique is suggested for the detailed design of the wall as a single element considering the proposed post-tensioning approach. For modelling the rocking walls in more complex cases such as in multi-story buildings or for NLTH analysis, it is preferred to keep the model simple and not to model the cable elements and the staged construction loading case. The details of the wall to base connection for each double acting or tension-only configuration is depicted in Fig. 5.25(b) and Fig. 5.25(c), respectively.

A numerical model for each configuration was made and analysed under the lateral cyclic loading. The internal forces were checked using the numerical model outputs. The distribution of the axial stresses in both the RSFJ shear wall and SSC shear wall are shown in Fig. 5.27(a) and Fig. 5.27(b), respectively. As predicted, tension stresses are eliminated using the proposed post-tensioning concept. Also, the maximum compression stress in the walls is equal to 14 MPa at the compression toe for the RSFJ shear wall and 18 MPa for the SSC shear wall at the toes which are less than the concrete compression strength of 40 MPa. The maximum compression force at the wall toe, F_{toe} , is equal to 107 kN and 170 kN for the RSFJ and SSC shear walls. These values are in agreement with the force calculated using Eq. 5.30 which verifies the analytical model developed.

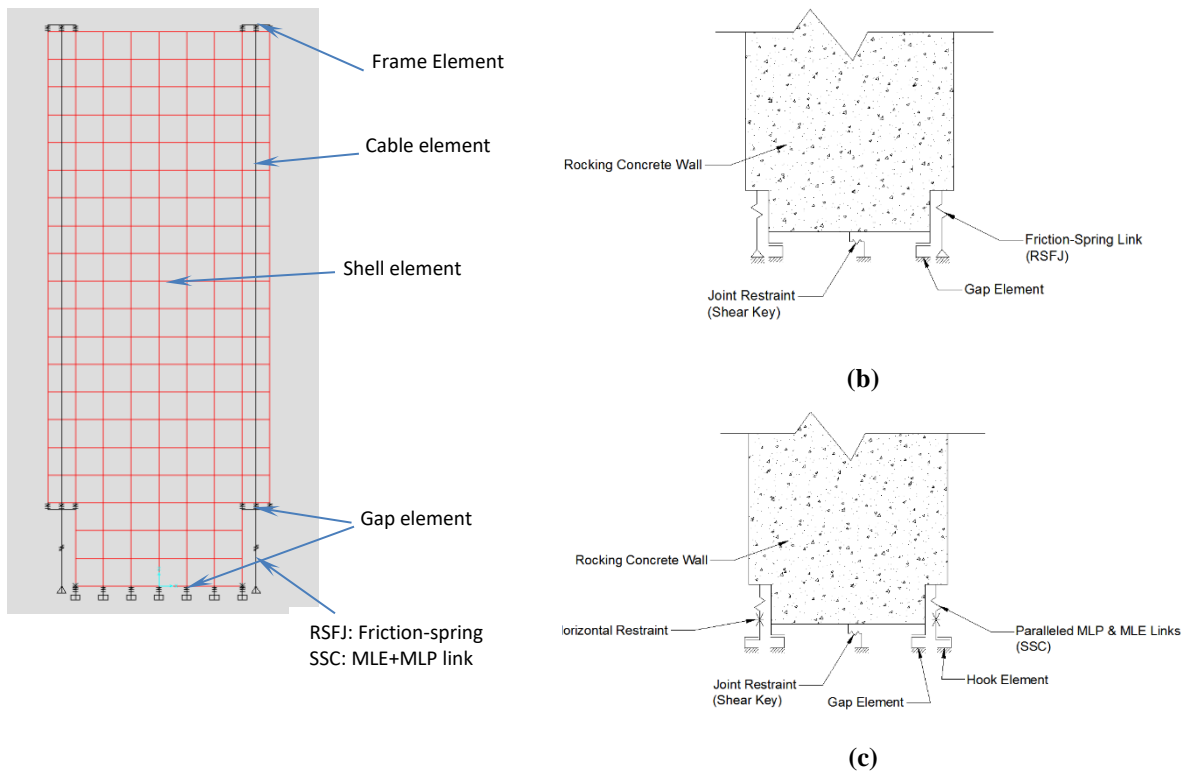


Figure 5.25. Numerical modelling of the proposed concept: a) general components, b) connection details for double-acting connections, and c) connection details for tension-only connections.

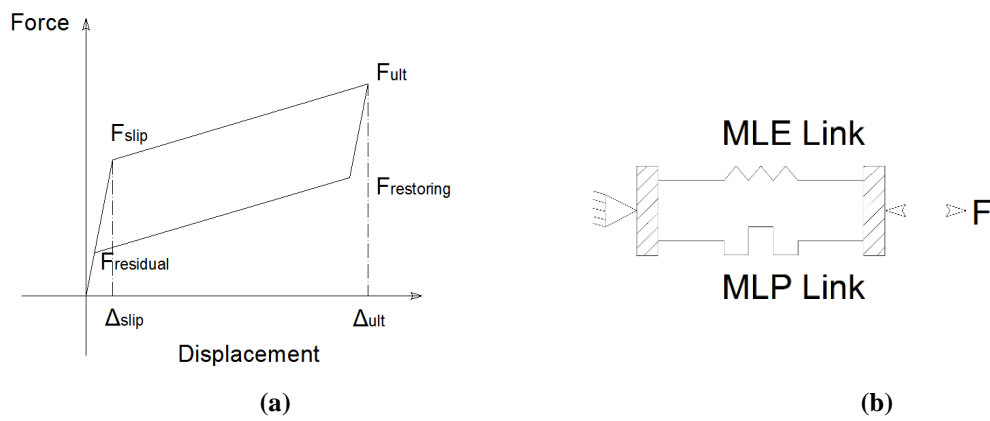


Figure 5.26. Combination of MLE and MLP links for modelling the SSC.

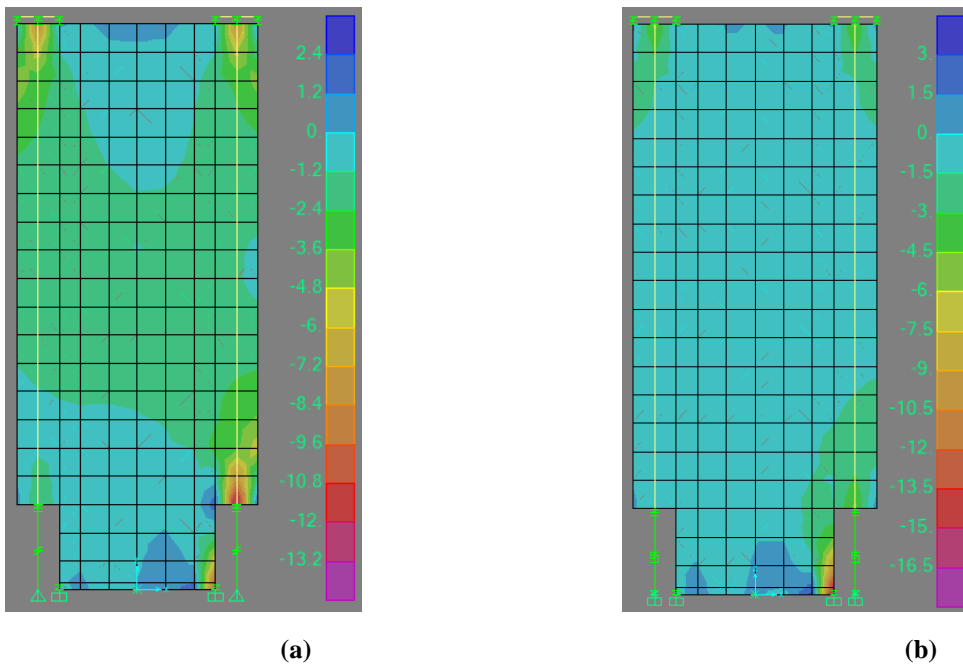


Figure 5.27. Axial stress distribution in the models: a) RSFJ shear wall, and b) SSC shear wall.

Cyclic pushover analysis is performed for each model to capture the lateral load-displacement response of the systems. As shown in Figure 5.28, the numerical results are in agreement with the experimental observations presented in the previous sections. Therefore, the accuracy of the model is verified for designing different elements of the proposed structure based on the corresponding internal actions.

Even though the overall agreement between the experimental and numerical results in Fig. 5.28a is satisfying some differences can be observed. These differences are discussed as follows. In the RSFJ shear wall test, Fig 5.20a, brackets have been used to connect the RSFJs wall to the foundation. These brackets serve the shear key role at the same time preventing the wall from lateral sliding. Bracket bolts have been tightened enough in order to prevent the wall from lateral movement. However, this constraint resulted in minor friction being generated between the wall toe and the internal face of the bracket. This additional friction resulted in a small difference in loading and unloading lines between the predicted and observed responses.

Considering the results presented in Fig 5.28b, a good agreement between the numerical and experimental results can be observed for both loading and unloading. However, a small shift from

the origin of coordinate in the negative side of the graph can be seen in the experimental results. As mentioned in Fig. 2.23a, square-section bars are used as shear keys for SSC shear wall test. These bars are tightened to the foundation using bolts. However, the tightening force is small enough to allow the shear keys to slide slightly to prevent the formation of friction at the wall hill during rocking. The minor movement at the base has resulted in the small shift in the graph as observed in Fig 5.28b.

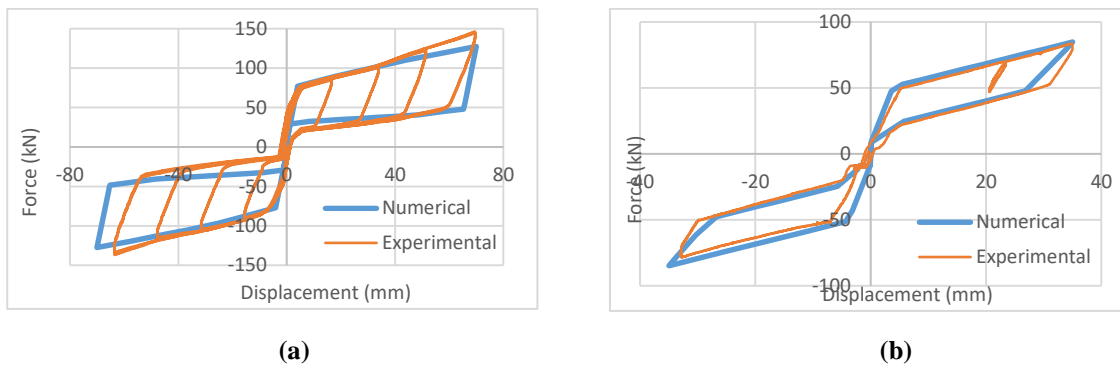


Figure 5. 28. Comparison of numerical and experimental results: a) RSFJ shear wall, b) SSC shear wall.

5.10 Non-linear time history analysis

In order to assess the seismic performance of the proposed system, a non-linear dynamic time-history analysis was carried out on a single degree of freedom model. The dimensions of the modelled rocking wall were similar to the dimensions of the wall presented in the experimental section of this paper. The load-displacement performance of the joints is shown in Fig. 5.29(a). A double-acting RSFJ was used for the structure. It was assumed that the structure was located on a soil type D zone (deep or soft soil) [164] with a 1000 year return period in Wellington, New Zealand. The hazard factor (Z), the near-fault factor (N) and the return period factor (R) were respectively determined as 0.4, 1.0 and 1.3 according to NZS1170.5 (New Zealand standard for earthquake actions) [135]. A seismic weight of 120kN was assumed and assigned to the top of the wall. A suite of three conventional earthquake records was selected and scaled in accordance with NZS1170.5 to match the Wellington 1000 year return period for Ultimate Limit State (ULS). Table

5.4 presents the selected seismic events and the associated scaled peak ground motions. The scaled acceleration records were applied at the base of the model.

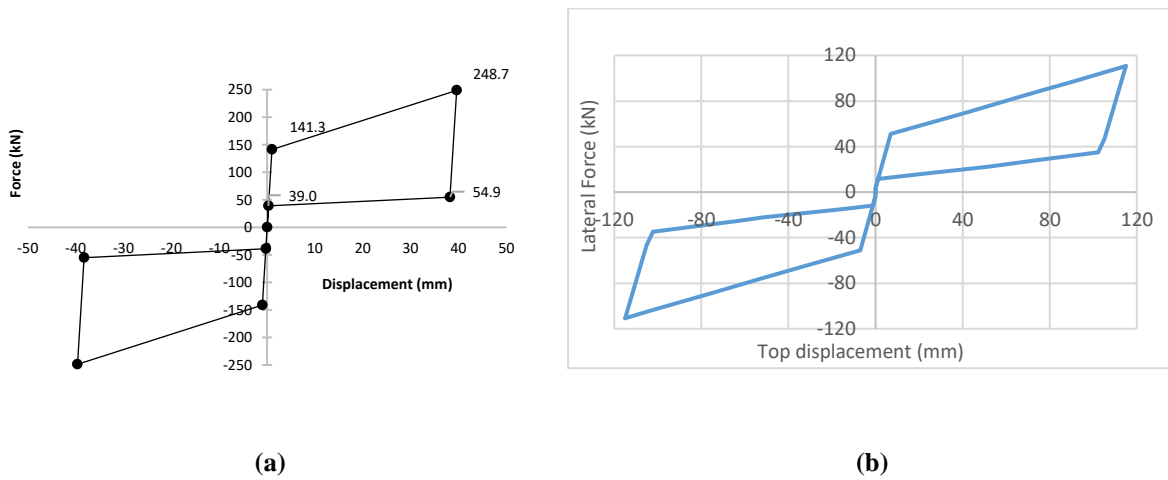


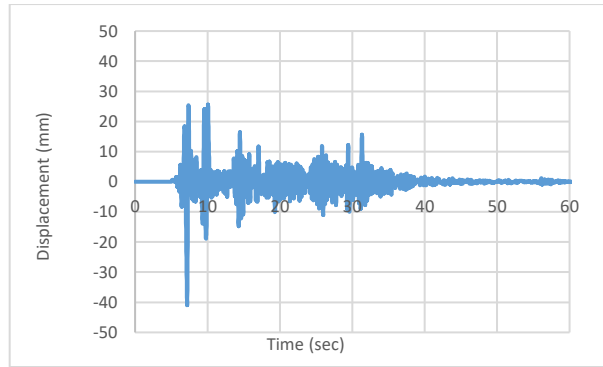
Figure 5. 29. Flag-shaped behaviour of the modelled RSFJs (Left), and Response of the proposed rocking wall system under cyclic loading for the lateral force acting at the top (H=4000mm) (Right)

Table 5. 4. Selected ground motions and scaling.

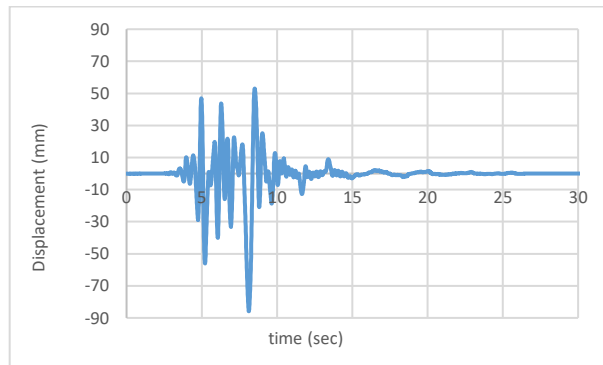
Event	Year	PGA	Scaled PGA
El Centro	1940	0.32	0.61
Christchurch	2011	0.36	0.72
Duzce	1999	0.53	0.74

The displacement responses for the three simulations are shown in Fig. 5.30. It should be emphasized that the self-centring behaviour is achieved without relying on any additional gravity loads.

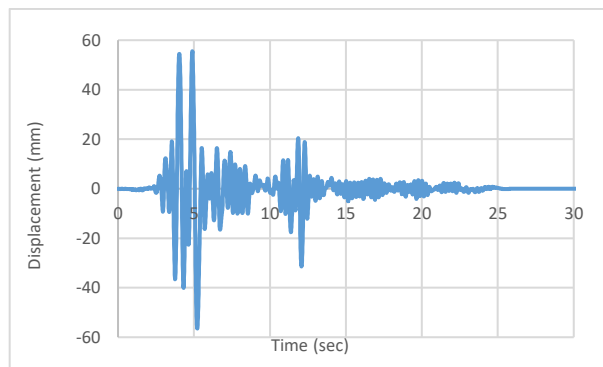
The New Zealand standard recommends a drift of 2.5% as the upper bound limit for the structures subjected to the ULS earthquakes. This limitation is indicated in Fig. 5.31. The uppermost recorded displacement among the events is for Christchurch which is approximately 2.15% of lateral drift. It can be seen that all of the recorded displacements are below the defined maximum allowable limit which indicates the efficiency of the proposed system in terms of satisfying the drift demands.



(a) El Centro 1940



(b) Christchurch 2011



(c) Duzce 1999

Figure 5. 30. Roof displacement demand for selected ground motions.

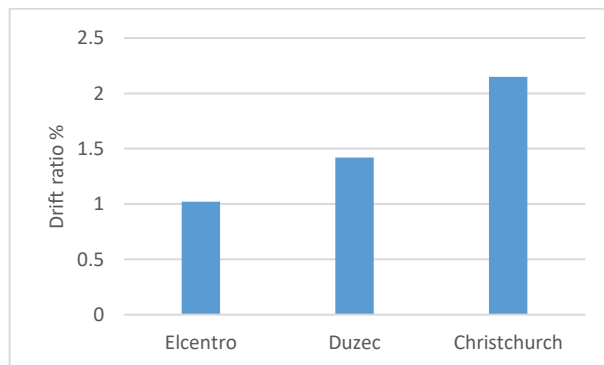


Figure 5. 31. Maximum top floor drift ratio for the selected earthquake events.

5.11 Discussion and Conclusion

This study proposes a rocking shear wall system with self-centring friction dampers as an alternative design to conventional fixed-base shear walls. Rocking shear walls can improve the seismic response of the structure considerably and mitigate the likelihood of irreparable damages. It should be noted that an additional energy dissipation mechanism helps to improve the response of the rocking wall systems by reducing the drift demand. In addition, when additional damping is employed in a rocking wall, associated damage with pounding between the wall toe and foundation, such as toe concrete crushing, will be controlled effectively.

Self-centring friction dampers have been used in this study to provide the required energy dissipation mechanism. It is proposed to use the dampers at the wall base to connect the wall boundary to the foundation.

The proposed self-centring friction devices in this study provide repetitive and reliable energy dissipation and can be considered as robust elements for the damage avoidance design (DAD) system developed in this study.

In this section, the findings of this study are discussed as follows.

1. It can be observed from the experimental results that tension-only SSC and double-acting RSFJ rocking concrete shear walls tested in this study provide viable solutions for seismic damage avoidance design of structures. The repetitive cyclic behaviour under high-frequency cyclic loading confirmed the reliability of the proposed systems.
2. the analytical procedure developed for predicting the load-displacement performance of the rocking walls were proved to be accurate when compared to the experimental results. Overall, there is less complexity in designing rocking walls with tension-only dampers used as hold-downs compared to double-acting dampers. The analytical equations developed for predicting the performance of the dampers have shown good agreement with the experimental results.

3. It should be noted that when dampers are used as hold-downs, large bending moments are expected at the base of the wall. This bending moment results in highly reinforced sections at the base. Also, additional reinforcement is required for anchoring the dampers to the bottom of the wall. In addition, bending tension cracks decrease the stiffness of the wall significantly. Consequently, the effectiveness of the damping devices will be sacrificed as less deformation is to be transferred to the dampers due to wall flexibility as the result of cracking. A new pre-stressing method has been proposed in this study to overcome cracking related issues. In this concept, before mounting the rocking wall, the wall is internally pre-stressed before being mounted on the construction site. The benefits of the proposed pre-stressing method are as follows.

- Tension stresses and tension cracks are eliminated.
- Highly-reinforced sections are not required and usually, a minimum code reinforcement will suffice.
- There is no need to design and use embedded anchors for connecting the dampers to the wall. The end plates used for wall pre-stressing can be used for connecting the dampers to the wall.
- Complex and costly on-site unbonded post-tensioning, which is common for other rocking wall systems, is not required in the proposed system make it more efficient compared to the conventional rocking systems.
- the system can be optimised for mass production and modular construction as minimum site work is required for mounting and assembly.

4. A simplified numerical analysis with widely used commercial software was used to determine the level of the internal stresses within the wall. There has been a reasonable agreement between the proposed analytical procedure and the numerical results. Minor concrete spalling at the wall toe was observed during the test. Also, tension cracks were not detected within the wall after the test. These observations verify that the level of damage is within a DAD desired performance. Therefore, the system is proved to be a robust solution for DAD.

5. Nonlinear time-history analysis was carried out to evaluate the seismic response of the proposed system with double-acting connections. Three different scaled ground motions were used, and the maximum displacement response of the system was evaluated against the design objectives. The response in all three cases was less than the code (NZS 1170.5) specified requirement confirming the reliability of the proposed system.

6. For future studies, it is recommended to further assess the performance of the proposed system through large scale three-dimensional shake table tests. The effect of deformation compatibility with the gravity structure, bi-directional loading and concurrency effects should be studied throughout the shake table testing program. More importantly, the effect of vertical accelerations on the behaviour of rocking structures should be studied experimentally as currently there is a lack of extensive study in this area.

Chapter 6: Conclusions

6.1 Conclusions

In the first chapter of this thesis, a comprehensive literature review was carried out in order to investigate the previous research done related to the scopes of this study. A summary of Chapter 1 is presented herein.

Even though achieving the life-safety performance is the main seismic design objective of a structure, minimising damages to structural and non-structural components is also important. It has been some decades since the researchers have been emphasising the need to shift from conventional ductile design to low-damage and damage avoidance designs. However, the importance of minimising damages was a lesson learnt by the rest of the New Zealand community after the 2010 and 2011 Canterbury earthquakes. For example, in the 2011 Christchurch earthquake, while most of the code-compliant structures performed as expected and saved lives, community expectations were not met as the result of the social and economic impacts of the lost properties[201]. Accordingly, a serious movement from conventional ductile design concepts to low-damage and damage avoidance design was required and therefore, emphasised by the community and authorities as well. Damage avoidance solutions should be cost-efficient yet buildable using the available resources and by building practitioners with a medium level of skills set.

Pauly's ductile link concept is still the base of the seismic design of low-damage systems. In traditional ductile design, the ductile link will be sacrificed and lose its ability to maintain the energy dissipation characteristics in future earthquakes. The link could not be repaired or replaced by a reasonable effort and cost. Also, residual deformations persist and structural integrity for resisting gravity loads might be endangered. However, equivalent ductile links, fuses, in low-damage structures can be repaired or replaced if required after severe earthquakes. A variety of

low-damage systems have been developed, tested and even used in real constructions in recent years. Some of them have consequently experienced moderate to severe seismic events and responded well to the actions and loadings imposed by the earthquakes. The common characteristic amongst fuses in low-damage systems is a predictable and repeatable energy dissipation property. This damping characteristic is usually provided either using yielding, friction or viscous damping. However, low-damage structures have been criticised for the expected residual deformation after earthquakes. It is interruptive, complex, timely and costly to set the deformed structure back to its upright status.

The Damage Avoidance Design (DAD) concept has solved the residual deformation problem. DAD requires a stable and robust energy dissipation to be combined with reliable re-centring capability. Self-centring capability is usually provided using pre-stressing. A residual force being kept within either the structure or the energy dissipation fuses can provide the potential energy required for bringing the structure back to a zero-deformation status when the earthquake loading has disappeared.

Friction has been used as a source for seismic energy dissipation in several different low-damage concepts. The load-displacement performance of friction dampers can be easily predicted as they are an equivalent of an elastic-perfectly-plastic response. Also, the cyclic response of friction-based dampers is repetitive which is suitable for seismic resisting structures. Friction-damped structures have performed well in past earthquakes. When combined with self-centring, a robust system is achieved in which the damage is minimised and there will be no residual displacement after earthquakes. Therefore, post-event realignment is not required, and the building can be reoccupied quickly after the event resulting in minimising business interruption. Accordingly, structural systems utilising self-centring friction dampers are of desired seismic performance to form a DAD system and are therefore worth development and then adopted in real construction.

The lack of previous research on developing concrete structures equipped with self-centring friction dampers has been addressed in this research. Rocking concrete shear walls have been developed and studied in several previous studies. Post-tensioned cables and additional yielding dampers have been used for controlling the rocking motion in these structures. The pros and cons of these systems were reviewed in Chapter 1 and compared to those of traditional ductile reinforced concrete (RC) walls. It was mentioned that even though the damage is considerably controlled in rocking walls, complexity and additional site work and measurements are required to install and pre-stress these walls. Also, yielding dampers should be inspected after moderate to severe events and repaired or replaced if required as they are prone to low-cycle fatigue and local instability failures. Accordingly, it was required to develop a rocking wall concept with compact self-centring friction dampers to be used in DAD of structures. The developed system should simplify construction and minimise post-event maintenance. This study aimed to develop such systems.

The first stage of developing the concrete rocking wall system was to adopt suitable self-centring friction dampers. This stage of the study was presented in Chapter 2 and Chapter 3 of this thesis. In Chapter 2, Resilient Slip-Friction Joint (RSFJ), a self-centring friction damper, was selected and studied analytically and experimentally. The purpose of this study was to review the previously conducted research on the RSFJ and the feasibility of adopting the damper in developing the structural system in the next phases of this research. As the RSFJ was a new concept at the time of this study, the pros and cons of the damper were investigated and new unique contributions have been made to improve the design and performance of the RSFJ.

Unique contributions of the research presented in Chapter 2 are summarised as follows.

- The performance prediction equations were improved by implementing the use of only one coefficient of friction (μ), instead of using two different static (μ_s) and dynamic (μ_k) coefficients of friction. The need for this new improvement was verified through experimental investigations in this Chapter.

- A new simplified mechanics-based analytical method was developed for the first time to optimise the analysis and design process of the RSFJ. This new model negates the need for complex and timely computer-based finite-element modelling. Internal forces and elastic deformations can be derived easily by spreadsheets developed based on the new analytical model.
- The RSFJ locks at its maximum displacement. When the damper locks during an earthquake stronger than the design level, a shock can be imposed on the supporting structure resulting in damage and even catastrophic failure in the gravity structure. As one of the unique and important contributions of this research, a new Anti-Locking Mechanism (ALM) was introduced, developed and experimentally verified in Chapter 2. The concept was developed analytically and then investigated and verified experimentally as one of the main contributions of Chapter 2.

As discussed in Chapter 1, to achieve a robust damage avoidance design (DAD) system, self-centring is crucial. Self-centring devices were reviewed in Chapter 1 including viscous, HF2V, ESD and friction ring springs. Later on, within the thesis, the RSFJ concept was introduced and novel contributions were made to improve the performance of the damper.

Viscus and HF2V dampers are rate dependent dampers with reliable energy dissipation characteristics. However, viscous dampers are rather expensive and it is quite challenging to design the structures equipped with these dampers. Also, they get quite big when designed for high capacities limiting their use for architectural considerations. HF2V dampers are cost-efficient dampers developed based on the lead extrusion concept. These dampers have been used successfully in real construction projects. One of the deficiencies of viscous and HF2V dampers from a mass-production point of view is that each individual product represents the force-displacement performance it is designed to. Therefore, dampers that are designed for a specific

project are not adjustable to be used for another project with different load-deformation requirements.

ESD dampers have mentioned reliable self-centring and energy dissipation characteristics. However, as described for HF2V dampers, they are not suitable when it comes to mass production. Friction dampers have shown reliable hysteretic damping for seismic input energy dissipation. Also, the friction force can be easily adjusted by the applied normal force making the dampers more flexible in terms of design. Ring springs, as discussed in Chapter 1, are self-centring friction devices with superior damping and self-centring performance. Flexibility in design with adjustable force-displacement characteristics for each individual product making them excellent choices for mass production. However, damping and self-centring are coupled in ring-springs so by changing one, the other one is changed as well. Also, axial pre-stressing absorbs a portion of displacement capacity.

Resilient Slip Friction Joint, RSFJ (invented by others), was adopted for the purpose of this study. The RSFJ incorporates the same conceptual framework as friction ring springs in a different way. Friction rings have been replaced by grooved plates pre-stressed and clamped together using Belleville springs. In the RSFJ, the pre-stressing is applied perpendicular to the main axis of the damper making it more flexible to be used in different applications. The RSFJ has pros and cons. It can be designed to accommodate large forces while keeping its robust self-centring ability and repetitive energy dissipation. However, the RSFJ is prone to in-plane and out-of-plane instability and internal (within the RSFJ) or external (in the supporting structure) arrangements are required to deal with the instability issue. Also, it is not suitable for outdoor and corrosive environment applications as the moving parts are exposed. Also, friction and pre-stressing (Damping and self-centring) are coupled together and controlled using the cap-plate clamping bolts. Coupled damping and self-centring results in less flexibility in design and performance optimisation.

To overcome the RSFJ issues, a unique, new, patentable concept was invented and proposed by the author (main inventor) and scoped to be developed during this research. Accordingly, extensive concept development, patentability research, analytical and experimental investigations were conducted during this research. The damping concept, Self-Centring structural connector (SSC), which is presented in Chapter 3 is the unique contribution of the candidate.

The SSC was introduced in chapter 3 with new contributions as listed below.

- The mechanism and different components of the new damper were explained and the equations governing the damper behaviour were developed for the first time.
- The prototype of the damper (tension-only variation) was designed and tested. The self-centring and energy dissipation characteristics of the damper were observed during the experiments. Therefore, the overall performance of the concept was proved to be as expected for the first time as one of the important outcomes of this thesis.
- New developed analytical equations were verified against experimental results and the effect of different parameters such as pre-stressing force and friction in the response of the damper were investigated.
- Various configurations and variations of the damper were proposed and the potential applications of the SSC in different lateral load resisting systems were discussed.
- A general approach for numerical modelling of the damper using structural analysis software was introduced.

The benefits of the SSC can be summarised as follows. SSC is flexible in design as uncoupled and adjustable damping and Self-centring making it excellent for mass production purposes. SSC is cost-efficient and easy to manufacture and no costly and complicated manufacturing methods such as casting is required. Robust uniaxial performance without in-plane and out-of-plane instability issues are one of the SSC advantages compared to other self-centring dampers. Optimised

repetitive damping the ratio of friction to normal force F_c/F_{fr} is 0.95 in the SSC which means that the friction and normal force are almost the same. Therefore, unlike other friction dampers, the huge normal force is not required in the SSC making the design less challenging and more cost-efficient. SSC is excellent for applied outdoor and corrosive environment applications as the moving parts can be sealed easily.

The study related to the component level of this thesis was undertaken and presented in Chapter 2 and Chapter 3. In Chapter 4, the seismic performance and design of structures equipped with self-centring dampers with an emphasis on rocking wall systems were investigated. It was assumed that the dampers were used as based connections of the rocking wall system. The outcome of Chapter 4 can be summarised as below.

- A new design procedure was proposed based on Direct Displacement Based Design method.
- The proposed design procedure was developed based on equivalent damping ratio and effective stiffness instead of ductility and yielding concepts. In fact, it was assumed that a self-centring system with supplemental damping is equivalent to an elastic system with viscous damping with a ductility factor of one.
- A five-story prototype building equipped with concrete rocking shear walls utilizing RSFJ and SSC as hold-downs was designed based on the proposed design procedure.
- Resilient Slip-Friction Joint (RSFJ) was selected to represent the performance of a double-acting connection and Self-centring Structural Connector (SSC) was selected to represent the performance of a tension-only connection.
- The structure was designed for two different systems based on the proposed procedure. Non-linear pushover analysis was used to capture the load-displacement performance of the systems. Also, Nonlinear time-history analysis was carried out in order to verify the seismic performance of the designed buildings.

- The seismic response of the structure was assessed against the desired response parameters such as the roof displacement and the maximum inter-story drift. The structures performed as expected and the response parameters were in compliance with the maximum intended design limits.
- The proposed design procedure can be used for the seismic design of rocking wall structures equipped with self-centring dampers. The main contribution of Chapter 4 is to prove that it is not required to adopt a ductility factor for direct displacement-based design (DDBD) of damage avoidance designed (DAD) structures. Ductility means unrestorable deformation which is not the case in DAD structures. A DAD structure can be looked at as an elastic system with supplemental damping modelled as equivalent viscous damping.

When the seismic response of the buildings designed using the proposed rocking wall system was investigated through the research presented in Chapter 4, a comprehensive study was carried out as presented in Chapter 5 to develop and detail the proposed rocking wall system. As mentioned in the primary phases of this study, the objective of this part of the study was to achieve an efficient system that not only minimises damage and provides self-centring but also decreases any required post-event maintenance work (suitable for DAD philosophy). Also, improving the construction simplicity compared to current rocking walls with post-tensioning cables was another objective of this part of the research. Chapter 5 can be summarised as follows.

- An extensive large-scale experimental study was carried out to develop a new rocking-concrete wall system equipped with self-centring friction dampers as one of the unique contributions of this thesis. The developed system and relevant design procedure are another contribution of this research to the knowledge in the field of this study.
- The conceptual framework and the analytical model were developed and used to design the experimental study.

- The test results verified the accuracy of the developed analytical procedure. The robustness of the proposed structural system as a reliable seismic resisting system was approved considering the predictability and repeatability of the performance.
- A numerical procedure using widely available software was introduced and verified. This was undertaken in order that the analysis and design of the proposed system could be completed by the wider engineering community without the need for specialist or bespoke software.
- The seismic performance of the system was examined using Nonlinear Time-History Analysis (NLTH) analysis on a prototype building and compared to New Zealand seismic design code [164] requirements. The results verified that the performance criteria of the design code are met by the designed system.

In summary, the new low-damage structural system developed in this research has met the requirements defined in the scope of the research and is capable of being used as an efficient solution for Damage Avoidance Design (DAD).

The author suggests potential further research to be carried out in the areas mentioned in the next section.

6.2 Future studies

The proposed future studies are classified into two main categories as follows. First, suggestions are made for future research related to Chapter 3. The dampening concept (the SSC) has a lot of potential for further development and research. As discussed in Chapter 3, There are different applications and configurations of the damper that are worth further detailed development. Second, the proposed rocking wall system has potential for further future studies as described later on in this chapter.

Self-centring Structural Connector (SSC)

In this study, the tension-only variation of the damper was designed and studied. As it was mentioned in Chapter 3, compression-only and double-acting configurations of the damper can be designed. The double-acting configuration can be used in lots of different applications such as braces and rocking wall systems and different retrofitting applications. It is suggested that the double-acting variation of the damper be designed for high force and displacement capacities (for example more than 1000 kN force and 100mm displacement) and tested under different loading seismic load scenarios.

Furthermore, the proposed arrangement in Chapter 3 for the application of the SSC in steel moment-resisting frames is cost-efficient suitable for modular construction of steel buildings. Steel moment resisting frames (MRF) are common seismic resisting systems, especially where the use of braces or walls is restricted due to architectural considerations. Common problems of conventional ductile structures such as brittle and unexpected failure modes, design complexity and residual deformations remain with ductile MRF's. Therefore, developing an SSC based damage avoidance MRF carrying the desired characteristics of DAD philosophy is an interesting topic for future studies. In addition to satisfying DAD requirements, the developed MRF system should be cost-efficient and construction friendly.

Concrete Rocking Wall

In this research, it was assumed that the gravity load resisting system is separated from the seismic load resisting system and the rocking wall system resists earthquake loads only. In the structural system developed in this study, the considered gravity load is only the self-weight of the wall. If the building design requires transferring the roof gravity loads to the rocking wall system, it will affect the seismic response of the wall and therefore the design of the dampers.

The effect of the gravity load should be investigated for two aspects. First, the seismic response of the system; when the lateral displacements are within the drift requirements of the system, the

gravity load tends to re-centre the system. The tendency for re-centring results in a decrease in the damping ratio of the system. In fact, as no additional damping is involved in the re-centring effect of the gravity load, the damped energy area in the load-displacement performance graph will be decreased. Therefore, an analytical and numerical parametric study on the effect of the floor gravity loads on the design of the system is suggested for further future research.

Second, Wall floor connection, especially when gravity loads are transferred from the floor to the rocking wall, is of special concern. Accordingly, it is suggested to perform a further study on the suitable detailing and design of the wall to floor connection. The designed connection should be able to continuously and safely transfer the gravity load to the wall while compatible with the vertical movements of the wall due to the rocking motion.

Higher mode effects in the response of the multi-degree of freedom structures equipped with the proposed system are also suggested to be studied in the future. The seismic response of multi-story buildings with the developed rocking wall system was studied in Chapter 4. It was assumed in developing the equations presented in Chapter 4 that the seismic response of the multi-degree of freedom system can be analyzed using an equivalent single degree of freedom system. The rocking motion is inherently intended to follow the first translational mode of vibration with a triangular distribution throughout the height of the structure. When the seismic masses, especially in high rise buildings, tend to vibrate based on the higher modes of the system, higher demands are expected in the rocking wall. Accordingly, the required future study on the higher mode effects can be suggested on two different aspects as follows.

First, extensive NLTH analysis should be carried out in order to assess the effect of various parameters on the demands imposed by the higher vibration modes. Second, suitable solutions should be found where the higher mode demands result in an uneconomical design. Using walls with multiple rocking sections through the height of the structure is one of the possible solutions as each section can oscillate independently according to the dominant vibration mode for that

section. Finding the optimum location of the rocking sections could be a potentially significant topic for future studies and technical refinement of the concepts presented in this thesis. It should be noted that researchers have studied the design of multiple rocking walls to mitigate the higher mode effects [193, 202]. However, those studies have been mostly carried out on cable-based rocking systems. Further study is proposed to investigate how higher mode effects can be mitigated in rocking systems equipped with self-centring dampers.

As for another topic for future studies, the response of a system consisting of the proposed rocking wall system paralleled to another system can be investigated. In architecturally complex buildings, designers may prefer to use parallel systems in order to effectively distribute the seismic actions between lateral resisting systems. For example, a steel Moment Resisting Frame (MRF) or a braced frame might be used in parallel to the proposed rocking wall system. It is suggested to conduct further study on the seismic performance and design of such systems in order to provide the required scientific background for the engineering community aiming to adopt damage avoidance design (DAD) solutions in their everyday design. Damage avoidance solutions have been developed through research programs in which the main focus has been on the development of the system itself and not on how this system can be combined with other systems. Once the solution is developed, it is important to investigate how it can work in combination with other common systems. This will provide the designers with the required knowledge and then flexibility to use different structural systems in their designs. Initial stiffness distribution, post-slip or post-yielding strength distribution and the interaction between the systems and deformation compatibility should be studied analytically and numerically. Design procedures and recommendations should be provided as an important scope of the suggested future study.

Also, it is suggested to investigate the optimum position of the damper at the base of the wall. In this study, the dampers were positioned at the base of the wall close to the edges. This arrangement results in the smallest force demand and the largest displacement demand. When the dampers are

mounted closer to the centre-line of the wall, bigger force and smaller displacement demands are expected. The effect of this positioning in both the performance of the system and the design of the self-centring connections should be studied in the future. The aim should be on improving the response and minimizing the construction cost and complexity.

Finally, it is suggested to perform a comprehensive shake table testing on a three-dimensional structure subjected to tri-directional earthquake loading. The scopes of the shake table test can be defined as follows. Firstly, the accuracy of the design procedure presented in Chapter 4 of this research can be verified based on the shake table results. Analytical investigations should be carried out in order to study the effect of vertical accelerations on the response of the developed rocking wall system. Also, the out-of-plane compatibility of the rocking wall system with the ground-shaking perpendicular to the rocking wall direction can be examined via shake table testing. Finally, it is suggested to consider the effect of mass eccentricity in the response of buildings subjected to simulated earthquakes using shake table testing. A robust damage avoidance design (DAD) is achieved when the system survives the structure from real earthquakes. Therefore, shake table testing of the proposed system is an important requirement for future studies.

REFERENCES

1. Sritharan, S., et al. *Lessons from 2011 Christchurch Earthquake for Improving Seismic Performance of Concrete Walls*. in *Proc Second European Conference on Earthquake Engineering Second European Conference on Earthquake Engineering and Seismology*. 2014.
2. Sritharan, S., et al., *Understanding poor seismic performance of concrete walls and design implications*. *Earthquake Spectra*, 2014. **30**(1): p. 307-334.
3. Wallace, J.W., et al., *Damage and implications for seismic design of RC structural wall buildings*. *Earthquake Spectra*, 2012. **28**(S1): p. S281-S299.
4. Kam, W.Y., S. Pampanin, and K. Elwood, *Seismic performance of reinforced concrete buildings in the 22 February Christchurch (Lyttleton) earthquake*. 2011.
5. Elwood, K.J., *Performance of concrete buildings in the 22 February 2011 Christchurch earthquake and implications for Canadian codes*. *Canadian Journal of Civil Engineering*, 2013. **40**(3): p. 759-776.
6. Wallace, J.W., *Behavior, design, and modeling of structural walls and coupling beams—Lessons from recent laboratory tests and earthquakes*. *International Journal of Concrete Structures and Materials*, 2012. **6**(1): p. 3-18.
7. Maffei, J., et al., *Recommendations for Seismic Design of Reinforced Concrete Wall Buildings Based on Studies of the 2010 Maule, Chile Earthquake*. 2014.
8. Paulay, T. and M.N. Priestley, *Seismic design of reinforced concrete and masonry buildings*. 1992.
9. Mander, J.B., *Beyond ductility*. *Bulletin of the New Zealand Society for Earthquake Engineering*, 2004. **37**(1): p. 35-44.
10. Mander, J.B. and C.-T. Cheng, *Seismic resistance of bridge piers based on damage avoidance design*, in *Seismic resistance of bridge piers based on damage avoidance design*. 1997. p. 109-109.
11. Buchanan, A.H., et al., *Base isolation and damage-resistant technologies for improved seismic performance of buildings*. 2011.
12. Pekcan, G., J.B. Mander, and S.S. Chen, *Fundamental considerations for the design of non-linear viscous dampers*. *Earthquake engineering & structural dynamics*, 1999. **28**(11): p. 1405-1425.
13. Holden, T., J. Restrepo, and J.B. Mander, *Seismic performance of precast reinforced and prestressed concrete walls*. *Journal of Structural Engineering*, 2003. **129**(3): p. 286-296.
14. Ajrab, J.J., G. Pekcan, and J.B. Mander, *Rocking wall-frame structures with supplemental tendon systems*. *Journal of Structural Engineering*, 2004. **130**(6): p. 895-903.
15. Mulligan, K.J., et al., *Semi-active rocking wall systems for enhanced seismic energy dissipation*. 2006.
16. Rodgers, G.W., et al., *Performance of a damage-protected beam-column subassembly utilizing external HF2V energy dissipation devices*. *Earthquake Engineering & Structural Dynamics*, 2008. **37**(13): p. 1549-1564.
17. Solberg, K., et al., *Performance of a damage-protected highway bridge pier subjected to bidirectional earthquake attack*. *Journal of structural engineering*, 2009. **135**(5): p. 469-478.
18. Hamid, N. and J.B. Mander, *Damage avoidance design for buildings*. *KSCE Journal of Civil Engineering*, 2014. **18**(2): p. 541-548.
19. Rodgers, G.W., J.B. Mander, and J.G. Chase, *Semi-explicit rate-dependent modeling of damage-avoidance steel connections using HF2V damping devices*. *Earthquake engineering & structural dynamics*, 2011. **40**(9): p. 977-992.
20. Toranzo, L., et al., *Shake-table tests of confined-masonry rocking walls with supplementary hysteretic damping*. *Journal of Earthquake Engineering*, 2009. **13**(6): p. 882-898.
21. Pekcan, G., J.B. Mander, and S.S. Chen, *Balancing lateral loads using tendon-based supplemental damping system*. *Journal of structural engineering*, 2000. **126**(8): p. 896-905.

22. Pekcan, G., J.B. Mander, and S.S. Chen, *Experiments on steel MRF building with supplemental tendon system*. Journal of structural engineering, 2000. **126**(4): p. 437-444.
23. Henry, R., *Self-centering precast concrete walls for buildings in regions with low to high seismicity*. 2011, ResearchSpace@ Auckland.
24. Priestley, M.N., et al., *Preliminary results and conclusions from the PRESSS five-story precast concrete test building*. PCI journal, 1999. **44**(6): p. 42-67.
25. Housner, G.W., *The behavior of inverted pendulum structures during earthquakes*. Bulletin of the seismological society of America, 1963. **53**(2): p. 403-417.
26. Nazari, M., *Seismic performance of unbonded post-tensioned precast wall systems subjected to shake table testing*. 2016, Iowa State University.
27. Kurama, Y., et al., *Seismic behavior and design of unbonded post-tensioned precast concrete walls*. PCI journal, 1999. **44**(3): p. 72-89.
28. Rahman, A.M. and J.I. Restrepo-Posada, *Earthquake resistant precast concrete buildings: seismic performance of cantilever walls prestressed using unbonded tendons*. 2000.
29. Holden, T.J., *A comparison of the seismic performance of precast wall construction: Emulation and hybrid approaches*. 2001.
30. Sritharan, S., et al. *Introduction to PreWEC and key results of a proof of concept test*. in *MJ Nigel Priestley Symposium*. 2008.
31. Priestley, M.N. and J.R. Tao, *Seismic response of precast prestressed concrete frames with partially debonded tendons*. PCI journal, 1993. **38**(1): p. 58-69.
32. Kurama, Y.C., *Unbonded post-tensioned precast concrete walls with supplemental viscous damping*. ACI Structural Journal, 2000. **97**(4): p. 648-658.
33. Kurama, Y.C., *Simplified seismic design approach for friction-damped unbonded post-tensioned precast concrete walls*. Structural Journal, 2001. **98**(5): p. 705-716.
34. Sritharan, S., et al., *Precast concrete wall with end columns (PreWEC) for earthquake resistant design*. Earthquake Engineering & Structural Dynamics, 2015. **44**(12): p. 2075-2092.
35. Marriott, D., et al., *Dynamic testing of precast, post-tensioned rocking wall systems with alternative dissipating solutions*. 2008.
36. Marriott, D.J., *The development of high-performance post-tensioned rocking systems for the seismic design of structures*. 2009.
37. Twigden, K. and R. Henry. *Experimental response and design of O-connectors for rocking wall systems*. in *Structures*. 2015. Elsevier.
38. López, W.A. and R. Sabelli, *Seismic design of buckling-restrained braced frames*. Steel tips, 2004. **78**.
39. Grigorian, C.E., T.-S. Yang, and E.P. Popov, *Slotted bolted connection energy dissipators*. Earthquake Spectra, 1993. **9**(3): p. 491-504.
40. Grigorian, C.E. and E.P. Popov, *Energy dissipation with slotted bolted connections*. 1994, University of California, Berkeley.
41. Bishay-Girges, N.W. and A.J. Carr, *Ring spring dampers*. Bulletin of the New Zealand Society for Earthquake Engineering, 2014. **47**(3): p. 173-180.
42. Hazaveh, N.K., et al., *Seismic behavior of a self-centering system with 2–4 viscous damper*. Journal of Earthquake Engineering, 2020. **24**(3): p. 470-484.
43. Makris, N., M.C. Constantinou, and A.M. Reinhorn, *Viscous dampers: testing, modeling and application in vibration and seismic isolation*. 1990: National Center for Earthquake Engineering Research Buffalo, NY.
44. Constantinou, M.C. and M. Symans, *Experimental and analytical investigation of seismic response of structures with supplemental fluid viscous dampers*. 1992: National Center for earthquake engineering research Buffalo, NY.
45. Miyamoto, H.K., et al., *Limit states and failure mechanisms of viscous dampers and the implications for large earthquakes*. Earthquake engineering & structural dynamics, 2010. **39**(11): p. 1279-1297.

46. Hazaveh, N.K., et al., *Passive direction displacement dependent damping (D3) device*. Bulletin of the New Zealand Society for Earthquake Engineering, 2018. **51**(2): p. 105-112.
47. Rodgers, G.W., J.G. Chase, and J.B. Mander, *Repeatability and High-Speed Validation of Supplemental Lead-Extrusion Energy Dissipation Devices*. Advances in Civil Engineering, 2019. **2019**.
48. Robinson, W. and L. Greenbank, *An extrusion energy absorber suitable for the protection of structures during an earthquake*. Earthquake Engineering & Structural Dynamics, 1976. **4**(3): p. 251-259.
49. Rodgers, G.W., J.B. Mander, and J. Geoffrey Chase, *Modeling cyclic loading behavior of jointed precast concrete connections including effects of friction, tendon yielding and dampers*. Earthquake engineering & structural dynamics, 2012. **41**(15): p. 2215-2233.
50. Rodgers, G.W., et al., *High-force-to-volume seismic dissipators embedded in a jointed precast concrete frame*. Journal of structural engineering, 2012. **138**(3): p. 375-386.
51. Rodgers, G.W., et al., *Beyond ductility: parametric testing of a jointed rocking beam-column connection designed for damage avoidance*. Journal of Structural Engineering, 2016. **142**(8): p. C4015006.
52. Pekcan, G., J.B. Mander, and S.S. Chen, *The seismic response of a 1: 3 scale model RC structure with elastomeric spring dampers*. Earthquake spectra, 1995. **11**(2): p. 249-267.
53. Wikander, O.R., *Cushioning-spring construction*. 1931: United States.
54. Wahl, A.M., *Mechanical springs*. 1944: Penton Publishing Company.
55. Bishay-Girges, N.W., *Seismic protection of structures using passive control system*. 2004.
56. Khoo, H., et al. *Experimental studies of the self-centering Sliding Hinge Joint*. in *2012 NZSEE Conference*. 2012.
57. Gledhill, S., G. Sidwell, and D. Bell. *The damage avoidance design of tall steel frame buildings-fairlie terrace student accommodation project, victoria university of wellington*. in *New Zealand Society of Earthquake Engineering Annual Conference*. 2008.
58. Golzar, F.G., G.W. Rodgers, and J.G. Chase. *Design and experimental validation of a re-centring viscous dissipater*. in *Structures*. 2018. Elsevier.
59. Zarnani, P. and P. Quenneville, *A resilient slip friction joint*. Patent No. WO2016185432A1, NZ IP Office, 2015.
60. Shiravand, M., M. Nashtae, and S. Veismoradi, *Seismic assessment of concrete buildings reinforced with shape memory alloy materials in different stories*. The Structural Design of Tall and Special Buildings, 2017. **26**(15): p. e1384.
61. FEMA, P., *58-1 (2012) Seismic performance assessment of buildings (volume 1-Methodology)*. Federal Emergency Management Agency, Washington, 2012.
62. Veismoradi, S., A. Cheraghi, and E. Darvishan, *Probabilistic mainshock-aftershock collapse risk assessment of buckling restrained braced frames*. Soil Dynamics And Earthquake Engineering, 2018. **115**: p. 205-216.
63. Bradley, B.A., et al., *Experimental multi-level seismic performance assessment of 3D RC frame designed for damage avoidance*. Earthquake Engineering & Structural Dynamics, 2008. **37**(1): p. 1-20.
64. Li, L., J.B. Mander, and R.P. Dhakal, *Bidirectional cyclic loading experiment on a 3D beam-column joint designed for damage avoidance*. Journal of Structural Engineering, 2008. **134**(11): p. 1733-1742.
65. Solberg, K., et al., *Seismic performance of damage-protected beam-column joints*. 2008.
66. Miller, D.J., L.A. Fahnestock, and M.R. Eatherton, *Development and experimental validation of a nickel-titanium shape memory alloy self-centering buckling-restrained brace*. Engineering Structures, 2012. **40**: p. 288-298.
67. Eatherton, M.R., L.A. Fahnestock, and D.J. Miller, *Computational study of self-centering buckling-restrained braced frame seismic performance*. Earthquake Engineering & Structural Dynamics, 2014. **43**(13): p. 1897-1914.

68. Liu, L., J. Zhao, and S. Li, *Nonlinear displacement ratio for seismic design of self-centering buckling-restrained braced steel frame considering trilinear hysteresis behavior*. Engineering Structures, 2018. **158**: p. 199-222.
69. Xu, L.H., X.W. Fan, and Z.X. Li, *Cyclic behavior and failure mechanism of self-centering energy dissipation braces with pre-pressed combination disc springs*. Earthquake Engineering & Structural Dynamics, 2017. **46**(7): p. 1065-1080.
70. Hashemi, A., et al. *Seismic resistant cross laminated timber (CLT) structures with innovative resilient slip friction (RSF) joints*. in *16th World Conference on Earthquake Engineering, (16WCEE 2017)*. 2017.
71. Kang, Y.-j. and L.-y. Peng, *Development and Analysis of the Control Effect of a Reid Damper with Self-Centering Characteristics*. Shock and Vibration, 2018. **2018**.
72. Xu, L.-H., X.-S. Xie, and Z.-X. Li, *Development and experimental study of a self-centering variable damping energy dissipation brace*. Engineering Structures, 2018. **160**: p. 270-280.
73. Qiu, C.-X. and S. Zhu, *Performance-based seismic design of self-centering steel frames with SMA-based braces*. Engineering Structures, 2017. **130**: p. 67-82.
74. Zhou, Z., et al., *Hysteretic performance analysis of self-centering buckling restrained braces using a rheological model*. Journal of Engineering Mechanics, 2016. **142**(6): p. 04016032.
75. Erochko, J. and C. Christopoulos, *Self-centering energy-dissipative (sced) brace: Overview of recent developments and potential applications for tall buildings*, in *Sustainable Development of Critical Infrastructure*. 2014. p. 488-495.
76. Hashemi, A., et al., *Experimental Testing of Rocking Cross-Laminated Timber Walls with Resilient Slip Friction Joints*. Journal of Structural Engineering, 2017. **144**(1): p. 04017180.
77. Xu, L.-H., X.-W. Fan, and Z.-X. Li, *Development and experimental verification of a pre-pressed spring self-centering energy dissipation brace*. Engineering Structures, 2016. **127**: p. 49-61.
78. DARANI, F.M., P.J.H. QUENNEVILLE, and P. ZARNANI, *A Structural Connector*. 2020: Patent Number: WO2020008422A1, NZ IP Office.
- .
79. Darani, F., et al. *Application of new resilient slip friction joint for seismic damage avoidance design of rocking concrete shear walls*. in *NZSEE2018*. 2018. Auckland.
80. Hashemi, A., et al., *Damage Avoidance Self-Centering Steel Moment Resisting Frames (MRFs) Using Innovative Resilient Slip Friction Joints (RSFJs)*. Key Engineering Materials, 2018. **763**: p. 726-734.
81. Ramirez, J. and L. Tirca. *Numerical Simulation and Design of Friction-Damped Steel Frame Structures damped*. in *Proceedings of 15th World Conference in Earthquake Engineering, Lisbon, Portugal*. 2012.
82. Roik, K., U. Dorka, and P. Dechent, *Vibration control of structures under earthquake loading by three-stage friction-grip elements*. Earthquake engineering & structural dynamics, 1988. **16**(4): p. 501-521.
83. Lukkunaprasit, P., A. Wanitkorkul, and A. Filiatrault. *Performance deterioration of slotted-bolted connection due to bolt impact and remedy by restrainers*. in *Thirteen World Conference on Earthquake Engineering, Vancouver, BC*. 2004.
84. FEMA, P., *Commentary for the seismic rehabilitation of buildings*. FEMA-356, Federal Emergency Management Agency, Washington, DC, 2000.
85. Zarnani, P., A. Valadbeigi, and P. Quenneville. *Resilient slip friction (RSF) joint: A novel connection system for seismic damage avoidance design og timber structures*. in *World Conf. on Timber Engineering WCTE2014, Vienna Univ. of Technology, Vienna, Austria*. 2016.
86. Cedolin, L., *Stability of structures: elastic, inelastic, fracture and damage theories*. 2010: World Scientific.
87. Valadbeigi, A., *Application of a Resilient Slip Friction Joint in Steel-Timber Hybrid Structures*. 2019, University of Auckland.

88. Wallace, J.W., et al., *Damage and implications for seismic design of RC structural wall buildings*. Earthquake Spectra, 2012. **28**(1_suppl1): p. 281-299.
89. Kam, W.Y., S. Pampanin, and K. Elwood, *Seismic performance of reinforced concrete buildings in the 22 February Christchurch (Lyttelton) earthquake*. Bulletin of the New Zealand Society for Earthquake Engineering, 2011. **44**(4): p. 239-278.
90. Tremblay, R., et al., *Performance of steel structures during the 1994 Northridge earthquake*. Canadian Journal of Civil Engineering, 1995. **22**(2): p. 338-360.
91. McCormick, J., et al. *Permissible residual deformation levels for building structures considering both safety and human elements*. in *Proceedings of the 14th world conference on earthquake engineering*. 2008. Seismological Press Beijing.
92. Robinson, W.H., *Lead-rubber hysteretic bearings suitable for protecting structures during earthquakes*. Earthquake engineering & structural dynamics, 1982. **10**(4): p. 593-604.
93. Symans, M. and M. Constantinou, *Passive fluid viscous damping systems for seismic energy dissipation*. ISET Journal of Earthquake Technology, 1998. **35**(4): p. 185-206.
94. Kiggins, S. and C.-M. Uang, *Reducing residual drift of buckling-restrained braced frames as a dual system*. Engineering Structures, 2006. **28**(11): p. 1525-1532.
95. Mualla, I. and B. Belev, *Analysis, design and applications of rotational friction dampers for seismic protection*. Czasopismo Inżynierii Łądowej, Środowiska i Architektury, 2015. **62**(4): p. 335-346.
96. Barmo, A., I.H. Mualla, and H.T. Hasan, *The behavior of multi-story buildings seismically isolated system hybrid isolation (friction, rubber and with the addition of rotational friction dampers)*. Open Journal of Earthquake Research, 2014. **4**(01): p. 1.
97. De Domenico, D., G. Ricciardi, and I. Takewaki, *Design strategies of viscous dampers for seismic protection of building structures: a review*. Soil Dynamics and Earthquake Engineering, 2019. **118**: p. 144-165.
98. Spencer Jr, B.F., et al. *Smart dampers for seismic protection of structures: a full-scale study*. in *Proceedings of the second world conference on structural control*. 1998. Kyoto.
99. Sasaki, T., et al. *NEES/E-defense base-isolation tests: effectiveness of friction pendulum and lead-rubber bearing systems*. in *Proceedings of the 15th World Conference of Earthquake Engineering*. 2012.
100. Morgan, T.A. and S.A. Mahin, *Achieving reliable seismic performance enhancement using multi-stage friction pendulum isolators*. Earthquake Engineering & Structural Dynamics, 2010. **39**(13): p. 1443-1461.
101. Becker, T.C. and S.A. Mahin, *Experimental and analytical study of the bi-directional behavior of the triple friction pendulum isolator*. Earthquake Engineering & Structural Dynamics, 2012. **41**(3): p. 355-373.
102. Chung, R.M., *January 17, 1995 Hyogoken-Nanbu (Kobe) earthquake: Performance of structures, lifelines, and fire protection systems (NIST SP 901)*. 1996.
103. Ghosh, S., *Observations on the Performance of Structures in the Kobe Earthquake of January 17, 1995*. PCI journal, 1995. **40**(2): p. 14-22.
104. Naeim, F., et al., *Performance of tall buildings in Santiago, Chile during the 27 February 2010 offshore Maule, Chile earthquake*. The Structural Design of Tall and Special Buildings, 2011. **20**(1): p. 1-16.
105. Wallace, J.W. *February 27, 2010 Chile earthquake: preliminary observations on structural performance and implications for US building codes and standards*. in *Structures Congress 2011*. 2011.
106. Clifton, C., et al., *Steel structures damage from the Christchurch earthquake series of 2010 and 2011*. Bulletin of the New Zealand Society for Earthquake Engineering, 2011. **44**(4): p. 297-318.
107. MacRae, G.A. and G.C. Clifton. *Research on seismic performance of steel structures*. in *Steel Innovations Conference, Auckland, New Zealand*. 2015.

108. Christopoulos, C., et al., *Self-centering energy dissipative bracing system for the seismic resistance of structures: development and validation*. Journal of structural engineering, 2008. **134**(1): p. 96-107.
109. Erochko, J., C. Christopoulos, and R. Tremblay, *Design, testing, and detailed component modeling of a high-capacity self-centering energy-dissipative brace*. Journal of Structural Engineering, 2015. **141**(8): p. 04014193.
110. Darani, F., et al., *Application of new resilient slip friction joint for seismic damage avoidance design of rocking concrete shear walls*. 2018.
111. Darani, F.M., et al., *Rocking concrete shear walls with self-centring friction dampers for seismic protection of building structures*. 2018.
112. Chase, J.G., et al., *Re-shaping hysteretic behaviour using semi-active resettable device dampers*. Engineering Structures, 2006. **28**(10): p. 1418-1429.
113. Hazaveh, N.K., et al., *Seismic Behavior of a Self-Centering System with 2–4 Viscous Damper*. Journal of Earthquake Engineering, 2018: p. 1-15.
114. Hamid, N. and J.B. Mander, *A comparative seismic performance between precast hollow core walls and conventional walls using incremental dynamic analysis*. Arabian Journal for Science and Engineering, 2012. **37**(7): p. 1801-1815.
115. Nazari, M., *Seismic performance of unbonded post-tensioned precast wall systems subjected to shake table testing*. 2016.
116. Chi, P., et al., *Development of a self-centering tension-only brace for seismic protection of frame structures*. Steel and Composite Structures, 2018. **26**(5): p. 573-582.
117. Keivan, A. and Y. Zhang, *Nonlinear seismic performance of Y-type self-centering steel eccentrically braced frame buildings*. Engineering Structures, 2019. **179**: p. 448-459.
118. Devereux, C., et al., *NMIT arts & media building-damage mitigation using post-tensioned timber walls*. 2011.
119. Newcombe, M., et al., *Section analysis and cyclic behavior of post-tensioned jointed ductile connections for multi-story timber buildings*. Journal of Earthquake Engineering, 2008. **12**(S1): p. 83-110.
120. Buchanan, A., et al., *Post-tensioned timber frame buildings*. Structural Engineer, 2011. **89**(17): p. 24-30.
121. Shu, Z., et al., *Seismic design and performance evaluation of self-centering timber moment resisting frames*. Soil Dynamics and Earthquake Engineering, 2019. **119**: p. 346-357.
122. Guan, X., H. Burton, and S. Moradi, *Seismic performance of a self-centering steel moment frame building: From component-level modeling to economic loss assessment*. Journal of Constructional Steel Research, 2018. **150**: p. 129-140.
123. Wilson, A.W., et al., *Seismic Response of Post-Tensioned Cross-Laminated Timber Rocking Wall Buildings*. Journal of Structural Engineering, 2020. **146**(7): p. 04020123.
124. Geng, X. and W. Zhou, *Cyclic experimental response of self-centering concrete frames with slotted columns*. Construction and Building Materials, 2019. **195**: p. 363-375.
125. Christopoulos, C., et al., *Posttensioned energy dissipating connections for moment-resisting steel frames*. Journal of Structural Engineering, 2002. **128**(9): p. 1111-1120.
126. Nobahar, E., et al., *A post-tensioned self-centering yielding brace system: development and performance-based seismic analysis*. Structure and Infrastructure Engineering, 2020: p. 1-21.
127. Twigden, K.M. and R.S. Henry, *Snap back testing of unbonded post-tensioned concrete wall systems*. Earthquakes and Structures, 2019. **16**(2): p. 209-219.
128. Twigden, K.M., *Dynamic response of unbonded post-tensioned concrete walls for seismic resilient structures*. 2016, University of Auckland.
129. Miller, D.J., L.A. Fahnestock, and M.R. Eatherton. *Self-centering buckling-restrained braces for advanced seismic performance*. in *Structures Congress 2011*. 2011.
130. Zhu, S. and Y. Zhang, *Seismic analysis of concentrically braced frame systems with self-centering friction damping braces*. Journal of Structural Engineering, 2008. **134**(1): p. 121-131.

131. Rojas, P., J. Ricles, and R. Sause, *Seismic performance of post-tensioned steel moment resisting frames with friction devices*. Journal of structural engineering, 2005. **131**(4): p. 529-540.
132. Golzar, F.G., G.W. Rodgers, and J.G. Chase, *Nonlinear spectral analysis for structures with re-centring D3 viscous dissipaters*. Journal of Earthquake Engineering, 2020. **24**(10): p. 1530-1546.
133. Zarnani, P., A. Valadbeigi, and P. Quenneville. *Resilient slip friction (RSF) joint: A novel connection system for seismic damage avoidance design of timber structures*. in *World Conf. on Timber Engineering WCTE2014, Vienna Univ. of Technology, Vienna, Austria*. 2016.
134. Mottier, P., R. Tremblay, and C. Rogers. *Shake Table Test of a Half-Scale 2-Storey Steel Building Seismically Retrofitted Using Rocking Braced Frame System*. in *Key Engineering Materials*. 2018. Trans Tech Publ.
135. Sahami, K., P. Zarnani, and P. Quenneville, *Introducing a low damage system incorporating rocking braced frame and resilient slip friction joint as a shear key*. 2020.
136. Yousef-beik, S.M.M., et al., *A new self-centering brace with zero secondary stiffness using elastic buckling*. Journal of Constructional Steel Research, 2020. **169**: p. 106035.
137. Bagheri, H., et al., *The resilient slip friction joint tension-only brace beyond its ultimate level*. Journal of Constructional Steel Research, 2020. **172**: p. 106225.
138. Veismoradi, S., et al., *Seismic retrofitting of RC-frames using Resilient Slip Friction Joint toggle-bracing system*. 2020.
139. Cook, J., G.W. Rodgers, and G.A. MacRae, *Design and Testing of Ratcheting, Tension-Only Devices for Seismic Energy Dissipation Systems*. Journal of Earthquake Engineering, 2020. **24**(2): p. 328-349.
140. AISC, A., *AISC 341-10*. "Seismic provisions for structural steel buildings". Chicago (IL): American Institute of Steel Construction, 2010.
141. Engineers, A.S.o.C. *Minimum Design Loads for Buildings and Other Structures (ASCE/SEI 7-10)*. 2013. American Society of Civil Engineers.
142. Chopra, A.K., *Dynamics of structures*. 2012: Pearson Education Upper Saddle River, NJ.
143. Computers and Structures, I.C., *SAP2000: Integrated Finite Element Analysis and Design of Structures, Version 19.2.2, software*,. Berkeley, CA, 2017.
144. Hidalgo, P.A., C.A. Ledezma, and R.M. Jordan, *Seismic behavior of squat reinforced concrete shear walls*. Earthquake Spectra, 2002. **18**(2): p. 287-308.
145. Fintel, M., *Performance of buildings with shear walls in earthquakes of the last thirty years*. PCI journal, 1995. **40**(3): p. 62-80.
146. Park, R. and T. Paulay, *Reinforced Concrete Structures*, John Wiley & Sons. NY, USA, 1975.
147. Segura Jr, C.L. and J.W. Wallace, *Seismic performance limitations and detailing of slender reinforced concrete walls*. ACI Structural Journal, 2018. **115**(3): p. 849-859.
148. Nazari, M., S. Sritharan, and S. Aaleti, *Single precast concrete rocking walls as earthquake force-resisting elements*. Earthquake Engineering & Structural Dynamics, 2017. **46**(5): p. 753-769.
149. Kurama, Y.C., et al., *Seismic-resistant precast concrete structures: state of the art*. 2018, American Society of Civil Engineers.
150. Moehle, J. and G.G. Deierlein. *A framework methodology for performance-based earthquake engineering*. in *13th world conference on earthquake engineering*. 2004.
151. Priestley, M., G. Calvi, and M. Kowalsky. *Direct displacement-based seismic design of structures*. in *2007 NZSEE conference*. 2005.
152. Aragaw, L.F. and P.M. Calvi, *Comparing the performance of traditional shear-wall and rocking shear-wall structures designed using the direct-displacement based design approach*. Bulletin of Earthquake Engineering, 2020. **18**(4): p. 1345-1369.
153. Mohammadi Darani, F., P. Zarnani, and P. Quenneville, *A Structural Connector*. Patent No. WO2020008422A1, NZ IP Office, 2018.
154. Blandon, C.A. and M. Priestley, *Equivalent viscous damping equations for direct displacement based design*. Journal of earthquake Engineering, 2005. **9**(sup2): p. 257-278.

155. Wang, W., et al., *Manufacturing and performance of a novel self-centring damper with shape memory alloy ring springs for seismic resilience*. *Structural Control and Health Monitoring*, 2019. **26**(5): p. e2337.
156. Mualla, I.H. and B. Belev, *Performance of steel frames with a new friction damper device under earthquake excitation*. *Engineering Structures*, 2002. **24**(3): p. 365-371.
157. Pall, A. *Performance-based design using pall friction dampers-an economical design solution*. in *13th World Conference on Earthquake Engineering, Vancouver, BC, Canada*. 2004.
158. Soong, T. and B. Spencer Jr, *Supplemental energy dissipation: state-of-the-art and state-of-the-practice*. *Engineering structures*, 2002. **24**(3): p. 243-259.
159. Mohammadi Darani, F., et al., *Resilient Slip Friction Joint Performance, Damper Analysis and Anti Locking Mechanism*. Submitted paper under review, 2020.
160. Hashemi, A., et al., *Experimental testing of rocking cross-laminated timber walls with resilient slip friction joints*. *Journal of Structural Engineering*, 2018. **144**(1): p. 04017180.
161. Yousef-Beik, S.M.M., et al. *New seismic damage avoidant timber brace using innovative resilient slip friction joints for multi-story applications*. in *2018 World Conference on Timber Engineering (WCTE2018)*. 2018.
162. Bagheri, H., et al., *New Self-Centering Tension-Only Brace Using Resilient Slip-Friction Joint: Experimental Tests and Numerical Analysis*. *Journal of Structural Engineering*, 2020. **146**(10): p. 04020219.
163. Mohammadi Darani, F., P. Zarnani, and P. Quenneville, *Development of a New Self-Centering Structural Connector for Seismic Protection of Structures*. Paper Under review, 2020.
164. Standards New Zealand, *Structural design actions Part 5: Earthquake actions*. NZS 1170.5, 2004.
165. Bruneau, M. and G. MacRae, *Reconstructing Christchurch: a seismic shift in building structural systems*. The Quake Centre, University of Canterbury, Christchurch, 2017.
166. Australian Standard, A., *NZS 1170.0: 2002*. *Structural Design Actions Part 0: General Principles*, Standards Australia, 2002.
167. Wiebe, L., et al. *Modelling inherent damping for rocking systems: results of large-scale shake table testing*. in *Proceedings of the 15th World Conference on Earthquake Engineering*. 2012.
168. Mohammadi Darani, F., P. Zarnani, and P. Quenneville, *Development of a New Rocking Concrete Shear Wall with Self-Centering Friction Connections, Experimental Verification*. Paper Under review, 2020.
169. Standards New Zealand, *Steel Structures Standard*. NZS 3404, 1997.
170. Henry, R., J. Ingham, and S. Sritharan. *Wall-to-floor interaction in concrete buildings with rocking wall systems*. in *Proceedings of the (2012) NZSEE Annual Conference*. Christchurch, New Zealand. 2012.
171. Liu, Q., *Study on interaction between rocking-wall system and surrounding structure*. 2016.
172. Moroder, D., et al. *Experimental investigation of wall-to-floor connections in post-tensioned timber buildings*. in *NZSEE conference, Auckland*. 2014.
173. Standards New Zealand, *Structural Design Actions part 5: Earthquake actions*. NZS1170.5–Commentary, 2004.
174. DeJong, M.J. and E.G. Dimitrakopoulos, *Dynamically equivalent rocking structures*. *Earthquake engineering & structural dynamics*, 2014. **43**(10): p. 1543-1563.
175. Psycharis, I.N., *Dynamic behavior of rocking structures allowed to uplift*. 1981.
176. Acikgoz, S. and M.J. DeJong, *The interaction of elasticity and rocking in flexible structures allowed to uplift*. *Earthquake Engineering & Structural Dynamics*, 2012. **41**(15): p. 2177-2194.
177. Makris, N., *A half-century of rocking isolation*. *Earthquakes and Structures*, 2014. **7**(6): p. 1187-1221.
178. Reggiani Manzo, N. and M.F. Vassiliou, *Displacement-based analysis and design of rocking structures*. *Earthquake Engineering & Structural Dynamics*, 2019. **48**(14): p. 1613-1629.
179. Zhou, Y. and X. Lu, *State-of-the-art on rocking and self-centering structures*. *Jianzhu Jieqou Xuebao*(Journal of Building Structures), 2011. **32**(9): p. 1-10.

180. Deng, L., B.L. Kutter, and S.K. Kunnath, *Centrifuge modeling of bridge systems designed for rocking foundations*. Journal of Geotechnical and Geoenvironmental Engineering, 2012. **138**(3): p. 335-344.
181. Antonellis, G. and M. Panagiotou, *Seismic response of bridges with rocking foundations compared to fixed-base bridges at a near-fault site*. Journal of Bridge Engineering, 2014. **19**(5): p. 04014007.
182. Saad, A.S., D.H. Sanders, and I.G. Buckle, *Experimental evaluation of bridge column foundation rocking behavior*. Journal of Bridge Engineering, 2018. **23**(11): p. 04018088.
183. Deierlein, G., et al., *Earthquake resilient steel braced frames with controlled rocking and energy dissipating fuses*. Steel Construction, 2011. **4**(3): p. 171-175.
184. Deierlein, G., et al. *Large-scale shaking table test of steel braced frame with controlled rocking and energy dissipating fuses*. in *9th US National and 10th Canadian Conference on Earthquake Engineering*. 2010.
185. Mottier, P., R. Tremblay, and C. Rogers, *Seismic retrofit of low-rise steel buildings in Canada using rocking steel braced frames*. Earthquake Engineering & Structural Dynamics, 2018. **47**(2): p. 333-355.
186. Dowden, D.M., R. Purba, and M. Bruneau, *Behavior of self-centering steel plate shear walls and design considerations*. Journal of Structural Engineering, 2012. **138**(1): p. 11-21.
187. Dowden, D.M. and M. Bruneau, *Dynamic shake-table testing and analytical investigation of self-centering steel plate shear walls*. Journal of Structural Engineering, 2016. **142**(10): p. 04016082.
188. Dowden, D.M. and M. Bruneau, *Quasi-static cyclic testing and analytical investigation of steel plate shear walls with different post-tensioned beam-to-column rocking connections*. Engineering Structures, 2019. **187**: p. 43-56.
189. Jin, Z., et al., *Simplified mechanistic model for seismic response prediction of coupled cross-laminated timber rocking walls*. Journal of Structural Engineering, 2019. **145**(2): p. 04018253.
190. Pei, S., et al., *Experimental Seismic Response of a Resilient 2-Story Mass-Timber Building with Post-Tensioned Rocking Walls*. Journal of Structural Engineering, 2019. **145**(11): p. 04019120.
191. Gu, A., et al., *Experimental study and parameter analysis on the seismic performance of self-centering hybrid reinforced concrete shear walls*. Soil Dynamics and Earthquake Engineering, 2019. **116**: p. 409-420.
192. Hashemi, A., et al., *Seismic resistant rocking coupled walls with innovative Resilient Slip Friction (RSF) joints*. Journal of Constructional Steel Research, 2017. **129**: p. 215-226.
193. Wiebe, L. and C. Christopoulos, *Mitigation of higher mode effects in base-rocking systems by using multiple rocking sections*. Journal of Earthquake Engineering, 2009. **13**(S1): p. 83-108.
194. Kelly, T.E., *Tentative seismic design guidelines for rocking structures*. Bulletin of the New Zealand Society for Earthquake Engineering, 2009. **42**(4): p. 239-274.
195. Grigorian, M., et al., *Methodology for developing earthquake-resilient structures*. The Structural Design of Tall and Special Buildings, 2019. **28**(2): p. e1571.
196. Hogg, S.J., et al., *Case Studies on the Practical Application of Resilient Building Technologies Applied in New Zealand*. Structural Engineering International, 2020. **30**(2): p. 232-241.
197. Mohammadi Darani, F., P. Zarnani, and P. Quenneville, *Seismic Performance and Design of Rocking-wall Structures Equipped with Self-Centring Friction Connections*. Paper Under Review, 2020.
198. SAP, C., *v20 Integrated Finite Element Analysis and Design of Structures*. Computers and Structures Inc.: Berkely, CA, USA, 2018.
199. Mander, J.B., M.J. Priestley, and R. Park, *Theoretical stress-strain model for confined concrete*. Journal of structural engineering, 1988. **114**(8): p. 1804-1826.
200. Standards New Zealand, *Concrete structures standard*. NZS3101, 2006.
201. Parker, M. and D. Steenkamp, *The economic impact of the Canterbury earthquakes*. Reserve Bank of New Zealand Bulletin, 2012. **75**(3): p. 13-25.

202. Wiebe, L., et al., *Mechanisms to limit higher mode effects in a controlled rocking steel frame. 1: Concept, modelling, and low-amplitude shake table testing*. Earthquake engineering & structural dynamics, 2013. **42**(7): p. 1053-1068.

Appendix A, Self-Centring Structural Connector SSC Patent

Patent filed for Self-centring Structural Connector (SSC)

Link to the international patent application: [Link](#)

Link to the US patent application: [Link](#)



(51) International Patent Classification:

F16F 7/08 (2006.01) F16F 15/02 (2006.01)
F16F 13/04 (2006.01) E04H 9/02 (2006.01)

(21) International Application Number:

PCT/IB20 19/055737

(22) International Filing Date:

05 July 2019 (05.07.2019)

(25) Filing Language:

English

(26) Publication Language:

English

(30) Priority Data:

744156 06 July 2018 (06.07.2018) NZ
2019901741 22 May 2019 (22.05.2019) AU

(71) Applicant: AUT VENTURES LIMITED [NZ/NZ]; Aut, 7thFloor, WaBuilding, 55 Wellesley Street East, Auckland (NZ).

(72) Inventors; and

(71) Applicants: MOHAMMADI DARANI, Farhad [IR/NZ]; Unit 1214B, 21 Whitaker Place, Grafton, Auckland, 1010 (NZ). ZARNANI, Pouyan [IR/NZ]; 1/3C Appleyard Cres, Meadowbank, Auckland (NZ). QUENNEVILLE, Pierre Joseph Henri [CA/NZ]; 39 Tephra Boulevard, Stonefields, Auckland (NZ).

(74) Agent: AJ PARK; Level 22 Aon Centre, 1 Willis Street, Wellington (NZ).

(81) Designated States (unless otherwise indicated, for every kind of national protection available): AE, AG, AL, AM, AO, AT, AU, AZ, BA, BB, BG, BH, BN, BR, BW, BY, BZ, CA, CH, CL, CN, CO, CR, CU, CZ, DE, DJ, DK, DM, DO, DZ, EC, EE, EG, ES, FI, GB, GD, GE, GH, GM, GT, HN, HR, HU, ID, IL, IN, IR, IS, JO, JP, KE, KG, KH, KN, KP, KR, KW, KZ, LA, LC, LK, LR, LS, LU, LY, MA, MD, ME, MG, MK, MN, MW, MX, MY, MZ, NA, NG, NI, NO, NZ, OM, PA, PE, PG, PH, PL, PT, QA, RO, RS, RU, RW, SA, SC, SD, SE, SG, SK, SL, SM, ST, SV, SY, TH, TJ, TM, TN, TR, TT, TZ, UA, UG, US, UZ, VC, VN, ZA, ZM, ZW.

(84) Designated States (unless otherwise indicated, for every kind of regional protection available): ARIPO (BW, GH, GM, KE, LR, LS, MW, MZ, NA, RW, SD, SL, ST, SZ, TZ, UG, ZM, ZW), Eurasian (AM, AZ, BY, KG, KZ, RU, TJ, TM), European (AL, AT, BE, BG, CH, CY, CZ, DE, DK, EE, ES, FI, FR, GB, GR, HR, HU, IE, IS, IT, LT, LU, LV, MC, MK, MT, NL, NO, PL, PT, RO, RS, SE, SI, SK, SM, TR), OAPI (BF, BJ, CF, CG, CI, CM, GA, GN, GQ, GW, KM, ML, MR, NE, SN, TD, TG).

(54) Title: A STRUCTURAL CONNECTOR

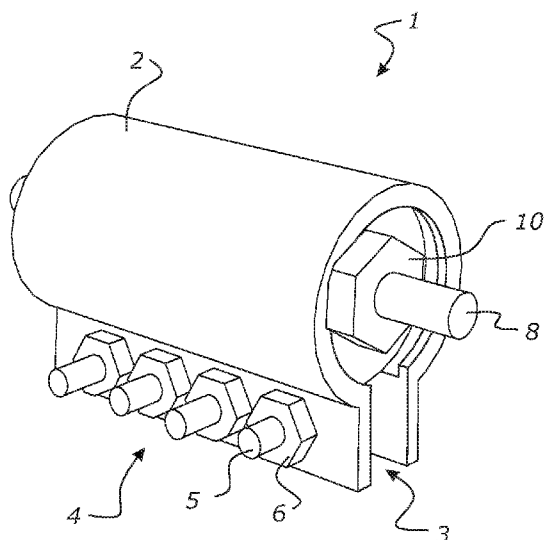


FIG. 1A

(57) Abstract: A connector for connecting two structural components. The connector has a casing engaged and to move with a first of said structural components. The casing is of an elongate constant cross section interior within which is operative in a frictional sliding engagement a spring and damper assembly. This comprising of at least one damper to move with a second of said structural components and contacting the interior of the casing and able to slide in frictional contact with the casing. A spring is able to be elastically deformed by and between the damper and the casing when the damper and casing are in relative motion to bias the two structural components towards their initial relative position.



Published:

- *with international search report (Art. 21(3))*
- *in black and white; the international application as filed contained color or greyscale and is available for download from PATENTSCOPE*

A STRUCTURAL CONNECTOR

FIELD OF THE INVENTION

The present invention relates to a structural connector of or for a structure for
5 resisting and damping external forces such as seismic and vibration forces, and to aid
in the restoration of any residual displacement following an external forcing event.

BACKGROUND TO THE INVENTION

Structures such as buildings commonly experience external loadings such as
10 seismic loadings or vibration loadings. These loadings may create forces between
members of the structure. Structural connectors may be used to facilitate these
connections, to hold the members of the structure together.

It may be desirable, rather than fixedly holding the members of the structure
together, to allow some relative displacement between them when subjected to
15 external forces.

Where relative displacement is allowed between members of a structure it
may also be desirable to provide for damping, to absorb energy of the external
forcing. Such damping may be provided by way of plastic deformation of structural
connectors.

20 Such structural connectors commonly however require maintenance due to
plastic deformation of their materials following an external loading. This maintenance
may be costly, and may require significant interference with the structure itself
because the structural connectors are commonly integrated with the structure.

Viscous dampers are also known. Dampers using a viscous material often use
25 a piston and cylinder arrangement, the design of which can be difficult and time
consuming as it is necessary to provide fluid tight seal to prevent leakage of the
viscous material.

Friction dampers are also known and may for example be seen in EP1467115.
These dampers rely on a frictional interface to absorb energy when the damper is set
30 in motion due to an event such as an earthquake or other events.

The damper of EP1467115 when used in a building may not encourage a
return of the building components that it is attached to, to their initial position pre-
displacement. This means that a building that has been subject to an event is not
encouraged to move back towards its initial condition and can mean that a building
35 following a first event is more vulnerable to collapse or further damage in a
subsequent event which may occur relatively shortly after the first event because the
building is not in a more stable shape, being the shape that it was originally built in.

In this specification where reference has been made to patent specifications, other external documents, or other sources of information, this is generally for the purpose of providing a context for discussing the features of the invention. Unless specifically stated otherwise, reference to such external documents is not to be construed as an admission that such documents, or such sources of information, in any jurisdiction, are prior art, or form part of the common general knowledge in the art.

It is an object of the present invention to provide a structural connector which overcomes or at least partially ameliorates some of the abovementioned disadvantages or which at least provides the public with a useful choice.

SUMMARY OF THE INVENTION

In a first aspect, the present invention may be said to broadly consist in a double acting slip friction energy damping connector for use between a first structural member and a second structural member of a ground supported structure that may be subjected to induced motion that can cause the first and second structural member to relatively translate towards and away from each other from an initial static position facilitated by the connector that comprises:

- i. an elongate casing having a notional straight axis with an interior surface or surfaces, the casing connected to the second structural member to translate with the second structural member,
- ii. a spring and damper assembly to travel along the axis inside the casing and comprising of
 - a. at least two spaced apart damper members each damper member having a friction surface or surfaces contacting the interior surface of surfaces of the casing to be able to slide with frictional resistance along the axis along at least part of the interior surface or surfaces,
 - b. a pre-loaded spring arrangement intermediate of and forcing, when the first and second structural members are in their initial static position, the two adjacent damper members apart in the axial direction each against a respective bearing member of one of (1) the casing located at or towards each end of the casing, and (2) the second structural member, yet allowing the two damper members to move towards each other against the load of the spring by a connection rod that is connected to the first structural member and to translate with the first structural member, the connection rod

having a stop positioned at each end of the spring and damper assembly,

- 5
- i. a first of said stops to act, when the connector acts in compression when the first and second structural members translate towards each other, on a first of said two damper members to displace the first of said two damper members away from its respective bearing member and towards the second of said two damper members and its respective bearing member, and
- 10
- ii. a second of said stops to act, when the connector acts in tension when the first and second structural members translate away from each other, on the second of said two damper members to displace the second of said two damper members away from its respective bearing member and towards the first of said two damper members and its
- 15
- respective bearing member.

Preferably at least one intermediate damper member is located between the first and second dampers, the spring arrangement comprising of at least two spring sets, a said set located between each adjacent damper members.

20 Preferably the frictional engagement of each damper member with the casing is substantially the same and is preferably constant.

Preferably each damper member has a friction surface or surfaces shaped commensurate the interior surface of surfaces of the casing to be able to slide with frictional engagement along the interior surface or surfaces.

25 Preferably the contact of the friction surface or surfaces of each damper member with the interior surface or surfaces of the casing is such as to create a normal force on the damper member acting normal to the surfaces at their point of contact to establish said frictional resistance.

30 Preferably the normal force can be varied by changing the cross sectional shape of the casing.

Preferably the normal force is fixed and determined by the compression fit of the casing about the damper members.

Preferably the damper members and the casing are in a compression fit relationship with each other.

35 Preferably damper members have been assembled in said casing by compression fitting.

Preferably the intermediate damper members can translate along the axis relative the first and second structural members.

Preferably the first of said damper members in use remains fixed in translation relative said first structural member and said second of said damper members remains fixed in translation relative said second structural member.

Preferably the frictional engagement of the intermediate damper members with the casing is substantially the same and is preferably constant.

Preferably the frictional engagement of the intermediate damper members with the casing is substantially the same as the first mentioned damper members and is preferably constant.

Preferably the spring and damper assembly comprises of an array of damper members comprising the first and second of said damper members and at least one intermediate damper member each said damper member spaced apart from each other along the axis.

Preferably the connection rod passes through each damper member.

Preferably the connection rod can translate relative to each damper member along the axis.

Preferably the spring arrangement comprises of discrete spring sets that are each located intermediate of adjacent said damper members of the array of damper members of the spring and damper assembly.

Preferably as a force is applied to cause the first of said damper member to move away from its respective bearing member its initial displacement causes the adjacent spring set to compress more without displacing the adjacent intermediate damper member.

Preferably as the displacement of the first of said damper members increases beyond said initial displacement the compression force of the adjacent spring set increases to cause said adjacent intermediate damper member to displace, its initial displacement causes the next spring set in the array to compress.

Preferably each spring set is of the same spring constant.

Preferably the frictional resistance to sliding of each damping member relative the casing is the same.

Preferably the frictional resistance to sliding of the two damping members relative the casing is the different.

Preferably said damper members are able to slide along the axis in both directions relative to the interior surface of surfaces of the casing.

Preferably the elongate casing has an interior surface or surfaces defining a constant interior cross section for the or each damping member to slide along parallel the axis.

5 Preferably the elongate casing has an interior surface or surfaces of cylindrical cross section.

Preferably the elongate casing has an interior surface or surfaces between which the damper members can be captured to apply a compression loading onto the damper members to establish a friction force between the casing and the damper members.

10 Preferably the elongate casing has an interior surface or surfaces along which said damper members can slide that do not taper toward each other in the elongate direction.

Preferably the elongate casing has an interior surface or surfaces defining a polygonal cross sectional internal shape of the casing.

15 Preferably all the damper members are acted on by the spring arrangement.

Preferably all the damper members are acted on by the spring arrangement over the full range of travel of the spring and damper assembly in the casing.

Preferably the bearing members and the stops are able to act on the spring and damper assembly to cause it to be compressed.

20

Preferably there are at least two spaced apart damper members each damper member having a friction surface or surfaces contacting the interior surface of surfaces of the casing to be able to slide with constant frictional resistance parallel the axis along at least part of the interior surface or surfaces.

25

In a second aspect the present invention may be said to be a resilient slip friction connector for connecting to and allowing displacement between a first structural member and second structural member of a building structure and providing resistance to and damping of external forces that induce relative linear displacement between said first and second members and to provide a bias on the first and second structural members following external force caused relative linear displacement of the first and second structural members from an initial relative position to a displaced relative position, the bias being such as to return the first and second structural members towards their initial relative position from their displaced relative position, the connector comprising:

35

an elongate hollow casing,

an elongate spring and damping assembly having two opposed ends and to slide inside the casing in frictional engagement with the casing and for connection to the first structural member to thereby be caused to slide inside the casing, and

at least one bearing element for bearing against an end of the spring and
5 damping assembly,

wherein one of the at least one bearing element and the elongate hollow casing are for connection to said second structural member to move therewith, and

wherein the spring and damping assembly is able to be elastically deformed by its compression between one of its ends and an at least one bearing element due
10 to a relative linear displacement of the first and second structural members to their displaced relative position, and upon a sufficient reduction of an external force that caused the compression of the spring and damping assembly, the bias of the compressed spring and damping assembly exceeds the frictional force between the spring and damping assembly and the casing, and the first and second structural
15 members are then caused to return under the bias of the compressed spring and damping assembly towards their initial relative position.

Preferably the casing comprising at least one elongate split allowing the casing to expand and contract its internal cross-sectional shape or area.

Preferably an adjustable member is provided for applying a force to the casing
20 for setting and varying the sliding frictional engagement between the spring and damping assembly and the casing by virtue of the casing comprising said split.

Preferably a rod is provided within the casing for association with the elongate spring and damping assembly, and the rod is for connection to the first structural member.

Preferably the adjustable member acts at least in part as a bias towards a
25 predetermined degree of frictional engagement between the casing and the elongate spring and damping assembly.

Preferably upon a ceasing of the external forcing the first and second structural members are caused to return under the bias of the spring and damping
30 assembly to their initial position.

Preferably the reduction of the external forcing comprises a reduction below a first threshold.

Preferably upon the reduction of the external forcing below a second threshold, being a threshold lower than the first threshold, the first and second
35 structural members are caused to return to their initial position.

Preferably the at least one bearing element is fixed relative the casing, and the casing is for connection to the second structural member.

Preferably the at least one bearing element is of the casing.

Preferably the casing comprises at least one bearing element only at or adjacent one end of the spring and damping assembly so as to provide for the elastic deformation of the spring and damping assembly only under relative displacement of
5 the first and second structural members away from each other, being a utilisation of the connector in tension, or only under relative displacement of the first and second structural member towards each other, being a utilisation of the connector in compression.

Preferably under relative displacement of the first and second structural
10 members wherein the connector does not provide for elastic deformation of the spring and damping assembly along the rod, the rod and casing are able to move freely relative each other.

Preferably under relative displacement of the first and second structural members where the connector does not provide for elastic deformation of the spring
15 and damping assembly along the rod, the rod and casing are substantially prevented from relative displacement.

Preferably the casing comprises a bearing element and a stop of the rod at each end of the spring and damping assembly to provide for the elastic deformation of the spring and damping assembly under either of relative displacement of the first and
20 second structural members away from each other, being a utilisation of the connector in tension, or under relative displacement of the first and second structural member towards each other, being a utilisation of the connector in compression.

Preferably the at least one bearing element is for connection to the first structural member and is associated with a sleeve provided about the casing, the
25 sleeve being moveable relative the casing.

Preferably under a relative displacement of the first and second structural members the at least one bearing element of the sleeve and the stop of the rod act on opposing sides of the spring and damping assembly to elastically deform the spring
and damping assembly.

Preferably the elastic deformation of the spring and damping assembly from
30 both sides occurs substantially simultaneously.

Preferably the sleeve comprises at least one bearing element only at one end of the spring and damping assembly and one stop of the rod at the opposite end of the spring and damping assembly so as to provide for the elastic deformation of the spring
35 and damping assembly

only under relative displacement of the first and second structural members away from each other, being a utilisation of the connector in tension, or

only under relative displacement of the first and second structural members towards each other, being a utilisation of the connector in compression.

Preferably under relative displacement of the first and second structural members wherein the connector does not provide for elastic deformation of the spring and damping assembly along the rod, the rod and sleeve are able to move freely relative each other.

Preferably under relative displacement of the first and second structural members where the connector does not provide for elastic deformation of the spring and damping assembly along the rod, the rod and casing are substantially prevented from relative displacement.

Preferably the sleeve comprises at least one bearing element and a stop of the rod at each end of the spring and damping assembly to provide for the elastic deformation of the spring and damping assembly under either of relative displacement of the first and second structural members away from each other, being a utilisation of the connector in tension, or under relative displacement of the first and second structural members towards each other, being a utilisation of the connector in compression.

Preferably the spring and damping assembly comprises at least one damping member for frictional engagement with the casing inside the casing and at least one spring member for providing the bias on the structural members.

Preferably the spring and damping assembly comprises a damping member at each end of the spring and damping assembly.

Preferably the damping assembly comprises a plurality of arrays of at least one damping member and at least one spring member.

Preferably the spring and damping assembly comprises a plurality damping members spaced apart by at least one spring member intermediate of the damping members.

Preferably the damping members substantially correspond with the unbiased cross-sectional shape or area of the casing.

Preferably the damping members comprise at least one coned-disc spring.

Preferably the at least one spring element is sized so as to also frictionally engage with the casing inside the casing.

Preferably the elastic deformation of the spring and damping assembly is provided by a compression of the at least one spring member, such as by an elastic bending.

Preferably the elastic deformation of the spring and damping assembly is provide by a stretching of the at least one spring member, such as by an elastic bending.

5 Preferably the spring and damping assembly comprises at least one combined spring and damping member.

Preferably each at least one combined spring and damping member is capable of both frictional engagement with the casing inside the casing and providing the bias on the members.

10 Preferably each at least one combined spring and damping member is sized so as to be capable of frictionally engaging with the casing inside the casing.

Preferably each at least one spring and damping member comprises a coned-disc spring.

15 Preferably each coned-disc spring under compression expands laterally to the direction of its compression, the lateral expansion of each coned-disc spring resulting in an increased degree of frictional engagement of the spring and damping assembly with the casing.

Preferably the elastic deformation of the spring and damping assembly is provided by a compression of the at least one spring and damping member, such as by an elastic bending.

20 Preferably the elastic deformation of the spring and damping assembly is provided by a stretching of the at least one spring and damping member, such as by an elastic bending.

Preferably the internal cross-sectional shape or area of the connector is substantially perpendicular to its elongate direction.

25 Preferably the at least one elongate split is partial or complete over the length of the casing.

Preferably the adjustable member of the casing is provided to act along the at least one elongate split.

30 Preferably the bias of the casing is towards a contracted cross-sectional shape or area of the casing.

Preferably the bias of the casing is provided by a clamping of the casing along the at least one elongate split plane.

Preferably the clamping of the casing comprises a clamping along at least a substantial portion of the at least one elongate split.

35 Preferably the bias is adjustable to provide a predetermined frictional engagement of the damping assembly and the casing.

Preferably the connector is a double acting slip friction earthquake energy damper connector.

Preferably the connector is for use between a first structural member and a second structural member of a ground supported structure that may be subjected to earthquake induced motion that can cause the first and second structural members to relatively translate towards and away from each other from an initial static position facilitated by the connector.

Preferably the elongate casing has a notional straight axis with an interior surface or surfaces defining one or more constant interior cross sections of the casing.

Preferably the casing is connected to the second structural member to translate with the second structural member.

Preferably the spring and damper assembly is to travel along the axis inside the casing.

Preferably the spring and damper assembly comprises at least two spaced apart damper members each damper member having a friction surface or surfaces commensurate the interior surface of surfaces of the casing to slide with frictional resistance along at least part of the interior surface of surfaces.

Preferably the spring and damper assembly comprises a pre-loaded spring arrangement intermediate of and forcing, when the first and second structural members are in their initial static position, the two adjacent damper members apart in the axial direction

Preferably the forcing apart is to force each damper of the two damper members against a respective bearing member of the casing located at or towards each end of the casing, yet allowing the two damper members to move towards each other against the load of the spring by a connection rod that is connected to the first structural member and to translate with the first structural member.

Preferably the connection rod has a stop at each end of the spring and damper assembly, a first of said stops to act, when the connector acts in compression when the first and second structural members translate towards each other, on a first of said two damper members to displace the first of said two damper members away from its respective bearing member and towards the second of said two damper members and its respective bearing member and a second of said stops to act, when the connector acts in tension when the first and second structural members translate away from each other, on the second of said two damper members to displace the second of said two damper members away from its respective bearing member and towards the first of said two damper members and its respective bearing member.

Preferably at least one intermediate damper member is provided between the two first mentioned damper members the spring assembly comprising of spring sets each acting between each adjacent said damper members.

In a further aspect the present invention may broadly be said to be a method of manufacture of a connector as hereinbefore described, the method comprising the steps of

- a) providing a predetermined desired restorative force capacity of the connector for a predetermined amount of elastic deformation of the spring and damping assembly,
- 10 b) providing a predetermined desired damping capacity of the connector,
- c) determining a resultant required frictional force at each at least one damping member,
- d) selecting the at least one spring member of the spring and damping member such that at the predetermined amount of elastic deformation of the spring and damping assembly the spring force is greater than the desired damping capacity, 15 and
- e) adjusting the bias of the casing or selecting an appropriate interference fit between the casing and the damping members so as to provide the predetermined desired damping capacity of the connector.

20 Preferably the predetermined desired restorative force capacity is dependent on at least the mass and configuration of the first and second structural members.

Preferably the predetermined restorative force capacity is dependent on at least the maximum allowable deflection of the structure at the first and second structural members between which the connector is to be connected.

25 Preferably when the damping and spring assembly comprises a damping member at each end of the spring and damping assembly the determination of the resultant required frictional force comprises dividing the predetermined desired damping capacity by the number of damping members minus one.

30 Preferably the casing and the spring and damper assembly have been assembled together in an interference-fit manner.

In a further aspect the present invention may broadly be said to be a connector for connecting two structural components together in an initial relative position, the connector comprising

35 a casing, engaged and to move with a first of said structural components, comprising an elongate constant cross section interior within which is operative in a frictional sliding engagement a spring and damper assembly comprising of at least one damper engaged and to move with a second of said structural components and

contacting the interior of the casing and able to slide in frictional contact with the casing in the elongate direction and a spring able to be elastically deformed by and between the damper and the casing when the damper and casing are in relative motion and to bias the relative position of the two structural components, during
5 motion of the damper and casing, towards their initial relative position.

In a further aspect the present invention may be said to be a resilient slip friction connector for connecting and allowing displacement between a first structural member and second structural member of a structure and providing resistance to and damping of external forces that induce relative displacement between said two
10 members and to provide a bias on the structural members following external force caused relative displacement of the structural members from an initial relative position to a displaced relative position, the bias being such as to return the structural members towards the initial relative position from their displaced position, the connector comprising

15 an elongate hollow casing, the casing comprising at least one elongate split allowing the casing to expand and contract its internal cross-sectional shape or area, a elongate spring and damping assembly provided for sliding inside the casing in frictional engagement with the casing and for connection to the first structural member to displace therewith, and

20 at least one bearing element for bearing against an end of the spring and damping assembly,

an adjustable member for applying a force to the casing for setting and varying the sliding frictional engagement between the spring and damping assembly and the casing by virtue of the casing comprising said split,

25 wherein one of the at least one bearing element and the elongate hollow casing are for connection to said the second structural member, and

wherein the spring and damping assembly is able to be elastically deformed by compression between one of its ends and an at least one bearing element due to a relative displacement of the first and second structural members to their displaced
30 relative position, and upon a sufficient reduction of an external force that caused the compression of the spring and damping assembly, the bias of the compressed spring and damping assembly exceeds the frictional force between the spring and damping assembly and the casing, and the first and second structural members are then caused to return under the bias of the compressed spring and damping assembly
35 towards their initial relative position.

Preferably the interior surface of surfaces of the casing are of a circular cross section and the damper members are of a circular perimeter to allow the damper members to rotate in the casing.

Preferably the connection rod is coaxial the axis of the casing.

5 Preferably the connection rod is able to swivel relative the spring and damper assembly.

Preferably the connection rod is able to bend in force inducing event relative the spring and damper assembly.

10 Preferably the connection rod is held in a cantilevered manner by the first structural member.

In a further aspect the present invention broadly comprises a method of controlling the movement between a first structural member and a second structural member comprising connecting a connector as herein before described to said first and second structural members and adjusting the force applied by the casing to the spring and damping assembly to set a frictional resistance force of the connector for resisting movement between the first and second structural members.

15 In a further aspect the present invention may be said to be a slip friction earthquake energy damping connector for use between a first structural member and a second structural member of a ground supported structure that may be subjected to earthquake induced motion that can cause the first and second structural member to relatively translate towards and away from each other from an initial static position facilitated by the connector that comprises:

25 i. an elongate casing having a notional straight axis with an interior surface or surfaces, the casing connected to the second structural member to translate with the second structural member,

ii. a spring and damper assembly to travel along the axis inside the casing and comprising of

30 a. at least 3 spaced apart damper members each damper member having a friction surface or surfaces contacting the interior surface of surfaces of the casing to be able to slide parallel the axis with frictional resistance along at least part of the interior surface of surfaces,

35 b. springs located intermediate of each adjacent said damper members to each bias the damper members apart in the axial direction at least when the first and second structural members are displaced from their initial static position (and preferably also when in the initial static position), as least one of said damper

members able to press on and preferably against a bearing member of the casing or of the second structural member located at or towards an end of the casing, yet allowing the damper members to move towards each other against the bias of the springs by a connection rod that is connected to the first structural member and to translate with the first structural member, the connection rod having a stop located (preferably at the opposite end of the casing) at an end of the spring and damper assembly to be able to apply force to the spring and damper assembly towards the bearing member to increase the compression of the springs when then first and second structural members move from their initial static position.

Preferably the connector applies a force-displacement profile of the two structural members that is non-linear over the full range of travel of the spring and damper assembly in the casing when the two structural members translate relative each other in at least one direction from their initial static position.

Preferably the connector applies a force-displacement profile of the two structural members that is non-linear over the full range of travel of the spring and damper assembly in the casing when the two structural members translate relative each other in two directions from their initial static position.

In a further aspect the present invention broadly comprises a structure comprising at least two structural members connected using a connector as herein described.

As used herein the term "and/or" means "and" or "or", or both.

As used herein "(s)" following a noun means the plural and/or singular forms of the noun.

The term "comprising" as used in this specification means "consisting at least in part of". When interpreting each statement in this specification that includes the term "comprising", features other than that or those prefaced by the term may also be present. Related terms such as "comprise" and "comprises" are to be interpreted in the same manner.

This invention may also be said broadly to consist in the parts, elements and features referred to or indicated in the specification of the application, individually or collectively, and any or all combinations of any two or more said parts, elements or features, and where specific integers are mentioned herein which have known

equivalents in the art to which this invention relates, such known equivalents are deemed to be incorporated herein as if individually set forth.

To those skilled in the art to which the invention relates, many changes in construction and widely differing embodiments and applications of the invention will suggest themselves without departing from the scope of the invention as defined in the appended claims. The disclosures and the descriptions herein are purely illustrative and are not intended to be in any sense limiting.

Other aspects of the invention may become apparent from the following description which is given by way of example only and with reference to the accompanying drawings.

BRIEF DESCRIPTION OF THE DRAWINGS

Preferred embodiments of the invention will be described by way of example only and with reference to the drawings, in which:

Figure 1A shows an embodiment of a connector with a casing with a split.

Figure 1B shows a connector with a casing with no split.

Figures 2A-2C show various components of the connector of Figure 1A.

Figure 3A shows a side cut-away view of an embodiment of a double acting connector.

Figures 3B-3D show stages of action of the connector of Figure 3A under a compressive loading of the connector.

Figures 4A-C show stages of action of the connector of Figure 3A under a tension loading of the connector.

Figures 5A to 8E show various configurations of cross-sectional shape or area and elongate splits of a casing of a connector.

Figure 9 shows a theoretical hysteresis performance being the applied force and displacement of an embodiment of a connector of the present invention.

Figures 10 and 11 show embodiments of a connector which acts in one direction only.

Figure 12A shows a further embodiment of a connector which acts in compression direction only.

Figure 12B is a view of a connector that includes a universal connection between structural components to illustrate that rotation in three axis of rotation can be accommodated by the connector,

Figure 12C is a view of a connector connected to two structural components to illustrate that the connection may also act in bending wherein the connection rod is able to elastically bend.

Figures 13 and 14 show a variation of the connector of Figures 10 and 11 respectively.

Figure 15 shows an embodiment of a connector.

Figure 16 shows a further embodiment of a connector having combined spring
5 and damping members.

Figure 17A shows a cut-away view of a combination connector according to an embodiment of the invention.

Figure 17B shows a cross-section through the lines AA of Figure 17A.

Figure 18 shows a combination configuration of a connector according to an
10 embodiment of the invention.

Figure 19 shows an embodiment of a connector.

Figures 20-22 show embodiments of a connector which is able under certain conditions of varying the frictional engagement of the elongate spring and damping assembly along the displacement of the connector.

Figure 23 shows a combination configuration of a connector according to the
15 invention.

Figures 24A-D show potential applications of connectors according to the invention in various different structures.

Figures 25A-C show various views of an embodiment of a connector.
20

DETAILED DESCRIPTION OF PREFERRED EMBODIMENTS

The present invention relates to a structural connector for connecting between two structural members of a structure. The two structural members may herein be referred to as a first structural member and a second structural member. The
25 structural members may be for example structural beams or columns of a building. One structural member may be a beam or column and the other may be a foundation or footing or pile as an example.

The connector is a resilient slip friction connector and may be single acting or double acting. It acts between two structural members or components that may be
30 subjected to external forces that can push or pull the structural members or components to or away from each other in a translational manner.

Above a first predetermined threshold of external forces on the structural members, the connector may act to allow slip and hence relative displacement of the two structural members with which it is connected. The external force may arise from
35 an external event such as an earthquake.

The connector can act to resist at least some relative displacement between the two structural members towards and/or away from each other when an external

force is applied to the two structural members and may store energy, caused by relative displacement of the structural members to each other. During such relative displacement the connector may also provide damping to the displacement motion.

The connector may bias the two structural members to or towards a relative
5 position of the two structural members relative to each other. Upon the ceasing or reduction below a second predetermined threshold of the external force the bias provided by the connector on the two structural members may act to return them from any relative displacement of the two structural members from an initial relative position, to or towards their initial relative positions. The initial relative position is
10 preferably one established pre-event during construction or assembly of the connection with the two structural members. It is preferably one defined by a steady state of the structure. For a building or other civil engineered structure the steady state is likely to be initial static position of the structure, being preferably the state it is in when constructed. As such, the connector of the present invention may be
15 described to exhibit positional restorative functions.

The connector of the present invention preferably comprises an elongate hollow casing. It has a notional axis that passes through the casing. The interior surface or surfaces of the casing are parallel the notional axis. The interior surface or surfaces define a substantially constant internal cross section of the casing.

20 The casing may be directly or indirectly connected to the second structural member to remain in a fixed relative position therewith.

The connector comprises an elongate spring and damping assembly. The spring and damping assembly, in use, is able to translate linearly within the elongate casing in a frictional engagement with the inside surface or surfaces of the casing in
25 order to provide at least in part a damping function of the connector. The spring and damping assembly also acts in combination with other components of the connector to be able to provide a bias force on the two structural members to encourage them back toward on initial relative position if moved away from such.

The spring and damping assembly is preferably operatively connected to the
30 first structural member to displace therewith. In the preferred form, the connection to the first structural member is by a connection at an end of the elongate spring and damping assembly.

In an alternative form, a rod may be located in the casing. Where provided, the rod is for connection to the first structural member and to remain in a fixed
35 relative position therewith. About the rod is provided the elongate spring and damping assembly. To provide a limit of travel of the spring and damping assembly on the rod, the rod may comprise of a stop or stops.

In one preferred version of the connector the casing preferably comprises at least one split extending over its elongate length allowing the casing internal cross-sectional shape or area to be changed (e.g. by expansion or contraction) by active adjustment. This version is shown in most figures attached. The expansion and
5 contraction may be an actual expansion or contraction, or a bias towards an expansion or contraction of cross-sectional area or shape. An alternative version of the casing is shown in figure 1B where the casing has no split.

Expansion and contractions may occur preferably under the application of a force to the casing as for example shown in figure 1A, to change the shape of the
10 internal cross section. The force may be applied directly or via a bias such as may be provided by a spring or springs. An adjustable member may be associated with the casing for applying the force to the casing and for setting and varying the sliding frictional engagement between an elongate spring and damping assembly, and the casing. The varying of the frictional engagement may occur due to the split of the
15 casing, which allows at least a portion of the casing to assume a more expanded or contracted internal cross sectional area or shape. In the version of the casing of figure 1B, the force between the casing and the spring and damping assembly may be set at the time of assembly. A friction fit can be established at assembly to ensure that the casing applies a radial force to the spring and damping assembly for use. The casing
20 may be heated during assembly to cause it to expand allowing an easier locating of the spring and damping assembly inside the casing. As the casing cools, it will apply greater radial force to the spring and damping assembly so that the connector is then presented ready for use.

The expansion or contraction of the casing may occur due to a bias towards
25 an expansion or contraction of cross-sectional area or shape that acts against the spring and damping assembly. For example, when the casing is not yet engaged with the spring and damping assembly, the casing may be in a more contracted in cross-sectional area or shape. However, when already frictionally engaged with the spring and damping assembly, a further application of force towards a more contracted
30 cross-sectional area or shape of the casing may not change the cross-sectional area or shape, but rather increase the frictional engagement of the casing with the spring and damping assembly.

At least one bearing element is preferably provided to bear against an end of the spring and damping assembly. In forms where the connector is to be operative
35 under only one direction of linear displacement of the casing and spring and damping assembly, a bearing element may be provided only at one end of the spring and damping assembly. In forms where the connector is to act under both directions of

linear displacement a bearing element is preferably provided at each end of the spring and damping assembly.

Whilst in a preferred form the casing is to be connected to the second structural member, in some forms the at least one bearing element is for connection
5 to the second structural member.

Adjustment of the internal shape of the casing is preferably able to be made to vary the frictional engagement of the casing with the spring and damping assembly, in order to vary the damping effect of the connector on the displacement between the two structural members.

10 In use, the first and second structural members, and thus the connector connected between them, may be subjected to an external force. Once the external force exceeds a first predetermined threshold, the spring and damping assembly is able to be elastically deformed. Where a rod is provided within the casing and for connection to the first structural member, this deformation of the spring and damping
15 assembly preferably occurs along the rod between the at least one bearing element and the stop of the rod. The elastic compression of the spring and damping assembly causes displacement of components of the spring and damping assembly relative with the casing, and the frictional engagement of the spring and damping assembly with the casing provides damping.

20 The maximum relative displacement of the connected first and second structural members may be determined by the maximum elastic compression of the spring and damping assembly.

Upon the reduction of the external forcing below a second predetermined threshold the bias caused by the springs of the spring and damping assembly exceeds
25 the frictional engagement between the displaced portions of the spring and damping assembly and the casing, and the first and second structural members are caused to return under the bias towards their initial relative positions. An ability to return to their initial position can be achieved in some embodiments of the connector where the spring is pre-loaded when in the initial relative position.

30 The external forces to which the connector is to be exposed may include forces resulting from earthquakes or other seismic activity, vibration, wind, or other natural or man-made external loadings.

The connector of the present invention may commonly be used for connecting between two structural members of buildings, but may also be used in any other
35 application where any force is to be resisted. In a building, the two structural members might be, for example a post, beam, joist, rafter, brace, wall or panel, or a foundation or footing. The connector or a plurality of such connectors may be utilised

in connections of different lateral load resistant systems such as braced frames, moment resisting frames, or shear walls.

As described, the connector of the present invention may return at least some of the residual relative displacement of two connected structural members following an external forcing event. However, in preferred forms the connector provides for the returning of all or substantially all residual displacement between first and second structural members so that such are returned to their initial relative position on the basis that the forces on the two structural members permit such return. In order to provide for the full returning of all relative displacement of the first and second structural members to an initial relative position after an event, the spring force of the spring and damping assembly at all times exceed the frictional engagement of the spring and damping assembly with the casing.

Under external forcing of the first and second structural members below the level of the first predetermined threshold the connector may not allow for elastic deformation of the spring and damping assembly and relative displacement of the first and second structural members. This may be desirable in order to limit drift of a structure under serviceability loads. The first predetermined threshold may be determined by the frictional engagement of the relevant outer-most portion of the spring and damping assembly which is in frictional engagement with the casing. The adjustment of the adjustable member of the casing may therefore be used to set the first predetermined threshold.

Under a reduction of the external forcing below the second predetermined threshold the connector may begin to return displacement of the two structural members. The second predetermined threshold may be determined at least in part by a degree of pre-stressing or pre-loading of the spring and damping assembly. This pre-stressing provides an initial degree of elastic deformation of the spring and damping assembly. For example, this pre-stressing may be provided by an initial compression of the spring and damping assembly between stops of the rod, and/or bearing members.

The degree of pre-stressing may influence both the second predetermined threshold at which the connector will begin to return displacement, and also the rate of return of displacement under a ceasing or reduction of the external force.

The spring and damping assembly may comprise one or more spring and damping stages. Each of these spring and damping stages may provide specific spring and damping characteristics. In the preferred form, each of these spring and damping stages are individually and progressively elastically deformed over the stroke of the

connector. Preferably each stage is designed to provide the same spring and damping characteristics, though it is envisaged that stages may be different to each other.

The degree of adjustment of the internal cross-sectional shape of the casing may be substantially homogeneous over the length of the casing. Alternatively, it may
5 be varied along the length to provide for variable resistance and damping characteristics over the stroke the connector.

The bias acting on the casing may bias the casing towards a smaller cross-section, or may bias it towards a larger cross-section. For example, the unbiased cross-section of the casing may be greater in size than the cross-section of the spring
10 and damping assembly, and thus require biasing towards a smaller size in order to frictionally engage with the spring and damping assembly. Alternatively, the unbiased casing may be smaller in cross-section than the spring and damping assembly, and thus require biasing toward a larger size in order to allow the entry of the spring and
15 damping assembly therein, and to reduce the frictional engagement with the spring and damping assembly.

In a preferred form the frictional engagement of the inside of the casing with the spring and damping assembly, and the physical characteristics of the casing and
spring and damping assembly, are such that under action of the connector only elastic deformation of the spring and damping assembly and sliding at the friction surfaces
20 occur. In this manner the connector may be resilient.

It is considered desirable to prevent plastic deformation of the spring and damping assembly, particularly at the friction surfaces, in order to increase the service life of the connector and reduce the requirement for maintenance between external
forcing events. However some degree of plastic deformation at the friction surfaces
25 may occur under particular circumstances.

Embodiments of the connector may be provided allowing for the action of the connector by the compression of the spring and damping assembly under only one of tension or compression on the connector. In such connectors where the spring and
damping assembly is elastically deformed only under one of tension or compression of
30 the connector, the connector may either allow substantially un-resisted relative displacement of the structural members, or may prevent relative displacement of the structural members.

In preferred forms which will now be described, the elastic deformation of the spring and damping assembly comprises an elastic compression of the spring and
35 damping assembly. However other spring and damping assemblies may elastically deform in other ways during the action of the connector, such as by stretching under tension.

Examples of the invention will now be described with reference to the drawings. Shown in Figure 1A is an embodiment of the resilient slip friction connector of the present invention. The connector 1 is for connecting between two structural members of a structure.

The connector 1 has two main functions. First, the connector 1 provides resistance to and damping of an external force which induces relative moment between the two structural members to which the connector 1 is connected. Secondly, the connector 1 is to provide a bias on the two structural members when they are displaced away and/or towards each other, following external force caused relative displacement of the members from an initial relative position. This bias of the connector is to be such that it causes or aids in causing the return of the structural members to or towards their initial relative position from a translated relative position.

As seen in the embodiment of Figure 1A, the connector 1 comprises a casing 2. Preferably, the casing 2 is in the form of an elongate hollow casing having at least one elongate split 3 allowing the casing 2 to expand and contract its internal cross-sectional area or change its cross-sectional shape. The split may be linear and along the entire length of the casing.

The casing may be of one component having a split or not of two or more components assembled together to define an internal surface or surfaces 600 to an internal cross sectional area.

The casing has a national axis 700 x-x as shown in Figure 3B. The connector 1 may comprise an adjustable member 4 for the casing 2 for adjusting the cross section shape for applying a force to the casing for setting and varying the sliding frictional engagement between the spring and damping assembly and the casing.

As seen in the configuration of Figure 1A, the casing 2 comprises an elongate substantially cylindrical body having an elongate split 3 extending along one side of the body. In this configuration, the adjustable member 4 of the casing is provided by a plurality of bolts 5 and nuts 6 connected across the elongate split and arrayed along the elongate split 3. The tensioning of a bolt 5 and nut 6 of Figure 1A would be such as to effect a contraction of the internal cross-sectional area of the casing 2. In alternate configurations where the expansion of the casing 2 along the elongate split is to be desired, a similar bolt and nut connection may be provided to expand the casing 2 at the elongate split plane, thus expanding the cross-sectional area of the casing 2. The internal surface or surfaces may be cylindrical in shape defining one constant cross section region for sliding engagement. It may be of multiple shapes of constant cross section for each or several of the damper members to slide. The surfaces may

be of polygonal cross section. They are preferably not tapered surfaces. This helps ensure that the friction force between the damper member and its casing surface or surfaces it slides along remains constant over its range of travel.

The purpose of the adjustable member 4 of the casing 2 where provided is to
5 allow control of the frictional engagement of the internal surfaces 600 of the casing 2 with a spring and damping assembly 7. The spring and damping assembly is for connection to a first structural member. The spring and damping assembly 7 acts in combination with other components of the connector 1 to provide resistance to external forces, damping of external forces caused relative displacement, and the bias
10 on the structural members to encourage return of them to or towards their initial relative position from a displaced position.

The spring and damping assembly 7 is preferably provided about a rod 8. In this configuration the rod 8 is for connection to the first structural member.

The rod 8 is not limited to being a substantially cylindrical rod, but may be a
15 rod of many cross-section and dimensions such that it is able to be connected to a structural member and apply a load from the first structural member to at least one end of the spring and damping assembly 7. Furthermore, the rod may be of a substantially rigid form, or may be flexible such as in the form of a cable or chain.

The connector 1 further comprises at least one bearing member 9 for bearing
20 against an end of the spring and damping assembly 7. There may be two bearing members 9 for bearing against both ends of the assembly 7.

A linear displacement of the first and second structural members relative each other will result in relative displacement of the casing 2 and the spring and damping assembly 7. Preferably the connection of the first structural member to the spring and
25 damping assembly is a connection at one end of the spring and damping assembly. The relative movement is preferably such as to cause the spring and damping assembly to be elastically deformed by compression between one of its ends, preferably the connected end, and an at least one bearing element.

In embodiments wherein the connector comprises a rod 8 connected to the
30 first structural member, the respective connections of the rod 8 and casing 2 to the first structural member and second structural member of the structure will result in elastic deformation by compression of the spring and damping assembly along the rod 8 between a bearing member 9 and a stop 10 of rod.

The compression of the spring and damping assembly 7 may comprise one or
35 more stages of compression and damping.

Preferably the operative distance between the two stops 10a and 10b is the same as the distance between the two bearing members at each end of the casing.

The stops 10 of the rod 8 are preferably configured such that they may be adjusted along the rod so as to control a degree of pretension applied to the spring and damping assembly 7. While one such convenient form may be nuts and bolts threaded onto the rod 8, any other configuration able to provide for a limit of the spring and damping assembly on the rod and preferably also able to be adjusted in position along the length of the rod are contemplated within the scope of the invention. For example, one stop 10 may be permanently affixed or integrally formed with the rod 8, while the other stop 10 at the opposed end of the rod 8 is able to be adjusted in its position along the rod. In the configuration shown in Figure 3A the distance between the two stops 10a and 10b is the same as the distance between the two bearing members 9 at each end of the assembly 7. Pre-stressing or compression of the springs may hence be due to the spacing of the stops and/or the bearing members.

The connector 1 is configured such that the bias of the spring and damping assembly 7 exceeds the frictional force between the spring and damping assembly 7 and the casing 2 when the external forcing event ceases or is decreased below a predetermined threshold. The result is that, when the external force ceases or decreases below a threshold, the rod 8 and casing 2, and their associated first and second structural members, are caused to return towards their initial position. In some forms the return of the first and second structural members may comprise simply a return towards their initial position, but preferably it comprises a return to their initial position. A sufficient pre-stressing or compression of the springs helps to achieve this to ensure that the force of the springs can overcome the resistance to movement due to friction between the casing and the assembly.

Figures 2A-2C show further details of the constituent components of the connector 1 of the embodiment of Figure 1A. Shown in Figure 2A is the casing 2 of the connector, and its elongate split 3 extending along the length of the casing. Also shown in Figure 2A is an adjustable member 4 of the casing, being a bolt 5 and nut 6 for clamping of the casing 2 along the elongate split 3.

Figure 2B shows the different components of the spring and damping assembly 7 and rod 8 of the connector 1 of Figure 1A. The shown spring and damping assembly 7 comprises at least one damping member 12 and a spring arrangement that may comprise of at least one spring member or spring set 11. Also seen in Figure 2B is a stop 10 of rod 8, for bearing against the end of the spring and damping assembly 7 on the rod 8.

Figure 2C shows the assembled spring and damping assembly 7 on the rod 8 of the configuration of Figure 1A. This spring and damping assembly comprises a

plurality of spring and damping stages 13 arrayed between the stops 10 of the rod 8. Each spring and damping stage 13 comprises at least one spring member or spring set 11 and at least one damping member 12. In a preferred form seen in Figure 2C, the spring and damping assembly 7 comprises at each end adjacent the stop 10 of the rod a damping member 12. In other forms however, the spring and damping assembly 7 may comprise only a damping member 12 adjacent one of the stops 10 and a spring member 11 adjacent the other, or it may alternately comprise spring members 11 at each of its ends adjacent the stops 10.

The spring set may comprise of one or more individual spring elements such as a stack of Belleville washers.

The operation of a connector 1 according to the present invention will now be described with reference to Figures 3A-3D. The views of Figures 3A-3D show a cross-section of an embodiment of the connector.

Figure 3A shows a connector 1 comprising a casing 2 and spring and damping assembly 7 provided about a rod 8 located within the casing 2. The spring and damping assembly 7 is constrained on the rod 8 between two spaced apart stops 10 of the rod. It is also constrained within the casing 2 at each end between bearing members 9, here provided at both ends of the casing 2. The casing 2 is for connection to a second structural member (400), and the rod 8 is for connection to a first structural member (401). As previously described in relation to the embodiment of Figure 1A, though not shown in the cross-sections of Figures 3A-3D, the casing 2 comprises an elongate split 3 and adjustable member 4 for setting and varying the sliding frictional engagement between the spring and damping assembly and the casing.

The connector of Figure 3A has a spring and damping assembly 7 comprising three spring sets 11a, 11b, 11c and four damper members 12a-d defining damping stages 13A, 13B and 13C. Each spring and damping stage may comprise a damping member 12 and a plurality of spring members 11. The spring and damping assembly 7 of Figure 3A also demonstrates the preferred form wherein damping members 12 are provided at each end of the spring and damping assembly adjacent the stops 10A and 10B of the rod 8 to press there against.

In the configuration of Figure 3A-3D, the connector is able to act by the compression of the spring and damping assembly 7 under relative motion of the casing 2 and rod 8 in both longitudinal directions as denoted by the arrows 14. Such a connector 1 may be known as a bi-directional connector, double acting connector, or as a connector capable of acting in both tension and compression, where tension and

compression refer to the overall forces acting on the connector 1 due to resistance of and the relative displacements of the associated first and second structural members.

Figure 3B shows the first stage of action of the connector 1 of Figure 3A under the compression of the connector, being the displacement of the rod 8 in the direction of the arrow 15 and the displacement of the casing 2 in the direction of the arrows 16. The displacement of the rod 8 relative the casing 2 in the direction of the arrow 15 causes the stop 10A of the rod to act against the first damping member 12A of the spring and damping assembly 7.

The displacement of the rod 8 causes the compression of the first stage 13A of the spring and damping assembly. Under the compression of the first stage 13A the damping member 12A is moved in the direction of the arrow 15, and the array of spring members 11A are compressed in the direction of the arrow 15. As the spring and damping stage 13A is compressed, the damping member 12A absorbs energy due to its sliding frictional engagement with the inside of the casing 2 and the array of spring members 11A absorb energy due to their compression.

During the compression of the first spring and damping stage 13A, the spring force of the compressed spring member or array of spring members 11A is supported in the direction of the arrow 16 by the adjacent damping member 12B. Once the first spring and damping stage 13A is compressed such that the spring force of the spring member or array of spring members 11A is greater than the frictional engagement of the second damping member 12B with the casing 2, the second damping member 12B will also start to move in the direction 15. This causes the compression of the second spring and damping stage 13B as shown in Figure 3C.

As seen in Figure 3C, the compression of the spring member 11A of the first spring and damping stage 13A has been such that the frictional resistance to movement of the second damping member 12B with the casing 2 has been overcome, and the second stage 13B of the second spring and damping stage 13B has been compressed.

Figure 3D shows the connector 1 having a fully compressed spring and damping assembly 7, wherein each of the spring and damping stages 13A, 13B, and 13C have been fully compressed. The damping member 12D acts against the bearing members 9 to prevent the sliding of the damping member 12D in the direction of the arrow 15. Unless the spring members 11 of each spring and damping stage is capable of further compression, this state defines a limit of relative displacement of the rod 8 with respect to the casing 2.

Figures 4A-4C show the action of a connector 1 under the reverse relative displacement as shown in Figures 3A-3D. Figures 4A-4C show the action of the

connector under tension, being a relative displacement of its connected first and second structural members away from each other.

In Figure 4A, the rod 8 has been moved in the direction of the arrow 16 and the casing 2 has been moved in the direction of the arrow 15 such as to compress the spring and damping stage 13C. To effect the compression of the damping stage 13C, the stop 10B of the rod acts against the damping member 12D causing it to slide within the casing 2. The displacement of the damping member 12D causes the compression of the spring member 11C.

As previously described in relation to the action of the connector 1 in compression, continued displacement of the rod 8 in the direction of the arrow 16 will cause continued compression of the spring member 11C and an increase in its spring force. Once the spring force of the spring member 11C is sufficient to overcome the frictional engagement of the damping member 12C with the casing 2, the damping member 12C will begin to slide relative the casing and cause the compression of the second spring and damping stage 13B.

Figure 4B shows this next stage of action of the connector, wherein the spring and damping stage 13B has been compressed. Once the spring force of the spring member 11B overcomes the frictional engagement of the damping member 12B with the casing 2 the damping member 12B will also begin to move in the direction of the arrow 16 and result in the compression of the spring and damping stage 13A. Once all three spring and damping stages 13A, 13B, and 13C have been fully compressed, the damping member 12A is most forced against the bearing members 9 and further displacement of the spring and damping assembly relative to the casing is restricted.

During an external forcing event, such as an earthquake, vibration or other external forcing, a connector 1 may be acted on so as to displace the rod 8 relative the casing 2 as has been described in relation to Figures 3A-3D, and 4A-4C. Upon the ceasing or sufficient reduction of the external forcing event, the first and second structural members may still be displaced from their initial translational position, meaning that the connected rod 8 and casing 2 of the connector 1 will also be displaced from their initial position. Under the action of the connector through any of the stages or part stages of compression of the spring and damping stages 13 seen from Figure 3A-4C, the connector 1 acts to aid in the return its components and the connected first and second structural members towards their initial positions. This functionality is provided by the interrelationship of the spring force of the spring members 11 and the frictional engagement of the damping members 12 with the casing 2.

In order to provide for returning of relative displacement by the connector, the spring force of a compressed spring member 11 should exceed force resisting movement due to the frictional engagement of its associated damping member 12 with the casing 2 over its full range of travel. Provided that the spring force of the spring member 11 exceeds force resisting movement due to the frictional engagement of the damping member 12 with the casing 2, upon ceasing of the external force the stored energy of spring members 11 can overcome the resistance to movement caused by the frictional force on damping members 12 by the casing, and to return the rod 8 and casing 2 to their initial relative positions.

An example of such returning of relative displacement will now be described with reference to Figure 4B. Were the external forcing in the directions of the arrows 15 and 16 reduce below a threshold or to cease, the stored energy of the compressed spring and damping stages 13B and 13C can be released, and the damping members 12C and 12D can be forced in the direction of the arrows 15 towards their initial position.

A preferred theoretical design procedure of an example connector will now be described. The variables to be referred to in the design procedure are listed below.

$F_{friction}$	Total friction force
μ	Coefficient of friction
n_{bolt}	Number of clamping bolts
$F_{pr, bolt}$	Pre-stressing force in each clamping bolt
$F_{pr, rod}$	Pre-stressing force of the longitudinal rod
m	Number of individual spring stacks between friction discs
n	Number of the friction discs
$F_{slip, i}$	Slip force corresponds to the slip of i^{th} friction disk
$\Delta s_{slip, i}$	Displacement corresponds to the slip of i^{th} disc
k_i	Stiffness of i^{th} spring stack
F_{ult}	Ultimate loading capacity
Δ_j	Displacement of j^{th} spring stack at the slip of i^{th} friction disk

- $\Delta_{max,j}$ Maximum displacement of the j^{th} spring stack when the stack is fully compressed
- F_j force in the j^{th} spring stack at the slip of i^{th} friction disk
- $F_{restoring,i}$ restoring force corresponds to the re-centring slip of i^{th} friction disk
- $F_{residual}$ The residual unloading force in the damper

The following table lists a set of theoretical design equations which may be used in the design and to determine the characteristics of a connector of the present invention.

5

	Equation	Description
(1)	$F_{friction} = 2\pi\mu F_{pr,bolt} n_{bolt}$	Total friction force
(2)	$F_{pr,rod} > F_{friction}$	Self-centring condition
(3)	$F_{slip,0} = F_{pr,rod} + \frac{f_{friction}}{n}$	First slip force
(4)	$F_{slip,1} = F_{slip,0} + \frac{f_{friction}}{n}$ and $\Delta_{slip,1} = \frac{f_{friction}}{n * k_1}$	Second slip force and its corresponding displacement
(5)	$F_{slip,i} = F_{slip,i-1} + \frac{f_{friction}}{n}$ and $\Delta_{slip,i} = \sum_{j=1}^{i-1} \Delta_j + \frac{f_{friction}}{n * k_i}$	The i^{th} slip force and its corresponding displacement. It should be noted that the sign "Σ" refers to the displacement of other disk stacks which should be added to the i^{th} one.
(6)	$\Delta_j = \min \left\{ \frac{F_j}{k_j}, \Delta_{max,j} \right\}$	Displacement of j^{th} spring stack at the slip of i^{th} friction disk.

(7)	$F_j = F_{slip,i} - j * \frac{f_{friction}}{n}$	Force in the j^{th} spring stack at the slip of i^{th} friction disk.
(8)	$F_{ult} = F_{slip,m-1} + k_m * \Delta_{max,m}$	Ultimate loading capacity.
(9)	$F_{restoring,m} = k_m * \Delta_{max,m} - \frac{f_{friction}}{n}$	Restoring force at the maximum displacement.
(10)	$\begin{aligned} F_{restoring,m-1} &= F_{restoring,m} \\ &- \frac{f_{friction}}{n} \text{ and } \Delta_{restoring,m-1} \\ &= \Delta_{ult} - \Delta_{slip,1} \end{aligned}$	Restoring force at the second re-centring slip.
(11)	$\begin{aligned} F_{restoring,i} &= F_{restoring,i+1} \\ &- \frac{f_{friction}}{n} \text{ and } \Delta_{restoring,m-1} \\ &= \Delta_{ult} - \Delta_{slip,i} \end{aligned}$	Restoring force at the i^{th} re-centring slip.
(12)	$F_{residual} = F_{restoring,0} = F_{pr,rod} - \frac{f_{friction}}{n}$	The residual unloading force in the damper.

With reference to the list of variables and the equations provided above, a theoretical design procedure to predict various characteristics of a connector will now be described.

5 The total frictional engagement of a casing with its spring and damping assembly may be determined by equation (1).

In order to restore displacement of a connector, the degree of pre-stressing of the spring and damping assembly should be greater than the total frictional force calculated in equation (1). See equation (2).

10 The primary variables in the calculation of the slip forces of the connector, as listed above, are:

- Number of damping members $i=0$ to n , and
- Number of individual spring members between the damping members $j=0$ to m .

15 The external force to result in slipping of each successive damping member 12 may be calculated by equations (3)-(5) as the sum of the pre-stressing force applied between the stop 10 of the rod 8, and the ratio of the total frictional engagement with the number of damping members:

$$F_{slip,0} = F_{pr,rod} T \frac{f_{friction}}{n}$$

$$F_{slip,i} = F_{slip,0} + \frac{f_{friction}}{n} \text{ and } \Delta_{slip,1} = \frac{f_{friction}}{n * k_1}$$

$$F_{slip,i} = F_{slip,i-1} + \frac{f_{friction}}{n} \text{ and } \Delta_{slip,i} = \sum_{j=1}^{i-1} \Delta_j + \frac{f_{friction}}{n * k_i}$$

As shown above, the displacement due to the compression of each spring and damping stage 13 is determined by the total frictional force divided by the number of damping members and the spring constant of the spring being compressed. The total displacement due to the compression of multiple spring and damping stages 13 is the sum of each individual stage's displacement.

The compression of each spring member 11 of each spring and damping stage 13 may be calculated as being the minimum of a) the force applied at the spring member divided by its spring constant, and b) its maximum compression. Per equation (6):

$$\Delta_j = \min \left\{ \frac{F_j}{k_j}, \Delta_{max,j} \right\}$$

The force applied at each spring stage may be calculated from taking the slip friction threshold at the next associated damping member, and subtracting the multiple of the frictional engagement force with the number of the spring and damping member in that spring and damping stage divided by the number of total damping members. See equation (7):

$$F_j = F_{slip,i} - j * \frac{f_{friction}}{n}$$

The ultimate external force at which all stages of the spring and damping assembly are fully compressed and the displacement of the connector is maximised may be calculated by the sum of the force at the slip threshold of the second to final damping member and the product of the spring constant of that stage's spring with its maximum compression, per equation (8):

$$F_{ult} = F_{slip,m-1} + k_m * \Delta_{max,m}$$

The forces during restoring may then be calculated as follows, according to equations (10)-(12):

$$F_{\text{restoring},m} = k_m * \Delta_{\text{max},m} - \frac{f_{\text{friction}}}{n}$$

$$F_{\text{restoring},m-i} = F_{\text{restoring},m} - \frac{f_{\text{friction}}}{n} \text{ and } \Delta_{\text{restoring},m-i} = \Delta_{\text{ult}} - \Delta_{\text{slip},i}$$

$$F_{\text{restoring},i} = F_{\text{restoring},i+1} - \frac{f_{\text{friction}}}{n} \text{ and } \Delta_{\text{restoring},i} = \Delta_{\text{ult}} - \Delta_{\text{slip},i}$$

5 The residual unloading force in the connector may be calculated per equation (12) as:

$$F_{\text{residual}} = F_{\text{restoring},0} = F_{\text{pr.rod}} - \frac{f_{\text{friction}}}{n}$$

10

Figure 9 shows the predicted hysteresis characteristics of a connector according to the present invention. Figure 9 will now be described, with reference to the variables and equations defined above.

15 Seen in the second quadrant 17 of the graph of Figure 9, the connector 1 is utilised in tension as previously described.

In order to cause initial compression of the spring and damping assembly 7 an initial force $F_{\text{slip},0}$ at 19 must be provided between the rod 8 and the casing 2. The force $F_{\text{slip},0}$ at 19 is determined by the frictional engagement of the first damping member 12 with the casing 2. External force beyond this threshold results in
20 compression of the first spring member 11. Once the force reaches the threshold $F_{\text{slip},i}$ at 20 the slipping of the second damping member 12 will begin to occur, along with the compression of its associated spring member 11. This process of stage-wise compression of each spring and damping stage 13 continues until F_{ult} at 23 at which the spring and damping assembly has been fully compressed.

25 For a number of damping member from $i = 0$ to n , and a number of spring members $j = 0$ to m , the values shown in the graph of Figure 9 for the compression of the spring and damping assembly are:

- $F_{\text{slip},0}$ at 19,
- $F_{\text{slip},i}$ at 20,
- 30 • $F_{\text{slip},i}$ at 21,
- $F_{\text{slip},m-i}$ at 22, and
- F_{ult} at 23.

Figure 9 also shows the restoring action of the connector upon the reduction and ceasing of the external force. As the external force reduces from F_{uit} at 23 it reaches a threshold $F_{restoring,mat}$ 24 at which the first of the spring members 11 is able to overcome the frictional engagement of its associated damping member 12 with the casing 2. Further decreasing of the external force reduces the displacement of the connector as the first spring and damping stage decompresses. Further decreases of the external force will reach successive thresholds at which each of the following adjacent spring and damping segments can overcome the frictional engagement of their associated damping member 12 and decompress preferably all stages have their springs under pre-compression.

The predicted characteristics of the connector of Figure 9 comprise a residual spring force of the spring member 11 such that all displacement of the connector may be returned. This is seen by $F_{residual}$ at 28 in Figure 9.

For the restoring action of the connector, the values shown in Figure 9 are:

- F_{uit} at 23,
- $F_{restoring, mat}$ 24,
- $F_{restoring, m} 1$ at 25,
- $F_{restoring, j}$ 3t 26,
- $F_{restoring, l}$ 3t 27, and
- $F_{residual}$ at 28.

As shown in the predicted characteristics of Figure 9, the connector exhibits a fully self-centring capacity, such that upon the sufficient reduction below $F_{residual}$ at 28 of the external forcing, all residual displacement of the connector is returned. Self-centring or re-centring being in reference to restoring to the original relative position.

The residual force, $F_{residual}$ at 28, may be provided by pre-compression of the spring and damping assembly between the stops 10 of the rod. For example in the embodiment of Figure 1, the stops comprise bolts which may be tightened or loosened along the rod in order to provide for a desired amount of residual force, $F_{residual}$ at 28, of the connector.

The total energy damped by the connector is represented by the shaded area 29 of Figure 9.

Increases in the degree of residual force may be desirable for particular applications, such as to allow for total returning of the connector even in the presence of some remaining threshold of external forcing. However increases in the degree of residual forcing will decrease the total energy damped by the connector, as illustrated at the shaded area 29 in Figure 9.

The action of the connector in the reverse relative motion as described in relation to quadrant 2 at 17 is shown in quadrant 3 at 18. If the action in relation to quadrant 2 at 17 is an action in tension, the action of the connector in quadrant 3 at 18 is to be an action in compression. The action in quadrant 3 is substantially identical to that described for the connector in tension, except that the external force is exerted in the opposite direction, and the displacement of the rod 8 and casing 2 relative each other is opposite. The use of multiple spring and damping stages results in a non linear force/displacement profile over the full range of motion of the spring and damper assembly in the casing.

10 In the embodiment of figure 1 B the spring and damping assembly may be assembled into the casing of which the cross-sectional shape is fixed. The casing may not include a split as can be seen. The assembly may be established as a interference fit. Reference is made to, and which is hereby incorporated by way of reference to the publication Advanced Materials Research Vol 668 (2013) pp 495-499, FEM Analyses of Stress on Shaft-sleeve Interference Fits. Trans Tech Publications, Switzerland
15 doi: 10.4028/www.scientific.net/AMR.668.495

As has been previously described, different applications may have use of the connector such that it acts by the elastic deformation of the spring and damping assembly 7 under either or both action of the connector in tension or compression.

20 In a configuration wherein the connector 1 provides its spring and damping action only under one of tension or compression on the connector, the connector only needs to comprise bearing members at one end of the spring and damping assembly 7.

For example, shown in Figure 10 is an embodiment of the connector 1 wherein the connector provides its compression and damping action only under exposure of the connector 1 to tension. The connector under tension is indicated by the forcing of the rod 8 leftwards in the direction of the arrow 16, and the forcing of the casing 2 rightwards in the direction of the arrows 15. Under tension, the connector of Figure 10 will cause the spring and damping assembly to be elastically deformed by compression between the bearing members 9 of the casing 2 and the stop 10 of the rod. Under the reverse relative displacement, being a forcing of the rod in the opposite of the direction of arrows 16, and a forcing of the housing of Figure 10 in the opposite of the direction of the arrows 15, the spring and damping assembly is not compressed.

Figure 11 shows a connector capable of providing relative displacement, damping, and positional restorative functions only under compression of the connector. In tension, the rod 8 is not prevented from moving relative to the casing 2 but preferably no damping or positional restorative functions are provided.

Figure 12A shows a further variation of the connector 1 for use only in compression. As seen in Figure 12A, the connector 1 comprises two separate rods 8A and 8B. The first rod 8A is connected to a first damping member 12A and the second rod 8B is connected to a further damping member 12D. The damping members 12A and 12D are provided as part of a spring and damping assembly 7 as previously described. The spring and damping assembly comprises three spring and damping stages 13. Under forcing of the rod 8A in the direction of the arrow 15, and the forcing of the rod 8B in the direction of the arrow 16, the spring and damping assembly may be progressively compressed as previously described, except that in this configuration it may be compressed from both ends simultaneously. In the variation of Figure 12A, each of the rods 8A and 8B are for connection to the first and second structural members of the structure, rather than connecting such to a rod and the casing 2.

Were the connector of Figure 12A to be exposed to opposite forcing, being forcing of rod 8A in the direction of arrow 16 and forcing of rod 8B in the direction of arrow 15, the bearing members 9 of the casing would act against the damping members 12A and 12D to prevent relative displacement of the rods with respect to the casing 2.

Figure 12B illustrates a variation of a connector where the casing 2 captures a spring and damping assembly 7 between bearing members 9 in a pre-stressed or compressed condition and where a ball and knuckle connection 406 exists between the first and second structural members and the spring and damper assembly 7 as seen. The ball 407 is able to locate in rebate 408 of a damper and this may be repeated at the other end of the connector 7. In this configuration there are degrees of freedom of rotation about the axis 409 and 410 allowing for drift or pivoting or other rotational or rotation inducing forces to be accommodated in or by the connector in the structural assembly utilising the connector 1. It may be that only at one end of the connector is such degree of freedom of rotation enabled. It may also be that alternative of such arrangements to allow for a degree of rotational freedom to be established between the connector 2 and the structural member or members with which it is engaged.

In Figure 12C, there is shown a connector 1 comprising of a casing 2 from which there projects a rod 8 that may be secured to first structural member 401 in a cantilevered manner as seen in Figure 12C. The second structural member 402 may be connected to the casing 2 of the connector 1 and may move during translational displacement also in a rotational manner along the arc 421. The rod 8 may yield in an elastic manner to allow for such rotational displacement of the second structural member 402 to occur relative to the first structural member 401. The rod or other type of connection 8 between the connector 1 and the first structural member 401

may be such as to allow for an elastic yielding of the rod or other type of connector to occur during such displacement. Such elastic yielding will bias rotation of the first structural member relative to the second structural member back towards their initial rotational position. A translational displacement is provided for by the connector as is herein being described.

The use of a rod for example allows for omni-directional bending of the rod with a predictable response. The casing entrance where the rod enters is of a shape and configuration to not touch or constrain the rod from bending or pivoting relative to the spring and damping assembly. In order to provide for a connector providing damping and restorative characteristics under only one of tension or compression, but preventing relative displacement under the other, an assembly as shown in Figures 13 and 14 may be provided. As seen in Figures 13 and 14, the connectors 1 each comprise at least one limit element 30. The limit elements 30 act to hold a damping member 12 between the limit element 30 and the bearing member 9. As a result, the connectors of Figures 13 and 14 are able to provide relative displacement, damping, and position restorative functions under tension and compression respectively, but are substantially locked and prevented from relative displacement of the rod 8 and casing 2 under the opposite forcing.

The same functionality of either unrestricted or prevented relative displacement in the non-acting direction of a tension-only or compression-only connector may be provided in configurations where the bearing member 9 is of a sleeve 40 rather than of the casing 2.

The spring and damping assembly 7 and each of the at least one spring and damping stages 13 may comprise discrete spring members 11 and damping members 12. Alternatively, each at least one spring and damping stage 13 may comprise at least one unitary spring and damping member 31. Each such unitary spring and damping member 31 may be capable of both frictional engagement with the casing 2 inside the casing, and of providing the bias of the spring and damping assembly 7 in order to enable the positional restorative functions of the connector. One such damping and spring member 31 may be a spring sized to frictionally engage with the inside of the casing 2. An example of such a type of spring may be a coned disc spring as seen in Figure 16

The connector of Figure 16 comprises a rod 8, casing 2 and spring and damping assembly as described in relation to Figures 3 and 4, except the spring and damping assembly 7 comprises a plurality of combined spring and damping members 31. The spring and damping members 31 are shown in the configuration of opposing pairs of coned-disc springs provided along the rod 8 between limit members 32 and

the stops 10 of the rod. The limit member 32 may optionally be provided to assist with engagement of the spring and damping assembly 7 against the stops 10.

As seen in Figure 16, the pairs of unitary spring and damping members 31 are sized so as to frictionally engage with the inside of the casing 2. By this configuration, both the damping and positional restorative functions of the connector 1 may be provided without requiring separate spring members 11 to the damping members 12. The connector of Figure 16 may exhibit the same staged spring and damping characteristic as previously described with relation to Figure 9. Each opposed pair of coned-disc springs 31 will act as an individual stage.

While it has previously been described that either separate spring members 11 and damping members 12 may be provided, or alternatively a combined damping and spring member 31 may be provided in its place, in some embodiments the spring members 11 of the former configuration may still be sized for at least some frictional engagement with the inside of the casing 2. If the entirety or a substantial portion of the spring and damping assembly is in frictional engagement with the casing, the damping effect may be increased.

Furthermore, where a combined spring and damping member 31 is provided by a Belleville washer or other spring component which expands laterally under compression, the frictional engagement with the casing may be furthermore increased. For example in the case of a Belleville washer, it may expand radially as it is compressed, increasing its frictional engagement with the casing.

While previously described spring and damping assemblies have comprised a plurality of substantially identical spring and damping stages 13, the spring and damping assembly of the connector may comprise of differently configured spring and damping stages 13. For example in the configuration of Figure 15, the connector 1 comprises a plurality of different spring and damping stages 13. As shown, the damping members 12A-12F may comprise varying thicknesses and/or surface configurations in order to provide different damping characteristics. Similarly, the spring members 11A-11E of each spring and damping stage may comprise of a varying number of spring members 11, spring members of varying spring constants and other characteristics, spring members of different spring types, or spring members of larger and smaller diameters.

The sizing and configuration of each of the spring members 11 and damping members 12, and the location of each of those spring and damping members within the spring and damping assembly 7, may be customised to provide for desired resistance, damping, and restorative force characteristics over different segments of

displacement of the connector. The damping members are preferably of a shape and configuration to prevent their yielding during displacement especially plastic yielding.

The spring members 11 or combined damping and spring members 31 may comprise many forms of spring, such as but not limited to Belleville springs, Belleville washers, coned disc springs, conical spring washers, disc springs, cupped spring washers, or other spring washers of a generally frustoconical form. The spring members 11 or damping and spring members 31 may comprise conventional coil springs, die springs, shape memory alloy springs, metal, rubber and composite base springs, or rubber bearings. Each of these may be used singularly, or in a stack. Where Belleville washers are used, they may be stacked in the same or preferably in alternating directions. They should be selected to yield elastically during operation. In the preferred form the spring or springs act in compression.

In some embodiments the damping members 12 may comprise disc-like members. However, the damping members 12 may be of many desired cross-sections so as to substantially correspond with the internal cross-sectional shape and/or area of the casing 2 and may be of different thicknesses and having different surface characteristics. The damping members 12 may be of metallic or composite based materials.

Lubrication can be used between friction surfaces of the connector in order to achieve the desired and predictable damping performance. In addition to providing a lubricant between the friction surfaces of the connector, the use of self-lubricating materials is also contemplated.

While in preferred embodiments the damping members 12 may be located at either end of a spring and damping assembly, in other embodiments a spring and damping member 12 may not be located on at least one or both ends of the spring and damping assembly. Where a damping member 12 is not located at an end, a spring member 11 may be located at that end of the assembly.

In such a configuration, the operational characteristics of the connector may be varied. In such a configuration relative movement of the connector due to a compression at that end of the connector will result without first overcoming any frictional engagement of a damping member 12. Thus, compression of the associated spring and damping assembly and relative movement of the connector will occur upon the external force reaching the pre-stressing value, if any, of the spring member 11.

The casing 2 of the connector preferably comprises at least one elongate split 3. As seen in the connector of Figure 1A, the elongate split 3 comprises a complete split along the entire length of the casing 2. In other configurations, the split of the casing may be a partial split plane. Whether partial or complete, the configuration of

the split should be such as to allow adjustment of the bias of the casing against the spring and damping assembly to control the frictional engagement of the damping assembly 7 with the inside of the casing 2.

As previously described in relation to the connector of Figure 1A the adjustable member 4 of the casing may be provided by a clamping of the casing along at least a portion of the at least one elongate split 3. The clamping configuration shown in Figure 1A in relation to the embodiment of Figure 1A utilises a bolt and nut configuration to clamp the casing at its elongate split 3. While such a bolt and nut configuration may be useful in some applications, particularly for ease of adjustment for pre and post-installation loading of the casing, many other known means of providing a bias at the elongate split may be utilised. For example, many other forms of clamp may be utilised, such as a hose clamp.

Where a bolt and nut configuration are utilized, it may comprise washers in combination with the bolts and nuts. In particular, the washers may be provided in the form of disc springs or Belleville washers. By this configuration the bolted connection may become spring-loaded.

This may be desirable particularly where the adjustable member 4 is provided by clamping at discrete locations along the length of the casing 2. In such a configuration the frictional engagement with the spring and damping assembly 7 may vary within the casing dependent on the distance to the next adjacent clamping point. This may for example be due to deformation of the casing 2.

In such a situation, the presence of disc springs at the bolted connections providing the clamping points may compensate for these variations in the frictional engagement. This compensation may be provided by the compression of the disc springs and consequent reduction in the frictional engagement of the casing 2 with the spring and damping assembly 7 when the spring and damping assembly or the individual damping member is proximate to the clamping point.

While in the preferred form the clamping is substantially continuous along the at least a portion of the elongate split so as to provide a substantially continuous frictional engagement of the casing 2 with a damping member 12, the adjustment of the bias 4 along the split 3 may be varied along the elongate direction of the casing 2 in order to provide variable damping characteristics.

For example, in the connector of Figures 3 and 4, relatively greater clamping force towards an end of the spring and damping assembly 7 may provide for increased damping at the start of the displacement of the connector, relative to later stages of displacement. Conversely, if provided at the other end of the spring and damping assembly or under the other of tension or compression of the connector, it may

provide for increased damping at the later stages of the displacement of the connector relative to the earlier stages of displacement.

Corresponding effects may also be provided by relative increases or decreases in clamping forces at other particular points along a spring and damping assembly 7.

5 While shown in the embodiment as shown in Figure 1A as comprising a substantially circular elongate body having a single elongate split 3, the casing 2 of the connector may comprise more than one elongate split plane. The casing may hence be made from more than one component to define the internal cross section.

10 Examples of such configurations are shown in Figures 5B & 5C. In these configurations the adjustable member 4 will preferably be provided at each of the elongate splits 3 in order to allow for adjustment of the cross-sectional shape or area of the casing 2.

15 While the casing 2 may comprise a body having a substantially circular internal cross-section, any other desired cross-section may be provided within the scope of the invention. For example, Figures 6A-6C show a casing 2 comprising a substantially square internal cross-section. Figures 7A-7C show a casing having a substantially triangular internal cross-section. Figures 8A-8E show a casing 2 comprising a substantially pentagonal internal cross-section.

20 As also seen in Figures 6A-8E the casing 2 may comprise one or more elongate splits 3, and where multiple elongate splits are provided they may be either symmetric or non-symmetrically arranged about the perimeter of the casing.

25 The internal surfaces of the casing do not need to be of the same shape along the spring and damping assembly. As long as for the range of travel of a damper member the cross sectional shape is constant and does not taper then a constant frictional force will exist between the casing and a damper member.

So for example the first and second damper members 12a and 12d and the interior surfaces of the casing those members slide along may be of a larger diameter than the intermediate damper members 12b and 12c and their respective internal surfaces they slide along.

30 However, in a preferred form the interior surface or surfaces define a constant cross section for sliding engagement along the entire of the spring and damping assembly.

35 The frictional engagement of the spring and damping assembly 7 with at least part of the inside of the casing 2 during relative displacement of the connected first and second structural members of the structure provides damping of the external force causing relative displacement. The damping provided by the connector 1 may act

to dissipate the energy of the external force, and reduce the external force loads applied to the structural members of the structure.

The connector of the present invention may be configured to provide for high initial stiffness due to the frictional engagement of the spring and damping assembly with the casing. This means that high thresholds of external force can be required in order to result in slipping and displacement of the connector. This high initial stiffness can limit the drift of the structure under serviceability loads, and mean the connector only allows relative displacement under large external forces, such as those experienced during a seismic event.

Because the connector 1 operates with limited and preferably no plastic deformation of its frictional components or its other components, the connector may require limited or preferably no servicing between external forcing events. The reduction or elimination of the need for servicing of the connector following an external forcing event may significantly reduce the ongoing operational costs associated with the structure.

The positional restoring capacity or function of the connector may also provide for reduced servicing requirements of the structure, and improved performance of the structure, as the structural members are able to be returned to or towards its initial position after an external forcing event, with limited and preferably no residual displacement remaining between the structural members.

The connector of the present invention provides a customisable structural connector. For a given connector with a particular spring and damping assembly having set spring characteristics, the overall damping capacity, including the initial slipping threshold and ultimate resistance force of the connector, may simply be varied by the adjustment of the adjustable member 4 of the casing 2. Similarly, the threshold of external force below which the connector 1 will begin to restore residual displacement of the connector and the residual spring force in the connector at zero displacement may be adjusted by varying the precompression of the spring and damping assembly between the stops 10 of the rod 8 and/or bearing members 9. In this manner, a connector may be customised to provide particular damping and restoration characteristics.

While the bearing members 9 have previously been described as elements fixed in relation to the casing 2, in order to provide for further customisation of the characteristics of a connector 1 the bearing members 9 may be adjustable along the elongate direction of the casing 2. For example, the bearing members 9 may be able to be adjustably fixed at particular increments along the elongate direction of the casing. Alternatively, the bearing members 9 or at least one of the bearing members 9

may be threadingly engaged with the inside of the casing 2. The adjustment of the position of the bearing members 9 along the elongate direction of the casing allows for an adjustment of the maximum stroke length and thus maximum relative displacement of the connected structural members.

5 In addition to the previously described adjustments of a given connector in order to provide different initial and ultimate stiffness, damping, and restoration characteristics, the connector of the present invention may be scaled to different sizes in order to resist different loads.

10 Having described the functionality and operation of a connector 1 according to primary embodiments of the invention, further alternate configurations and combinations of connectors according to the invention will now be described.

Figure 19 shows a further embodiment of the connector of the present invention wherein under the action of the connector under either tension or compression the spring and damping assembly 7 is simultaneously compressed from
15 both ends.

In Figure 19 the connector 39 comprises a rod 8 for connection to a first structural member, and a sleeve 40 for connection to the second structural member. Provided about the rod and between stops 10 of the rod as previously described is a multistage spring and damping assembly 7. The spring and damping assembly 7 is
20 provided within a casing 2 that may comprise of an elongate split 3 and an adjustable member for the internal cross section, also as previously described.

In the connector 39 the sleeve 40 is provided about the casing 2, and the sleeve 40 is for connection to the second structural member of the structure. In the configuration of Figure 19, the casing 2 does not need to comprise any bearing
25 members 9. In place of the previously described bearing members 9, the sleeve 40 comprises at least one bearing elements 37 or 38 to act on a first damping member 12A. In a double-acting configuration at least one bearing element 37 at one end of the spring and damping assembly 7, and at least one bearing element 38 to act on a damping member 12D at the opposite end of the spring and damping assembly.

30 In the configuration of Figure 19, the connector 39 effectively isolates the casing 2 and spring and damping assembly 7 from relative displacement of the rod 8 and sleeve 40.

Exposure of the connector 39 to tension results in displacement of the rod 8 in the direction of the arrows 16, and the sleeve 40 in the direction of the arrow 15. At
35 the first end of the casing the bearing elements 37 act on the damping member 12A and once the frictional threshold with the casing 2 is met, and result in the compression of the first spring and damping stage 13A. Simultaneously at the

opposite end of the spring and damping assembly the stop 10B of the rod 8 acts on the damping member 12D and once its frictional engagement threshold with the casing 2 is met results in the compression of the spring and damping stage 13C. Further displacement of the rod and sleeve 40 in tension will result in slipping of the damping members 12B and 12C, and in compression of the spring and damping stage 13B.

Under the exposure of the connector 39 to compression the rod 8 is moved in the direction of the arrow 15, and the sleeve 40 is moved in the direction of the arrows 16. At the first end of the spring and damping assembly the stop 10A of the rod bears against the damping member 12A, and results in compression of the spring and damping stage 13A. At the opposite end of the spring and damping assembly the bearing element 38 of the sleeve 40 act on damping member 12D and cause the compression of the spring and damping stage 13C.

The connector assembly 39 of Figures 19 provide a double acting configuration, wherein under both exposure of the connector to tension and exposure of the connector to compression the spring and damping assembly 7 are able to be acted on simultaneously at each end. The result is that the spring and damping stages of each spring and damping assembly may simultaneously compressed from the outside to the inside of the spring and damping assembly.

A further combination configuration of a connector according to the present invention is shown in Figures 17A. This combination configuration utilises the sleeve 40 and bearing elements 37 and 38 as previously described in relation to Figure 19.

Figure 17A shows a cross-section along the longitudinal or elongate direction of the connector assembly 35, and Figure 17B shows a cross-section through the line AA of Figure 17A. Seen in the view of Figure 17B, the connector assembly 35 comprises a casing 2 having an elongate split 3. Provided within the casing 2 are four rods 8, each having arrays of spring members 11 provided about them. Provided about the four rods 8, and sized so as to substantially correspond with the internal cross-sectional shape or area of the casing 2, are damping members 12.

While not shown in Figure 17B, an adjustable member 4 is to be provided along the elongate split 3 of the casing 2 so as to apply a force to the casing for setting and varying the sliding frictional engagement with the damping members 12.

As in the configuration of Figure 19, a sleeve 40 is provided about the casing 2, for connection to the second structural member. The four rods 8 are connected together, such as by a connector plate 36, which is then able to be connected to the first structural member of the structure.

Under exposure of the connector assembly 35 to a tensile external force the connector assembly 35 operates substantially as previously described in relation to the embodiment of Figure 19. The connector plate 36 and rods 8 are forced in the direction of the arrows 16, and the sleeve 40 is forced in the direction of the arrows
5 15. The stops 10B of the rods 8 each act against the adjacent damping member 12 of each rod. Simultaneously, the bearing elements 37 of the sleeve 40 act against the opposite end of the casing 2.

Once the required threshold of force has been met, this can result in slipping of the damping members 12 adjacent the stops 10B relative to the casing 2 and
10 compression of the stage 13c of the spring and damping assembly 7. Subsequent stages are compressed upon further increases in the external force and further displacement of the connector.

The operation of the connector assembly 35 in compression comprises a forcing of the connector plate 36 and rods 8 in the direction of the arrows 15, and a
15 forcing of the sleeve 40 in the direction of the arrows 16. Under this action, the secondary stop 34 of each rod bears against the adjacent bearing member 9 of the casing, and consequently against the adjacent damping member 12.

At the opposite end of the spring and damping assemblies 7 the bearing element 38 of the sleeve 40 acts on the adjacent damping member 12 to cause its
20 sliding relative the casing 2, and the compression of its associated spring and damping stage.

The action of the secondary stops 34 against the casing 2 will result in relative displacement of the casing 2 with respect to the sleeve 40 under action of the connector assembly 35 in compression.

Figure 18 shows a further variation of the connector. The connector 41
25 comprises a first section 42 which is able to slide relative to the second section 43. Within each section is a spring and damping assembly 7, with rods 8 running through them. The first section and second section are each connected to a structural member. Under relative displacement of the first section in the direction of the arrow 15 and the
30 second section in the direction of the arrow 16, only the spring and damping assembly of the second section 43 is elastically deformed. Similarly, under the reverse displacement of each section, only the spring and damping assembly 7 of the first section 42 is elastically deformed. Such a configuration may be desirable to provide
35 customization of the way the connector acts in each direction. For example, the spring force or maximum travel of the spring and damping assembly or the frictional engagement of the casing may be individually set on each section 42, 43.

Figure 20 shows a further variation of the connector of the present invention. The connector 45 comprises a casing 2, rod 8 and spring and damping assembly 7 substantially as previously described in relation to the connector 1 of Figures 3 and 4.

The casing 2 however comprises a ramped or sloped external surface, to
5 correspond with a ramped or sloped surface of an external casing 44 provided about at least part of the casing 2. The interaction of the external casing 44 with the casing 2 is such as to provide a relative position dependent bias of the casing 2. This relative position dependent bias may be provided in place of, or in addition to the previously described adjustable member 4.

10 The rod 8 is fixed to the external casing 44, and the two are in turn connected to the second structural member. The casing 2 is connected to the second structural member.

Under relative displacement of the casing 2 and the external casing 44, the casing 2 may preferably be caused to ramp along the mutually ramped surfaces so as
15 to vary the bias of the casing 2 and vary the frictional engagement of the casing 2 with the spring and damping assembly 7.

For example, as seen in Figure 20, casing 2 and external casing 44 comprise a single mutual ramped surface above and below. The direction of the mutually ramped surfaces is such that the casing 2 may be forced into increased frictional engagement
20 with the spring and damping assembly 7 under a displacement of the casing 2 in the direction of arrow 15 and the external casing 44 in the direction of arrow 16.

The reverse configuration is shown in Figure 21, wherein the ramped surfaces are configured such that a displacement of the casing 2 in the direction of arrow 16 and the external casing 44 in the direction of arrow 15 is such as to increase the
25 frictional engagement with the spring and damping assembly 7. The angle of the ramped surfaces is exaggerated for illustrative purposes.

Figure 22 shows in effect a combination the connectors of Figures 20 and 21. In Figure 22 the connector 46 has a casing 47 and external casing 48 which each
30 comprise a pair of mutually ramped surfaces. The effect of the configuration of Figure 22 is that the casing 47 may be compressed and urged into increased frictional engagement with the spring and damping assembly 7 under relative displacement of the casing 47 and external casing 48 in either direction.

The configurations of Figures 20-22 will provide, under their ramping conditions, for increased damping properties of the connector as the relative
35 displacement of the first and second structural members from an initial position increase. This will provide increased resistance to relative displacement, and may act as an effective limit of the relative displacement.

The connector 49 combination of Figure 23 is similar to that described in relation to Figure 18. In Figure 23, the connector 49 comprises three portions 50, 51, and 52, each having its own spring and damping assembly 7. The casings of the outer portions are each able to slide within the inner portion. In this configuration the outer casings 50 and 52 are each for connection to a respective first or second structural member.

Under an exposure of the connector 49 to tension, the bearing members 9 of the outer casings act in combination with the stops 10 to compress the spring and damping assemblies of the outer portions 50, 52.

Under an exposure of the connector 49 to compression, the stops 10 of the rod 8 at each end of the connector 49 act against their spring and damping assemblies, and cause the compression of the first stages of the spring and damping assemblies. Once the outer portions 50, 52 are fully compressed, the bearing members 9 of each outer portion acts against an end of the middle portion 51, and its spring and damping assembly is compressed from each end.

By this configuration a connector 49 can be provided having different total maximum displacements of the first and second structural members in the operation of the connector in tension rather than in compression.

In some embodiments a secondary fuse may be associated with the elongate casing 2, and in sliding frictional engagement with the elongate casing. For example, the secondary fuse may be provided about the elongate casing 2. Alternatively, the secondary fuse may be provided within the elongate casing 2, intermediate of the casing and the spring and damping assembly. In such a configuration the elongate casing indirectly acts on the spring and damping assembly, through the secondary fuse.

The sliding frictional engagement between secondary fuse and the elongate casing is to always be greater than the resistive value of the spring and damping assembly 7 during its compression.

The purpose of the secondary fuse is to provide for further damped relative movement of the connector past the full compression of the spring and damping assembly 7. In a preferred form the fuse will act only under loading conditions greater than the design expectations of the connector.

Two potential embodiments of a connector comprising a secondary fuse 55 are shown in Figure 25A and Figure 25B. The other parts of the connector are substantially as have been previously described. Upon the full compression of the spring and damping assembly 7, the casing 2 and secondary fuse 55 are able to slide

relative to each other. Such a relative sliding provides further damping, but upon the reduction or ceasing of the external force, will mean that the components of the connector and the associated structural components will not be fully returned to their initial relative positions.

5 Figure 25C shows an end-on view of a casing 2 and secondary fuse 55 of Figure 25A or Figure 25B. As seen in Figure 25C, the secondary fuse 55 is provided within the casing 2 and intermediate of the casing and its spring and damping assembly (not shown). In such a configuration the clamping of the casing will provide or control the frictional engagement with the spring and damping assembly, but the
10 casing 2 is not in direct frictional engagement with the casing. Rather, the secondary fuse 55 is in direct frictional engagement with the casing.

The configuration of the secondary fuse described above is analogous to the sleeve 40 described in relation to previous embodiments, if the sleeve 40 was able to slide relative to the casing 2 and frictionally engaged with the casing 2 to a greater
15 degree than the maximum resistance of the spring and damping assembly 7 during its compression.

Figures 24A-D show various potential applications of the connector or of combinations of connectors according to the invention in a structure 53.

20 In Figure 24A the structure 53 is a bracing frame, and connectors 54 according to the invention are located between parts of the bracing frame.

In Figure 24B the structure 53 is a moment resisting frame, and connectors 54 are provided within it allow resisted moment action, and to return the moment resisting frame to its initial position following the external event.

25 The structure of Figure 24C is a shear wall, and connectors 54 are provided to allow resisted shear movement between the parts of the structure, but to dampen such movements and return the shear wall to its initial position following the external forcing event. Figure 24C may also illustrate the use of connectors to hold down storage tanks. As seen the rod is connected to the foundation 401 and the casing to
30 the tank 400.

Finally, Figure 24D shows the use of connectors 54 of the present invention in structure 53 as buckling-resistant bracing members.

The slip friction damped connector is not a viscous or hydraulic damper. Working fluids are not used to provide damping. This means the damping and
35 resistance forces are independent of velocity of displacement and of temperature.

Where in the foregoing description reference has been made to elements or integers having known equivalents, then such equivalents are included as if they were individually set forth.

5 Although the invention has been described by way of example and with reference to particular embodiments, it is to be understood that modifications and/or improvements may be made without departing from the scope or spirit of the invention.

CLAIMS

1. A double acting slip friction earthquake energy damping connector for use between a first structural member and a second structural member of a ground supported structure that may be subjected to earthquake induced motion that can cause the first and second structural member to relatively translate towards and away from each other from an initial static position facilitated by the connector that comprises:
- 5 i. an elongate casing having a notional straight axis with an interior surface or surfaces, the casing connected to the second structural member to translate with the second structural member,
 - 10 ii. a spring and damper assembly to travel along the axis inside the casing and comprising of
 - 15 a. at least two spaced apart damper members each damper member having a friction surface or surfaces contacting the interior surface of surfaces of the casing to be able to slide with frictional resistance along the axis along at least part of the interior surface of surfaces,
 - 20 b. a pre-loaded spring arrangement intermediate of and forcing, when the first and second structural members are in their initial static position, the two adjacent damper members apart in the axial direction each against a respective bearing member of the casing located at or towards each end of the casing, allowing the two damper members to move towards each other against the load of the spring by a connection rod that is connected to the first structural member and to translate with the first structural member, the connection rod having a stop located adjacent each end of the spring and damper assembly,
 - 25 i. a first of said stops to act, when the connector acts in compression when the first and second structural members translate towards each other, on a first of said two damper members to displace the first of said two damper members away from its respective bearing member and towards the second of said two damper members and its respective bearing member, and
 - 30 ii. a second of said stops to act, when the connector acts in tension when the first and second structural members translate away from each other, on the second of said two

damper members to displace the second of said two damper members away from its respective bearing member and towards the first of said two damper members and its respective bearing member.

- 5 2. A connector as claimed in claim 1 wherein at least one intermediate damper member is located between the first and second dampers, the spring arrangement comprising of at least two spring sets, each set located between each adjacent damper members.
3. A connector as claimed in claim 2 wherein each spring set is of the same
10 spring constant.
4. A connector as claimed in anyone of claims 1 to 3 wherein the frictional resistance to sliding of each damping member relative the casing is the same.
5. A connector as claimed in anyone of claims 1 to 3 wherein the frictional resistance to sliding of the two damping members relative the casing is the different.
- 15 6. A resilient slip friction connector for connecting to and allowing displacement between a first structural member and second structural member of a building structure and providing resistance to and damping of external forces that induce relative linear displacement between said first and second members and to provide a bias on the first and second structural members following external force caused
20 relative linear displacement of the first and second structural members from an initial relative position to a displaced relative position, the bias being such as to return the first and second structural members towards their initial relative position from their displaced relative position, the connector comprising:
- an elongate hollow casing,
- 25 an elongate spring and damping assembly having two opposed ends and to slide inside the casing in frictional engagement with the casing and for connection to the first structural member to thereby be caused to slide inside the casing, and
- at least one bearing element for bearing against an end of the spring and damping assembly,
- 30 wherein one of the at least one bearing element and the elongate hollow casing are for connection to said second structural member to move therewith, and
- wherein the spring and damping assembly is able to be elastically deformed by its compression between one of its ends and an at least one bearing element due to a relative linear displacement of the first and second structural members to their
35 displaced relative position, and upon a sufficient reduction of an external force that caused the compression of the spring and damping assembly, the bias of the compressed spring and damping assembly exceeds the frictional force between the

spring and damping assembly and the casing, and the first and second structural members are then caused to return under the bias of the compressed spring and damping assembly towards their initial relative position.

7. A connector as claimed in claim 6, wherein a rod is provided within the casing
5 for association with the elongate spring and damping assembly, and the rod is for connection to the first structural member to move therewith.
8. A connector as claimed in claims 6 or 7, wherein upon a ceasing of the external forcing the first and second structural members are caused to return under the bias of the spring and damping assembly to their initial position.
- 10 9. A connector as claimed in any one of claims 8 to 8, wherein the reduction of the external forcing comprises a reduction below a first threshold.
10. A connector as claimed in claim 9, wherein upon the reduction of the external forcing below a second threshold, being a threshold lower than the first threshold, the first and second structural members are caused to return to their initial position.
- 15 11. A connector as claimed in claim 7, wherein the at least one bearing element is fixed relative the casing, and the casing is for connection to the second structural member.
12. A connector as claimed in claim 11, wherein the at least one bearing element integral with the casing.
- 20 13. A connector as claimed in claims 11 or 12, wherein the casing comprises at least one bearing element only at or adjacent one end of the spring and damping assembly so as to provide for the elastic deformation of the spring and damping assembly only under relative displacement of the first and second structural members away from each other, being a utilisation of the connector in tension, or only under
25 relative displacement of the first and second structural member towards each other, being a utilisation of the connector in compression.
14. A connector as claimed in claim 13, wherein under relative displacement of the first and second structural members wherein the connector does not provide for elastic deformation of the spring and damping assembly along the rod, the rod and casing are able to move freely relative each other.
- 30 15. A connector as claimed in claim 13, wherein under relative displacement of the first and second structural members where the connector does not provide for elastic deformation of the spring and damping assembly along the rod, the rod and casing are substantially prevented from relative displacement.
- 35 16. A connector as claimed in claim 13 or 14, wherein the casing comprises a bearing element and a stop of the rod at each end of the spring and damping assembly to provide for the elastic deformation of the spring and damping assembly

under either of relative displacement of the first and second structural members away from each other, being a utilisation of the connector in tension, or under relative displacement of the first and second structural member towards each other, being a utilisation of the connector in compression.

5 17. A connector as claimed in claim 7, wherein the at least one bearing element is for connection to the first structural member and is associated with a sleeve provided about the casing, the sleeve being moveable relative the casing.

10 18. A connector as claimed in claim 17, wherein under a relative displacement of the first and second structural members the at least one bearing element of the sleeve and the stop of the rod act on opposing sides of the spring and damping assembly to elastically deform the spring and damping assembly.

19. A connector as claimed in 18, wherein the elastic deformation of the spring and damping assembly from both sides occurs substantially simultaneously.

15 20. A connector as claimed in any one of claims 17 to 19, wherein the sleeve comprises at least one bearing element only at one end of the spring and damping assembly and one stop of the rod at the opposite end of the spring and damping assembly so as to provide for the elastic deformation of the spring and damping assembly

20 a) only under relative displacement of the first and second structural members away from each other, being a utilisation of the connector in tension, or

b) only under relative displacement of the first and second structural members towards each other, being a utilisation of the connector in compression.

25 21. A connector as claimed in claim 20, wherein under relative displacement of the first and second structural members wherein the connector does not provide for elastic deformation of the spring and damping assembly along the rod, the rod and sleeve are able to move freely relative each other.

30 22. A connector as claimed in claim 20, wherein under relative displacement of the first and second structural members where the connector does not provide for elastic deformation of the spring and damping assembly along the rod, the rod and casing are substantially prevented from relative displacement.

35 23. A connector as claimed in any one of claims 17 to 19, wherein the sleeve comprises at least one bearing element and a stop of the rod at each end of the spring and damping assembly to provide for the elastic deformation of the spring and damping assembly under either of relative displacement of the first and second structural members away from each other, being a utilisation of the connector in

tension, or under relative displacement of the first and second structural members towards each other, being a utilisation of the connector in compression.

24. A connector as claimed in anyone of claims 6 to 23 wherein the elongate hollow casing comprising at least one elongate split allowing the casing to expand and contract its internal cross-sectional shape or area, and wherein an adjustable member is provided for applying a force to the casing for setting and varying the sliding frictional engagement between the spring and damping assembly and the casing by virtue of the casing comprising said split.

25. A connector as claimed in claim 24, wherein the adjustable member acts at least in part as a bias towards a predetermined degree of frictional engagement between the casing and the elongate spring and damping assembly.

26. A resilient slip friction connector for connecting to and allowing displacement between a first structural member and second structural member of a building structure and providing resistance to and damping of external forces that induce relative displacement between said first and second structural members and to provide a bias on the first and second structural members following external force caused relative displacement of the first and second structural members from an initial relative position to a displaced relative position, the bias being such as to return the first and second structural members toward the initial relative position from their displaced relative position, the connector comprising:

an elongate hollow casing, the casing comprising at least one elongate split allowing the casing to expand and contract its internal cross-sectional shape or area,

an elongate spring and damping assembly having two opposed ends and to slide inside the casing in frictional engagement with the casing and for connection to the first structural member to thereby be caused to slide inside the casing, and

at least one bearing element for bearing against an end of the spring and damping assembly,

an adjustable member for applying a force to the casing for setting and varying the sliding frictional engagement between the spring and damping assembly and the casing by virtue of the casing comprising said split,

wherein one of the at least one bearing element and the elongate hollow casing are for connection to the second structural member to move therewith, and

wherein the spring and damping assembly is able to be elastically deformed by its compression between one of its ends and an at least one bearing element due to a relative displacement of the first and second structural members to their displaced relative position, and upon a sufficient reduction of an external force that caused the compression of the spring and damping assembly, the bias of the

compressed spring and damping assembly exceeds the frictional force between the spring and damping assembly and the casing, and the first and second structural members are then caused to return under the bias of the compressed spring and damping assembly to their initial relative position.

5 27. A connector for connecting two structural components together in an initial relative position, the connector comprising

a casing, engaged and to move with a first of said structural components, comprising an elongate constant cross section interior within which is operative in a frictional sliding engagement a spring and damper assembly comprising of at least one
10 damper member engaged and to move with a second of said structural components and contacting the interior of the casing and able to slide in frictional contact with the casing in the elongate direction and a spring able to be elastically deformed by and between the damper member and the casing when the damper member and casing are in relative motion and to bias the relative position of the two structural
15 components, during motion of the damper member and casing, towards their initial relative position.

28. A connector as claimed in claim 27 wherein the force of the spring acting on the casing and the damper member always exceeds the frictional force between the damper member and the casing to ensure that the damper member is pushed back to
20 a position corresponding to the initial relative position.

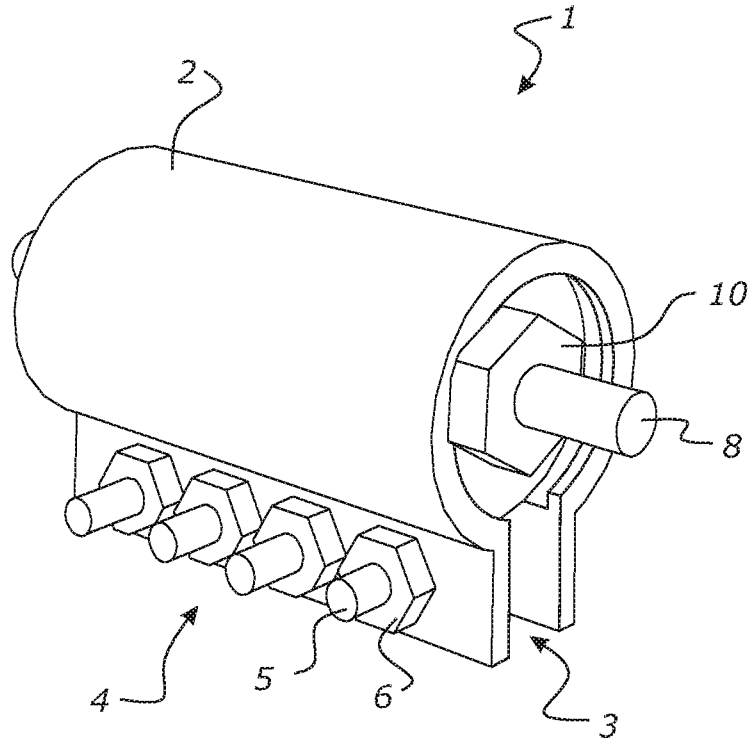


FIG. 1A

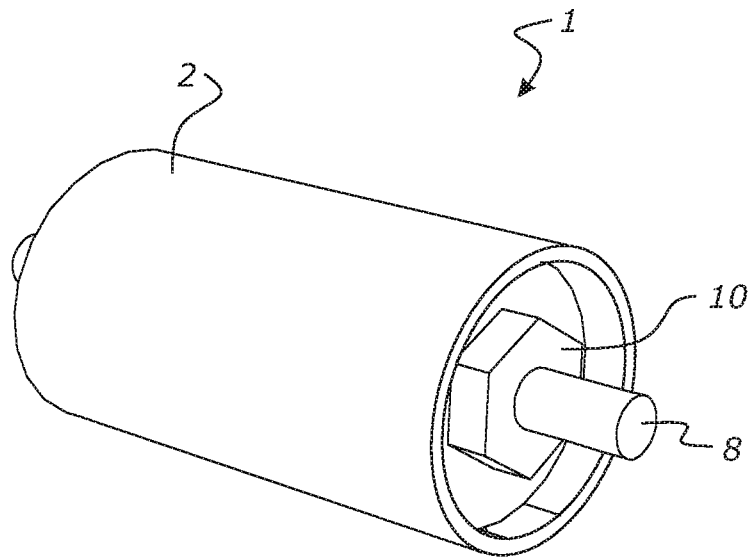


FIG. 1B

2 / 17

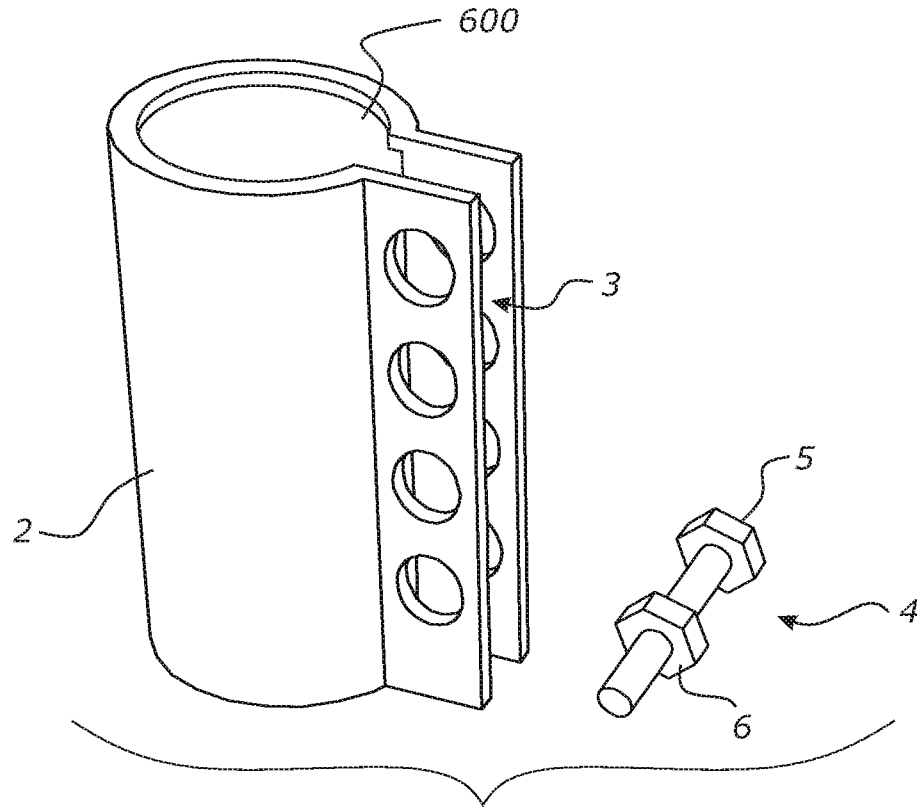


FIG. 2A

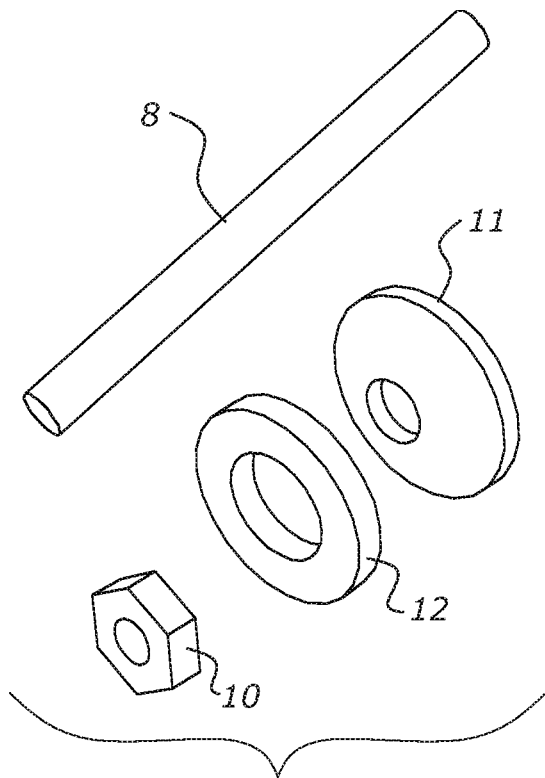


FIG. 2B

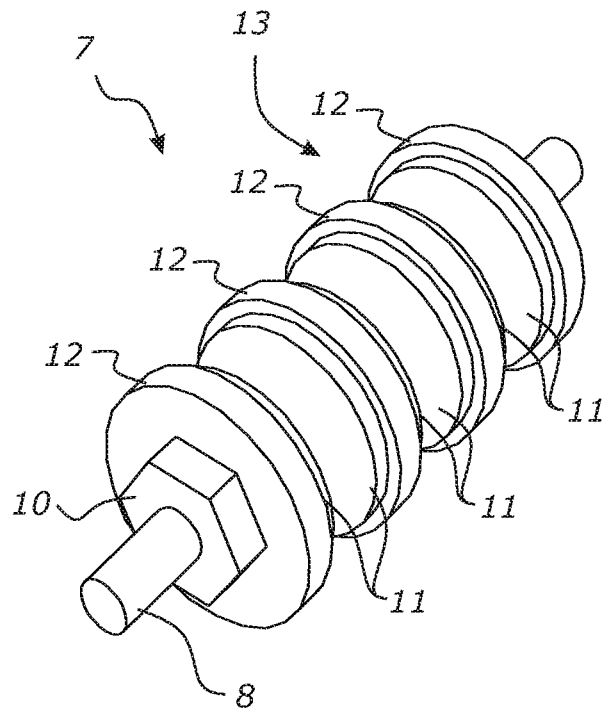


FIG. 2C

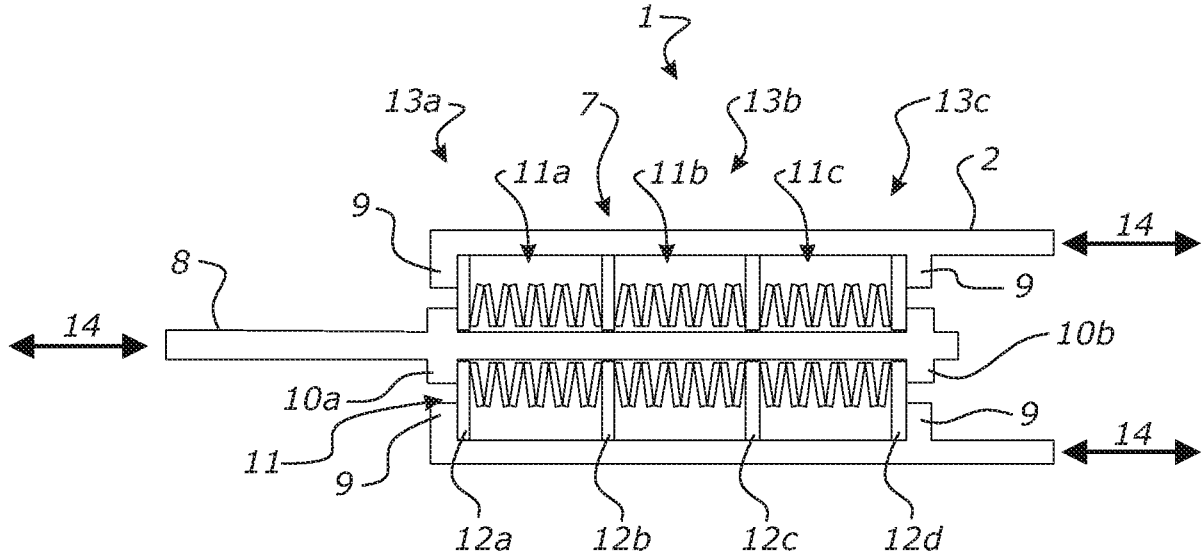


FIG. 3A

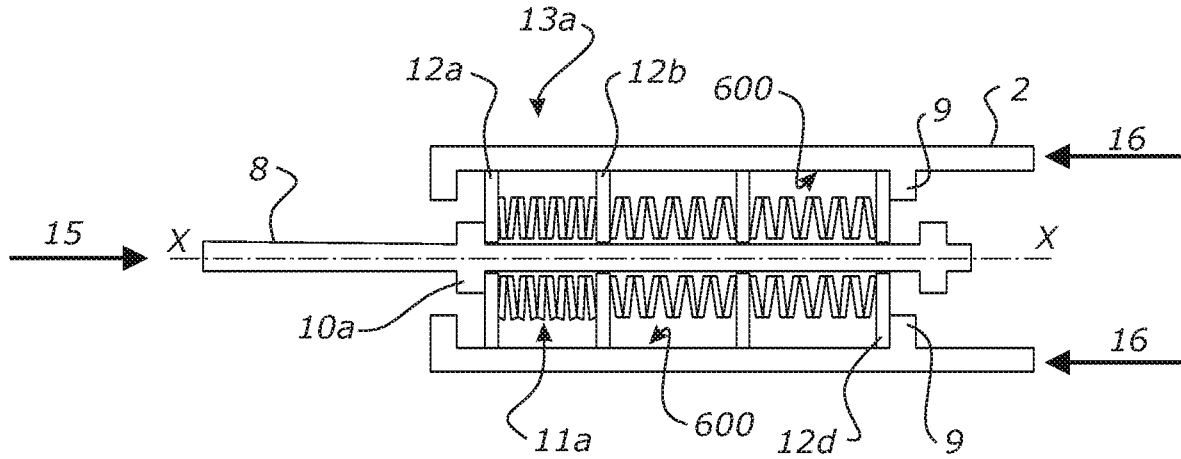


FIG. 3B

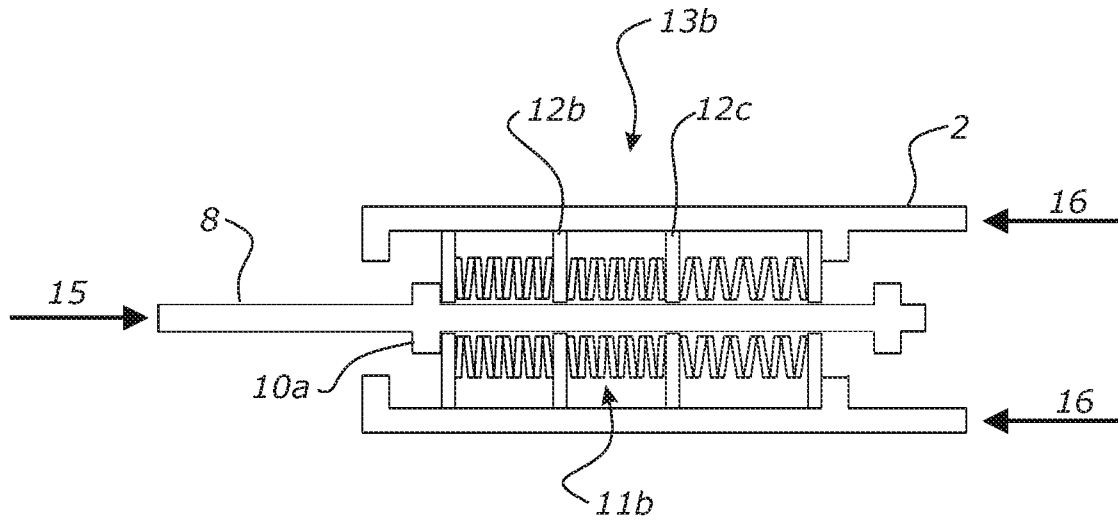


FIG. 3C

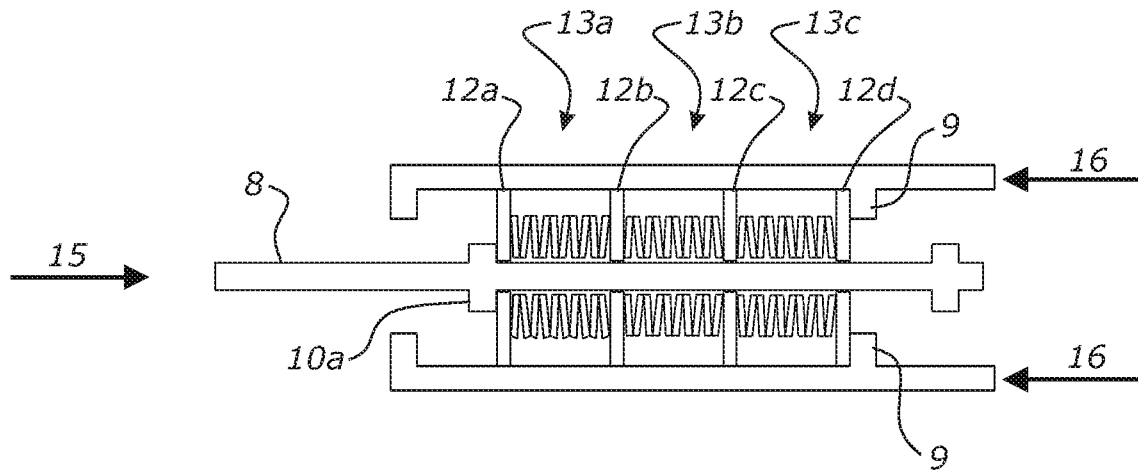


FIG. 3D

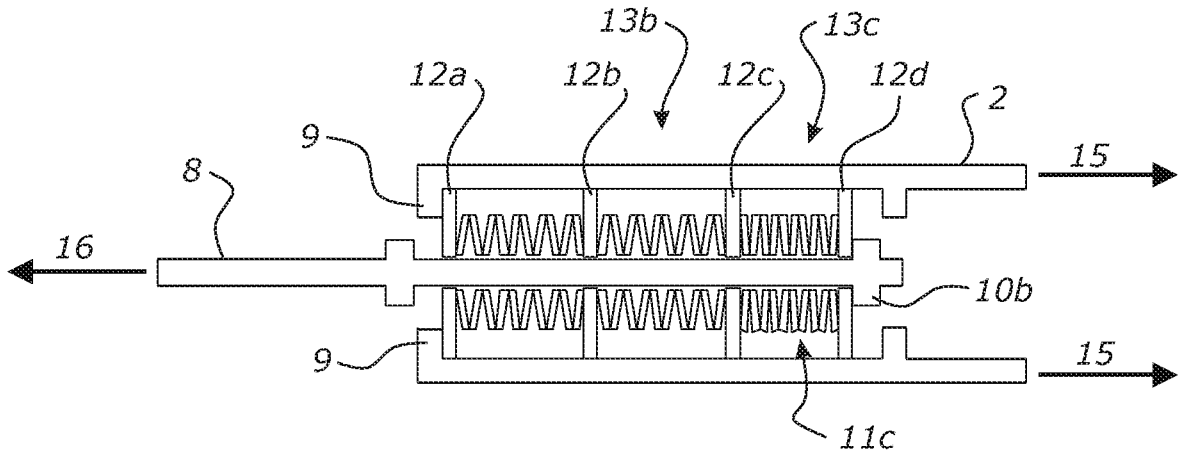


FIG. 4A

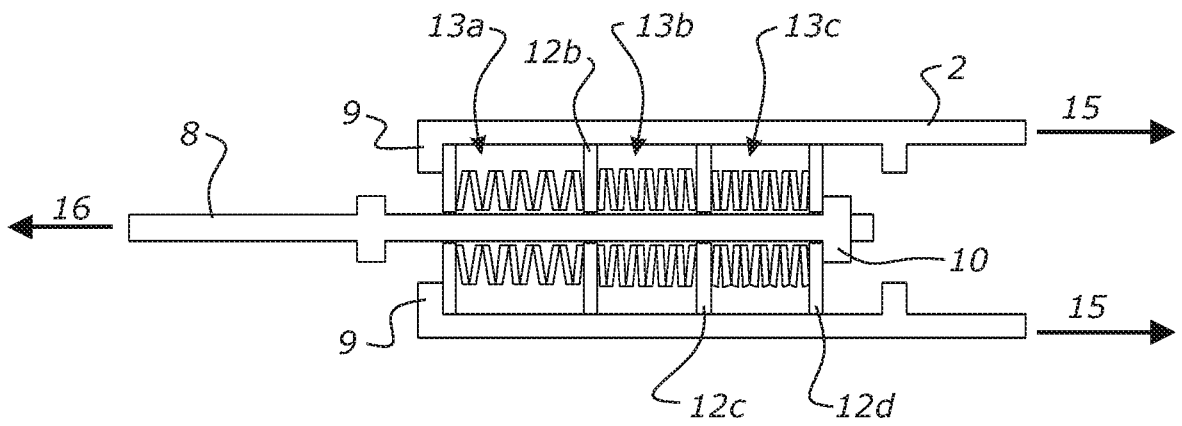


FIG. 4B

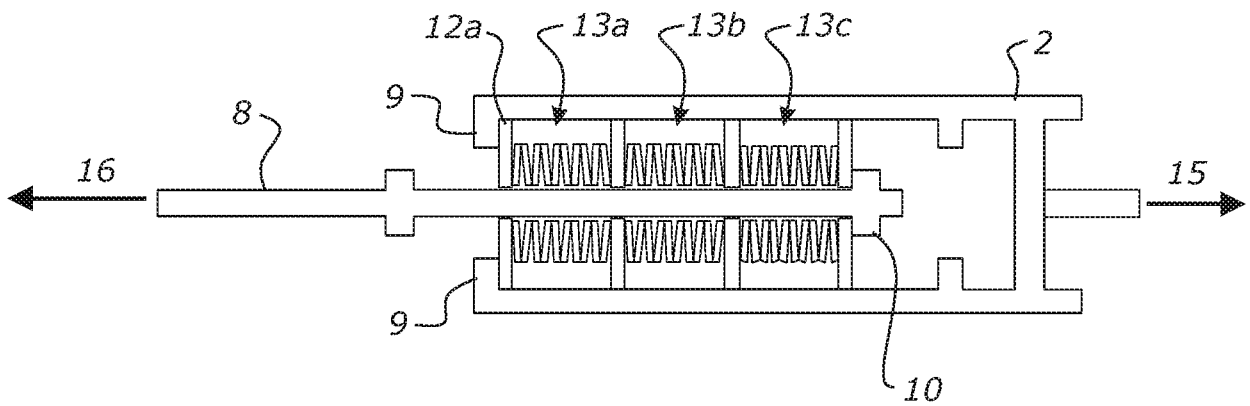


FIG. 4C

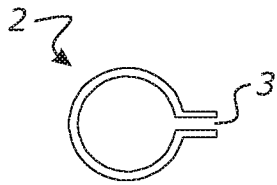


FIG. 5A

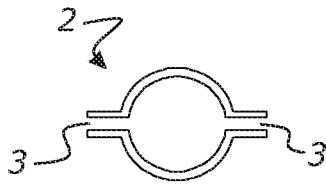


FIG. 5B

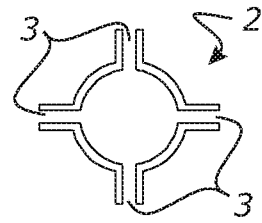


FIG. 5C

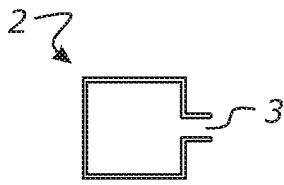


FIG. 6A

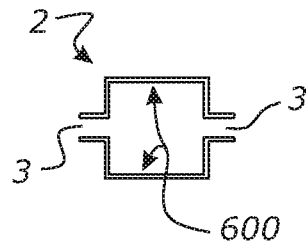


FIG. 6B

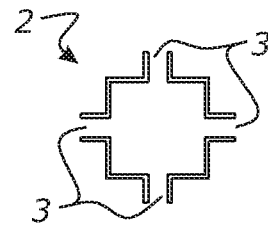


FIG. 6C

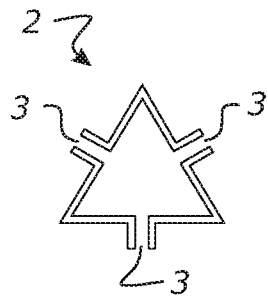


FIG. 7A

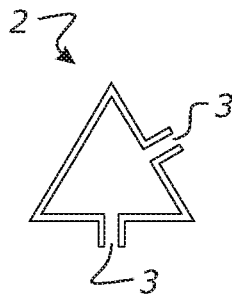


FIG. 7B

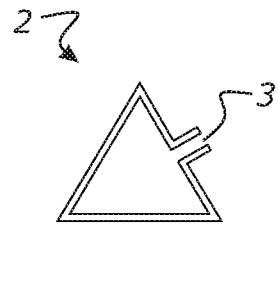


FIG. 7C

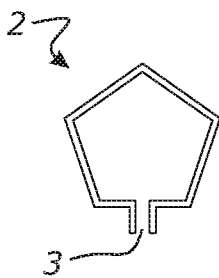


FIG. 8A

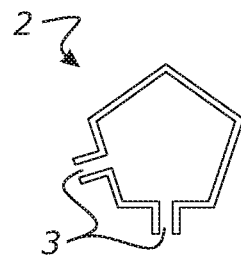


FIG. 8B

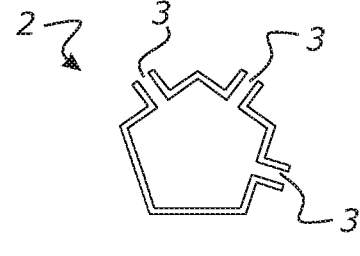


FIG. 8C

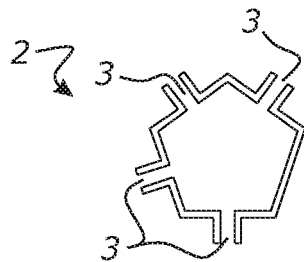


FIG. 8D

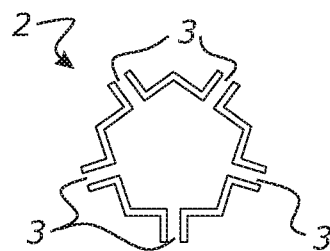


FIG. 8E

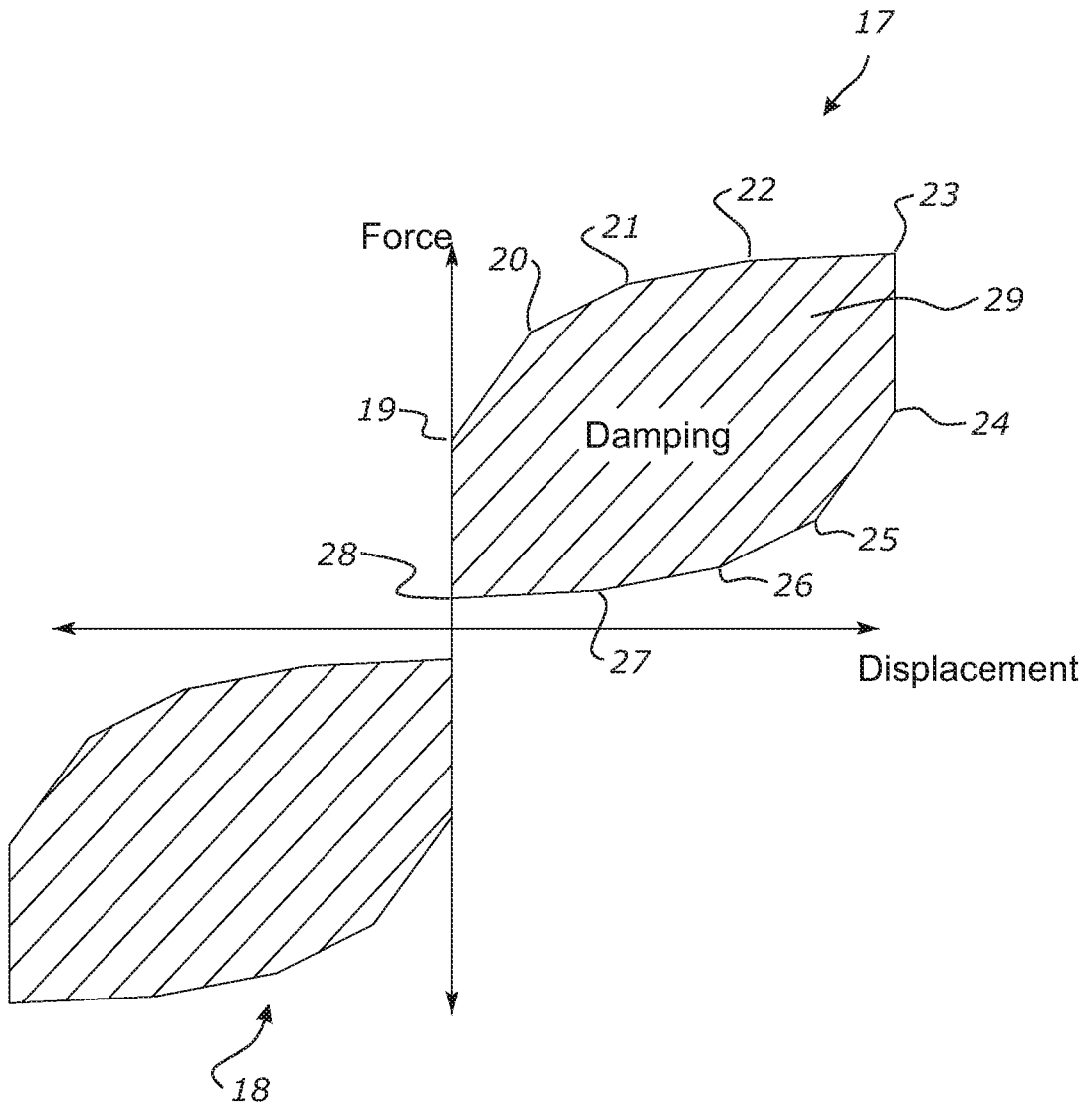


FIG. 9

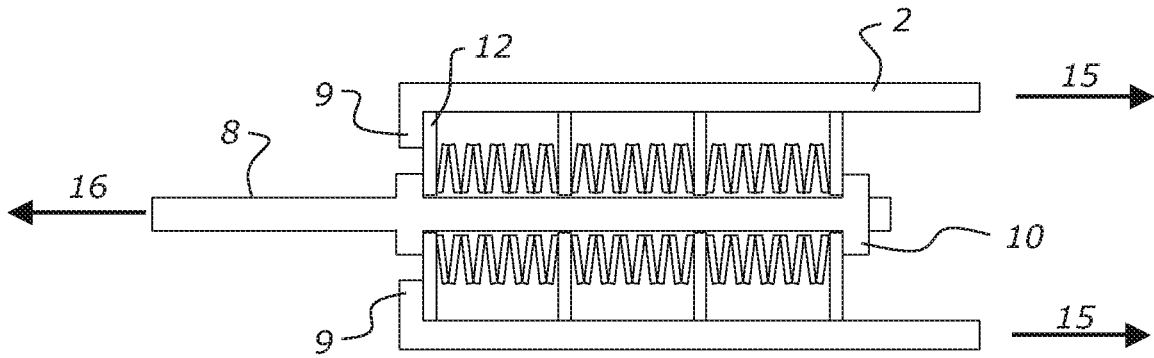


FIG. 10

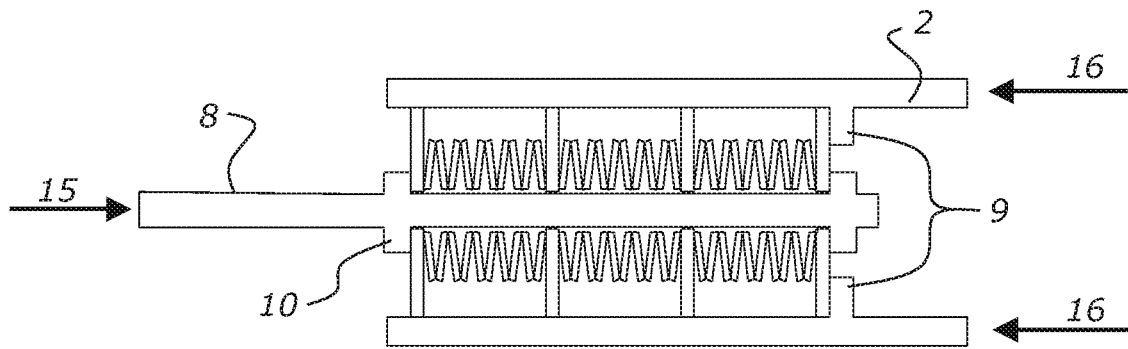


FIG. 11

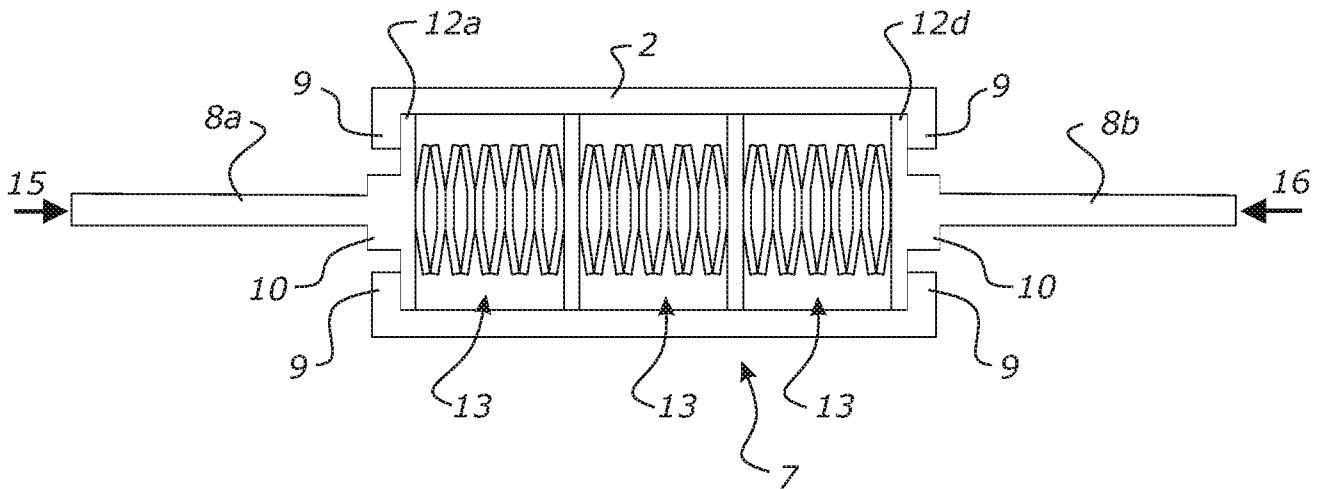


FIG. 12A

9 / 17

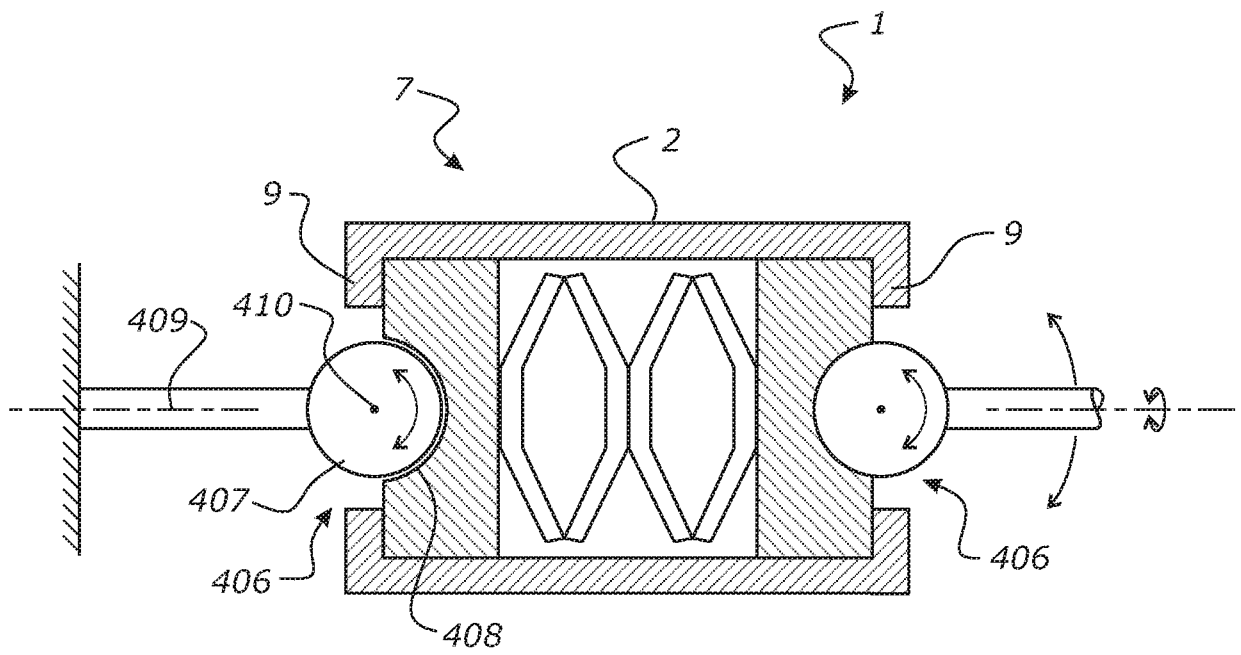


FIG. 12B

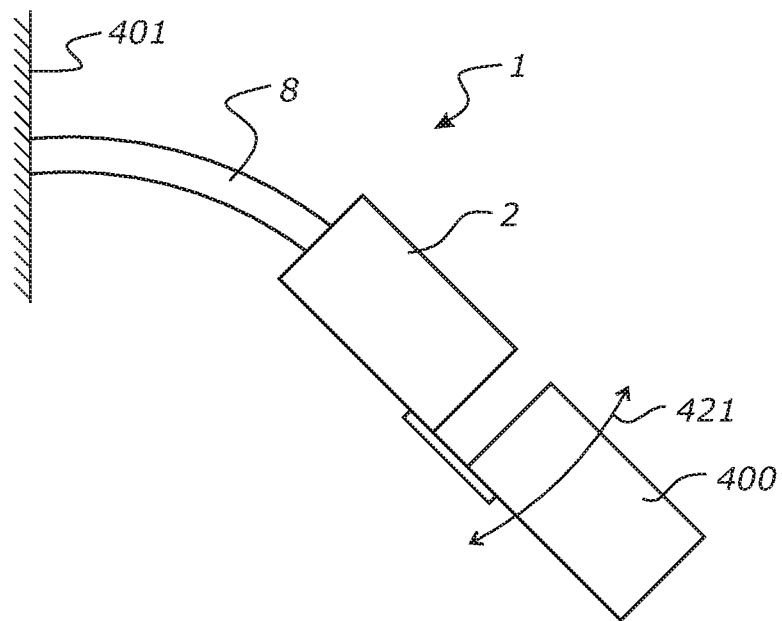


FIG. 12C

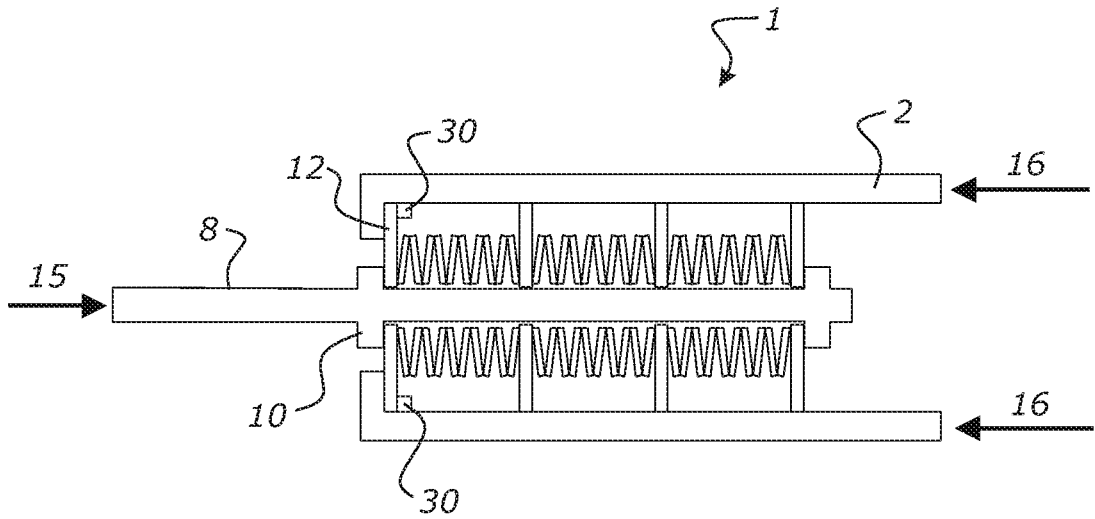


FIG. 13

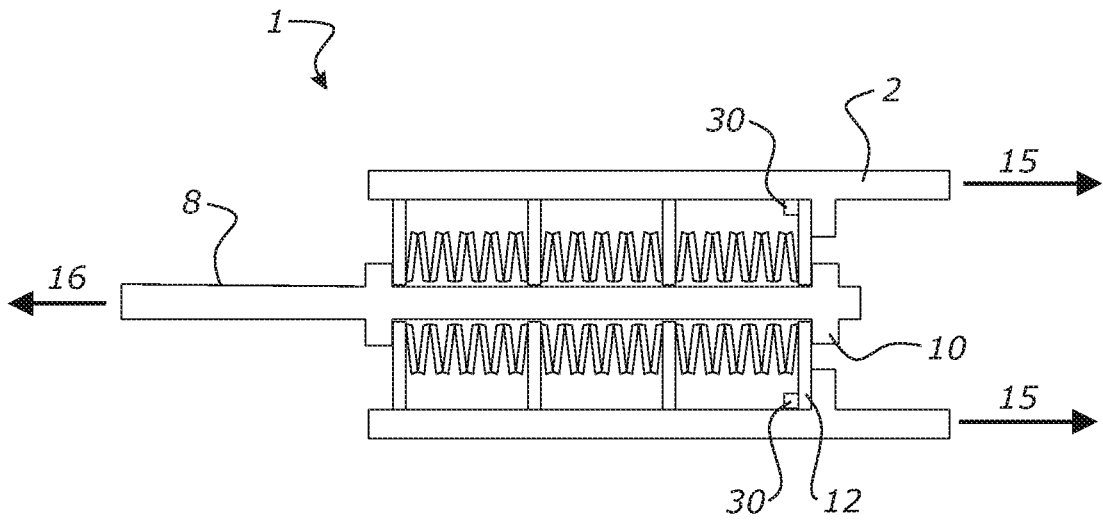


FIG. 14

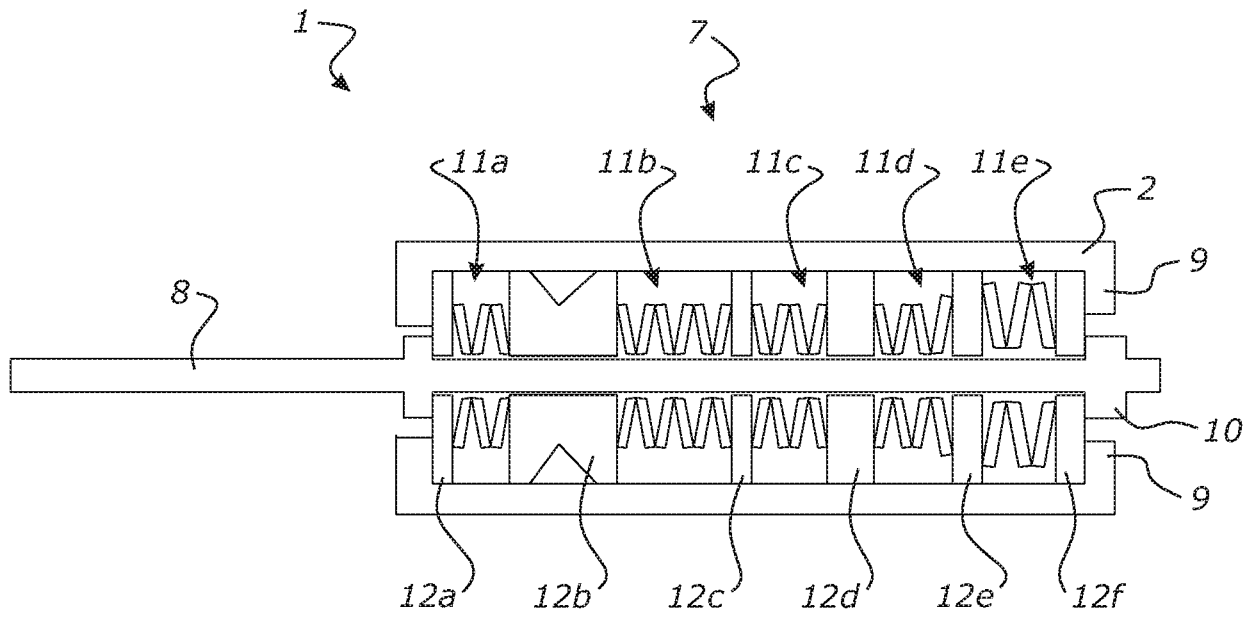


FIG. 15

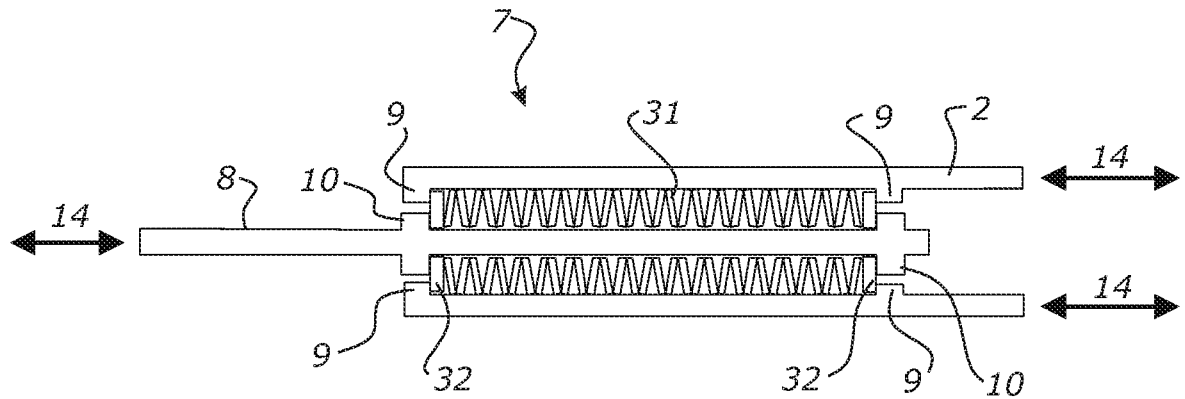


FIG. 16

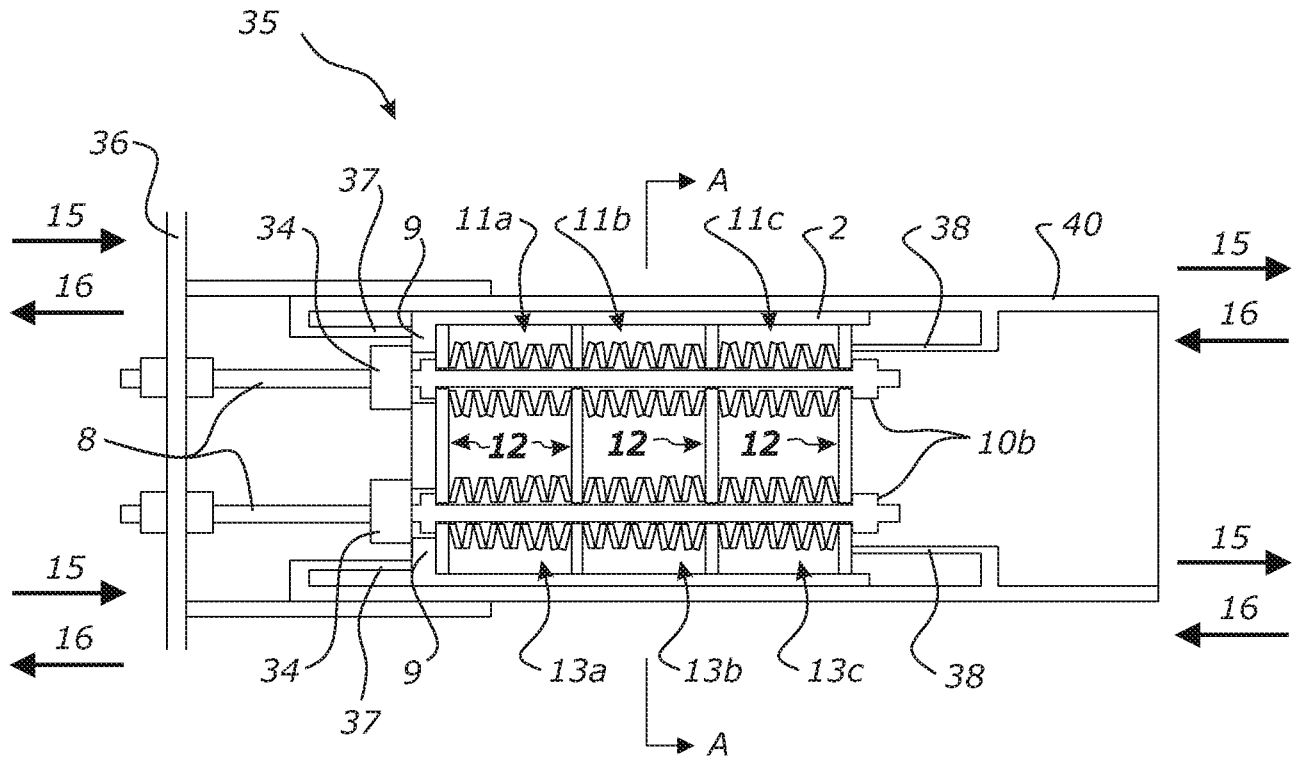


FIG. 17A

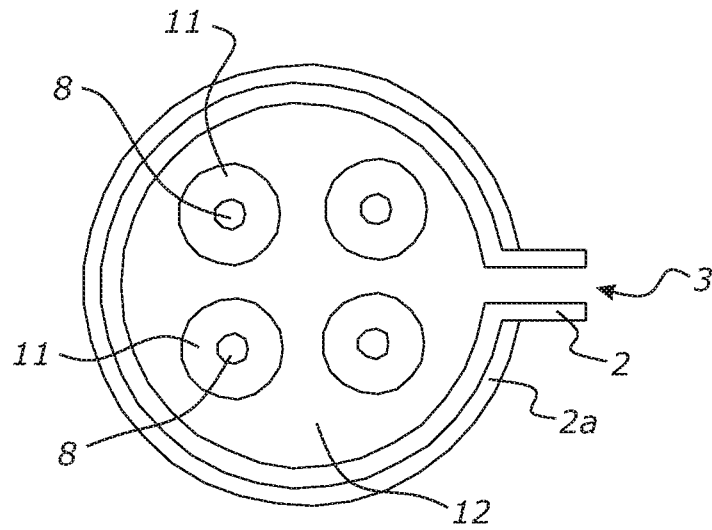


FIG. 17B

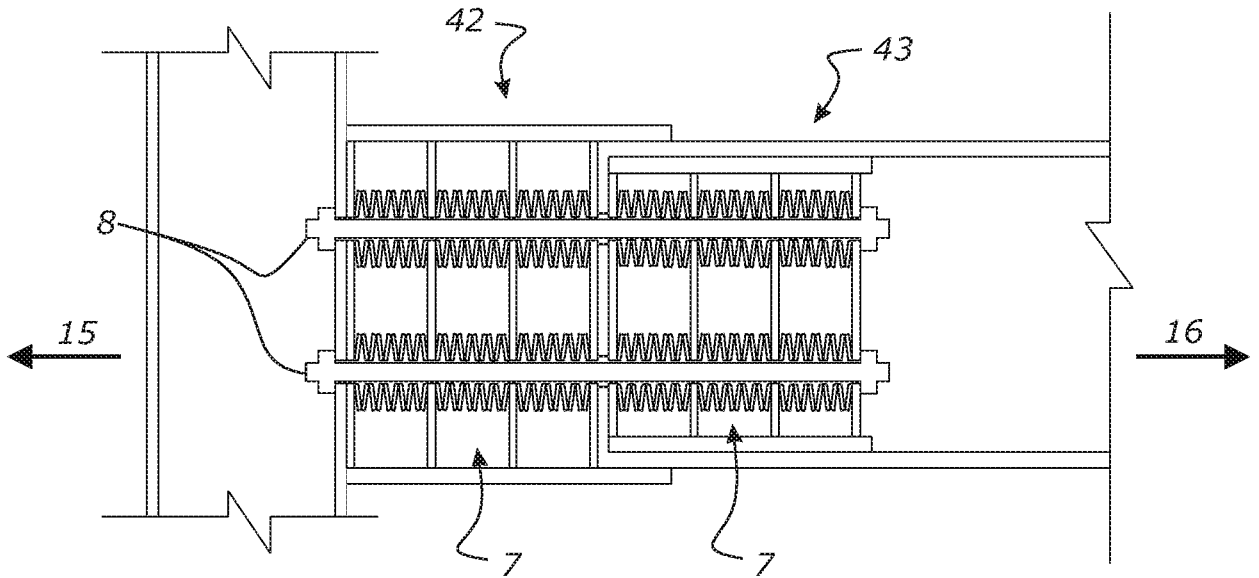


FIG. 18

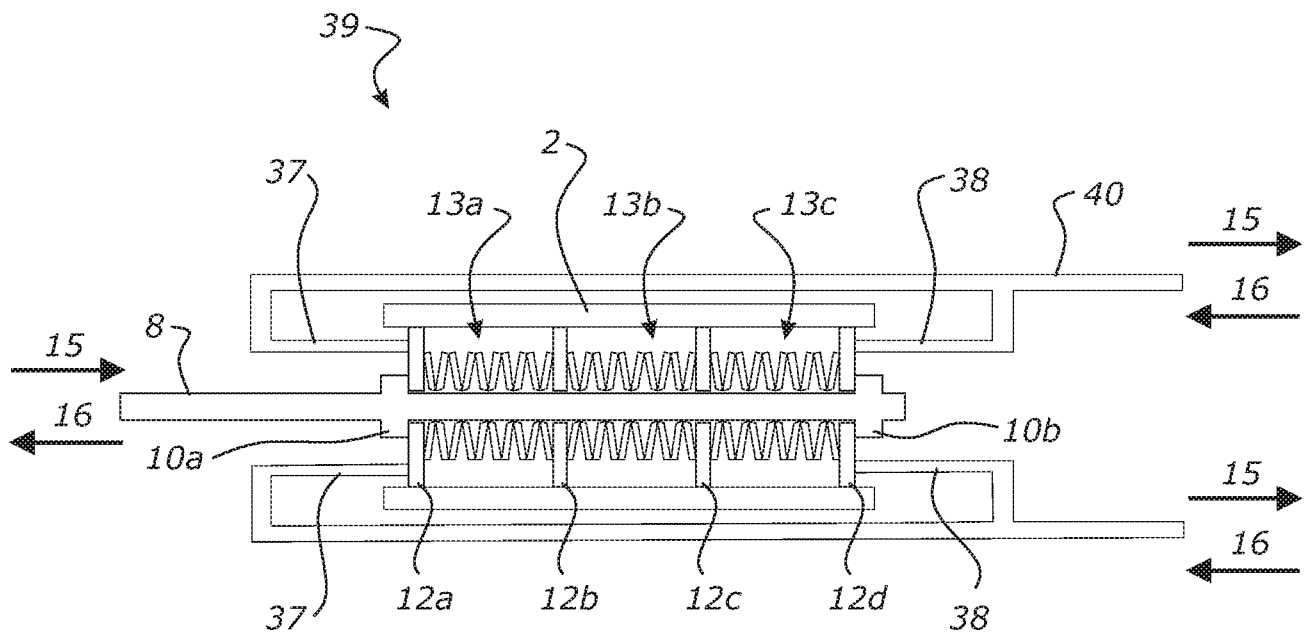


FIG. 19

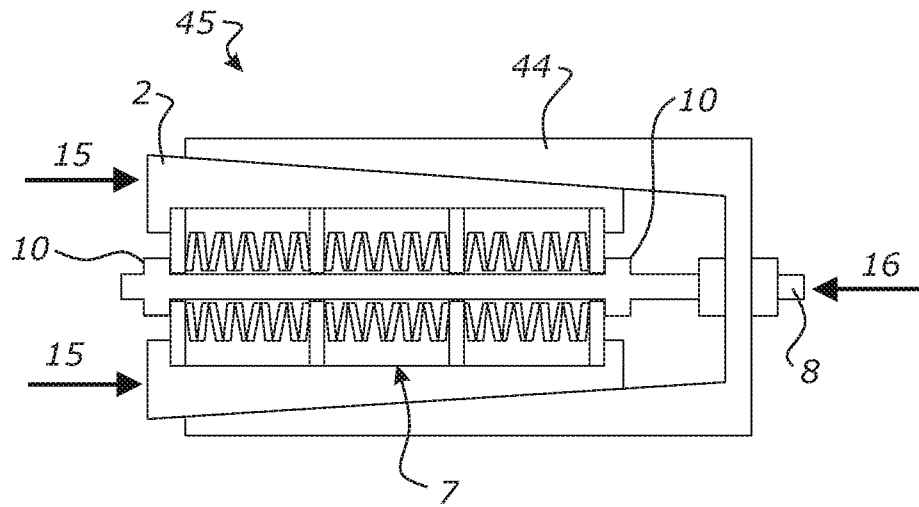


FIG. 20

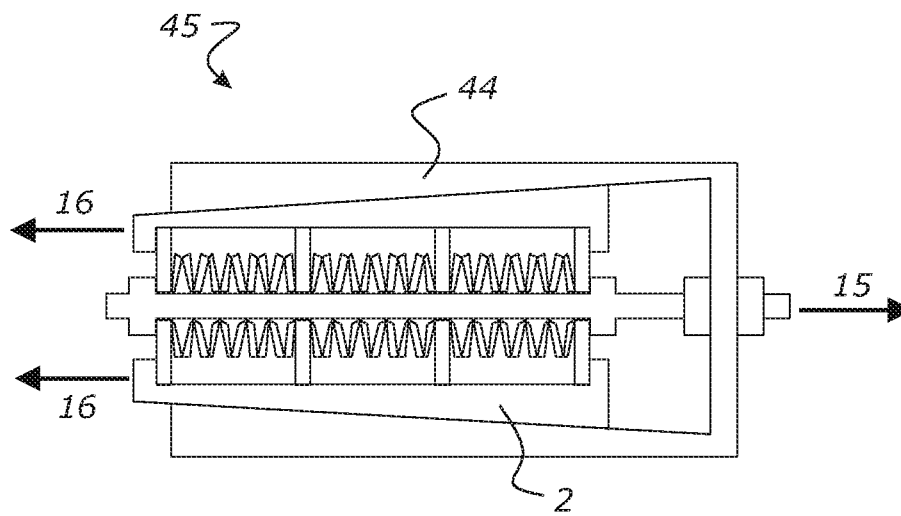


FIG. 21

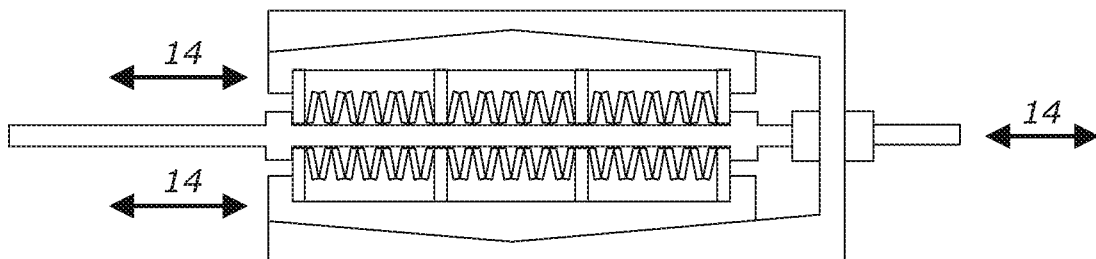


FIG. 22

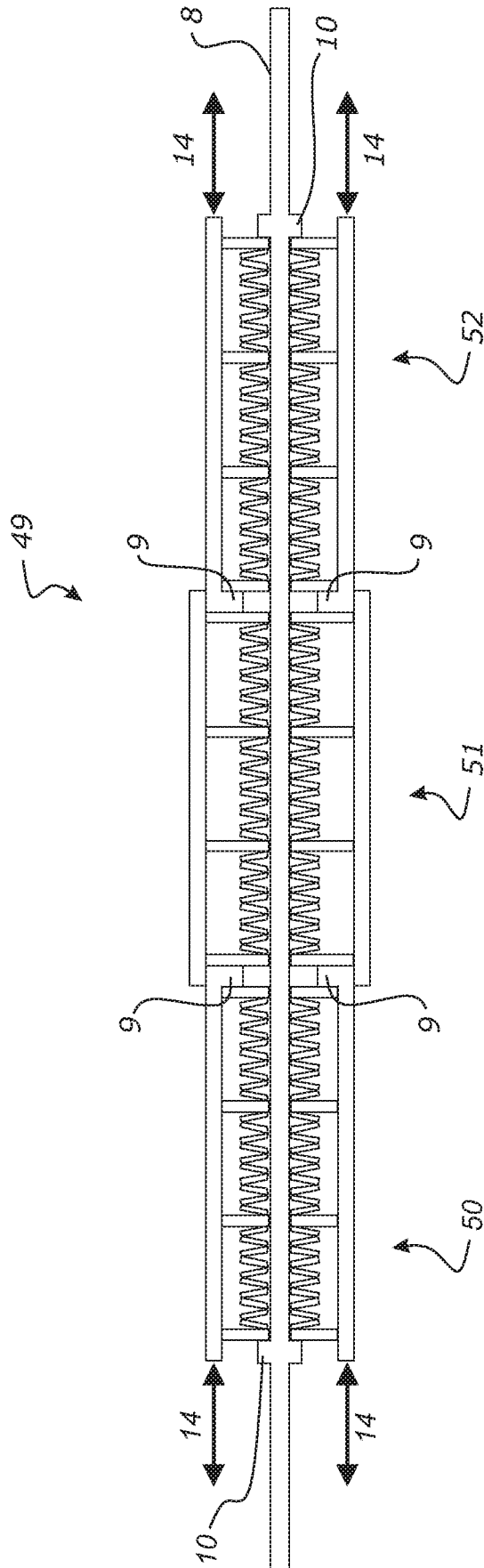


FIG. 23

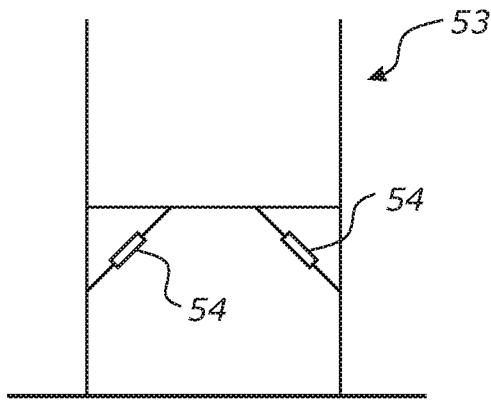


FIG. 24A

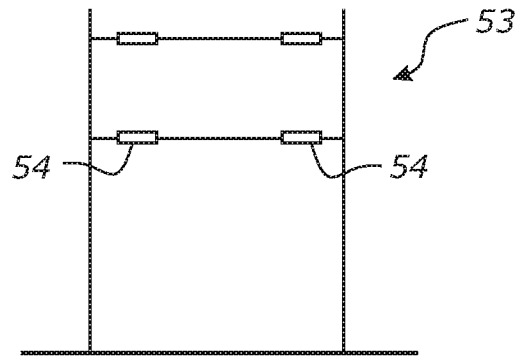


FIG. 24B

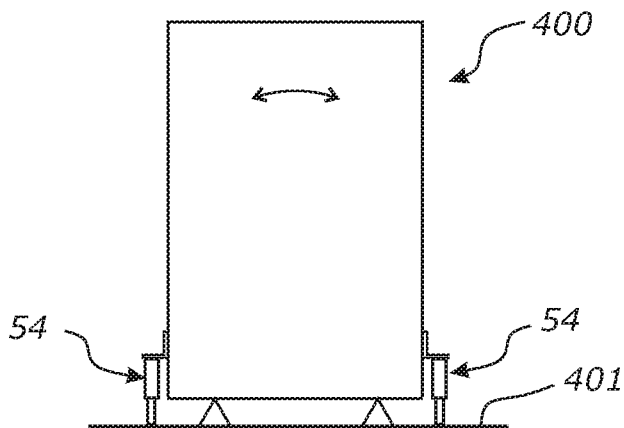


FIG. 24C

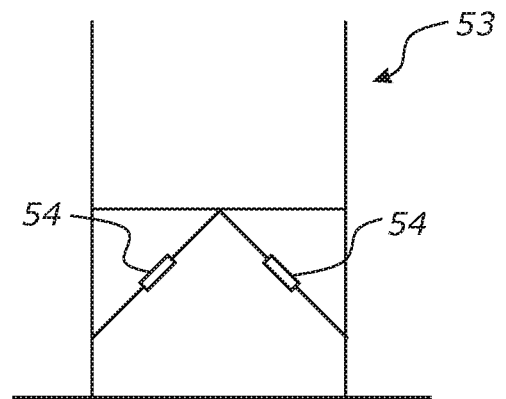


FIG. 24D

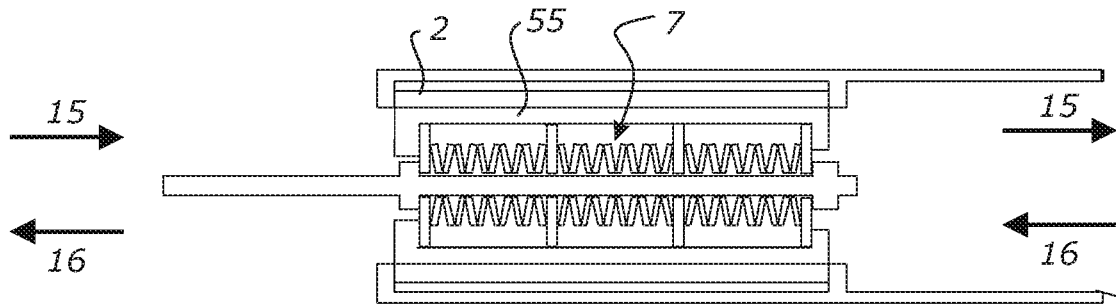


FIG. 25A

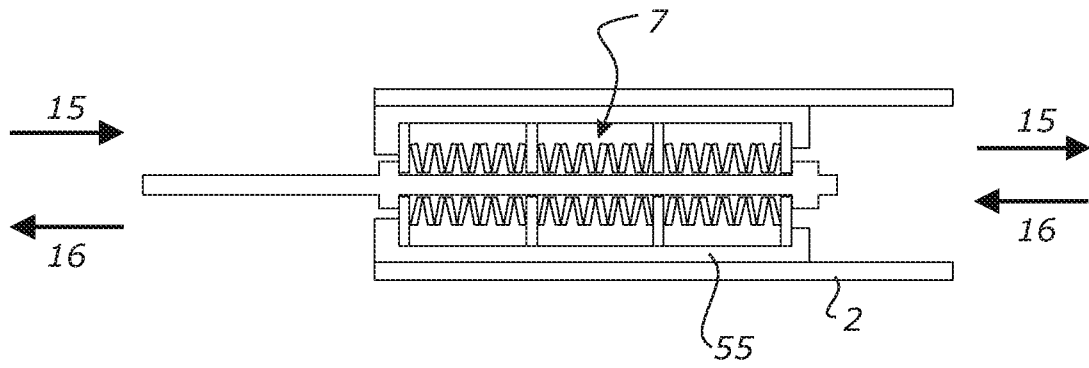


FIG. 25B

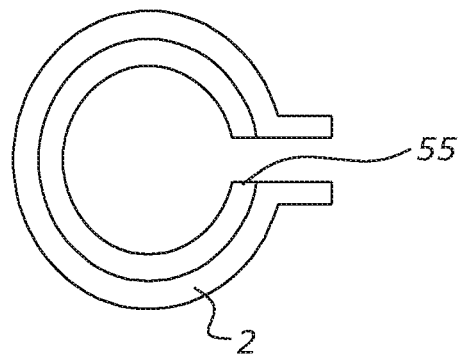


FIG. 25C

INTERNATIONAL SEARCH REPORT

International application No.

PCT/IB2019/055737

A. CLASSIFICATION OF SUBJECT MATTER

F16F 7/08 (2006.01) F16F 13/04 (2006.01) F16F 15/02 (2006.01) E04H 9/02 (2006.01)

According to International Patent Classification (IPC) or to both national classification and IPC

B. FIELDS SEARCHED

Minimum documentation searched (classification system followed by classification symbols)

Documentation searched other than minimum documentation to the extent that such documents are included in the fields searched

Electronic data base consulted during the international search (name of data base and, where practicable, search terms used)

PATENW/EPODOC/WPIAP/TXTE; IPC/CPC Marks F16F7/082/low, F16F13/005, F16F15/022, E04B 1/98, E04H9/021, F16F7/08/low, F16F13/1409, F16F 13/00/low, F16F1/32/low, F16F1/34, F16F3/00/low, F16F 15/02/low, F16F13/04/low and Keywords: friction, slip, damper, casing, earthquake, connector, spring, bias, bearing, sleeve, rod and similar terms.

Google Patents/Espacenet/Auspat/Google/PAMS Nose/INTESS; IPC/CPC F16F7, F16F7/08/low and Keywords: friction, slip, spring, damper, structural, connector and similar terms; applicant/inventor names searched.

C. DOCUMENTS CONSIDERED TO BE RELEVANT

Category*	Citation of document, with indication, where appropriate, of the relevant passages	Relevant to claim No.
	Documents are listed in the continuation of Box C	

 Further documents are listed in the continuation of Box C
 See patent family annex

* Special categories of cited documents:		
"A" document defining the general state of the art which is not considered to be of particular relevance	"T" later document published after the international filing date or priority date and not in conflict with the application but cited to understand the principle or theory underlying the invention	
"D" document cited by the applicant in the international application	"X" document of particular relevance; the claimed invention cannot be considered novel or cannot be considered to involve an inventive step when the document is taken alone	
"E" earlier application or patent but published on or after the international filing date	"Y" document of particular relevance; the claimed invention cannot be considered to involve an inventive step when the document is combined with one or more other such documents, such combination being obvious to a person skilled in the art	
"L" document which may throw doubts on priority claim(s) or which is cited to establish the publication date of another citation or other special reason (as specified)	"&" document member of the same patent family	
"O" document referring to an oral disclosure, use, exhibition or other means		
"P" document published prior to the international filing date but later than the priority date claimed		

Date of the actual completion of the international search 2 September 2019	Date of mailing of the international search report 02 September 2019
Name and mailing address of the ISA/AU AUSTRALIAN PATENT OFFICE PO BOX 200, WODEN ACT 2606, AUSTRALIA Email address: pct@ipaustralia.gov.au	Authorised officer Yew-Seng How AUSTRALIAN PATENT OFFICE (ISO 9001 Quality Certified Service) Telephone No. +61262832945

INTERNATIONAL SEARCH REPORT

International application No.

C (Continuation).

DOCUMENTS CONSIDERED TO BE RELEVANT

PCT/IB2019/055737

Category*	Citation of document, with indication, where appropriate, of the relevant passages	Relevant to claim No.
X	JP 2018096513 A (SHIMIZU CONSTRUCTION CO LTD) 21 June 2018 Figs 3a-4d; Paras 0001-0043 English translation from Espacenet	1-28
X	JP 2017078432 A (ASEISMIC DEVICES CO LTD) 27 April 2017 Fig 12; Paras 0044-0099 English translation from Espacenet	1-28
X	US 6244577 B1 (BUCHOLTZ) 12 June 2001 Figs 1-4; Col 1 Line 29 – Col 4 Line 10	1-28
X	CN 104482093 A (HUAQIAO UNIVERSITY et al.) 01 April 2015 Figs 1-5, 9; Pages 1-5 English translation from Espacenet	1-28
X	JP H0942346 A (IWATA DENKO KK) 10 February 1997 Figs 1-2; Paras 0005-0015 English translation from Espacenet	1-28
A	US 2005/0087414 A1 (OKIMURA et al.) 28 April 2005 Whole document	
A	CN 105604203 A (BEIJING UNIVERSITY OF TECHNOLOGY) 25 May 2016 Whole document	

Box No. 11 Observations where certain claims were found unsearchable (Continuation of item 2 of first sheet)

This international search report has not been established in respect of certain claims under Article 17(2)(a) for the following reasons:

1. Claims Nos.:
because they relate to subject matter not required to be searched by this Authority, namely:
the subject matter listed in Rule 39 on which, under Article 17(2)(a)(i), an international search is not required to be carried out, including
2. Claims Nos.:
because they relate to parts of the international application that do not comply with the prescribed requirements to such an extent that no meaningful international search can be carried out, specifically:
3. Claims Nos.:
because they are dependent claims and are not drafted in accordance with the second and third sentences of Rule 6.4(a)

Box No. III Observations where unity of invention is lacking (Continuation of item 3 of first sheet)

This International Searching Authority found multiple inventions in this international application, as follows:

See Supplemental Box for Details

1. As all required additional search fees were timely paid by the applicant, this international search report covers all searchable claims.
2. As all searchable claims could be searched without effort justifying additional fees, this Authority did not invite payment of additional fees.
3. As only some of the required additional search fees were timely paid by the applicant, this international search report covers only those claims for which fees were paid, specifically claims Nos.:
4. No required additional search fees were timely paid by the applicant. Consequently, this international search report is restricted to the invention first mentioned in the claims; it is covered by claims Nos.:

Remark on Protest

- The additional search fees were accompanied by the applicant's protest and, where applicable, the payment of a protest fee.
- The additional search fees were accompanied by the applicant's protest but the applicable protest fee was not paid within the time limit specified in the invitation.
- No protest accompanied the payment of additional search fees.

Supplemental Box**Continuation of: Box III**

This International Application does not comply with the requirements of unity of invention because it does not relate to one invention or to a group of inventions so linked as to form a single general inventive concept.

This Authority has found that there are different inventions based on the following features that separate the claims into distinct groups:

- Claims 1-5 are directed to a double acting slip friction earthquake energy damping connector that comprises an elongate casing, a spring and damper assembly comprising at least two spaced apart damper members, a pre-loaded spring arrangement, a respective bearing member of the casing, and a connection rod having a stop located adjacent each end of the spring and damper assembly. The feature of at least two spaced apart damper members, a respective bearing member of the casing, and a connection rod having a stop located adjacent each end of the spring and damper assembly is specific to this group of claims.
- Claims 6-25 are directed to a resilient slip friction connector comprising an elongate hollow casing, an elongate spring and damping assembly, at least one bearing element, the bias of the compressed spring and damping assembly exceeds the frictional force between the spring and damping assembly and the casing. The feature of at least one bearing element, the bias of the compressed spring and damping assembly exceeds the frictional force between the spring and damping assembly and the casing is specific to this group of claims.
- Claim 26 is directed to a resilient slip friction connector comprising an elongate hollow casing comprising at least one elongate split, an elongate spring and damping assembly, at least one bearing element, an adjustable member, the bias of the compressed spring and damping assembly exceeds the frictional force between the spring and damping assembly and the casing. The feature of an elongate hollow casing comprising at least one elongate split, at least one bearing element, an adjustable member, the bias of the compressed spring and damping assembly exceeds the frictional force between the spring and damping assembly and the casing is specific to this group of claims.
- Claims 27-28 are directed to a connector for connecting two structural components together in an initial relative position, the connector comprising a casing, a spring and damper assembly comprising at least one damper member, and a spring able to be elastically deformed and to bias the relative position of the two structural components. The feature of a spring and damper assembly comprising at least one damper member, and a spring able to be elastically deformed and to bias the relative position of the two structural components is specific to this group of claims.

PCT Rule 13.2, first sentence, states that unity of invention is only fulfilled when there is a technical relationship among the claimed inventions involving one or more of the same or corresponding special technical features. PCT Rule 13.2, second sentence, defines a special technical feature as a feature which makes a contribution over the prior art.

When there is no special technical feature common to all the claimed inventions there is no unity of invention.

In the above groups of claims, the identified features may have the potential to make a contribution over the prior art but are not common to all the claimed inventions and therefore cannot provide the required technical relationship. The only feature common to all of the claimed inventions and which provides a technical relationship among them is a connector for connecting two structural components together comprising a casing and a spring and damper assembly.

However it is considered that this feature is generic in this particular art. Therefore in this light this common feature cannot be a special technical feature. Hence there is no special technical feature common to all the claimed inventions and the requirements for unity of invention are consequently not satisfied *a priori*.

INTERNATIONAL SEARCH REPORT

Information on patent family members

International application No.

PCT/IB2019/055737

This Annex lists known patent family members relating to the patent documents cited in the above-mentioned international search report. The Australian Patent Office is in no way liable for these particulars which are merely given for the purpose of information.

Patent Document/s Cited in Search Report		Patent Family Member/s	
Publication Number	Publication Date	Publication Number	Publication Date
JP 2018096513 A	21 June 2018	JP 2018096513 A	21 Jun 2018
JP 2017078432 A	27 April 2017	JP 2017078432 A	27 Apr 2017
		JP 6529884 B2	12 Jun 2019
US 6244577 B1	12 June 2001	US 6244577 B1	12 Jun 2001
		CA 2312502 A1	12 Jan 2001
		EP 1069337 A1	17 Jan 2001
CN 104482093 A	01 April 2015	CN 104482093 A	01 Apr 2015
JP H0942346 A	10 February 1997	JP H0942346 A	10 Feb 1997
US 2005/0087414 A1	28 April 2005	US 2005087414 A1	28 Apr 2005
		US 7322451 B2	29 Jan 2008
		CA 2471499 A1	24 Jul 2003
		CN 1615409 A	11 May 2005
		CN 101067316 A	07 Nov 2007
		CN 101067316 B	17 Aug 2011
		CN 101463876 A	24 Jun 2009
		CN 101463876 B	16 Jan 2013
		EP 1467115 A1	13 Oct 2004
		EP 1467115 B1	17 Oct 2007
		EP 1808615 A1	18 Jul 2007
		EP 1808615 B1	18 Jun 2008
		EP 1862693 A1	05 Dec 2007
		EP 1862693 B1	25 Mar 2009
		JP 2003278828 A	02 Oct 2003
		JP 4366935 B2	18 Nov 2009
		KR 20040071309 A	11 Aug 2004
		KR 100661115 B1	22 Dec 2006
		NZ 534102 A	27 Jul 2007
		TW 200415316 A	16 Aug 2004
		TW I266837 B	21 Nov 2006
		US 2012073921 A1	29 Mar 2012
		US 8584821 B2	19 Nov 2013
		US 2007289828 A1	20 Dec 2007
		US 9488240 B2	08 Nov 2016

Due to data integration issues this family listing may not include 10 digit Australian applications filed since May 2001.

Form PCT/ISA/210 (Family Annex)(July 2019)

INTERNATIONAL SEARCH REPORT

Information on patent family members

International application No.

PCT/IB2019/055737

This Annex lists known patent family members relating to the patent documents cited in the above-mentioned international search report. The Australian Patent Office is in no way liable for these particulars which are merely given for the purpose of information.

Patent Document/s Cited in Search Report		Patent Family Member/s	
Publication Number	Publication Date	Publication Number	Publication Date
CN 105604203 A	25 May 2016	US 2013327607 A 1	12 Dec 2013
		US 9494207 B2	15 Nov 2016
		WO 03060344 A 1	24 Jul 2003
		CN 105604203 A	25 May 2016
		CN 105604203 B	31 Oct 2017

End of Annex